PRIFYSGOL BANGOR / BANGOR UNIVERSITY

3,4-Phenylenedioxythiophenes (PheDOTs) functionalized with electron-withdrawing groupsand their analogs for organic electronics. Remarkably efficient tuning the energy levels in flatconjugated polymers

Krompiec, Michal Piotr; Baxter, Sean; Klimareva, Elena L. ; Yufit, Dmitry S.; Congrave, Daniel G.; Britten, Thomas K.; Perepichka, Igor

Journal of Materials Chemistry C

DOI:
10.1039/C7TC05227H

Published: 14/04/2018

Peer reviewed version

Cyswllt i'r cyhoeddiad / Link to publication

Dyfyniad o'r fersiwn a gyhoeddwyd / Citation for published version (APA):
Krompiec, M. P., Baxter, S., Klimareva, E. L., Yufit, D. S., Congrave, D. G., Britten, T. K., & Perepichka, I. (2018). 3,4-Phenylenedioxythiophenes (PheDOTs) functionalized with electron-withdrawing groupsand their analogs for organic electronics. Remarkably efficient tuning the energy levels in flatconjugated polymers. *Journal of Materials Chemistry C*, *6*(14), 3746-3756. https://doi.org/10.1039/C7TC05227H

Hawliau Cyffredinol / General rights
Copyright and moral rights for the publications made accessible in the public portal are retained by the authors and/or other copyright owners and it is a condition of accessing publications that users recognise and abide by the legal requirements associated with these rights.

• Users may download and print one copy of any publication from the public portal for the purpose of private study or research.
• You may not further distribute the material or use it for any profit-making activity or commercial gain
• You may freely distribute the URL identifying the publication in the public portal ?

Take down policy
If you believe that this document breaches copyright please contact us providing details, and we will remove access to the work immediately and investigate your claim.

01. Jun. 2021

Check for updates

View Article Online
View Journal

Journal of Materials Chemistry C

Accepted Manuscript

This article can be cited before page numbers have been issued, to do this please use: M. Krompiec, S. N. Baxter, E. L. Klimareva, D. S. Yufit, D. G. Congrave, T. K. Britten and I. F. Perepichka, *J. Mater. Chem. C*, 2018, DOI: 10.1039/C7TC05227H.

This is an Accepted Manuscript, which has been through the Royal Society of Chemistry peer review process and has been accepted for publication.

Accepted Manuscripts are published online shortly after acceptance, before technical editing, formatting and proof reading. Using this free service, authors can make their results available to the community, in citable form, before we publish the edited article. We will replace this Accepted Manuscript with the edited and formatted Advance Article as soon as it is available.

You can find more information about Accepted Manuscripts in the author guidelines.

Please note that technical editing may introduce minor changes to the text and/or graphics, which may alter content. The journal's standard Terms & Conditions and the ethical guidelines, outlined in our author and reviewer resource centre, still apply. In no event shall the Royal Society of Chemistry be held responsible for any errors or omissions in this Accepted Manuscript or any consequences arising from the use of any information it contains.

ROYAL SOCIETY OF CHEMISTRY

rsc.li/materials-c

View Article Online
DOI: 10.1039/C7TC05227H

Graphical Abstracts

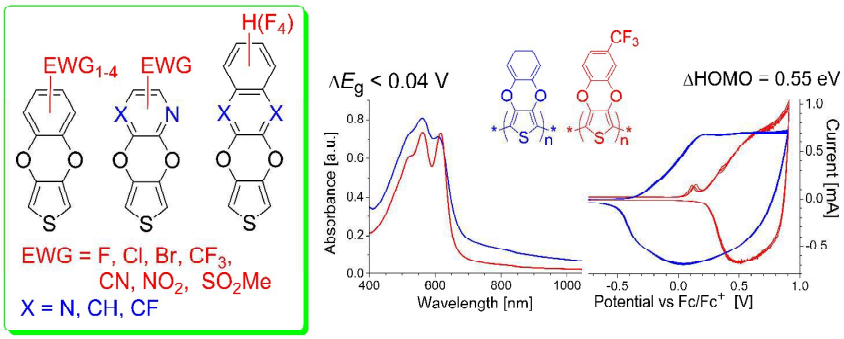

Facile one-pot microwave-assisted method of synthesis of novel functionalized arylenedioxythiophenes as promising building blocks for conjugated polymers with tuneable electronic properties is presented.

Published on 03 January 2018. Downloaded by McGill University on 03/01/2018 15:18:04.

Journal of Materials Chemistry C Accepted Manuscript

View Article Online
DOI: 10.1039/C7TC05227H

3,4-Phenylenedioxythiophenes (PheDOTs) functionalized with electron-withdrawing groups and their analogs for organic electronics. Remarkably efficient tuning the energy levels in flat conjugated polymers[†,‡]

Michal P. Krompiec,[a,§] Sean N. Baxter,[a] Elena L. Klimareva,[a,b] Dmitry S. Yufit,[c] Daniel G. Congrave,[a] Thomas K. Britten[a] and Igor F. Perepichka[a,*]

Published on 03 January 2018. Downloaded by McGill University on 03/01/2018 15:18:04.

Abstract

A novel, facile and efficient one-pot microwave-assisted method of synthesis allowing an access to a new series of 3,4-phenylenedioxy-thiophene derivatives with electron-withdrawing groups at the benzene ring (**EWG-PheDOT**) and their analogs (with expanded side π-system or with heteroaromatic rings, **ArDOT**) by reaction of 2,5-dialkoxycarbonyl-3,4-dihydroxythiophenes with electrophilic aromatic/heteroaromatic compounds in dipolar aprotic solvents has been described. Its applicability to a wide range of novel functionalized **ArDOTs** as promising building blocks for organic electronic materials have been demonstrated. The structures of selected **ArDOTs** have been determined by a single crystal X-ray diffraction. The electronic structure of conjugated polymers **p[ArDOTs]** based on synthesized novel thiophene monomers has been studied theoretically by DFT PBC/B3LYP/6-31G(d) method. The performed calculations reveal that while the side functional groups are formally not in conjugation with the polymer main chain, they have an unprecedentedly strong effect on the HOMO/LUMO energy levels of conjugated polymers, allowing their efficient tuning by over 1.6 eV range. In contrast to that, the energy gaps of the polymers are almost unaffected by such functionalizations and vary within a range of only ≤ 0.05 eV. Computational predictions have been successfully confirmed in experiments: cyclic voltammetry shows a strong anodic shift of p-doping for the electron-withdrawing CF_3 group functionalized polymer **p[4CF$_3$-PheDOT]** relative to the unsubstituted **p[PheDOT]** polymer(by 0.55 V; DFT predicted decrease of HOMO by 0.58 eV), while very similar Vis-NIR absorption spectra for both polymers in the undoped state indicate that their optical energy gaps near coincide (ΔE_g <0.04 eV).

[a] *School of Chemistry, Bangor University, Deiniol Road, Bangor LL57 2UW, UK. E-mail: i.perepichka@bangor.ac.uk; Tel: +44–(0)1248–382386; Fax: +44–(0)1248–370528*
[b] *Department of Organic Substances Technology, Ural Federal University, Ekaterinburg 620002, Russian Federation*
[c] *Department of Chemistry, Durham University, Durham DH1 3LE, UK*
[†] We dedicate this paper to Prof. Fred Wudl in celebration of 50 years of his contributions to the field of π-conjugated organic materials.
[‡] Electronic supplementary information (ESI) available: experimental procedures of synthesis of **ArDOTs**. ^{1}H, ^{13}C and ^{19}F NMR spectra and MS for characterized compounds; ^{13}C DEPT, HSQC and HMBC NMR spectra for selected compounds; UV-Vis spectra for selected **ArDOT** compounds; data on DFT calculations for **ArDOT** oligomers and polymers; cyclic voltammograms and Vis-NIR absorption spectra for two **p[ArDOT]** polymers; single crystal X-ray structure data for 8 selected compounds (CCDC 1553610–1553617). For ESI and crystallographic data in CIF or other electronic formats see DOI: #########
[§] Present address: Merck Chemicals Ltd, Southampton, UK.

Journal of Materials Chemistry C Accepted Manuscript

View Article Online
DOI: 10.1039/C7TC05227H

Published on 03 January 2018. Downloaded by McGill University on 03/01/2018 15:18:04.

Journal of Materials Chemistry C Accepted Manuscript

Introduction

Polythiophenes are one of the most fascinating classes of conjugated polymers,[1] and a large number of polythiophenes and oligothiophenes, as well as thiophene-based small molecules have been studied and used as materials for organic electronic applications,[2] including organic light-emitting devices (OLED),[3] field-effect transistors (OFET),[4] photovoltaics (OPV),[5] electrochromics,[6] photochromics,[7] electrode materials for batteries and capacitors,[8] sensors[9] and biosensors.[10] Among them, poly(3,4-ethylenedioxythiophene) (**PEDOT**) is of special interest and importance due to its high electrical conductivity, optical transparency and stability in the doped state, and it has found many applications in organic electronics.[11] Apart from the electronic effect of the ethylenedioxy substitution onto the thiophene moiety, an important reason for superior properties of **PEDOT** is the flat structure of its backbone due to the attractive S···O intermolecular interactions between the neighboring EDOT moieties, which was shown by X-ray crystallography for **EDOT** oligomers.[12,13,14] This attracted substantial interest into EDOT derivatives and a large number of functionalized **PEDOTs** have been synthesized and studied.[15] However, functionalization of **EDOT** monomer at the ethylene bridge does not provide means for tuning the properties of the polymers, because substituents attached to the bridge sp^3 carbon atoms are not conjugated to the thiophene ring and are directed out of the polymer plane (thereby disturbing the π-π stacking between the polymer chains).

3,4-(1,2-Phenylenedioxy)thiophene (**PheDOT**),[16,17] a benzo-fused analog of **EDOT**, represents a fascinating building block for π-functional oligo/polythiophene materials with the possibility of wider functionalization (at the benzene ring). Electrochemically prepared unsubstituted **PheDOT** polymer, **p[PheDOT]**, is oxidized at higher potentials (by 0.3–0.4 V) than **PEDOT** showing better environmental stability of its neutral form (highest occupied molecular orbital (HOMO) energy levels estimated from cyclic voltammetry data are –4.33 and –3.95 eV, respectively[17]) and giving a slightly larger band gap (1.80[17] eV and 1.6 eV,[11a] respectively). In contrast to **PEDOT**, the hydrogen atoms on the benzene ring of **p[PheDOT]** lie in the monomer plane, and therefore substitution should not increase inter-chain spacing. Also, the electronic effect of substituents on the benzene ring of **PheDOT** is expected to be stronger because the sp^2 hybridization of the carbon atoms should allow better coupling of substituents with the oxygen atoms of the dioxine ring via resonance. Reynolds *et al.* first reported a soluble electroactive PheDOT polymer with dodecyl groups, **p[$(C_{12})_2$-PheDOT]**, which showed a remarkable degree of intra- and interchain order, both in solution and in the solid state.[18] Other soluble alkyl-substituted **p[PheDOTs]** have been synthesized.[19] The polymers showed hole mobility of 1.92×10^{-3} cm^2 V^{-1} cm^{-1} in OFET devices and up to 0.91% PCE (power conversion efficiency) in OPV with $PC_{70}BM$. The **PheDOT** building

View Article Online
DOI: 10.1039/C7TC05227H

Published on 03 January 2018. Downloaded by McGill University on 03/01/2018 15:18:04.

Journal of Materials Chemistry C Accepted Manuscript

block has also been used in the design of an efficient hole-transporting material for perovskite solar cells which showed encouraging power conversion efficiency (PCE) up to 10.64%.[20] Another interesting behavior of some substituted **PheDOTs** was recently demonstrated by Darmanin and Guittard: on electropolymerization, they form well-ordered nanotubes of **p[PheDOT]** polymers on the surface without any template.[21] Such nanotubes create parahydrophobic surfaces with extremely high water contact angles (up to θ_W ~130–150 ^{o}) and high water adhesion, even if the nanotubes are prepared from the intrinsically hydrophilic polymers (i.e. Young's angle θ^Y ~ 60 ^{o}). This makes them attractive materials for advanced applications e.g. in membrane design, water transport and harvesting, as well as sensor design.

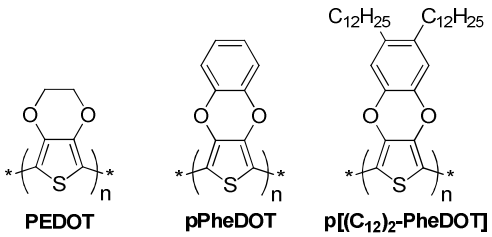

PheDOT itself and alkyl-substituted **PheDOTs** (in a more general case, **PheDOTs** with electron-donating groups (EDGs) at the benzene ring) have been prepared by a common method of coupling of 3,4-dimethoxythiophene with catechols catalyzed by *p*-toluenesulfonic acid.[16–19,21] However, synthesis of **PheDOTs** bearing electron-withdrawing groups (EWGs) by this route is problematic because even weak EWGs drastically decrease the nucleophilicity of the corresponding catechols and the yields of **PheDOTs**.[22] An alternative multi-step method, widely used in the synthesis of functionalized **EDOTs** and related thiophenes, is based on the reaction of 3,4-dihydroxy-2,5-di(alkoxycarbonyl)thiophene (**1**) with dihaloalkanes, followed by removal of the carbalkoxy groups by reaction with lithium bromide[23] or by alkali hydrolysis followed by high temperature decarboxylation in presence of copper chromite,[24] copper oxide[25] or silver carbonate.[26] We have isolated **PheDOT** in a low yield by this reaction,[16a] however its applicability toward a wider range of substituted **PheDOTs** is problematic (particularly because of problems with purification of intermediates). Also, this method required several synthetic steps and the use of highly toxic hexamethylphosphortriamide (in the case of decarboxyethylation with LiBr) that diminished its synthetic advantages.

Here we report the facile one-pot microwave-assisted synthesis of a wide range of substituted **PheDOTs** functionalized with EWGs at the benzene ring (**EWG-PheDOTs**) from thiophene **1**. We have also successfully expanded this reaction to the synthesis of some analogues structures with pyridine (**EWG-PyDOT**) and pyrazine (**PzDOT, QxDOT**) rings, as well as polyfluorinated

View Article Online
DOI: 10.1039/C7TC05227H

Published on 03 January 2018. Downloaded by McGill University on 03/01/2018 15:18:04.

arylenedioxythiophenes (**F_4-BnDOT, F_6-NaphDOT(1,2), F_6-NaphDOT(2,3)**). We have analyzed the properties of the derived polymers by computational, electrochemical and Vis-NIR electron absorption methods. We demonstrate a remarkably strong effect of substituents in **PheDOT** and its heteroanalogs on the frontier orbital energies of derived polymers with surprisingly small influence on their band gaps.

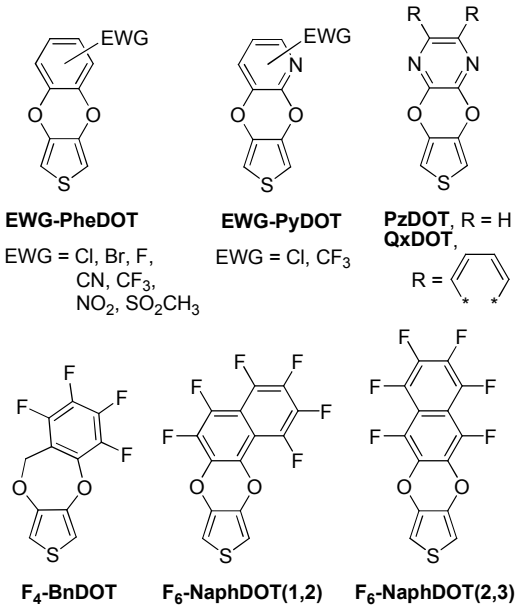

Results and discussion

Synthesis

The synthetic approach to the one-pot microwave-assisted (MW) synthesis of **PheDOT** derivatives with EWG groups at the benzene ring, **EWG-PheDOT,** is illustrated in Scheme 1. Double nucleophilic aromatic substitution (S_NAr) of the substituted benzenes **2–16** by anions generated from 3,4-dihydroxythiophene **1** by a weak base (K_2CO_3) led to the formation of intermediates **22** and **23**, which at high temperature in the presence of lithium bromide underwent decarboxyethylation to form the target **EWG-PheDOT** compounds. The reaction proceeded well in dipolar aprotic solvents (generally, in *N,N*-dimethylacetamide (DMA), but *N,N*-dimethylformamide (DMF) and pyridine have also been tested).

For more detailed studies, the reaction of thiophene **1** was first tested with hexafluorobenzene (**15**) with monitoring by GC-MS (Table S2 in ESI). No product **F_4-PheDOT** or intermediates **F_4-22** or **F_4-23** were detected in the reaction with conventional heating in DMA even at prolonged time at 100 ^oC (Table S2 in ESI). In MW-assisted conditions, heating at 220 ^oC showed a formation of mixture of **F_4-PheDOT** and an intermediate **F_4-23**. Addition of LiBr substantially increased the rate

Journal of Materials Chemistry C Accepted Manuscript

View Article Online
DOI: 10.1039/C7TC05227H

of decarboxyethylation of intermediate **F_4-23**, showing the yields of **F_4-PheDOT** of ca. 10–35% (Table S2, entries 6, 7). Further optimizations of the temperature, time and the amount of the solvent allowed to obtain **F_4-PheDOT** in 30–35% isolated yields in grams-scale reactions under MW conditions (Table S3 in ESI). Microwave irradiation is an important factor for the reaction: performing the reaction under similar conditions with conventional heating resulted in substantially lower yields of **F_4-PheDOT** (0–7%, Table S3 in ESI) and incomplete decarboxyethylation: apart from the target product **F_4-PheDOT**, substantial amounts of the intermediate **F_4-23** were formed. We have isolated an intermediate **F_4-23** when the reaction was performed at temperatures of 140–160 ^{o}C and its structure was confirmed by a single crystal X-ray diffraction (Figure S4 in ESI).

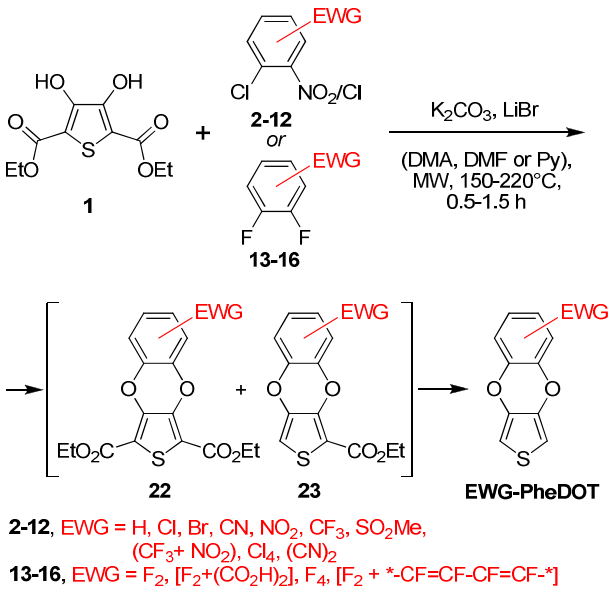

Scheme 1. Microwave-assisted synthesis of **EWG-PheDOT** (the structures of reactants **2-16** and the products are shown in the Table 1).

A large series of electron-deficient aromatic compounds (**3–16**) have been investigated in the reaction with thiophene **1** and functionalized **EWG-PheDOTs** have been successfully obtained (Table 1, entries 3–15). The reaction worked well with fluoro-, chloro- and nitro-substituted aromatic compounds. While NO_2 is a poor leaving group, the intramolecular nature of the second step of cyclization to form the **PheDOT** moiety makes the reaction efficient. It should be mentioned that *o*-chloronitrobenzene under these conditions showed a very low yield of unsubstituted **PheDOT** of only 2% (Table 1, entry 2), presumably due to its lower reactivity in a S_NAr reaction in an absence of an additional EWG.

In the reaction of thiophene **1** with tetrafluorophtalic acid (**14**), spontaneous decarboxylation of CO_2H groups at the benzene ring was also observed under the reaction conditions resulting in **36F_2-PheDOT** (Table 1, entry 13). For the reaction with octafluoronaphtalene (**16**), nucleophilic

Published on 03 January 2018. Downloaded by McGill University on 03/01/2018 15:18:04.
Journal of Materials Chemistry C Accepted Manuscript

View Article Online
DOI: 10.1039/C7TC05227H

substitution occurred at the both positions 2,3- and 1,2- of the naphthalene moiety to form two isomers (total yield 33%), symmetrical **F_6-NaphDOT(2,3)** and non-symmetrical **F_6-NaphDOT(1,2)** in a ratio of ca. 1.75:1 (Table 1, entry 15). In the case of dibromosubstituted 1,2-difluorobenzenes **24** and **25**, we observed partial debromination in the reaction and mixtures of substituted **PheDOTs** were formed. The mixtures were difficult to separate, so were analyzed by GC-MS and ^{1}H NMR, which indicated the removal of one or two bromine atoms in the products (see ESI).

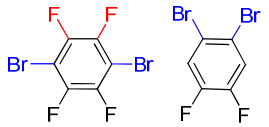

After the successful synthesis of a series of **EWG-PheDOTs** with various electron-withdrawing substituents at the benzene ring, we expanded the reaction to other electrophiles, namely perfluorobenzylbromide (**17**), substituted pyridines (**18**, **19**) and pyrazines (**20**, **21**). The reaction worked well in these cases to give **PheDOT** analogs, i.e. **F_4-BnDOT, EWG-PyDOTs, PzDOT** and **QxDOT**,[27] correspondingly (Scheme 2 and Table 1, entries 16–20). Electron-deficient pyridine and pyrazine rings are activated for S_NAr reactions and with these heterocycles the reaction worked well, even better than for EWG-functionalized benzenes, giving the target products in the yields of 17–74%.

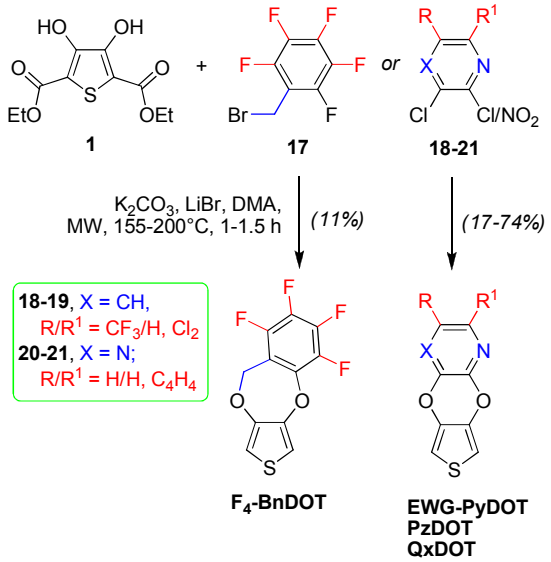

Scheme 2. Microwave-assisted synthesis of **PheDOT** analogs.

While the obtained yields in this one-pot microwave-assisted reaction (Schemes 1 and 2) were generally moderate to low, they are comparable with the total yields of the 3-steps "classical route"

Published on 03 January 2018. Downloaded by McGill University on 03/01/2018 15:18:04.
Journal of Materials Chemistry C Accepted Manuscript

View Article Online
DOI: 10.1039/C7TC05227H

of condensation of **1** → hydrolysis → decarboxylation (although for the reaction of pyridine **17**, we isolated **5CF$_3$-PyDOT** with high yield of 74%). We should mention that in most the cases we did not optimize the yields towards the reaction conditions (e.g. temperature, time, ratio of reagents, concentrations etc., so the yields can be further improved) but focussed on demonstration of the applicability of this facile and simple method for a wide range of functionalized **ArDOTs**. In addition, even for the low yielding reactions, the target products could be very easily separated from the intermediates, by-products and tag by column chromatography on silica gel, as they always eluted first with non-polar/modest polarity solvents (usually, PE, toluene, DCM or their mixtures; see Table 1). The synthesized **ArDOTs** are colorless to yellowish crystalline materials (see Fig. S1 and S2 in ESI for their UV-Vis absorption spectra), generally well soluble in common organic solvents (except of **F$_6$-NaphDOT(2,3)** and **F$_6$-NaphDOT(1,2)**, the solubility of which is much lower than for other compounds).

Table 1. Synthesis ArDOT derivatives by reaction of 3,4-dihydroxythiophene 1 under microwave-assisted conditions.[a,b]

Entry	Reactant (amount)	Conditions: (tempera-ture, time)	Product	Yield,[c] %
1	(1.04 eq.)	200 °C, 1 h	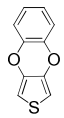 PheDOT	2% (PE)
2	(1.09 eq.)	200 °C, 1 h	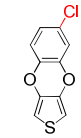 4Cl-PheDOT	17% (PE)
3	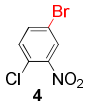 (1.10 eq.)	160 °C, 1 h	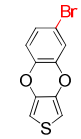 4Br-PheDOT	9%[d] (PE)
4	(1.09 eq.)	200 °C, 1 h	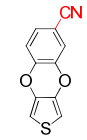 4CN-PheDOT	19% (toluene or DCM)
5	(1.00 eq.)	220°C, 0.5 h[e]	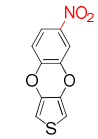 4NO$_2$-PheDOT	15% (toluene)

Published on 03 January 2018. Downloaded by McGill University on 03/01/2018 15:18:04.
Journal of Materials Chemistry C Accepted Manuscript

View Article Online
DOI: 10.1039/C7TC05227H

Published on 03 January 2018. Downloaded by McGill University on 03/01/2018 15:18:04.

6	7 (1.10 eq.)	200°C, 1 h	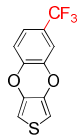 4CF$_3$-PheDOT	36% (PE)
7	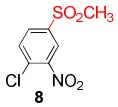 8 (1.11 eq.)	200°C, 1 h	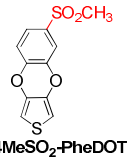 4MeSO$_2$-PheDOT	21% (DCM)
8	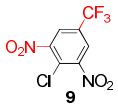 9 (1.10 eq.)	155°C, 1.5 h	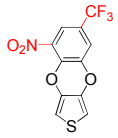 3NO$_2$,5CF$_3$-PheDOT	13% (PE:DCM, 1:3)
9	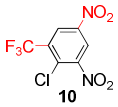 10 (1.09 eq.)	155°C, 1.5 h	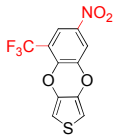 3CF$_3$,5NO$_2$-PheDOT	13% (DCM)
10	11 (1.09 eq.)	200°C, 1 h	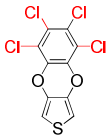 Cl$_4$-PheDOT	9%[g] (hot heptane)
11	12 (1.09 eq.)	170 °C, 1 h[f]	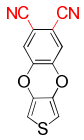 45(CN)$_2$-PheDOT	15% (toluene)
12	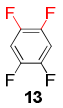 13 (1.11 eq.)	165°C, 1 h	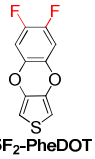 45F$_2$-PheDOT	2% (PE)
13	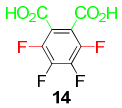 14 (1.11 eq.)	155°C, 1.5 h	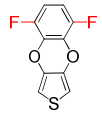 36F$_2$-PheDOT	7% (PE:EA, 20:1)
14	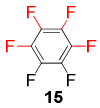 15 (1.28 eq.)	172°C, 0.5 h	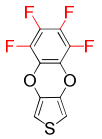 F$_4$-PheDOT	36% (toluene)

Journal of Materials Chemistry C Accepted Manuscript

View Article Online
DOI: 10.1039/C7TC05227H

Published on 03 January 2018. Downloaded by McGill University on 03/01/2018 15:18:04.

15	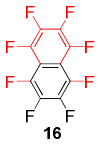 **16** (1.09 eq.)	200°C, 1 h	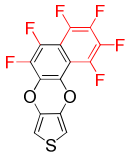 **F_6-NaphDOT(1,2)** 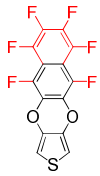 **F_6-NaphDOT(2,3)**	12%[h] (PE) 21%[h] (PE)
16	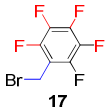 **17** (1.15 eq.)	200°C, 1 h	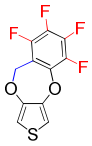 **F_4-BnDOT**	11% (PE)
17	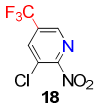 **18** (1.11 eq.)	155°C, 1.5 h	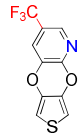 **$5CF_3$-PyDOT**	74% (PE:EA, 1:1, or DCM))
18	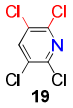 **19** (1.10 eq.)	200°C, 1 h	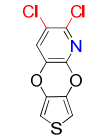 **$56Cl_2$-PyDOT**	17% (toluene)
19	**20** (1.04 eq.)	200°C, 1 h	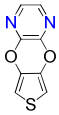 **PzDOT**	38% (PE:EA, 9:1)
20	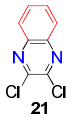 **21** (1.10 eq.)	155°C, 1.5 h	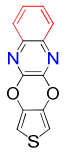 **QxDOT**	42%[i] (PE:DCM, 3:1 to DCM)

[a]**ArDOT** is a general abbreviation for all synthesized products, i.e. **PheDOT**, **EWG-PheDOTs**, and their analogs with aromatic/heteroaromatic side moieties. [b]Reaction conditions: DMA (2.6–3.1 mL/1 mmol of compound **1**), K_2CO_3 (1.0 eq.), LiBr (0.6 eq.), MW irradiation 100–150W. [c]Isolated yields. Solvents used for column purification are indicated in brackets (PE = petrol ether, DCM = dichloromethane, EA = ethyl acetate). [d]The yield was decreased to 1.9% when AcONa was used as a base; 200 °C / 1 h. [e]2,5-Dicarbomethoxy-3,4-dihydroxythiophene disodium salt, DMF (6.9 mL / 1 mmol), AcOH (1.0 eq.), no LiBr. [f]In pyridine, 0.44 eq. LiBr. [g]The yield was decreased to 5% in the reaction at 155 °C for 1.5 h. [h]For the reaction at 165 °C / 1.5 h, the yields of **F_6-NaphDOT(2,3)** and **F_6-NaphDOT(1,2)** were lowered to 6.4% and 2.1%, respectively (1 g scale synthesis). [i]The yield was decreased to <26% for the reaction at 200 °C / 1h.

Journal of Materials Chemistry C Accepted Manuscript

View Article Online
DOI: 10.1039/C7TC05227H

Published on 03 January 2018. Downloaded by McGill University on 03/01/2018 15:18:04.

Journal of Materials Chemistry C Accepted Manuscript

X-ray Crystallography of ArDOTs

For several synthesized **EWG-PheDOTs** and their analogs, we have confirmed their structures by X-ray crystallography. The molecular structures of single crystals for seven of the studied **ArDOTs** are shown in Figure 1 (see also Figure S3 in ESI for crystal packing).

Planar molecules of **36F$_2$-PheDOT** in the crystal structure form typical for polycyclic aromatic compounds inclined stacks with interplanar distances of 3.437(3) Å. C(thiophene)–H···O contacts link the stacks in layers, while weak C(Ph)–H···F interactions connect the layers in a 3D framework. In contrast to **36F$_2$-PheDOT**, molecules of **F$_4$-PheDOT** are arranged in an anti-parallel mode in stacks, probably due to the presence of two additional fluorine atoms creating an area of negative electrostatic potential. Only the heterocyclic parts of adjacent molecules are overlapped in stacks, the shortest interatomic distance between the molecules is 3.461(2) Å. The C(thiophene)-H···O interactions combine the stacks into corrugated layers.

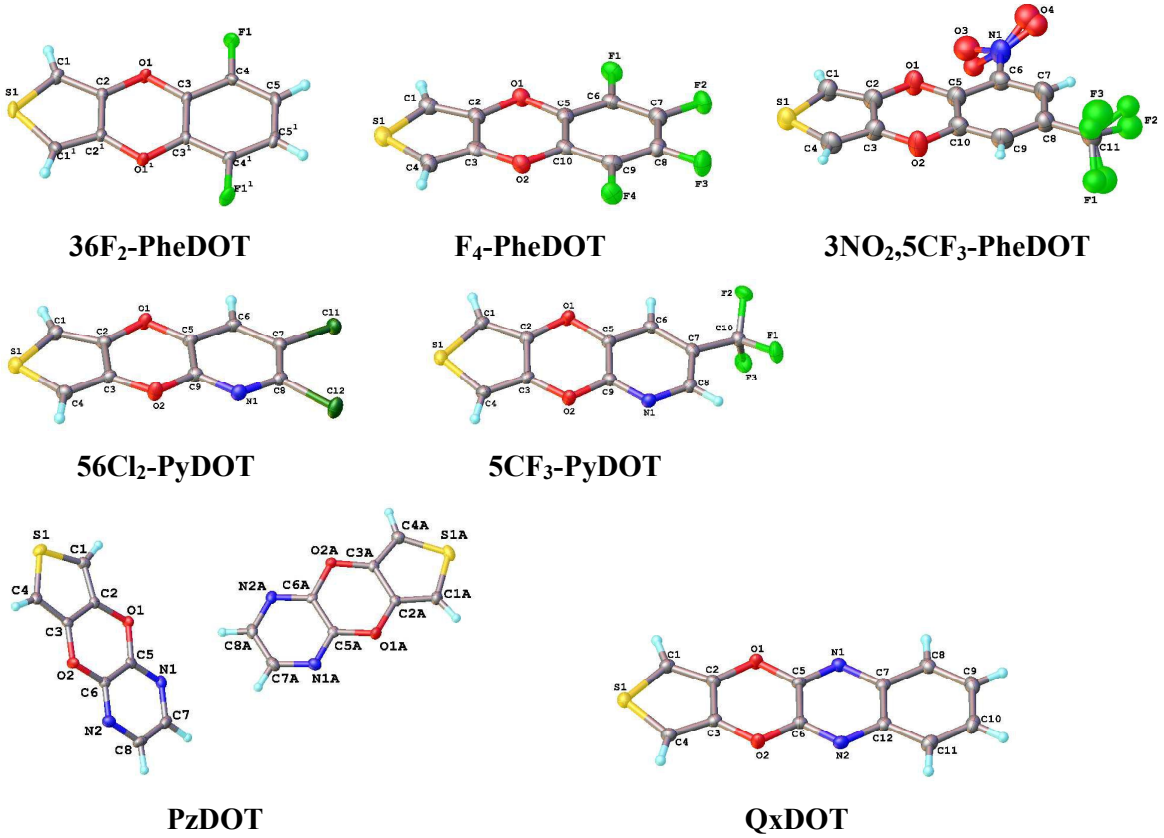

Figure 1. Molecular structures of **36F$_2$-PheDOT, F$_4$-PheDOT, 3NO$_2$,5CF$_3$-PheDOT, 56Cl$_2$-PyDOT, 5CF$_3$-PyDOT, PzDOT** and **QxDOT** by a single crystal X-ray diffractometry (**3NO$_2$,5CF$_3$-PheDOT** showed some disorder of NO_2/CF_3 groups in a crystal and **PzDOT** contains two independent molecules in a unit cell).

The presence of bulky EWG groups in the phenyl ring (especially, nitrogroup's oxygen atoms that are stronger acceptors of hydrogen bonds than heterocyclic oxygens), drastically change the packing motif. Instead of aromatic stacks, linked by CH···O interactions, the packing of

View Article Online
DOI: 10.1039/C7TC05227H

3NO$_2$,5CF$_3$-PheDOT molecules is dominated by C(thiophene)–H···O(nitro) and C–F···O contacts. The planar moieties are barely overlapped and adjacent layers are shifted relatively to each other forming a step-like arrangement in order to accommodate the bulky substituents.

The structure **PzDOT** contains two virtually identical independent molecules. These two molecules form two separate layers with a different orientation relatively to the crystallographic *a*-axis. The molecules are linked in layers by π···π interactions between the dioxythiophene fragments of adjacent molecules and by C(Ph)–H···N contacts. A variety of potential acceptors of hydrogen bonds in this molecule makes the pattern of intermolecular interactions quite complex. Both independent molecules are involved in a number of C(thiophene)–H···N and C(thiophene)–H···S interactions that connect the molecules of different layers into a 3D-network. Interestingly, the C(thiophene)–H···O interactions, which are present in all other structures, are not present in structure **PzDOT**.

The general packing motif of **56Cl$_2$-PyDOT** is similar: the chains of the molecules are linked by π···π interactions into layers. The peculiarity of the structure is the bonding between the molecules in the layer. Double C(thiophene)–H···N contacts are alternate with a combination of a pair of C(Py)–H···O interactions with another pair of C(thiophene)–H···Cl contacts. Weak Cl···Cl (and, probably, Cl···S) interactions exist between the layers.

The C(thiophene)–H···O and C(Py)···H···N interactions in **5CF$_3$-PyDOT** are far from being linear - the C–H···X angles are about 135°. Such deviation from linearity is apparently caused by the presence of the non-planar CF$_3$ substituent, similarly to the structure of **3NO$_2$,5CF$_3$-PheDOT**. The packing motif of **5CF$_3$-PyDOT** is probably better described as layers of shifted stacks. No apparent direction-specific inter-layer contacts can be found in the structure and the layers interdigitate by terminal CF$_3$ groups.

The extended polycyclic structure of **OxDOT** augments the formation of stacks in the crystal. Slightly shifted stacks are linked together in layers by pairs of bifurcated C(thiophene)–H···N,O contacts. C(Ph)–H···S contacts exist between the layers.

Generally, the packing of **PheDOT** derivatives is characterized by the presence of aromatic stacks (except for the cases, where the benzene ring is carrying non-planar groups (**3NO$_2$,5CF$_3$-PheDOT** and **5CF$_3$-PyDOT**) that are arranged in layers. The thiophene CH groups are the most active in the formation of weak C–H···X contacts that mainly determine the mutual arrangement of stacks within layers and orientation of the layers. It should be noted that the relative importance of the mentioned interactions and their role in the formation of crystal structures is impossible to estimate properly without calculations of pair-wise energies of intermolecular interactions. The geometrical parameters of intermolecular contacts alone cannot provide accurate description of packing motifs dominated by weak/non-directional interactions. For example, the chains of

Published on 03 January 2018. Downloaded by McGill University on 03/01/2018 15:18:04.
Journal of Materials Chemistry C Accepted Manuscript

View Article Online
DOI: 10.1039/C7TC05227H

molecules belonging to adjacent stacks may also be regarded as a basic motif of described structures.

Computational Studies

We have studied the geometries and the electronic structures of conjugated oligomers and polymers derived from synthesized **ArDOT** monomers by the density functional theory (DFT) method at the B3LYP/6-31G(d) level of theory in the gas phase. The structures of the dimers **(ArDOT)$_2$** optimized at B3LYP/6-31G(d) level have been used for calculations of the polymers by periodic boundary conditions (PBC) method at the same level of theory.[28] Apart from synthesized **ArDOTs**, several other related molecules have also been included into these calculations to obtain a more comprehensive picture of the influence of the side arylenedioxy fragments on the structure, orbital energies and the band gaps of the polymers (namely, **4MeO-PheDOT, 4Me-PheDOT**,[21a] **4F-PheDOT**, **NaphDOT(2,3)**[17] and **PyDOT**).

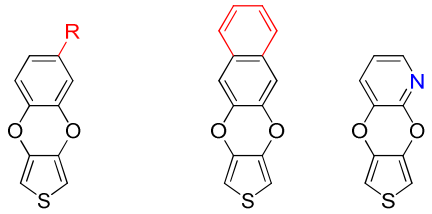

4MeO-PheDOT, R = MeO **NaphDOT(2,3)** **PyDOT**
4Me-PheDOT, R = Me
4F-PheDOT, R = F

The optimized geometries of **(ArDOT)$_n$** oligomers adopt an *anti* conformation of the adjacent monomer units and in the absence of steric repulsion between the side fragments in the monomer units (that are on the same side of the backbone[29]) DFT calculations give planar oligomer chains (Figure 2a) with short S···O contacts between the thiophene sulphur atoms and dioxine oxygen atoms (see below for more details). Small steric repulsions between the fluorine atoms in **(F$_4$-PheDOT)$_n$** makes the oligomer backbone slightly twisted (average dihedral angles ~6.4 ^{o}), adopting a spiral conformation (Figure 2b), although this small twisting weakly effects the total energies or frontier orbital energies of the oligomers.[30] So, we have compared an evolution of the HOMO and LUMO (highest occupied and lowest unoccupied molecular orbitals) energies and the HOMO–LUMO energy gaps (ΔE_{HL}) for planar **(PheDOT)$_n$** and spiral **(F$_4$-PheDOT)$_n$** with an increase of the main chain length "n" of the oligomers.

Chain length dependences of the HOMO, LUMO and ΔE_{HL}, when plotted versus the reciprocal number of repeating units (1/n), are linear for shorter oligomers (n ~3–10) with deviation from the linearity and "saturation" for longer oligomers chains, as is commonly observed for π-conjugated oligomers (Figures S5, S6, S8a and Table S5 in ESI).[31] This results in extrapolated (to 1/n = 0, i.e. n

Published on 03 January 2018. Downloaded by McGill University on 03/01/2018 15:18:04.
Journal of Materials Chemistry C Accepted Manuscript

View Article Online
DOI: 10.1039/C7TC05227H

Published on 03 January 2018. Downloaded by McGill University on 03/01/2018 15:18:04.

= ∞) energy levels and the energy gaps that are substantially different (by ca 0.2 eV) from those calculated for these polymers by PBC method (Figures S6 and S8a in ESI). Using a function $1/(n+0.1n^2)$ that takes into account quadratic dependence on the chain length for longer oligomers[32,33] gives excellent linear dependences (Figure 3 and Figures S7, S8b in ESI). The HOMO, LUMO and ΔE_{HL} energies extrapolated to n = ∞ nicely coincide with the highest occupied / lowest unoccupied crystal orbital energies (HOCO / LUCO) and the band gaps (E_g) for polymers calculated by PBC (deviations are ~5–21 meV only, Figure S7 in ESI).

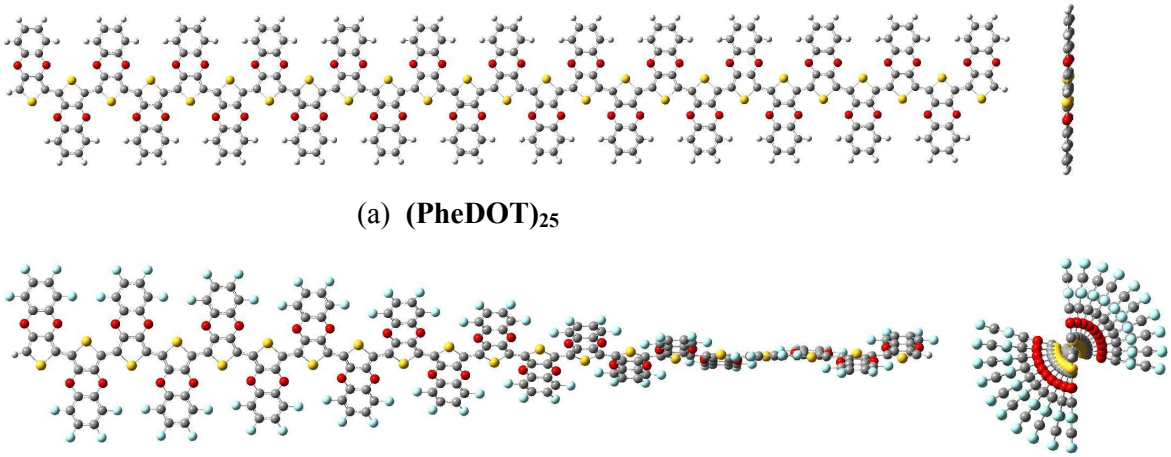

(a) **(PheDOT)$_{25}$**

(b) **(F$_4$-PheDOT)$_{20}$**

Figure 2. B3LYP/6-31G(d) optimized structures of (a) **(PheDOT)$_{25}$** and (b) **(F$_4$-PheDOT)$_{20}$**. Left structures – views perpendicular to the chain, right structures – views along the chain. Average dihedral angles / S···O distances between the adjacent monomer units are 0.0 º / 2.947 Å [**(PheDOT)$_{25}$**] and 6.4 º / 2.948 Å [**(F$_4$-PheDOT)$_{20}$**].

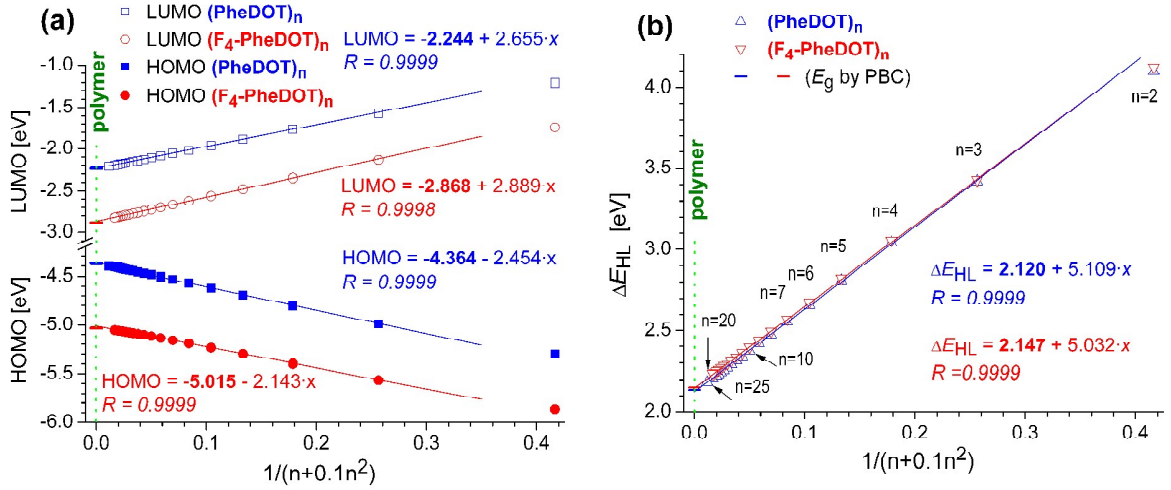

Figure 3. Chain length dependences of (a) HOMO and LUMO energies and (b) HOMO–LUMO energy gaps, ΔE_{HL}, for B3LYP/6-31G(d) optimized geometries of **(PheDOT)$_n$** and **(F$_4$-PheDOT)$_n$** oligomers, plotted as a function of an empirical parameter $1/(n + 0.1n^2)$. Symbols ▬ and ▬ correspond to the energies (HOCO, LUCO, E_g) for polymers calculated by PBC.

Journal of Materials Chemistry C Accepted Manuscript

View Article Online
DOI: 10.1039/C7TC05227H

Published on 03 January 2018. Downloaded by McGill University on 03/01/2018 15:18:04.

Considering excellent coincidence between the oligomeric approach [linear fitting vs $1/(n + 0.1n^2)$] and less time-consuming PBC method, further calculations of the energy levels and the band gaps for polymers have been performed by PBC using the optimized dimers as the unit cells (Figures S9, S10 and Table S6, S7 in ESI). For **p[ArDOTs]** without substantial steric repulsion in the side groups,[29] planarization of the backbone is facilitated by attractive interactions between the thiophene sulphur atoms and oxygen atoms of the dioxine ring of the neighboring monomer units. This is manifested by shortening interatomic S···O distances, which for the studied polymers are in the range of ca. 2.9–3.0 Å (see Table S8 in ESI),[34] i.e. substantially lower than the sum of van der Waals radii for sulphur and oxygen (1.80 + 1.52 = 3.32 Å). They are close to the experimental S···O distances from a single crystal X-ray diffraction structures of planar EDOT–EDOT (2.91–2.93 Å),[12] EDOT–thiophene (2.96 Å, 3.02 Å),[13] and EDOT–thieno[3,2-*b*]thiophene oligomers (2.87 Å)[14] where non-covalent S···O interactions is also supposed to be an origin of planarization of these systems.[35]

The energy levels calculated by PBC for the optimized geometries of the polymers, i.e. the highest occupied and lowest unoccupied crystal orbitals (HOCO and LUCO) and the band gaps (E_g) are presented in Figure 4.[36] DFT calculations show that functionalization of **PheDOT** at the benzene ring efficiently tune the orbital energy levels of the polymers. Thus, for **p[EWG-PheDOT]** polymers (first letter "**p**" designates the polymer), electron-withdrawing groups decrease the HOCO energy levels by up to 1.64 eV, from –4.374 eV for **p[PheDOT]** to –6.017 eV for **p[45(CN)$_2$-PheDOT]** (Figure 4a and Table S7 in ESI). An intriguing feature found from these calculations is that LUCO energy levels are decreased by the near the same magnitude (from –2.239 eV to –3.847 eV, respectively). As a result, the band gaps of the polymers remains almost the same (with variations of less than 0.05 eV) and for all **p[X-PheDOT]** polymers lie in the range of 2.123–2.170 eV (from **p[4Me-PheDOT]** to **p[45(CN)$_2$-PheDOT]**, Figure 4b and Table S7 in ESI)).[37] This is contrasting with the effect of an introduction of electron-withdrawing substituents in other classes of conjugated polymers when intramolecular donor-acceptor interaction is observed. For example, an introduction of cyano-groups into poly(*p*-phenylenevinylenes) and their analogs[38,39,40] or polythiophenes[38,41] (onto vinylene or thiophene moieties, respectively) result both in decrease of the LUMO energy levels and the band gaps contraction.

Thus, our results demonstrate that structural variations at the benzene ring in **p[PheDOT]** polymers might be an efficient way of controlling their frontier orbital energies and p-/n-doping abilities without affecting the band gaps of the polymers. These findings could also be exploited in the design of novel **PheDOT**-based copolymers, for which the fine tuning of their energy levels would be facilitated by functionalization of the **PheDOT** moieties at the benzene ring.

Journal of Materials Chemistry C Accepted Manuscript

View Article Online
DOI: 10.1039/C7TC05227H

Published on 03 January 2018. Downloaded by McGill University on 03/01/2018 15:18:04.

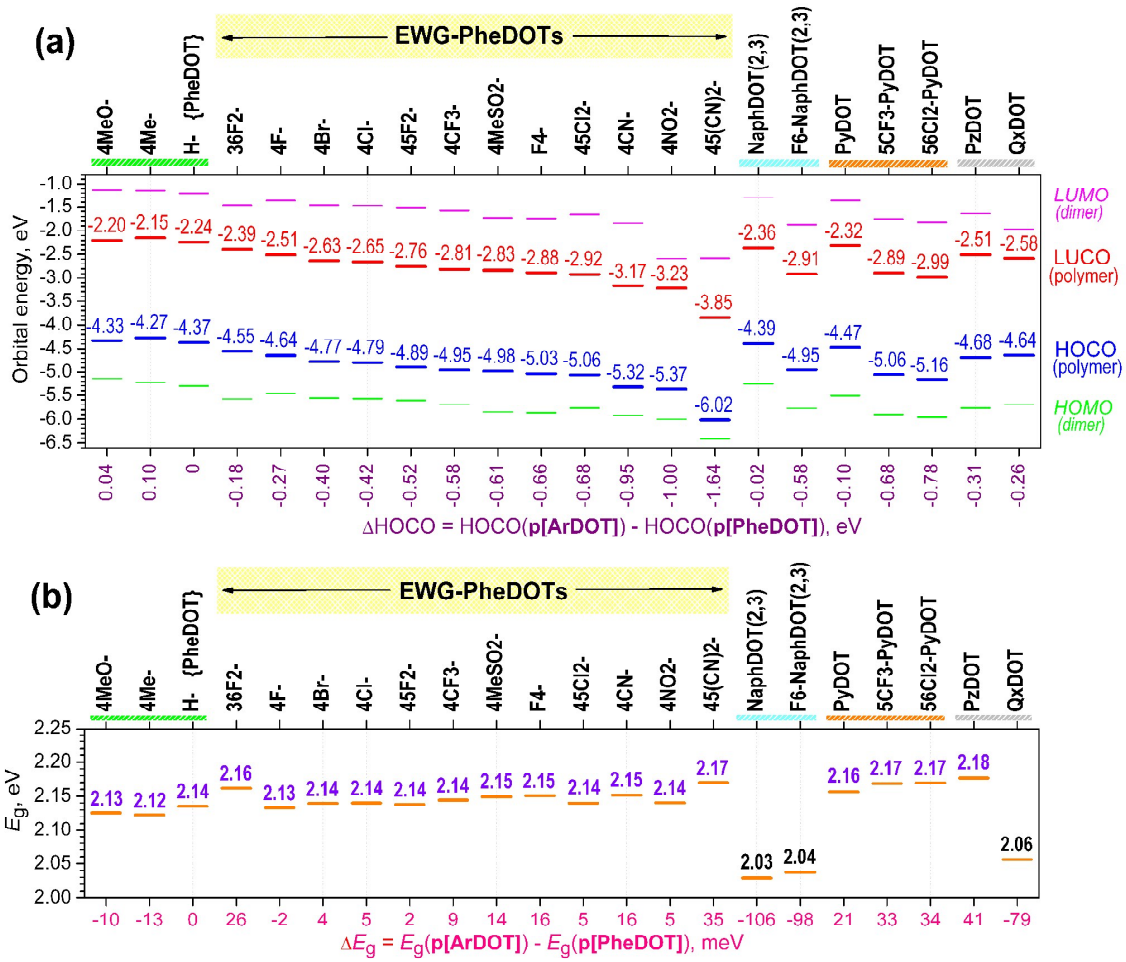

Figure 4. DFT B3LYP/6-31G(d) calculations in a gas phase (by PBC for polymers): (a) frontier orbital energies of **p[ArDOT]** polymers (HOCO and LUCO) and **(ArDOT)$_2$** dimers (HOMO and LUMO); bottom scale shows HOCO of **p[ArDOTs]** versus HOCO of **p[PheDOT];** (b) band gaps of **p[ArDOT]** polymers, E_g = LUCO – HOCO; bottom axis shows E_g of **p[ArDOTs]** versus E_g of **p[PheDOT]**.

Although the side benzene ring in **p[PheDOTs]** is not in direct conjugation with thiophene π-system, the resonance (and inductive) effects of the substituents in positions 4,5 of the benzene ring involving the oxygen atom of the dioxine ring strongly effect on the polymer backbone. This explains the efficient tuning of the frontier orbital energy levels of polymers (both HOMO and LUMO are on the main chain of the polymers). At the same time, the degree of this influence is incredibly high. For comparison: an attachment of the cyanogroups onto the main chain vinylene fragments of (2,7-carbazolylenevinylene)–(*p*-phenylenevinylene) copolymer decreases the LUMO energy by 0.62 eV (with a band gap contraction of 0.10 eV).[39] The effect of an attachment of one or two cyano-groups to the side benzene moiety of **PheDOT** (which are far from the main polymer chain and separated from it by the dioxine ring) is even more pronounced: in the series of **p[PheDOT] → p[4CN-PheDOT] → p[45(CN)$_2$-PheDOTs]**, the calculated LUCO are decreased by 0.93 eV and 0.68 eV, respectively (Figure 4a).

Journal of Materials Chemistry C Accepted Manuscript

View Article Online
DOI: 10.1039/C7TC05227H

Electron deficient nitrogen atoms in the side aromatic ring, i.e. pyridine and pyrazine, also lead to decrease in both the HOCO and LUCO energies (for **p[PyDOT**] and **p[PzDOT]**, decreases in HOCO/LUCO energies versus those in **p[PheDOT]** are 0.097/0.086 eV and 0.310/0.268 eV, respectively; Figure 4 and Table S7 in ESI). Again, the band gaps are only weakly affected by these structural changes: E_g = 2.135 eV (**p[PheDOT]**), 2.156 eV (**p[PyDOT]**), 2.177 eV (**p[PzDOT]**). On the other hand, an expanded conjugation at the side moiety by an additional annulated benzene ring (cf. **p[NaphDOT(2,3)]** and **p[F_6-NaphDOT(2,3)]** vs **p[PheDOT]** and **p[QxDOT]** vs **p[PzDOT]**) leads to more pronounced decrease in the band gaps by 79–106 meV to E_g ~ 2.029–2.056 eV (Figure 4 and Table S7 in ESI). It was recently demonstrated by computational methods that an extension of conjugation into the second dimension leads to materials with smaller band gaps compared to parent 1D polymers.[42]

Electrochemistry and Vis-NIR absorption spectroscopy

To confirm experimentally the predictions of DFT studies that functionalization of **p[PheDOTs]** at the benzene ring strongly effects on the HOMO/LUMO energies of the polymers while affording only minor changes in the band gaps, we have studied two polymers, **p[PheDOT]** and **p[4CF_3-PheDOT]**, by cyclic voltammetry and Vis-NIR electron absorption spectroscopy methods. The polymers were prepared by electrochemical polymerization of the corresponding monomers to form insoluble polymer films, which were deposited onto Pt disks (for cyclic voltammetry experiments (CV), Figure S11 in ESI) or onto ITO (indium tin oxide) glass substrates (for spectroscopic studies) from the monomer solutions in DCM under potentiodynamic conditions. Previously, we have shown that electropolymerization of **PheDOT** is more difficult compared to **EDOT** due to lower positive charge /spin densities at the position 2,5- of the thiophene, and requires high concentration of the monomer and proper choice of the solvents (works better in DCM).[16a] The selection of **4CF_3-PheDOT** as electron-deficient monomer, to compare it with **PheDOT**, was conditioned by DFT prediction of observable decrease of the HOMO energy level of its polymer (by 0.58 eV, Figure 4) but still straightforward electropolymerization to form smooth and stable polymer films (Figures S11d and S12b in ESI). The CV studies on the polymer films in 0.1 M Bu_4NPF_6 / acetonitrile demonstrated that both polymers are reversibly p-doped and show stable doping/dedoping on cycling (Figure 5a; see also Figure S12 in ESI). **p[4CF_3-PheDOT]** was oxidized (p-doped) at higher potential than **p[PheDOT]**, confirming its weaker electron donor ability (Figure 5a). Its oxidation onset potential (E_{ox}) was anodically shifted by 0.55 V (from –0.36 V to +0.19 V vs Fc/Fc^+ reference), which is in excellent agreement with DFT calculations (difference in HOCOs of **p[PheDOT]** and **p[4CF_3-PheDOT]** from DFT calculations is 0.58 V, Figure 4a). For **p[4CF_3-PheDOT]**, we observed electrochemically irreversible n-doping at E_{red} = –1.57 V (Figure 5a). From

Published on 03 January 2018. Downloaded by McGill University on 03/01/2018 15:18:04.
Journal of Materials Chemistry C Accepted Manuscript

View Article Online
DOI: 10.1039/C7TC05227H

the onsets of p- and n-doping processes, we estimated the band gap of this polymer as E_g^{CV} = 1.76 eV, which is close to estimation of E_g ~ 1.8 eV for **p[PheDOT]**.[17]

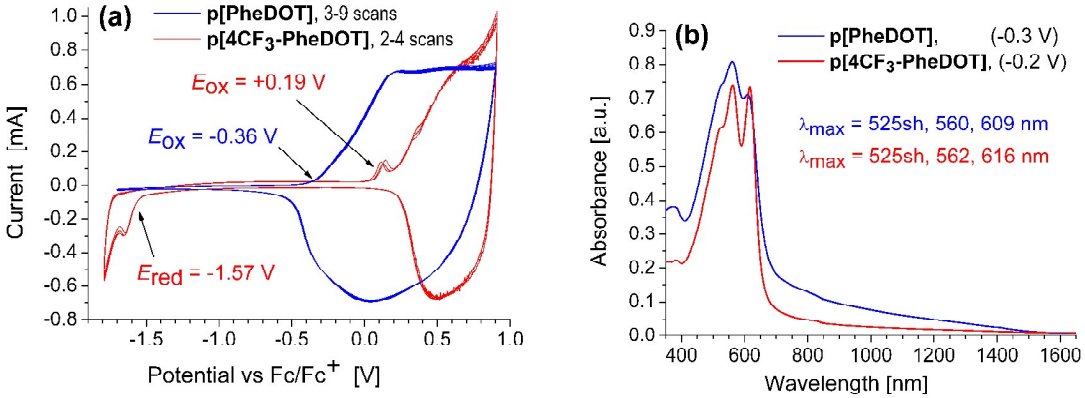

Figure 5. Comparison of properties of **p[PheDOT]** and **p[4CF$_3$-PheDOT]** in films: (a) cyclic voltammograms of polymer films (7 and 3 consecutive scans, respectively, are shown) in acetonitrile, 0.1 M Bu_4NPF_6, scan rate 100 mV/s (current for **p[4CF$_3$-PheDOT]** has been multiplied by a factor of ×6.5 for convenience of comparison); (b) Vis-NIR electron absorption spectra of **p[PheDOT]** and **p[4CF$_3$-PheDOT]** polymer films (electrodeposited on ITO glass substrate) in the undoped state; 0.1 M Bu_4NPF_6 / acetonitrile; potentials are vs. Ag wire reference electrode.

Vis-NIR electron absorption spectra of **p[PheDOT]** and **p[4CF$_3$-PheDOT]** polymer films (deposited on ITO glass substrates) in undoped states were recorded in a spectroelectrochemical setup (SEC) with 0.1 M Bu_4NPF_6/acetonitrile, with applied negative potentials of –(0.2–0.3) V, which correspond to the neutral states of the polymers. The results shown in Figure 5b demonstrate that the Vis-NIR spectra of two polymers near coincide (both by the maxima of absorption and by the red edge of the longest absorption band corresponding to the optical energy gaps of the polymers). The optical energy gaps of **p[PheDOT]** and **p[4CF$_3$-PheDOT]**, estimated from their absorption onsets were found to be very similar, 1.83 eV (676 nm) and 1.87 eV (662 nm), respectively.[43] These results confirm that the band gap of **p[PheDOT]** is unaffected by introduction of electron-withdrawing CF_3 groups and confirm the results of our DFT calculations and CV experiments. As the synthesized **ArDOT** monomers (Table 1) do not contain long-chain solubilizing groups, their polymers are expected to be insoluble materials (similar to **p[PheDOT]** and **p[4CF$_3$-PheDOT]**) that limits further expansion of these studies to chemically prepared polymers and requires synthesis of corresponding **EWG-PheDOT** analogs additionally decorated with linear or branched solubilizing groups.

Conclusions

We have reported a facile and efficient one-pot microwave-assisted method of synthesis of 3,4-phenylenedioxythiophene (**PheDOT**) derivatives substituted with electron-withdrawing groups at

Published on 03 January 2018. Downloaded by McGill University on 03/01/2018 15:18:04.
Journal of Materials Chemistry C Accepted Manuscript

View Article Online
DOI: 10.1039/C7TC05227H

the benzene rings and their analogs (with expanded side π-system or with heteroaromatic rings) by reaction of 2,5-dialkoxycarbonyl-3,4-dihydroxythiophenes with electrophilic aromatic/heteroaromatic compounds in dipolar aprotic solvents under basic conditions in the presence of lithium bromide at high temperature. This general method provides an easy access to a wide range of novel **ArDOT** derivatives as attractive building blocks for conjugated molecular and polymeric materials for organic electronic applications, which are inaccessible by other current methods. The structures of eight selected compounds have been established by single crystal X-ray diffraction crystallography, shedding light on the molecular structure and crystal packing of these materials.

DFT calculations predict that the HOMO and LUMO energies for conjugated polymers derived from these monomers can be efficiently tuned by more than 1.6 eV, whereas the band gaps are expected to be near-identical for all of the studied polymers (variations in ΔE_{HL} are ≤ 0.05 eV). This paves a way for efficient tuning of the HOMO energy levels of thiophene-based polymers in a wide range of over 1–1.5 eV without altering their band gaps.

These DFT predictions were further confirmed by cyclic voltammetry and Vis-NIR electron absorption spectroscopy experiments: an anodic shift by 0.55 V for p-doping of **p[4CF$_3$-PheDOT]** compared to **p[PheDOT]** corresponds well to the predicted difference in their HOCO orbital energies (0.58 eV), while good coincidence of their electron absorption spectra (λ_{max} = 616 and 609 nm, E_{onset} = 1.83 and 1.87 eV, respectively) is in excellent agreement with very small changes in the DFT calculated band gaps (E_g = 2.144 and 2.135 eV, respectively). On the other hand, an expansion of the π-system in the side moieties leads to the band gap contraction of the resulting polymers (an additional benzene ring decreases the E_g by ca. 0.1 eV to ≈ 2.03–2.06 eV).

The reported novel **ArDOT** molecules represent an interesting class of thiophene monomers for the design of conjugated homopolymers, with the ability to fine tune the optoelectronic properties of materials by side-chain functionalization. New **ArDOTs** also represent fascinating building blocks for incorporation into conjugated systems, including small conjugated molecules, cooligomers and copolymers, for design novel materials for organic electronic applications. The work on the synthesis of soluble conjugated oligomers and polymers/copolymers based on these **ArDOTs** as materials for electrochromic, field-effect transistor and photovoltaic applications is in progress and the results will be reported elsewhere.

Experimental

Microwave-assisted synthesis of EWG-substituted ArDOTs. General procedure. Diethyl 3,4-dihydroxy-2,5-thiophenedicarboxylate (**1**) (1.000 g, 3.84 mmol, 1.00 eq.), K_2CO_3 (531 mg, 3.84 mmol, 1.00 eq.), electrophilic reagent **2–21** (1.0–1.3 eq.) and LiBr (210 mg, 2.42 mmol, 0.6 eq.)

Published on 03 January 2018. Downloaded by McGill University on 03/01/2018 15:18:04.
Journal of Materials Chemistry C Accepted Manuscript

View Article Online
DOI: 10.1039/C7TC05227H

were combined in a 35 mL microwave tube, and DMA (10–12 mL) was added. The tube was sealed and bubbled with N_2 under stirring for ca. 5 min. The mixture was then heated with stirring in a microwave reactor (initially for 5–20 min at 80–100°C (for dissolution and homogenization of the reaction mixture), then at 150–200 ^{o}C for 0.5–1.5 h; see Table 1 in the paper). After cooling to room temperature, the dark brown mixture was diluted with water (100 mL) and extracted with DCM (3 × 100 mL). The combined organic layers were washed with water (2–3 times), dried over $MgSO_4$, and the solvent was evaporated. The residue was purified by column chromatography on silica gel with an appropriate solvent as an eluent (PE, toluene, DCM, PE/DCM or PE/EA). For full details on the experimental procedures and characterizations of novel compounds see ESI.

Conflict of Interests

There are no conflicts of interests to declare.

Acknowledgements

We thank the LCRI (Low Carbon Research Institute) programme for funding (Welsh European Funding Office, Grant WEFO-80366). M.P.K. thanks LCRI and Bangor University for a postdoctoral fellowship. E.L.K. thanks Ural Federal University for financial support of her visits to I.F.P. at Bangor University. We thank Robert Beaumont for participation in electrochemical experiments.

References and Notes

1 I. F. Perepichka and D. F. Perepichka (Eds), *Handbook of Thiophene-Based Materials: Applications in Organic Electronics and Photonics*, 2009, John Wiley & Sons, 865 pp.

2 (a) A. Mishra, C.-Q. Ma and P. Bäuerle, *Chem. Rev.*, 2009, **109**, 1141–1276. (b) M. E. Cinar and T. Ozturk, *Chem. Rev.*, 2015, **115**, 3036−3140. (c) D. Fichou, *J. Mater. Chem.*, 2000, **10**, 571–588. (d) T. Otsubo, Y. Aso and K. Takimiya, *J. Mater. Chem.*, 2002, **12**, 2565–2575. (e) S. C. Rasmussen and S. J. Evenson, *Progr. Polym. Sci.*, 2013, **38**, 1773–1804.

3 (a) I. F. Perepichka, D. F. Perepichka, H. Meng and F. Wudl, *Adv. Mater.*, 2005, **17**, 2281–2305. (b) D. F. Perepichka, I. F. Perepichka, H. Meng and F. Wudl, in: *Organic Light-Emitting Materials and Devices*, Z. Li, H. Meng (Eds.), CRC Press: Boca Raton, FL, 2007, Chapter 2, pp 45–293.

4 (a) K.-J. Baeg, M. Caironi and Y.-Y. Noh, *Adv. Mater.*, 2013, **25**, 4210–4244. (b) R. P. Ortiz, H. Yan, A. Facchetti and T. J. Marks, *Materials*, 2010, **3**, 1533–1558. (c) A. Salleo, *Mater. Today*, 2007, **10**, 38–45. (d) C. B. Nielsen and I. McCulloch, *Prog. Polym. Sci.*, 2013, **38**, 2053–2069.

5 (a) A. Mishra and P. Bäuerle, *Angew. Chem. Int. Ed.*, 2012, **51**, 2020–2067. (b) J. Roncali, *Chem. Soc. Rev.*, 2005, **34**, 483–495. (c) E. Bundgaard and F. C. Krebs, *Sol. Energy Mater. Sol. Cells*, 2007, **91**, 954–985.

6 (a) P. M. Beaujuge and J. R. Reynolds, *Chem. Rev.*, 2010, **110**, 268–320. (b) L. Beverina, G. A. Pagani and M. Sassi, *Chem. Commun.*, 2014, **50**, 5413–5430. (c) M. Zhu, W. Li, P. Xu, J. Shi, S. Shao, X. Zhu, Y. Guo, Y. He, Z. Hu, H. Yu, Y. Zhu, I. F. Perepichka and H. Meng, *Science China Chem.*, 2017, **60**, 63–76.

7 (a) T. J. Wigglesworth, A. J. Myles and N. R. Branda, *Eur. J. Org. Chem.*, 2005, 1233–1238. (b) C. Yun, J. You, J. Kim, J. Huh and E. Kim, *J. Photochem. Photobiol. C*, 2009, **10**, 111–129. (c) M. Irie, *Chem. Rev.*, 2000, **100**, 1685–1716. (d) H. Nishi, T. Namari and S. Kobatake, *J. Mater. Chem.*, 2011, **21**, 17249–17258.

Published on 03 January 2018. Downloaded by McGill University on 03/01/2018 15:18:04.

Journal of Materials Chemistry C Accepted Manuscript

View Article Online
DOI: 10.1039/C7TC05227H

Published on 03 January 2018. Downloaded by McGill University on 03/01/2018 15:18:04.

Journal of Materials Chemistry C Accepted Manuscript

8 (a) J. F. Mike and J. L. Lutkenhaus, J. *Polym. Sci. B*, 2013, **51**, 468–480. (b) G. A. Snooka, P. Kaob and A. S. Best, *J. Power Sources*, 2011, **196**, 1–12.

9 (a) M. Leclerc, *Adv. Mater.*, 1999, **11**, 1491–1498. (b) I. F. Perepichka, M. Besbes, E. Levillain, M. Sallé and J. Roncali, *Chem. Mater.,* **2002,** *14,* 449–457.

10 (a) H.-A. Ho, M. Béra-Abérem and M. Leclerc, *Chem. Eur. J.*, 2005, **11**, 1718–1724. (b) M. Béra Abérem, A. Najari, H.-A. Ho, J.-F. Gravel, P. Nobert, D. Boudreau and M. Leclerc, *Adv. Mater.*, 2006, **18**, 2703–2707. (c) G. Barbarella, M. Zambianchi, A. Ventola, E. Fabiano, F. D. Sala, G. Gigli, M. Anni, A. Bolognesi, L. Polito, M. Naldi and M. Capobianco, *Bioconjugate Chem.*, 2006, **17**, 58–67.

11 (a) L. "Bert" Groenendaal, F. Jonas, D. Freitag, H. Pielartzik and J. R. Reynolds, *Adv. Mater.,* 2000, **12**, 481–494; (b) S. Kirchmeyer and K. Reuter, *J. Mater. Chem.*, 2005, **15**, 2077–2088.

12 (a) J.-M. Raimundo, P. Blanchard, P. Frère, N. Mercier, I. Ledoux-Rak, R. Hierle and J. Roncali, *Tetrahedron Lett.*, 2001, **42**, 1507–1510. (b) P. Leriche, M. Turbiez, V. Monroche, P. Frère, P. Blanchard, P. J. Skabara and J. Roncali, *Tetrahedron Lett.*, 2003, **44**, 649–652. (c) M. Turbiez, P. Frère and J. Roncali, *J. Org. Chem.*, 2003, **68**, 5357–5360. (d) K. M. N. de Silva, E. Hwang, W. K. Serem, F. R. Fronczek, J. C. Garno and E. E. Nesterov, *ACS Appl. Mater. Interfaces*, 2012, **4**, 5430–5441.

13 M. Turbiez, P. Frère, M. Allain, C. Videlot, J. Ackermann and J. Roncali, *Chem. Eur. J.*, 2005, **11**, 3742–3752.

14 G. J. McEntee, P. J. Skabara, F. Vilela, S. Tierney, I. D. W. Samuel, S. Gambino, S. J. Coles, M. B. Hursthouse, R. W. Harrington and W. Clegg, *Chem. Mater.*, 2010, **22**, 3000–3008.

15 J. Roncali, P. Blanchard and P. Frère, *J. Mater. Chem.*, 2005, **15**, 1589–1610.

16 (a) S. Roquet, P. Leriche, I. Perepichka, B. Jousselme, E. Levillain, P. Frère and J. Roncali, *J. Mater. Chem.*, 2004, **14**, 1396–1400; (b) I. F. Perepichka, S. Roquet, P. Leriche, J.-M. Raimundo, P. Frère and J. Roncali, *Chem. Eur. J.*, 2006, **12**, 2960–2966. (c) J. Storsberg, D. Schollmeyer and H. Ritter, *Chem. Lett.*, 2003, **32**, 140–141.

17 E. Poverenov, Y. Sheynin, N. Zamoshchik, A. Patra, G. Leitus, I. F. Perepichka and M. Bendikov, *J. Mater. Chem.*, 2012, **22**, 14645–14655.

18 C. R. G. Grenier, W. Pisula, T. J. Joncheray, K. Müllen and J. R. Reynolds, *Angew. Chem. Int. Ed.*, 2007, **46**, 714–717.

19 (a) K. Shibasaki, M. Watanabe and M. Kijima, *Synth. Metals*, 2015, **205**, 18–22; (b) K. Shibasaki, T. Yasuda, and M. Kijima, *Electrochemistry*, 2017, **85**, 241–244.

20 J. Chen, B.-X. Chen, F.-S. Zhang, H.-J. Yu, S. Ma, D.-B. Kuang, G. Shao and C.-Y. Su, *Chem. Asian J.*, 2016, **11**, 1043–1049.

21 (a) C. R. Szczepanski, I. M'Jid, T. Darmanin, G. Godeau and F. Guittard, *J. Mater. Chem. A*, 2016, **4**, 17308–17323; (b) T. Darmanin and F. Guittard, *J. Mater. Chem. A*, 2016, **4**, 3197–3203. (c) T. Darmanin, J.-P. Laugier, F. Orange and F. Guittard, *J. Colloid Interf. Sci.,* 2016, **466**, 413–424.

22 Reaction of 4,5-dibromo- and 4,5-dichlorocatechols with 3,4-dimethoxythiophene gave corresponding **45Br$_2$-PheDOT** and **45Cl$_2$-PheDOTs** with low yields of only 1.3% and 5%, respectively (M. A. Krompiec, S. N. Baxter and I. F. Perepichka, unpublished results), compared to the yield of 20–25% for unsubstituted **PheDOT** [Ref. 16a].

23 M. V. Lakshmikantham and M. P. Cava, *J. Org. Chem.*, 1976, **41**, 882.

24 (a) K. Zong, L. Madrigal, L. "Bert" Groenendaal and J. R. Reynolds, *Chem. Commun.*, 2002, 2498–2499. (b) Z. Xu, J.-H. Kang, F. Wanga, S.-M. Paek, S.-J. Hwang, Y. Kim, S.-J. Kim, J.-H. Choy and J. Yoon, *Tetrahedron Lett.*, 2011, **52**, 2823–2825.

25 (a) S. Akoudad, P. Frère, N. Mercier and J. Roncali, *J. Org. Chem.*, 1999**, 64***,* 4267–4272. (b) D. M. Welsh, A. Kumar, E. W. Meijer and J. R. Reynolds, *Adv. Mater.*, 1999, **11**, 1379–1381.

26 (a) P. A. Cisneros-Pérez, B. A. Frontana-Uribe, D. Martínez-Otero and E. Cuevas-Yáñez, *Tetrahedron Lett.*, 2016, **57**, 5089–5093. (b) P. A. Cisneros-Pérez, D. Martínez-Otero, E. Cuevas-Yánez and B. A. Uribe-Frontana, *Synth. Commun.*, 2014**, 44**, 222–230.

27 A "dithio-analog" of **QxDOT**, thieno[3',4':5,6][1,4]dithiino[2,3-*b*]quinoxaline, was reported previously to be prepared by different synthetic route and showed (in contrast to **QxDOT**, see X-ray crystallography section below) non planar structure: P. J. Skabara, R. Berridge, K. Prescott, L. M. Goldenberg, E. Ortí, R. Viruela, R. Pou-Amérigo, A. S. Batsanov, J. A. K. Howard, S. J. Coles and M. B. Hursthouse, *J. Mater. Chem.*, 2000, **10**, 2448–2457.

28 In PBC calculations of non-symmetrical **ArDOTs** from the dimers as unit cells, we used head-to-tail (HT) connectivity of the monomer units in all the cases. In an absence of steric repulsions between the side aromatic moieties, which are on the same side of the polymer backbone (as in the case of **p[4R-PheDOTs]** and **p[5CF$_3$-PyDOT]**), the calculations of the polymers with HT and HH-TT (head-to-head / tail-to-tail) arrangement gave very close total energies (differences are 0.00 – 0.39 kcal/mol), as well as HOCO, LUCO and E_g (differences are 0 – 5

View Article Online
DOI: 10.1039/C7TC05227H

Published on 03 January 2018. Downloaded by McGill University on 03/01/2018 15:18:04.

meV) (Table S1 in ESI). Of course, these differences are substantially higher in the case of polymers with large steric repulsion between the side moieties, i.e. **p[3NO$_2$,5CF$_3$-PheDOT]**, **p[3NO$_2$,5CF$_3$-PheDOT]** and **p[F$_6$-NaphDOT(1,2)]**.

29 **(ArDOT)$_n$** oligomers with bulky side aryl groups, i.e. **Cl$_4$-PheDOT**, **3NO$_2$,5CF$_3$-PheDOT**, **3NO$_2$,5CF$_3$-PheDOT. F$_6$-NaphDOT(1,2)** and **F$_4$-BnDOT** showed substantial deviation from the planarity, with large dihedral angles between the adjacent **ArDOT** moieties and therefore they have not been used in further calculations.

30 For example, fully flat conformation of hexamer **(F$_4$-PheDOT)$_6$** has been calculated (local minimum, no frozen coordinates have been used) to have a total energy of 0.59 kcal/mol higher than that for the optimized spiral structure and very close frontier orbital energy levels: HOMO = –5.238 / –5.236eV, LUMO = –2.580 / 2.562 eV, ΔE_{HL} = 2.658 / 2.675 eV, for flat / spiral **(F$_4$-PheDOT)$_6$** optimized structures.

31 (a) J. Gierschner, J. Cornil and H.-J. Egelhaaf, *Adv. Mater.*, 2007, **19**, 173–191; (b) S. S. Zade, N. Zamoschik and M. Bendikov, *Acc. Chem. Res*., 2011, **44**, 14–24. (c) G. R. Hutchison, Y.-J. Zhao, B. Delley, A. J. Freeman, M. A. Ratner and T. J. Marks, *Phys. Rev. B,* 2003, **68**, 035204. (c) H. Meier, U. Stalmach and H. Kolshorn, *Acta Polymerica*, 1997, **48**, 379–384.

32 Several other empirical parameters (e.g $1/n^{0.7}$, $1/n^{1.5}$) have been used to obtain linear dependences of orbital energies and energy gaps: (a) S. S. Zade and M. Bendikov, *Chem. Eur. J.*, 2008, **14**, 6734–6741. (b) S. Shao, J. Shi, I. Murtaza, P. Xu, Y. He, S. Ghosh, X. Zhu, I. F. Perepichka and H. Meng, *Polym. Chem.*, 2017, **8**, 769–784. Non-linear fitting for longer oligomers was also exploited to adequately extrapolate the energies and energy gaps to n = ∞: (c) X.-H. Jin, D. Sheberla, L. J. W. Shimon and M. Bendikov, *J. Am. Chem. Soc.*, 2014, **136**, 2592−2601. (d) S. Sharma and M. Bendikov, *Chem. Eur. J.*, 2013, **19**, 13127–13139. (e) S. S. Zade and M. Bendikov, *J. Phys. Chem. C*, 2007, **111***,* 10662–10672. (f) S. S. Zade and M. Bendikov, *Org. Lett.*, 2006, **8**, 5243–5246.

33 An extrapolation of EDOT and PheDOT oligomers to the polymers limit (n = ∞) using different physical models was recently considered in: J. Torras, J. Casanovas and C. Alemán, *J. Phys. Chem. A*, 2012, **116**, 7571−7583.

34 Similar results have been obtained by us recently for calculations of EDOT–thieno[3,2-*b*]thiophene copolymers, see Ref. 32b.

35 Basing on the computational studies, Gierschner et al. assume that short S···O contacts in **EDOT** oligomers are non-bonding and vibronically resolved absorption/emission spectra of oligo-EDOTs (as opposite to non-resolved spectra of oligothiophenes) are not due to self-rigidification by attractive S···O interactions, but due to very similar out-of-plane modes in the electronic ground (S_0) and first excited (S_1) state, which exhibit surprisingly low frequencies: B. M. Medina, D. Wasserberg, S. C. J. Meskers, E. Mena-Osteritz, P. Bäuerle and J. Gierschner, *J. Phys. Chem. A,* 2008, **112,** 13282–13286.

36 In the case of monosubstituted non-symmetric **ArDOTs**, the polymer main chain can be arranged in HT (head-to-tail) and HH-TT (head-to-head / tail-to-tail) fashion. The total energies, HOCO, LUCO and E_g are almost the same for both regioisomers (Table S1 in ESI). The values reported in the paper are for HT-**p[R-ArDOT]** regiosomers.

37 The calculated band gap for **p[PheDOT]** (E_g = 2.135 eV, ΔE_{HL} = 2.120 eV) is ca. 0.3 eV higher than the experimental value for this polymer (1.8 eV [Ref. 17], 1.87 eV [this paper, see below]). However, it should be noted that the calculations have been performed for the isolated molecules in the gas phase and do not take into account the polarity of the environment and the solid state effect. Good correlations have been demonstrated between the experimental (cyclic voltammetry, Vis-NIR spectroscopy) and PBC/B3LYP/6-31G(d) calculated frontier orbital energy levels and band gaps for structurally related polythiophenes [Ref. 17], so changes in the HOMO, LUMO and E_g with the structural changes in **p[ArDOTs]** should be predicted by DFT with a high accuracy.

38 S. C. Moratti, R. Cervini, A. B. Holmes, D. R. Baigent, R. H. Friend, N. C. Greenham, J. Gruner and P. J. Hamer, *Synth. Metals,* 1995, **71**, 2117–2120.

39 J.-F. Morin, N. Drolet, Y. Tao and M. Leclerc, *Chem. Mater.*, 2004**, 16***,* 4619–4626.

40 (a) N. C. Greenham, S. C. Moratti, D. D. C. Bradley, R. H. Friend and A. B. Holmes, *Nature*, 1993, **365**, 628–630. (b) B. C. Thompson, Y.-G. Kim, T. D. McCarley and J. R. Reynolds, *J. Am. Chem. Soc.*, 2006, **128**, 12714–12725.

41 (a) A. E. Rudenko, P. P. Khlyabich and B. C. Thompson, *ACS Macro Lett.*. 2014, **3**, 387−392; (b) P. P. Khlyabich, A. E. Rudenko and B. C. Thompson, *J. Polym. Sci. A*, 2014, **52**, 1055–1058; (c) N. Hergué, C. Mallet, P. Frère, M. Allain and J. Roncali, *Macromolecules*, 2009, **42**, 5593–5599.

42 R. Gutzler and D. F. Perepichka, *J. Am. Chem. Soc.*, 2013, **135**, 16585−16594.

43 The tail absorption of **p[PheDOT]** in NIR region (900–1200 nm) is presumably due to trapped charges in the polymer as is sometimes observed for low band gap polymers. This might result in somewhat higher estimation of its band gap (see e.g. Ref 32b).

Journal of Materials Chemistry C Accepted Manuscript

Electronic Supplementary Material (ESI) for Journal of Materials Chemistry C.
This journal is © The Royal Society of Chemistry 2018

SUPPORTING INFORMATION

3,4-Phenylenedioxythiophenes (PheDOTs) functionalized with electron-withdrawing groups and their analogs for organic electronics. Remarkably efficient tuning the energy levels in flat conjugated polymers

Michal P. Krompiec,[a,‡] Sean N. Baxter,[a] Elena L. Klimareva,[a,b] Dmitry S. Yufit,[c] Daniel G. Congrave,[a] Thomas K. Britten[a] and Igor F. Perepichka[a]

[a] *School of Chemistry, Bangor University, Deiniol Road, Bangor LL57 2UW, UK*
[b] *Department of Organic Substances Technology, Ural Federal University, Ekaterinburg 620002, Russian Federation*
[c] *Department of Chemistry, Durham University, Durham DH1 3LE, UK*

*Corresponding author. Email: i.perepichka@bangor.ac.uk

CONTENTS

	page
Experimental part …….	S2
Materials ……...	S2
Instruments ……	S2
Computational methodology *(Table S1)* ……	S2
X-Ray crystallography …….	S4
Electrochemistry and Vis-NIR electron absorption spectroscopy of polymers	S4
Synthesis ……..	S5
(Tables S2, S3) ……..	S13, S14
UV-Vis spectra of ArDOT monomers *(Figures S1, S2)* …….	S21, S22
Crystal data and structure refinement parameters *(Table S4)* …….	S23
Molecular and crystal structures of compounds *(Figures S3 and S4)* ……..	S24, S27
Chain length dependence of HOMO, LUMO and ΔE_{HL} for ArDOT oligomers *(Figures S5–S8)* ……	S29–S33
Total energies, HOMO/LUMO and ΔE_{HL} for **(PheDOT)$_n$** and **(F$_4$-PheDOT)$_n$** oligomers by B3LYP/6-31G(d) *(Table S5)* ……	S34
HOMO, LUMO and ΔE_{HL} of dimers **(ArDOT)$_2$** by B3LYP/6-31G(d) *(Table S6)*	S35
HOCO, LUCO energy levels and the band gaps (E_g,) of **p[ArDOT]** polymers by PBC/B3LYP/6-31G(d) *(Table S7)* ……	S36
Short S···O contacts and selected bond distances in **p[ArDOTs]** by PBC/B3LYP/6-31G(d) *(Table S8)* …….	S37
Unit cells for the optimized structures of **p[Ar-PheDOT]** polymers calculated at PBC/B3LYP/6-31G(d) *(Figures S9, S10)* …….	S38
Cyclic voltammograms of **PheDOT** and **4CF$_3$-PheDOT**; electropolymerization of **PheDOT** and **4CF$_3$-PheDOT** *(Figure S11)* ……	S40
References ……	S41
Copies of ^{1}H, ^{13}C and ^{19}F NMR spectra of synthesized compounds ……	S42

Experimental Part

Materials

All starting materials were purchased from Aldrich, Fisher Scientific or Alfa Aesar and were used without further purification. Diethyl 3,4-dihydroxy-2,5-dicarboxylate (**1**) and dimethyl 3,4-dihydroxy-2,5-dicarboxylate (**27**) were synthesized according to the method described by Hinsberg[1] (syntheses by this protocol have also been described in later publications[2]). Disodium 2,5-bis(methoxycarbonyl)thiophene-3,4-bis(olate) (**26**) was obtained as an intermediate in synthesis of compound **27** by this method.

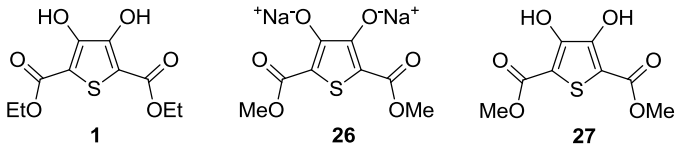

Instruments

^{1}H, ^{13}C, and ^{19}F NMR spectra were recorded using a Bruker Avance 400 instrument in $CDCl_3$. Tetramethylsilane (TMS) (δ_H , δ_C = 0.00 ppm) and C_6F_6 (δ_F = –163.0 ppm) were used as internal standards. For assigning H and C signals, DEPTQ and 2D NMR (^{1}H-^{1}H COSY, ^{13}C-^{1}H HSQC and HMBC spectroscopy have been used). Enumerations of H and C atoms used in description of ^{1}H and ^{13}C NMR spectra are shown below:

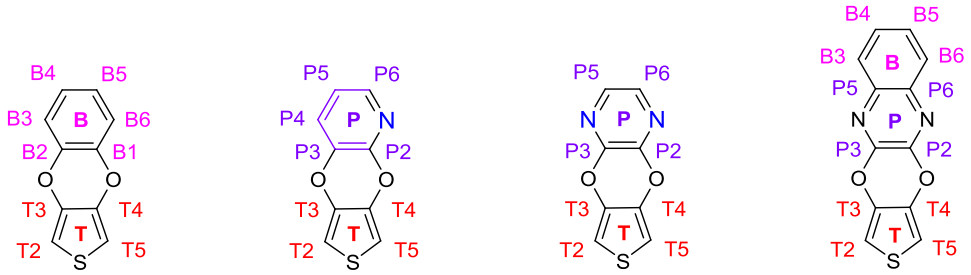

Electron impact mass spectra (positive mode) were recorded on a GC-MS system consisting of a HP 5890 gas chromatograph with a HP 8971 EI-MS detector, operating at 70KeV. Thin layer chromatography (TLC) was carried out throughout all syntheses using Merck TLC silica gel 60 aluminium sheets. Microwave assisted reactions were carried out in a CEM Discover SP microwave reactor, with a maximum power output of 300 W and controlling the temperature of the reaction mixture. Purification of synthesised compounds by flash chromatography was performed manually on glass columns or on Teledyn ISCO Combiflash Rf 200 flash chromatograph on silica gel 40-60 μm (40–250 mesh). UV-Vis electron absorption spectra of **ArDOT** monomers were recorded on a Shimadzu UV-3600 spectrophotometer in dichloromethane in quartz cells of 10 mm path length.

Computational methodology

Computational studies were carried out using density functional theory (DFT) with the Gaussian 09[3] package of programs. Becke's three-parameter hybrid exchange functional[4] with the Lee–Yang–Parr gradient-corrected correlation functional (B3LYP)[5] and Pople's 6-31G split valence basis set supplemented by d-polarization functions for heavy atoms were employed [B3LYP/6-31G(d)]. The restricted Hartree-Fock formalism was used. The geometries of the oligomers, **(ArDOT)$_n$**, were fully optimized for isolated molecules in a gas phase, with no constraints, and the electronic structures for the optimised geometries were calculated at the same level of theory.

Optimization of the geometries of the polymers, **p[ArDOTs]**, and calculation of their electronic structures were performed using periodic boundary conditions formalism (PBC) at the PBC/B3LYP/6-31G(d) level, which generally gives a good estimate of the band gaps of conjugated

polymers, including polythiophenes.[6] The unit cells for PBC calculations of the polymers presented in the paper have been prepared from the optimized structures of corresponding dimers. Presented in the paper PBC calculations of non-symmetrical **ArDOTs** (as in the case of **p[4R-PheDOT]** and **p[5CF$_3$-PyDOT]**) from the dimers as unit cells, are for head-to-tail (HT) connectivity of the monomer units in all the cases. For comparison, we also performed calculations for head-to-head/tail-to-tail (HH-TT) arrangement of the monomer units in the polymer backbone.The results show that in the absence of steric repulsions between the side aromatic moieties, which are on the same side of the polymer backbone (as in the case of **p[4R-PheDOT]** and **p[5CF$_3$-PyDOT]**), the calculations of the polymers with HT and HH-TT arrangement give very close total energies (differencies are 0.00 – 0.39 kcal/mol), as well as HOCO, LUCO and E_g (differences are 0 – 5 meV) (Table S1). Of course, these differences are substantially higher in the case of polymers with substantial steric repulsion between the the side moieties, i.e. **p[3NO$_2$,5CF$_3$-PheDOT]**, **p[3NO$_2$,5CF$_3$-PheDOT]** and **p[F$_6$-NaphDOT(1,2)]**, and PBC calculations for these polymer were not performed.

Table S1. Total energies (E_{total}), HOCO/LUCO energy levels and the band gaps (E_g,) of regioisomeric **p[ArDOTs]** by PBC/B3LYP/6-31G(d) calculations in the gas phase

Polymer	Regio-isomer[a]	E_{total}, hartree	ΔE_{total} (HT–HHTT), kcal/mol	HOCO, eV	LUCO, eV	E_g, eV
p[4Me-PheDOT]	HT	–1942.8090085	–0.08	–4.270	–2.147	2.123
	HHTT	–1942.8088779		–4.268	–2.139	2.129
p[4F-PheDOT]	HT	–2062.6355280	0.00	–4.644	–2.511	2.133
	HHTT	–2062.6355222		–4.644	–2.512	2.132
p[4Br-PheDOT]	HT	–7006.3793017	0.00	–4.770	–2.631	2.139
	HHTT	–7006.3793007		–4.770	–2.631	2.140
p[4Cl-PheDOT]	HT	–2783.3613276	0.00	–4.790	–2.650	2.140
	HHTT	–2783.3613268		–4.790	–2.650	2.140
p[4CF$_3$-PheDOT]	HT	–2538.2463064	–0.39	–4.953	–2.809	2.144
	HHTT	-2538.246926		–4.955	–2.806	2.149
p[4MeSO$_2$-PheDOT]	HT	–3039.9466487	–0.09	–4.980	–2.831	2.149
	HHTT	–3039.9465101		–4.982	–2.834	2.147
p[4CN-PheDOT]	HT	–2048.6563942	–0.01	–5.324	–3.173	2.152
	HHTT	–2048.6563817		–5.325	–3.174	2.151
p[4NO$_2$-PheDOT]	HT	–2273.1744023	–0.03	–5.370	–3.230	2.140
	HHTT	–2273.1743528		–5.371	–3.235	2.136
p[5CF3-PyDOT]	HT	–2570.3264606	–0.10	–5.055	–2.887	2.169
	HHTT	–2570.32631		–5.055	–2.891	2.164

[a]HT – head-to-tail arrangement of 4R groups in the polymer backbone. [a]HH-TT – head-to-head / tail-to-tail arrangement of 4R groups in the polymer backbone.

The PBC calculated HOCO/LUCO and E_g of **p[ArDOTs]** were compared with the results based on the oligomers approach of extrapolations of HOMO/LUMO energies and the HOMO–LUMO energy gaps (ΔE_{HL}) of **(ArDOT)$_n$** to the infinite chain length to (n = ∞) by linear fitting of E vs $1/(n + 0.1n^2)$, showing good coincidence.

X-Ray crystallography

Single crystals of studied **ArDOTs** have been obtained by recrystallization of pure samples from appropriate solvents (petrol ether, dichloromethane, toluene, ethylacetate or their mixtures) or by slow evaporation of their solution at room temperature. The X-ray single crystal data have been collected using λMoKα radiation (λ = 0.71073Å) on a Bruker D8Venture (Photon100 CMOS detector, IμS-microsource, focusing mirrors; compounds **F$_4$-23, 36F$_2$-PheDOT**, and **PzDOT**) and Agilent XCalibur (Sapphire-3 CCD detector, fine-focus sealed tube, graphite monochromator; comounds **F$_4$-PheDOT**, **3NO$_2$5CF$_3$-PheDOT**, **56Cl$_2$-PyDOT**, **5CF$_3$-PyDOT** and **QxDOT**) diffractometers equipped with a Cryostream (Oxford Cryosystems) open-flow nitrogen cryostats at the temperature 120.0(2) K. The crystals of compound **3NO$_2$5CF$_3$-PheDOT** shuttered during the flash-freezing, so the crystal of this compound was placed on a goniometer at 250 K and slowly cooled down to 200 K where the data were collected. All structures were solved by direct method and refined by full-matrix least squares on F^2 for all data using Olex2[7] and SHELXTL[8] software. All non-disordered non-hydrogen atoms were refined anisotropically. The hydrogen atoms in the structures of **F$_4$-PheDOT** and **PzDOT** were placed in the calculated positions and refined in riding mode. The hydrogen atoms in the other structures were refined isotropically. The disordered atoms in the structure of **3NO$_2$5CF$_3$-PheDOT** were refined isotropically with fixed SOF = 0.5. Crystal data and parameters of refinement are listed in Table S4 and molecular structures and crystal packings are shown in Figures S3 and S4.

Crystallographic data for the structure have been deposited with the Cambridge Crystallographic Data Centre as supplementary publications CCDC 1553610–1553517.

Electrochemistry and Vis-NIR electron absorption spectroscopy of polymers.

Electrochemical experiments were carried out using an Autolab PGSTAT-302N potentiostat-galvanostat. Cyclic voltammetry (CV) measurements were performed in a three-electrode cell equipped with a platinum disk (d = 1.6 mm) as the working electrode, platinum wire as a counter electrode and a non-aqueous Ag/Ag^+ reference electrode (0.01 M $AgNO_3$ and 0.1 M Bu_4NPF_6 in MeCN). Cyclic voltammograms of monomers **PheDOT** and **4CF$_3$-PheDOT** were recorded at room temperature in dichloromethane (DCM) at low concentrations (~ 1mM) with 0.2 M Bu_4NPF_6 as supporting electrolyte, with ohmic drop compensation (Figure S9a,c). The potentials were corrected with ferrocene/ferrocenium redox pair (Fc/Fc^+) as an internal standard. At such low monomer concentrations, no electropolymerization was observed on cycling (we have observed previously that electropolymerization of **PheDOT** is more difficult than **EDOT** and requires higher concentrations of the monomer[9,10]). Their electropolymerization was performed under potendiodynamic conditions in 0.2 M Bu_4NPF_6 / DCM at higher monomer concentrations of ~100 mM, cycling between 0 and + 1.3 V for **PheDOT**, and between 0 and +1.6 V for **4CF$_3$-PheDOT** (vs. Ag/Ag^+ reference electrode) (Figure S9b,d). After being electrodeposited onto working electrodes, the films of the polymers **p[PheDOT]** and **p[4CF$_3$-PheDOT]** were rinsed with acetonitrile and their electrochemical response was recorded in dry acetonitrile with 0.1 M Bu_4NPF_6 as supporting electrolyte.

For measurements of Vis-NIR electron absorption spectra, the films of **p[PheDOT]** and **p[4CF$_3$-PheDOT]** were electrodeposited on ITO glass substrate working electrodes in the same manner as described above. As the polymers have low oxidation potentials, they can be partly self-doped under air. Therefore, their Vis-NIR spectra were measured (Shimadzu UV-3600 spectrophotometer) in a spectroelectrochemical setup (0.1 M Bu_4NPF_6 / acetonitrile, ITO working

electrode, Ag wire reference electrode) applying potentials corresponding to the neutral state of the polymers.

Synthesis

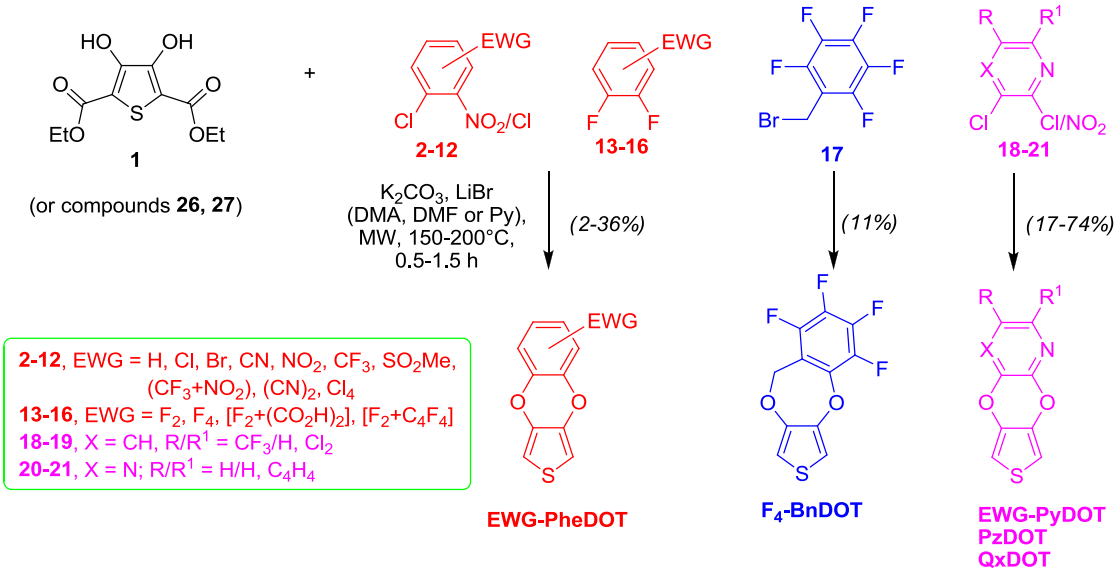

<u>Microwave-assisted synthesis of PheDOTs and their analogs. General procedure.</u>

Diethyl 3,4-dihydroxy-2,5-thiophenedicarboxylate (**1**) (1.000 g, 3.84 mmol, 1.00 eq.), K_2CO_3 (531 mg, 3.84 mmol, 1.00 eq.), electrophilic reagent **2–21** (1.0–1.3 eq.) and LiBr (210 mg, 2.42 mmol, 0.60 eq.) were combined in a 35 mL microwave tube, and DMA (10–12 mL) was added. The tube was sealed and bubbled with N_2 under stirring for ca. 5–10 min. The mixture was then heated with stirring in a microwave reactor (initially for 5–20 min at 80–100°C (for dissolution and homogenization of the reaction mixture), then at 150–200 ^{o}C for 0.5–1.5 h). After cooling to room temperature, the dark brown mixture was diluted with water (100 mL) and extracted with DCM (3 × 100 mL). The combined organic layers were washed with water (2–3 times), dried over $MgSO_4$, and the solvent was evaporated. The residue was purified by column chromatography on silicagel with an appropriate solvent as an eluent (PE, toluene, DCM, PE/DCM or PE/EA).

Benzo[b]thieno[3,4-e][1,4]dioxine (PheDOT)

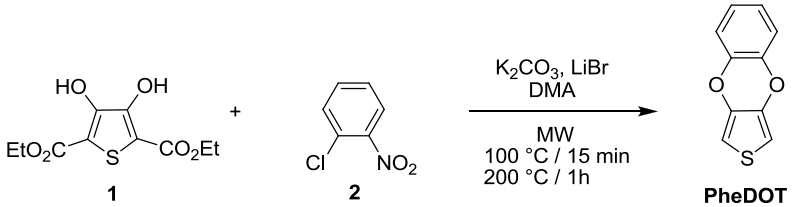

Diethyl 3,4-dihydroxy-2,5-thiophenedicarboxylate (**1**) (1.004 g, 3.86 mmol, 1.00 eq.), K_2CO_3 (0.533 g, 3.86 mmol, 1.00 eq.), 1-chloro-2-nitrobenzene (**2**) (0.632 g, 4.01 mmol, 1.04 eq.), LiBr (0.200 g, 2.30 mmol, 0.60 eq.) and DMA (10 mL) were placed in a 35 mL MW tube. The tube was sealed, degassed by bubbling with nitrogen (stirring) for 3 min and heated with stirring in a microwave reactor in 4 steps: 1) 50 °C / 5 min; 2) 80 °C / 15 min; 3) 100 °C / 15 min, 4) 200 °C / 1 h. The reaction was repeated at the same conditions using diethyl 3,4-dihydroxy-2,5-thiophenedicarboxylate (**1**) (1.002 g, 3.85 mol, 1.00 eq.), K_2CO_3 (0.548 g, 3.97 mol, 1.03 eq.), 1-chloro-2-nitrobenzene (**2**) (0.653 g, 4.14 mol, 1.08eq.) and LiBr (0.211 g, 2.43 mol, 0.63 eq.) in DMA (10 mL). The combined mixtures from both syntheses were poured into water (200 mL), stirred and the precipitate was filtered off. The solid was dissolved in DCM (200 mL), stirred for 1 h, dried over $MgSO_4$, filtered and the solvent was evaporated. The crude product was purified by flash chromatography on silica gel (eluent: PE) to yield compound **PheDOT** (24.1 mg, 1.6%) as a white solid.

Analytical data (^{1}H and ^{13}C NMR, MS) were consistent with the data published in the literature.[9]

^{1}H NMR (400 MHz, $CDCl_3$): δ (ppm) 6.92 (4H, m, $H^{B1–4}$), 6.43 (2H, s, $H^{T2,5}$).

FTIR (cm^{-1}): 3102, 3075.

6-Chlorobenzo[b]thieno[3,4-e][1,4]dioxine (4Cl-PheDOT)

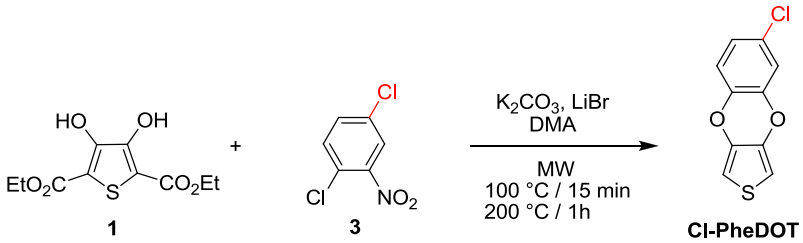

Diethyl 3,4-dihydroxy-2,5-thiophenedicarboxylate (**1**) (1.001 g, 3.85 mmol, 1.00 eq.), K_2CO_3 (0.542 g, 3.92 mmol, 1.02 eq.), 2,5-dichloronitrobenzene (**3**) (0.804 g, 4.19 mmol, 1.09 eq.), LiBr (0.218 g, 2.51 mmol, 0.65 eq.) and DMA (10 mL) were placed in a 35 mL MW reaction tube. The tube was sealed, degassed by bubbling with nitrogen (stirring) for 3 min and heated with stirring in a microwave reactor in 4 steps: 1) 50 °C / 5 min; 2) 80 °C / 15 min; 3) 100 °C / 15 min, 4) 200 °C / 1 h. After cooling to room temperature, the mixture was poured into DCM (100 mL) and stirred for 1 h before adding water (100 mL). The mixture was filtered, the organic layer was separated, washed with water (4 × 50 mL), dried over $MgSO_4$ and the solvent was evaporated. The residue was purified by flash chromatography on silica gel (eluent: PE) to yield compound **4Cl-PheDOT** (0.145 g, 16.8%) as a white solid.

^{1}H NMR (400 MHz, $CDCl_3$): δ (ppm) 6.93 (1H, d, $J_{B3–B5}$ = 2.3 Hz, H^{B3}), 6.90 (1H, dd, $J_{B5–B6}$ = 8.6 Hz, $J_{B3–B5}$ = 2.3 Hz, H^{B5}), 6.84 (1H, d, $J_{B5–B6}$ = 8.6 Hz, H^{B6}), 6.46 (1H, d, $J_{T2–T5}$ = 3.6 Hz, $H^{T2/5}$), 6.44 (1H, d, $J_{T2–T5}$ = 3.6 Hz, $H^{T2/5}$).

^{13}C NMR (DEPTQ, 100 MHz, $CDCl_3$): δ (ppm) 141.29, 139.70, 138.61, 138.32, 128.16 (C^{B4}), 123.55 (CH, C^{B5}), 117.57 (CH, C^{B6}), 117.07 (CH, C^{B3}), 101.57 (CH, $C^{T2/5}$), 101.38 (CH, $C^{T2/5}$).

MS (EI+): *m/z* 223.95 (M^+, 100%), 225.95 (37.61%); calcd. for $C_{10}H_5ClO_2S$: 223.97 (100.0%), 225.97 (37.0%).

6-Bromobenzo[b]thieno[3,4-e][1,4]dioxine (4Br-PheDOT)

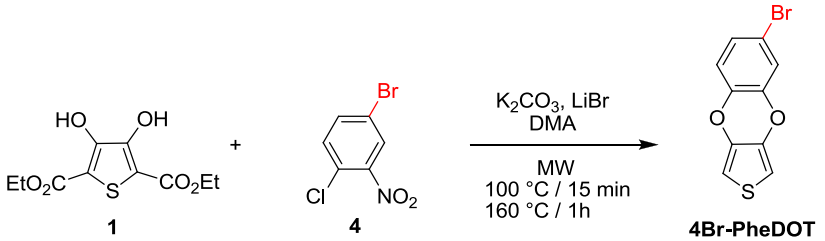

Diethyl 3,4-dihydroxy-2,5-thiophenedicarboxylate (**1**) (1.500 g, 5.76 mmol, 1.00 eq.), K_2CO_3 (0.840 g, 6.08 mmol, 1.05 eq.), 2-chloro-5-bromonitrobenzene (**4**) (1.781 g, 6.34 mmol, 1.10 eq.), LiBr (0.320 g, 3.68 mmol, 0.64 eq.) and DMA (15 mL) were placed in a 35 mL MW reaction tube. The tube was sealed, degassed by bubbling with nitrogen (stirring) for 3 min and heated with stirring in a microwave reactor in 4 steps: 1) 50 °C / 5 min; 2) 80 °C / 15 min; 3) 100 °C / 15 min, 4) 160 °C / 1 h. The mixture was cooled to room temperature, diluted with DCM (100 mL) and filtered. The filtrate was washed with water (3 × 200 mL), dried over $MgSO_4$ and the solvent was evaporated. The residue was purified by flash chromatography on silica gel (eluent: PE) to yield compound **4Br-PheDOT** (139 mg, 9.0%) as a white solid.

^{1}H NMR (400 MHz, $CDCl_3$): δ (ppm) 7.07 (1H, d, $J_{B3–B5}$ = 2.3 Hz, H^{B3}), 7.03 (1H, dd, $J_{B5–B6}$ = 8.6 Hz, $J_{B3–B5}$ = 2.3 Hz, H^{B5}), 6.79 (1H, d, $J_{B5–B6}$ = 8.6 Hz, H^{B6}), 6.46 (1H, d, $J_{T2–T5}$ = 3.6 Hz, $H^{T2/5}$), 6.44 (1H, d, $J_{T2–T5}$ = 3.6 Hz, $H^{T2/5}$).

^{13}C NMR (DEPTQ, 100 MHz, $CDCl_3$): δ (ppm) 141.5 ($C^{B1/2}$), 140.2 ($C^{B1/2}$), 138.6 ($C^{T3/4}$), 138.3 ($C^{T3/4}$), 126.5 (CH,C^{B4}), 119.9 (CH, C^{B3}), 118.0 (CH, C^{B6}), 115.1 (C^{B4}), 101.6 (CH, $C^{T2/5}$), 101.4 (CH, $C^{T2/5}$).

MS (EI+): *m/z* 267.95 (M^+, 100.0%, ^{79}Br), 270.00 (M^+, 99.47%, ^{81}Br); calcd. for $C_{10}H_5BrO_2S$: 267.92 (97.8%, ^{79}Br), 269.92 (100.0%, ^{81}Br).

Benzo[b]thieno[3,4-e][1,4]dioxine-6-carbonitrile (4CN-PheDOT)

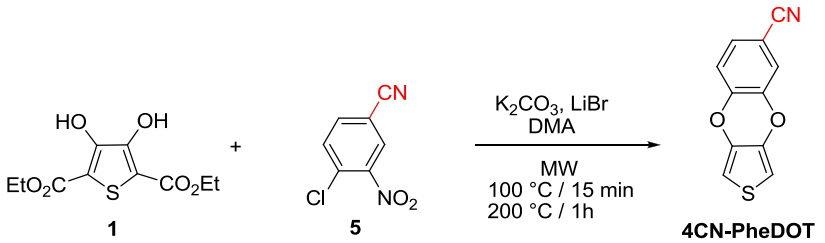

Diethyl 3,4-dihydroxy-2,5-thiophenedicarboxylate (**1**) (1.508 g, 5.79 mmol, 1.00 eq.), K_2CO_3 (0.802 g, 5.80 mmol, 1.00 eq.), 1-chloro-2-nitro-4-cyanobenzene (**5**) (1.150 g, 6.30 mmol, 1.09 eq.), LiBr (0.215 g, 2.48 mmol, 0.43 eq.) and DMA (15 mL) were placed in a 35 mL MW reaction tube. The tube was sealed, degassed by bubbling with nitrogen (stirring) for 3 min and heated with stirring in a microwave reactor in 4 steps: 1) 50 °C / 5 min; 2) 80 °C/ 15 min; 3) 100 °C/ 15 min, 4) 200 °C / 1 h. After cooling, the mixture was diluted with DCM (100 mL), filtered and the filtrate was washed with water (5 × 100 mL). The organic phase was dried over $MgSO_4$, filtered and evaporated to dryness. The residue was purified by flash chromatography on silica gel (eluent: toluene) to yield compound **4CN-PheDOT** (242 mg, 19.4%) as a white solid.

^{1}H NMR (400 MHz, $CDCl_3$): δ (ppm) 7.24 (1H, dd, $J_{B5–B6}$ = 8.4 Hz, $J_{B3–B5}$ = 1.9 Hz, H^{B5}), 7.19 (1H, d, $J_{B3–B5}$ = 1.9 Hz, H^{B3}), 6.98 (d, $J_{B5–B6}$ = 8.4 Hz, H^{B6}), 6.52 (d, $J_{T2–T5}$ = 3.6 Hz, $H^{T2/5}$), 6.50 (d, $J_{T2–T5}$ = 3.6 Hz, $H^{T2/5}$).

^{13}C NMR (100 MHz, $CDCl_3$): δ (ppm) 144.68 ($C^{B1/2}$), 141.30 ($C^{B1/2}$), 137.75 ($C^{T3/4}$), 137.67 ($C^{T3/4}$), 128.24 (CH, C^{B5}), 120.63 (CH, C^{B3}), 117.95 (CN), 117.85 (CH, C^{B6}), 107.17 (C^{B4}), 102.53(CH, $C^{T2/5}$), 102.27 (CH, $C^{T2/5}$).

MS (EI+): *m/z* 214.95 (M^+, 100.0%); calcd. for $C_{11}H_5NO_2S$: 215.00.

6-Nitrobenzo[b]thieno[3,4-e][1,4]dioxine (4NO$_2$-PheDOT)

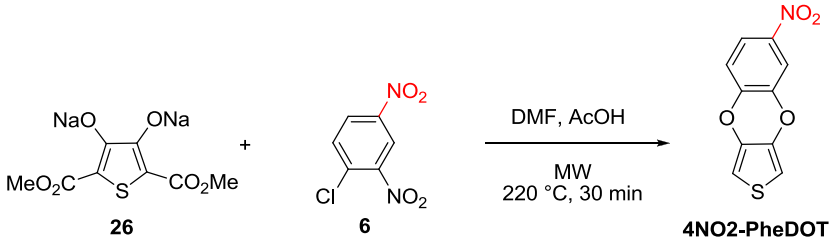

Dimethyl 3,4-dihydroxy-2,5-thiophenedicarboxylate disodium salt (**26**) (201 mg, 0.73 mmol, 1.00 eq.), 1-chloro-2,4-dinitrobenzene (**6**) (147 mg, 0.73 mmol, 1.00 eq.), acetic acid (44 mg, 0.73 mmol, 1.00 eq.) and DMF (5 mL) were placed in a 10 mL microwave tube. The tube was sealed, degassed by bubbling with nitrogen (stirring) for 3 min and heated with stirring in a microwave reactor at 220 °C for 30 min. After cooling, the mixture was poured into water (25 mL) and extracted with ethyl acetate (2 × 20 mL). The organic layer was dried over $MgSO_4$, evaporated to dryness and purified by flash chromatography on silica gel (eluent: toluene) to afford **4NO$_2$-PheDOT** (23.6 mg, 15%) as a light yellow solid.

^{1}H NMR (400 MHz, $CDCl_3$): δ (ppm) 7.87 (1H, dd, $J_{B5–B6}$ = 8.9 Hz, $J_{B3–B5}$ = 2.6 Hz, 1H^{B5}), 7.82 (1H, d, $J_{B3–B5}$ = 2.6 Hz, H^{B3}), 7.02 (1H, d, $J_{B5–B6}$ = 8.9 Hz, H^{B6}), 6.56 (1H, d, $J_{T2–T5}$ = 3.6 Hz, H$^{T2/5}$), 6.54 (1H, d, $J_{T2–T5}$ = 3.6 Hz, H$^{T2/5}$).

^{13}C NMR (100 MHz, $CDCl_3$): δ (ppm) 146.08, 143.52, 140.92, 137.55, 137.10 (C^{B4}), 119.72 (CH, C$^{B3/5/6}$), 116.99 (CH, C$^{B3/5/6}$), 112.96 (CH, C$^{B3/5/6}$), 102.81 (CH, C$^{T2/5}$), 102.43 (CH, C$^{T2/5}$).

MS (EI+): *m/z* 235.05 (M$^+$, 100%); calcd. for: $C_{10}H_5NO_4S$: 234.99.

6-(Trifluoromethyl)benzo[b]thieno[3,4-e][1,4]dioxine (4CF$_3$-PheDOT)

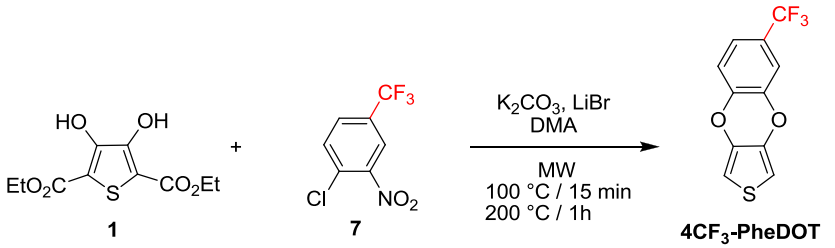

Diethyl 3,4-dihydroxy-2,5-thiophenedicarboxylate (**1**) (1.009 g, 3.88 mmol, 1.00 eq.), K_2CO_3 (0.536 g, 3.88 mmol, 1.00 eq.), 4-chloro-3-nitrobenzotrifluoride (**7**) (0.964 g, 4.27 mmol, 1.10 eq.), LiBr (0.267 g, 3.07 mmol, 0.79 eq.) and DMA (10 mL) were placed in a 35 mL MW tube The tube was sealed, degassed by bubbling with nitrogen (stirring) for 3 min and heated with stirring in a microwave reactor in 4 steps: 1) 50 °C / 5 min; 2) 80 °C / 15 min; 3) 100 °C / 15 min, 4) 200 °C / 1 h. Another batch of diethyl 3,4-dihydroxy-2,5-thiophenedicarboxylate (**1**) (1.021 g, 3.92 mmol, 1.00 eq.), K_2CO_3 (0.537 g, 3.89 mmol, 1.01 eq.), 4-chloro-3-nitrobenzotrifluoride (**7**) (0.976 g, 4.33, 1.12 eq.), LiBr (0.221 g, 2.54, 0.66 eq.), DMA (10 mL) was run under the same conditions. The two reaction mixtures were combined, diluted with DCM (200 mL), stirred and filtered to remove insoluble material. The filtrate was washed with water (6 × 150 mL), dried over $MgSO_4$ and the solvent was evaporated to dryness. The crude product was purified by flash chromatography on silica gel (eluent: PE) to yield compound **4CF$_3$-PheDOT** (0.715 g, 35.8%) as a white solid.

^{1}H NMR (400 MHz, $CDCl_3$): δ (ppm) 7.19 (2H, m, H^{B3,5}), 6.98 (1H, d, $J_{B5–B6}$ = 8.4 Hz, H^{B6}), 6.49 (1H, d, $J_{T2–T5}$ = 3.6 Hz, H$^{T2/5}$), 6.48 (1H, d, $J_{T2–T5}$ = 3.6 Hz. H$^{T2/5}$).

^{13}C NMR (100 MHz, $CDCl_3$): δ (ppm) 143.46 (C$^{B1/2}$), 141.00 (C$^{B1/2}$), 138.24 (C$^{T3/4}$), 138.18 (C$^{T3/4}$), 126.12 (q, $^2J_{C–F}$ = 33.4 Hz, C^{B4}), 123.51 (q, $^1J_{C–F}$ = 271.6 Hz, CF_3), 120.89 (CH, q, $^3J_{C–F}$ = 3.9 Hz, C^{B5}), 117.21 (CH, C^{B6}), 114.44 (CH, q, $^3J_{C–F}$ = 3.9 Hz, C^{B3}), 101.97 (CH, C$^{T2/5}$), 101.82 (CH, C$^{T2/5}$).

^{19}F NMR (376 MHz, $CDCl_3$): δ (ppm) –63.52 (s, CF_3).

MS (EI+): *m/z* 258.05 (M$^+$, 100%); calcd. for $C_{11}H_5F_3O_2S$: 258.00.

6-(Methylsulfonyl)benzo[b]thieno[3,4-e][1,4]dioxine (4MeSO$_2$-PheDOT)

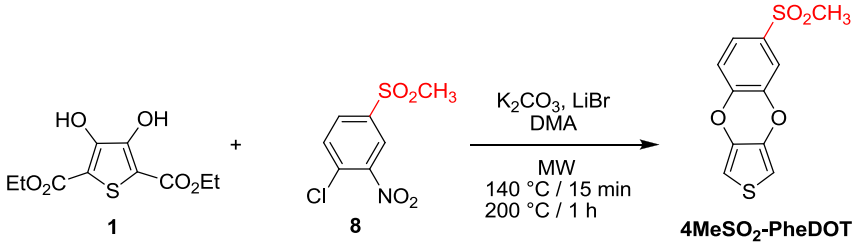

Diethyl 3,4-dihydroxy-2,5-thiophenedicarboxylate (**1**) (1.001 g, 3.85 mmol, 1.00 eq.), K_2CO_3 (0.566 g, 4.10 mmol, 1.06 eq.), 2-chloro-5-methylsulfonyl-1-nitrobenzene (**8**) (1.009 g, 4.28 mmol, 1.11 eq.), LiBr (0.217 g, 2.49 mmol, 0.65 eq.) and DMA (11 mL) were placed in a 35 mL MW tube. The tube was sealed, degassed by bubbling with nitrogen (stirring) for 3 min and heated with stirring in a microwave reactor in 2 steps: 1) 140 °C / 15 min (80 W), 2) 200 °C / 1 h. After cooling, the mixture was diluted with DCM (50 mL) and water (100 mL) and filtered. The organic phase was washed with water (3 × 50 mL), dried over $MgSO_4$, filtered and the solvent was evaporated. The residue was dissolved in hot toluene (50 mL) and passed through a short silica gel column eluting with DCM. After solvent evaporation the solvent, the crude product was purified by flash chromatography on silica gel (eluent: DCM) to afford compound **4MeSO$_2$-PheDOT** (216 mg, 20.9 %) as a white solid (purity 98%, by ^{1}H NMR). Analytically pure product (193 mg, 18.7%) was obtained by recrystallization from heptane/chloroform (7:1).

^{1}H NMR (400 MHz, $CDCl_3$): δ (ppm) 7.52 (1H, dd, $J_{B5–B6}$ = 8.4 Hz, $J_{B3–B5}$ = 2.0 Hz, H^{B5}), 7.50 (1H, d, $J_{B3–B5}$ = 2.0 Hz, H^{B3}), 7.07 (1H, d, $J_{B5–B6}$ = 8.4 Hz, H^{B6}), 6.54 (1H, d, $J_{T2–T5}$ = 3.6 Hz, $H^{T2/5}$), 6.52 (1H, d, $J_{T2–T5}$ = 3.6 Hz, $H^{T2/5}$), 3.05 (3H, s, CH_3).

^{13}C NMR (100 MHz, $CDCl_3$): δ (ppm) 145.19, 141.32, 137.84, 137.71, 135.69, 123.39, 117.74, 116.57, 102.51, 102.27, 44.63 (CH_3).

MS (EI+): *m/z* 268.10 (M^+, 100%); calcd. for $C_{11}H_8O_4S_2$: 267.99.

5-Nitro-7-(trifluoromethyl)benzo[b]thieno[3,4-e][1,4]dioxine (3NO$_2$,5CF$_3$-PheDOT)

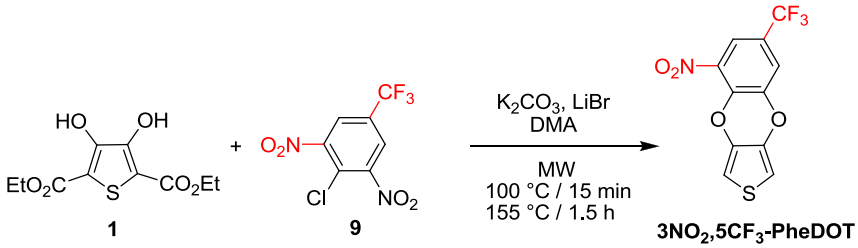

Diethyl 3,4-dihydroxy-2,5-thiophenedicarboxylate (**1**) (1.004 g, 3.86 mmol, 1.00 eq.), K_2CO_3 (0.531 g, 3.84 mmol, 1.00 eq.), 4-chloro-3,5-dinitrobenzotrifluoride (**9**) (1.144 g, 4.23 mmol, 1.10 eq.), LiBr (0.200 mg, 2.30 mmol, 0.60 eq.) and DMA (11 mL) were placed in a 35 mL MW tube. The tube was sealed, degassed by bubbling with nitrogen (stirring) and heated with stirring in a microwave reactor in 2 steps: 1) 100 °C / 10 min, 2) 155 °C / 1.5 h). After cooling, the mixture was diluted with DCM (50 mL) and water (50 mL), stirred and filtered to remove insoluble material. The organic layer was washed with water (3 × 50 mL), dried over $MgSO_4$, filtered and evaporated to dryness. The crude product was purified by flash chromatography on silica gel (eluent: PE:DCM, 7:3) to yield compound **3NO$_2$,5CF$_3$-PheDOT** (150 mg, 12.8%) as a light yellow solid.

^{1}H NMR (400 MHz, $CDCl_3$): δ (ppm) 7.83 (1H, d, $J_{B3–B5}$ = 2.0 Hz, $H^{B3/5}$), 7.39 (1H, d, $J_{B3–B5}$ = 2.0 Hz, $H^{B3/5}$), 6.72 (1H, d, $J_{T2–T5}$ = 3.6 Hz, $H^{T2/5}$), 6.59 (1H, d, $J_{T2–T5}$ = 3.6 Hz, $H^{T2/5}$).

^{13}C NMR (100 MHz, $CDCl_3$): δ (ppm) 142.92, 138.56, 138.25, 136.76, 136.02, 122.35 (q, $^1J_{C-F}$ = 272.7 Hz, CF_3), 125.31 (q, $^2J_{C–F}$ = 35.2 Hz, C^{B4}), 118.13 (CH, q, $^3J_{C–F}$ = 3.5 Hz, $C^{B3/5}$), 117.24 (CH, q, $^3J_{C–F}$ = 4.0 Hz, $C^{B3/5}$), 104.50, 103.07.

^{19}F NMR (376 MHz, $CDCl_3$): δ (ppm) –64.13 (s, CF_3).

MS (EI+): *m/z:* 303.05 (100; calcd. for $C_{11}H_4F_3NO_4S$: 302.98.

7-Nitro-5-(trifluoromethyl)benzo[b]thieno[3,4-e][1,4]dioxine (3CF$_3$,5NO$_2$-PheDOT)

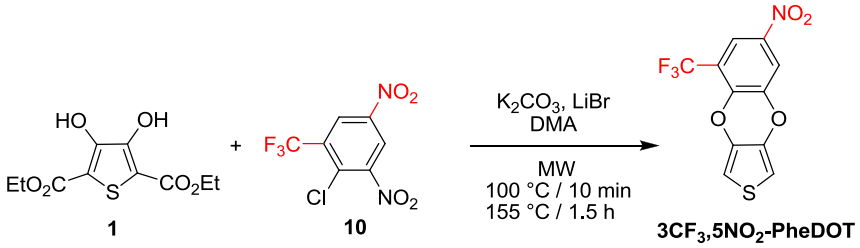

Diethyl 3,4-dihydroxy-2,5-thiophenedicarboxylate (**1**) (1.007 g, 3.87 mmol, 1.00 eq.), K_2CO_3 (0.537 g, 3.89 mmol, 1.00 eq.), 2-chloro-3,5-dinitrobenzotrifluoride (**10**) (1.144 g, 4.23 mmol, 1.09 eq.), LiBr (0.217 mg, 2.50 mmol, 0.65 eq.) and DMA (11 mL) were placed in a 35 mL MW tube. The tube was sealed, degassed by bubbling with nitrogen (stirring) for 3 min and heated with stirring in a microwave reactor in 2 steps: 1) 100 °C / 10 min, 2) 155 °C / 1.5 h. After cooling, the mixture was diluted with DCM (70 mL) and water (50 mL), stirred and filtered to remove insoluble material. The organic layer was washed with water (2 × 50 mL), dried over $MgSO_4$, filtered and the solvent was evaporated. The crude product was purified by flash chromatography on silica gel (eluent: DCM) to yield compound **3CF$_3$,5NO$_2$-PheDOT** (175 mg, 14.9%) as a light yellow solid. An analytically pure sample was obtained by recrystallization from heptane (154 mg, 13.1%).
^{1}H NMR (400 MHz, $CDCl_3$): δ (ppm) 8.16 (1H, d, $J_{B3–B5}$ = 2.6 Hz, $H^{B3/5}$), 7.98 (1H, d, $J_{B3–B5}$ = 2.6 Hz, $H^{B3/5}$), 6.71 (1H, d, $J_{T2–T5}$ = 3.6 Hz, $H^{T2/5}$), 6.60 (1H, d, $J_{T2–T5}$ = 3.6 Hz, $H^{T2/5}$).
^{13}C NMR (100 MHz, $CDCl_3$): δ (ppm) 144.35, 142.39, 142.02, 136.65, 136.20, 121.55 (q, $^1J_{C–F}$ = 273.8 Hz, CF_3), 119.18 (CH, q, $^2J_{C–F}$ = 34.0 Hz, C^{B5}), 117.28 (q, $^3J_{C–F}$ = 5.3 Hz, C^{B4}), 115.95, 104.34 (CH, $C^{T2/5}$), 103.17 (CH, $C^{T2/5}$).
^{19}F NMR (376 MHz, $CDCl_3$): δ (ppm) –63.63 (s, CF_3).
MS (EI+): *m/z* 303.05 (M^+, 100%); calcd. for $C_{11}H_4F_3NO_4S$: 302.98.

5,6,7,8-Tetrachlorobenzo[b]thieno[3,4-e][1,4]dioxine (Cl$_4$-PheDOT)

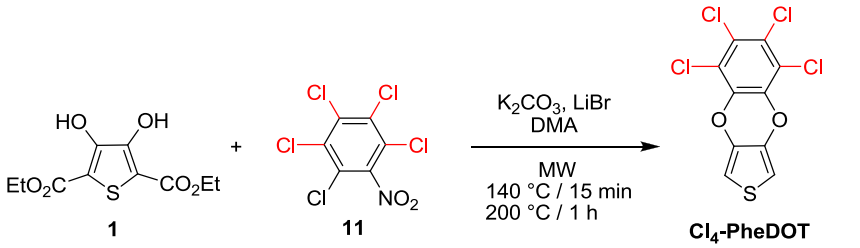

Diethyl 3,4-dihydroxy-2,5-thiophenedicarboxylate (**1**) (904 mg, 3.47 mmol, 1.00 eq.), K_2CO_3 (486 mg, 3.52 mmol, 1.01 eq.), pentachloronitrobenzene (**11**) (112 mg, 0.38 mmol, 1.09 eq.), LiBr (187 mg, 2.15 mmol, 0.62 eq.) and DMA (11 mL) were placed in a 35 mL MW tube. The tube was sealed, degassed by bubbling with nitrogen (stirring) for 3 min and heated with stirring in a microwave reactor in 2 steps: 1) 140 °C / 15 min (80 W), 2) 200 °C / 1 h. After cooling, the mixture was diluted with DCM (100 mL), washed with water (3 × 50 mL), dried with $MgSO_4$, and the solvent was evaporated. The crude product was purified by flash chromatography on silica gel (eluent: hot heptane) to yield compound **Cl$_4$-PheDOT** (105 mg, 9.2%) as a white powder.
^{1}H NMR (400 MHz, $CDCl_3$): δ (ppm) 6.65 (1H, s, $H^{T2,5}$).
^{13}C NMR (DEPTQ, 100 MHz, $CDCl_3$): δ (ppm) 137.87, 136.91, 127.08, 120.40, 103.16 (CH, $C^{T2,5}$).
MS (EI+): *m/z* 325.90 (80%), 327.95 (100%), 329.90 (51%) [M^+ with $^{35}Cl/^{37}Cl$ distribution]; calcd. for $C_{10}H_2Cl_4O_2S$ (for natural $^{35}Cl/^{37}Cl$ distribution): 325.85 (78.2%), 327.85 (100.0%), 329.85 (47.9%).

Benzo[b]thieno[3,4-e][1,4]dioxine-6,7-dicarbonitrile (45(CN)$_2$-PheDOT)

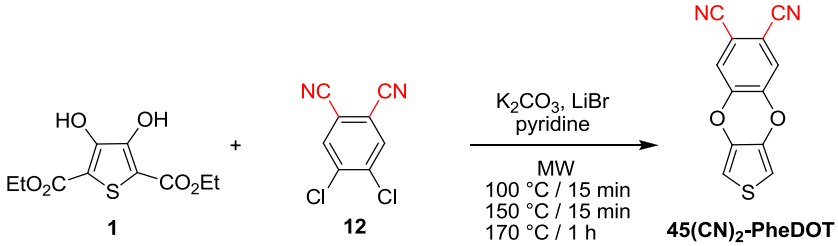

Diethyl 3,4-dihydroxy-2,5-thiophenedicarboxylate (**1**) (1.502 g, 5.77 mmol, 1.00 eq.), 4,5-dichlorophthalonitrile (**12**) (1.238 g, 6.28 mmol, 1.09 eq.), K_2CO_3 (0.797 g, 5.77 mmol, 0.99 eq.), LiBr (0.220 g, 2.55 mmol, 0.44 eq.) and pyridine (15 mL) were placed in a 35 mL MW tube. The tube was sealed, degassed by bubbling with nitrogen (stirring) for 3 min and heated with stirring in a microwave reactor in 2 steps (MW 150 W): 1) 100 ^{o}C / 10 min, 150 ^{o}/ 15 min, 170 ^{o}C / 1 h. After cooling, the mixture was diluted with water (100 mL) and extracted with DCM (8 × 25 mL). The combined DCM layers were washed with concentrated HCl (4 mL), water (2 × 25 mL) and filtered through a silica gel plug. The solvent was evaporated to yield the crude product (750 mg, 54%) as an orange solid. The crude product was purified by flash chromatography on silica gel (eluent: toluene) to yield pure compound **45(CN)$_2$-PheDOT** (208 mg (15 %) as a light yellowish solid.
^{1}H NMR (400 MHz, $CDCl_3$): δ (ppm) 7.29 (2H, s, $H^{B3,6}$), 6.61 (2H, s, $H^{T2,5}$).
^{13}C NMR (100 MHz, $CDCl_3$): δ (ppm) 144.65, 136.54, 122.12, 114.56, 111.32, 103.85.
^{13}C NMR (100 MHz, DMSO-d_6): δ (ppm) 144.23, 136.14, 122.67, 115.22, 110.25, 104.37.
MS (EI+): *m/z* 240.08 (M^+, 100%); calcd for $C_{12}H_4N_2O_2S$: 240.00.

6,7-Difluorobenzo[b]thieno[3,4-e][1,4]dioxine (45F$_2$-PheDOT)

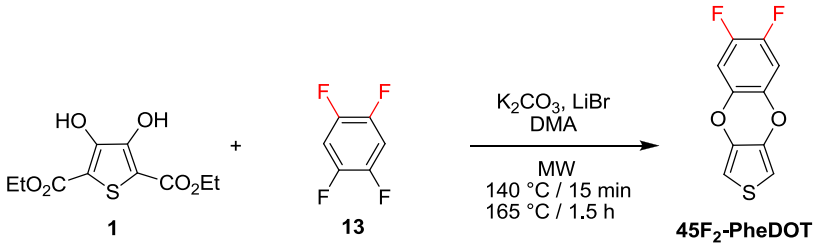

Diethyl 3,4-dihydroxy-2,5-thiophenedicarboxylate (**1**) (1.001 g, 3.86 mmol, 1.00 eq.), K_2CO_3 (0.562 g, 4.07 mmol, 1.06 eq.), 1,2,4,5-tetrafluorobenzene (**13**) (0.640 g, 4.26 mmol, 1.11 eq.), LiBr (0.199 g, 2.29 mmol, 0.60 eq.) and DMA (11 mL) were placed in a 35 mL MW tube. The tube was sealed, degassed by bubbling with nitrogen (stirring) for 3 min and heated with stirring in a microwave reactor in 2 steps: 1) 140 °C/ 15 min, 2) 165 °C / 1 h. After cooling, the mixture was diluted with DCM (100 mL) and filtered to remove insoluble material. The filtrate was washed with water (3 × 50 mL), dried with $MgSO_4$, filtered and evaporated to dryness. The crude product was purified by flash chromatography on silica gel (eluent: PE) to yield compound **45F$_2$-PheDOT** (17 mg, 2%) as a white solid.
^{1}H NMR (400 MHz, $CDCl_3$): δ (ppm) 6.78 (2H, dd, J = 9.2 Hz, 8.8 Hz, $H^{B3,6}$), 6.45 (2H, s, $H^{T2,5}$).
^{13}C NMR (100 MHz, $CDCl_3$): δ (ppm) 145.70 (dd, $^{1}J_{C–F}$ = 246.1 Hz, $^{2}J_{C–F}$ = 15.8 Hz, $C^{B4,5}$), 138.06 ($C^{T3,4}$), 136.53 (dd, J = 6.4 Hz, J = 6.3 Hz), 105.74 (m), 101.62 (CH, $C^{T2,5}$).
^{19}F NMR (376 MHz, $CDCl_3$): δ (ppm) –143.85 (s, $F^{B4,5}$).
MS (EI+): 226.00 (M^+, 100%); calcd. for $C_{10}H_4F_2O_2S$: 225.99.

5,8-Difluorobenzo[b]thieno[3,4-e][1,4]dioxine (36F$_2$-PheDOT)

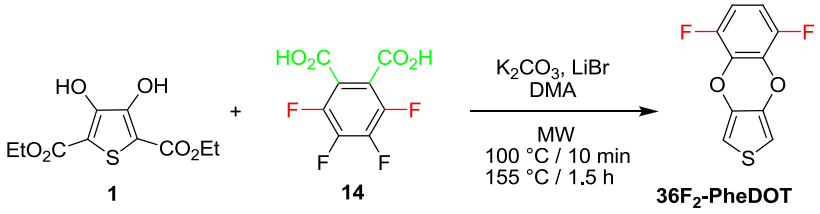

Diethyl 3,4-dihydroxy-2,5-thiophenedicarboxylate (**1**) (1.005 g, 3.86 mmol, 1.00 eq.), K_2CO_3 (0.546 g, 3.95 mmol, 1.02 eq.), tetrafluorophthalic acid (**14**) (1.021 g, 0.004 mmol, 1.11 eq.), LiBr (0.207 g, 2.38 mmol, 0.62 eq.) and DMA (11 mL) were placed in a 35 mL MW tube. The tube was sealed, degassed by bubbling with nitrogen (stirring) for 3 min and heated with stirring in a microwave reactor in 2 steps: 1) 100 °C / 10 min (80 W), 2) 155 °C / 1.5 h. After cooling, the mixture was diluted with DCM (100 mL) and water (100 mL), stirred and filtered to remove insoluble material. The filtrate was acidified with a few drops of concentrated HCl, organic layer was separated, washed with water (3 × 50 mL), dried with $MgSO_4$, filtered and the solvent evaporated. The crude product was purified by flash chromatography on silica gel (eluent: PE to PE:EA, 95:5) to yield compound **36F$_2$-PheDOT** (58.5 mg, 6.7%)* as a white powder.

***Note:** The yield in the reaction is low (lower than e.g. in the case of **F$_4$-PheDOT**, see below). We can't guarantee that full decarboxylation took place in the reaction and possibly the products with one or two CO_2H on the benzene ring were formed as well but were lost with a tag during the column chromatography purification. Thus, CO_2H group at the benzene ring of **PheDOT** seems to be more stable toward decarboxylation than those at the 2,5-positions of the thiophenes ring.*

^{1}H NMR (400 MHz, $CDCl_3$): δ (ppm) 6.74–6.69 (2H, m, $H^{B4,5}$), 6.60 (2H, s, $HT^{2,5}$).

^{13}C NMR (100 MHz, $CDCl_3$): δ (ppm) 146.92 (dd, $^1J_{C–F}$ =245.0 Hz, $^4J_{C–F}$ = 3.9 Hz, $C^{B3,6}$), 137.27 ($C^{T3,4}$), 131.52 (dd, $^2J_{C–F}$ = 12.6 Hz, $^3J_{C–F}$ = 6.8 Hz, $C^{B2,3}$), 109.25 (CH, dd, $^2J_{C–F}$ = 16.8 Hz, $^3J_{C–F}$ = 11.2 Hz, $C^{B4,5}$), 102.71 (CH, $C^{T2,5}$).

^{19}F NMR (376 MHz, $CDCl_3$): δ (ppm) –140.53 (s, $F^{B3,6}$).

MS (EI+): *m/z* 226.05 (M^+, 100%); calcd. for $C_{10}H_4F_2O_2S$: 225.99 (100.0%).

5,6,7,8-Tetrafluorobenzo[b]thieno[3,4-e][1,4]dioxine (F$_4$-PheDOT)

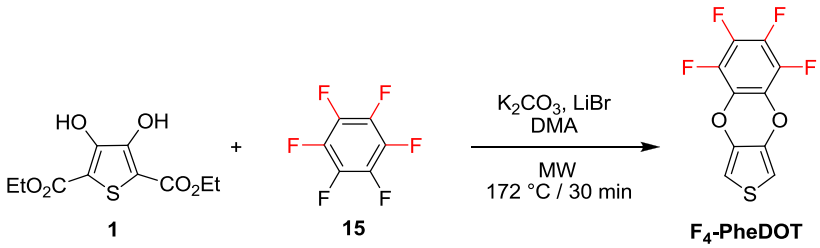

Diethyl 3,4-dihydroxy-2,5-thiophenedicarboxylate (**1**) (2.002 g, 7.69 mmol, 1.00 eq.), K_2CO_3 (1.068 g, 7.73 mmol, 1.00 eq.), hexafluorobenzene (**15**) (1.837 g, 9.87 mmol, 1.28 eq.), LiBr (0.400 g, 4.61 mmol, 0.60 eq.) and DMA (20 mL) were placed in a 35 mL microwave reaction tube. The tube was sealed, degassed by bubbling with nitrogen (stirring) for 3 min and heated with stirring in a microwave reactor at 172 °C for 30 min. The mixture was cooled down to room temperature, poured into DCM (100 mL) and filtered to remove insoluble material. The filtrate was washed with water (5 × 50 mL), dried over $MgSO_4$, filtered and evaporated to dryness. The crude product was purified by flash chromatography on a silica gel (eluent: toluene) to yield compound **F$_4$-PheDOT** (0.719 g, 35.6% yield) as a white solid.

^{1}H NMR (400 MHz, $CDCl_3$): δ (ppm) 6.63 (2H, s, $H^{T2,5}$).

^{13}C NMR (100 MHz, $CDCl_3$): δ (ppm) 138.16 (m, $C^{3,6/4,5}$), 136.42 (s, $C^{T3,4}$), 135.76 (m, $C^{3,6/4,5}$), 128.28 (m, $C^{B1,2}$), 103.27 (CH, s, $C^{T2,5}$).

^{19}F NMR (376 MHz, $CDCl_3$): δ (ppm) –163.27 – 163.43 (m, 2F), –166.23 – 166.39 (m, 2F).

^{19}F NMR (377 MHz, $CDCl_3$): δ (ppm) –(163.35–163.5) (m, 2F), –(166.3–166.5) (m, 2F).

MS (EI+): *m/z* 262.05 (M^+, 100%); calcd. for $C_{10}H_2F_4O_2S$: 261.97.

Optimization of the reaction conditions in synthesis of F_4-PheDOT

For more detailed studies in our initial experiments, the reaction of thiophene **1** was tested with hexafluorobenzene (**15**) with monitoring by GC-MS (Table S2). No product **F_4-PheDOT** or intermediates **F_4-22** or **F_4-23** were detected in the reaction with conventional heating even at prolonged time at 100 °C (Table S2, entries 1, 2).[11] In MW-assisted conditions, heating with K_2CO_3 in DMA at 220 °C showed formation of the target product **F_4-PheDOT** along with intermediate **F_4-23** (entries 3, 4). However, the yield was drastically decreased when the temperature was raised to 245 °C indicating decomposition of **F_4-PheDOT** at higher temperatures (entry 5). Addition of LiBr substantially increased the rate of decarboxyethylation of intermediate **F_4-23**, giving the yields of **F_4-PheDOT** of ca. 30% (entries 6, 7), although entry 8 indicates that decomposition of **F_4-PheDOT** occurs upon prolonged heating at 220 °C. Finally, variations in the amount of DMA solvent showed that the highest yields are achieved when the reaction temperature does not exceed 200 °C and ca. 10 mL of a solvent is used per 1 g of thiophene **1** (entries 10, 11).

Table S2. Reaction of thiophene **1** with hexafluorobenzene (**15**) at different conditions.[a]

Entry	T, °C	Time, h	LiBr, eq.	$V_{DMA}/1$[c] mL/g	Yield,[b] %	
					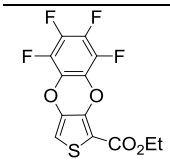 **F_4-23**	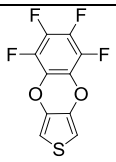 **F_4-PheDOT**
1[d]	100	16	0	60	0	0
2[e]	100	18	0	25	0	0
3	220	1.5	0	25	19.2	14.8
4	220	3	0	25	11.4	17.3
5	245	1.5	0	25	0	2.1
6	200	1.5	0.6	30	10.5	29.3
7	220	0.5	0.6	25	0	31.5
8	220	1.5	0.6	25	0	10.4
9	200	1.5	0.6	6	0	19.9
10	200	1	0.6	10	0	34.3
11	200	0.5	0.6	9.5	0	34.5

[a]Reaction conditions: thiophene **1** (1.0 eq.), hexafluorobenzene **15** (1.1 eq.), K_2CO_3 (1.0 eq.), LiBr (0–0.6 eq.), in DMA, MW irradiation. [b]Yields by GC-MS analysis. The intermediate **F_4-22** (with two CO_2Et groups at the thiophenes ring) was not detected in any experiment.[12] [c]Amount of DMA per 1 g of thiophene **1**. [d]In DMF, conventional heating. [e]In DMF, conventional heating, 3 eq. Cs_2CO_3 instead of 1 eq. K_2CO_3.

Microwave irradiation is an important factor for the reaction: performing the reaction under similar conditions with conventional heating resulted in substantially lower yields of **F_4-PheDOT** (0–7%, Table S3) and incomplete decarboxyethylation: apart from the target product **F_4-PheDOT**, substantial amount of the intermediate **F_4-23** was formed. It was isolated and is characterized below.

Table S3. Optimization of the reaction conditions and the yields of **F_4-PheDOT** in MW-asisted reaction of thiophene **1** with hexafluorobenzene (**15**):[a]

Entry.	Thiophene **1**	C_6F_6 (**15**)	Base (1.0 eq.)	Solvent: DMA	MW, temp. / time	Yield,[b] %	Number of reactions
1	2.00 g	1.1 eq.	K_2CO_3	20 mL	172 °C / 0.5 h	35.6%	1
2	1.50 g	1.1 eq.	*t*-BuOK	10 mL	178 °C / 1 h	31.7%	1
3	2.00 g	1.1 eq.	K_2CO_3	20 mL	160–170 °C / 1 h	32.3%	4
4	1.50 g	1.1 eq.	K_2CO_3	10 mL	164 °C / 1 h	29.3%	3
5	1.00 g	1.1 eq.	K_2CO_3	10 mL	190–200 °C / 1 h	23%	3
6[c]	2.00 g	1.0 eq.	K_2CO_3	20 mL	120 °C / 38 h 140 °C / 18 h	4%	1
7[c]	1.00 g	1.1 eq.	K_2CO_3	9 mL	160 °C / 2.5 h	7%	1
8[c]	8.00 g	1.1 eq.	K_2CO_3	72 mL	180 °C / 2.5 h	6%	1
9[c]	5.00 g	1.5 eq.	K_2CO_3	40 mL (DMF)	149 °C / 28 h	0%	1

[a]0.6 eq. LiBr has been used in all reactions. [b]Isolated yields. Average yields from several reactions (where appropriate). [c]Conventional heating in an autoclave.

Ethyl 5,6,7,8-tetrafluorobenzo[b]thieno[3,4-e][1,4]dioxine-1-carboxylate (**F_4-23**)

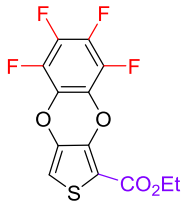

F_4-23

Compound **F_4-23** was isolated from a tag after an isolation of **F_4-PheDOT**. After purification of **F_4-PheDOT**, the resiude from the column was washed with DCM, the crude product was collected and was purified twice by flash chromatography on a silica gel (eluent: gradient from PE to PE:DCM, 1:1) to afford pure compound **F_4-23**.

R_f (PE:DCM, 1:1) = 0.32.

^{1}H NMR (400 MHz, $CDCl_3$): δ (ppm) 6.83 (1H, s, H^{T5}), 4.38 (2H, q, *J* = 7.1 Hz, CH_2), 1.40 (3H, t, *J* = 7.1 Hz, CH_3).

^{13}C NMR (100 MHz, $CDCl_3$): δ (ppm) {only thiophene aromatic carbons have been detected; benzene carbons appear as very low intensity multiplets due to H–F coupling}, 160.12 (s, C=O), 139.00 (s, C), 139.0–137.8 (m, C–F, C^B)136.36 (s, C), 137.0–135.5 (m, C–F, C^B), 128.2–127.8 (m, C–F, C^B), 108.12 (s, CH, C^{T5}), 61.65 (CH_2), 14.19 (CH_3).

^{19}F NMR (376 MHz, $CDCl_3$); δ (ppm) –161.64 (1F, ddd, *J* = 21.6, 5.7, 2.9 Hz, $F^{B3/6}$), –163.13 (1F, ddd, *J* = 21.5, 5.6, 3.3 Hz, $F^{B3/6}$), –164.75 (1F, td, *J* = 21.7, 2.8 Hz, $F^{B4/5}$), –165.30 (1F, td, *J* = 21.7, 3.3 Hz, $F^{B4/5}$).

MS (EI+): *m/z* 334.01; calcd for $C_{13}H_6F_4O_4S$: 333.99.

1,2,3,4,5,6-Hexafluoronaphtho[2,1-b]thieno[3,4-e][1,4]dioxine {F_6-NaphDOT(1,2)}
and
5,6,7,8,9,10-hexafluoronaphtho[2,3-b]thieno[3,4-e][1,4]dioxine {F_6-NaphDOT(2,3)}

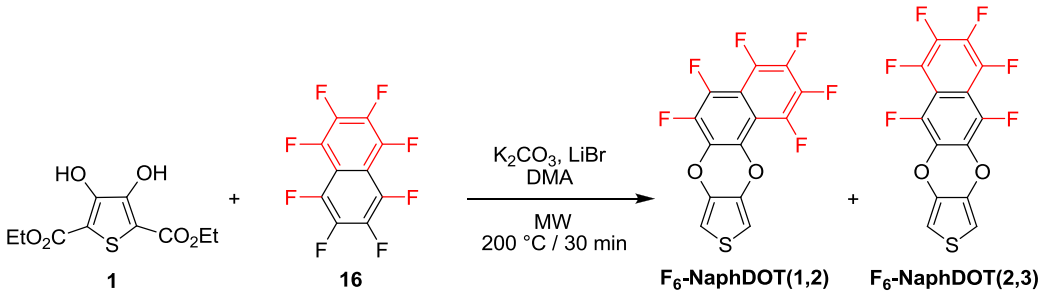

Diethyl 3,4-dihydroxy-2,5-thiophenedicarboxylate (**1**) (101 mg, 0.39 mmol, 1.00 eq.), K_2CO_3 (55.7 mg, 0.40 mmol, 1.03 eq.), octafluoronaphthalene (**16**) (115 mg, 0.42 mmol, 1.09 eq.), LiBr (20 mg, 0.23 mmol, 0.60 eq.) and DMA (1.0 mL) were placed in a 10 mL MW reaction tube. The tube was sealed, degassed by bubbling with nitrogen (stirring) for 3 min and heated with stirring in a microwave reactor at 200 °C for 30 min. The mixture was cooled to room temperature and poured into DCM (20 mL). The solution was filtered from insoluble material, the filtrate was washed with water (5 × 15 mL), dried over $MgSO_4$, filtered and the solvent was removed by evaporation. The residue, which contains a mixture of isomers **F_6-NaphDOT(1,2)** and **F_6-NaphDOT(2,3)** (two closely spaced spots on TLC in non-polar solvents, which are not separated in more polar solvents) was purified by column chromatography on silica gel (eluent: PE) first eluting compound **F_6-NaphDOT(1,2)** (16.6 mg, 12.2% yield, white solid), followed by compound **F_6-NaphDOT(2,3)** (28.9 mg, 21.3% yield, white solid). The total combined yield of both isomers was 33.5% (with a ratio of **F_6-NaphDOT(1,2):F_6-NaphDOT(2,3)** ≈ 1:2). Both isomers, especially **F_6-NaphDOT(2,3)**, are very insoluble materials, so their flash chromatography separation can only be performed on a small scale.

Non-symmetric compound **F_6-NaphDOT(1,2):**
^{1}H NMR (400 MHz, $CDCl_3$): δ (ppm) 6.64 (1H, d, $J_{T2–T5}$ = 3.6 Hz, $H^{T2/5}$), 6.62 (1H, d, $J_{T2–T5}$ = 3.6 Hz, $H^{T2/5}$).
^{13}C NMR (100 MHz, $CDCl_3$): δ (ppm) 137.22, 136.40, 103.32 (2C, $C^{T2,5}$), {identification of other peaks in the region of 133–144 ppm was difficult because of low solubility of the compound and low intensity of the signals due to C–F coupling}.
^{19}F NMR (376 MHz, $CDCl_3$): δ (ppm) –144.0–144.2 (m, 1F), –144.5–147.9 (m, 1F), –150.3–150.6 (m, 1F), –155.1–155.2 (m, 1F), –157.0–157.2 (m, 1F), –157.4–157.6 (m, 1F).
MS (EI+): *m/z* 348.01 (M^+, 100.0%); calcd. for $C_{14}H_2F_6O_2S$: 347.97.

Symmetric compound **F_6-NaphDOT(2,3):**
^{1}H NMR (400 MHz, $CDCl_3$, TMS): δ (ppm) 6.74 (2H, s, $H^{T2,5}$).
^{13}C NMR (DEPTQ, 100 MHz, $CDCl_3$): δ (ppm) 103.5 (2C, $C^{T2,5}$), {an identification of other peaks was difficult because of very low solubility of the compound and low intensity of the signals due to C–F coupling}.
^{19}F NMR (376 MHz, $CDCl_3$): δ (ppm) –146.5–146.8 (m, 2F), –147.7–148.1 (m, 2F), –157.6–157.8 (m, 2F).
MS (EI+): *m/z* 348.05 (M^+, 100.0%); calcd. for $C_{14}H_2F_6O_2S$: 347.97.

5,6,7,8-Tetrafluoro-9H-benzo[e]thieno[3,4-b][1,4]dioxepine (F$_4$-BnDOT)

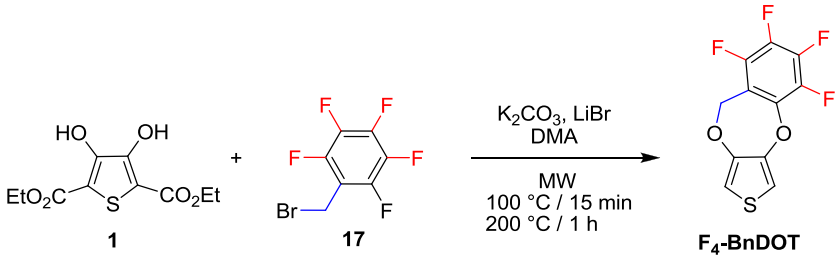

Diethyl 3,4-dihydroxy-2,5-thiophenedicarboxylate (**1**) (1.018 g, 3.91 mmol, 1.00 eq.), K_2CO_3 (0.558 g, 4.04 mmol, 1.03 eq.), 2,3,4,5,6-pentafluorobenzylbromide (**17**) (1.170 g, 4.48 mmol, 1.15 eq.), LiBr (0.215 g, 2.48 mmol, 0.63 eq.) and DMA (10 mL) were placed in a 35 mL MW tube The tube was sealed, degassed by bubbling with nitrogen (stirring) for 3 min and heated with stirring in a microwave reactor in 4 steps: 1) 1) 50 °C / 5 min; 2) 80 °C / 15 min; 3) 100 °C / 15 min, 4) 200°C / 1 h. After cooling, the mixture was diluted with water (100 mL), stirred for 1h and the solid was filtered off by suction. The solid was transferred into DCM (150 mL), stirred for 30 min, dried over $MgSO_4$, filtered and the solvent was evaporated. The crude product was purified by flash chromatography on silica gel (eluent: PE) to yield compound **F$_4$-BnDOT** (0.120 g, 11.1%) as a white solid.

^{1}H NMR (400 MHz, $CDCl_3$): δ (ppm) 6.87 (1H, d, $J_{T2–T5}$ = 4.2 Hz, $H^{T2/5}$), 6.44 (1H, d, $J_{T2–T5}$ = 4.2 Hz, $H^{T2/5}$), 5.24 (2H, d, $J_{H–F}$ = 1.5 Hz, CH_2).

^{13}C NMR (100 MHz $^{13}C\{^1H\}$): δ (ppm) 145.35 (s), 145.0 (m), 142.7 (m), 142.31 (s), 140.8 (m), 140.3 (m), 138.5 (m), 136.2 (m), 114.40 (dd, J =16.1 Hz, J = 3.6 Hz), 108.76 (CH, s, $H^{T2/5}$), 104.39 (CH, s, $C^{T2/5}$), 60.38 (d, $^3J_{C–F}$ = 4.3 Hz, CH_2).

^{19}F NMR (376 Hz): δ (ppm) –146.16 (1F, ddd, J = 22.5 Hz, 11.1 Hz, 1.9 Hz), –154.91 (1F, td, J = 20.8 Hz, 1.9 Hz), –157.61 (1F, dd, J = 21.1 Hz, 10.5 Hz), –162.65 (1F, dd, J = 22.2 Hz, 20.7 Hz).

MS (EI+): *m/z* 276.05 (M^+, 100%); calcd. for $C_{11}H_4F_4O_2S$: 275.99.

3-Trifluoromethylthieno[3',4':5,6][1,4]dioxino[2,3-b]pyridine (5CF$_3$-PyDOT)

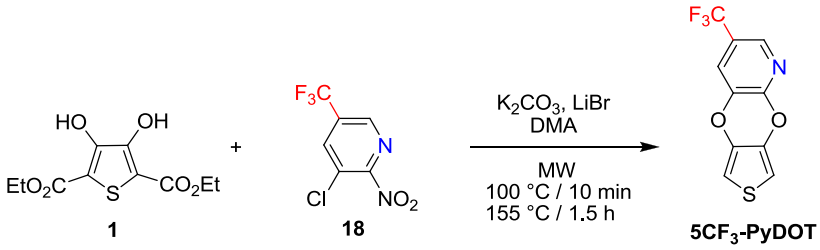

Diethyl 3,4-dihydroxy-2,5-thiophenedicarboxylate (**1**) (1.000 g, 3.84 mmol, 1.00 eq.), K_2CO_3 (531 mg, 3.84 mmol, 1.00 eq.), 2,3-difluoro-6-trifluoromethylpyridine (**18**) (778 mg, 4.25 mmol, 1.11 eq.), LiBr (210 mg, 2.42 mmol, 0.63 eq.) and DMA (11 mL) were placed in a 35 mL MW tube The tube was sealed, degassed by bubbling with nitrogen (stirring) for 3 min and heated with stirring in a microwave reactor in 2 steps: 1) 100°C / 10 min, 155°C / 90 min. After cooling, a clear, almost colorless layer was formed at the bottom of the tube. The mixture was partitioned between DCM (80 mL) and water (70 mL) (full dissolution was observed). The organic layer was separated, washed with water (3 × 25 mL), dried over $MgSO_4$, filtered and the solvent was evaporated. The crude product was analyzed by GC-MS, which showed the desired product, together with small amount of one by-product. The crude product was purified by flash chromatography on silica gel (eluent: PE to PE:EA, 9:1) to yield a relatively pure sample of compound **5CF$_3$-PyDOT** (841 mg, 96%) followed by an impure fraction (71 mg). The first fraction was additionally purified by flash chromatography on silica gel (eluent: PE:EA, 1:1) to afford pure compound **5CF$_3$-PyDOT** (641 mg, 74%) as a white solid.

^{1}H NMR (400 MHz, $CDCl_3$): δ (ppm) 8.16 (br.s, $H^{P5/6}$), 7.44 (d, $J_{P4–P6}$ = 1.9 Hz, $H^{P5/6}$), 6.65 (1H, d, $J_{T2–T5}$ = 3.6 Hz, $H^{T2/5}$), 6.55 (1H, d, $J_{T2–T5}$ = 3.6 Hz, $H^{T2/5}$).
^{13}C NMR (100 MHz, $CDCl_3$): δ (ppm) 150.55 (C^{P2}), 139.02 (CH, q, $^{3}J_{C–F}$ = 4.5 Hz, $C^{P4/6}$), 137.90 ($C^{T3/4}$), 137.04 ($C^{T3/4}$), 136.89 (C^{P3}), 124.00 (q, $^{2}J_{C–F}$ = 33.8 Hz, C^{P5}), 122.79 (q, $^{1}J_{C–F}$ = 272.0 Hz, CF_3), 121.92 (CH, q, $^{3}J_{C–F}$ = 3.3 Hz, $C^{P4/6}$), 103.75 (CH, $C^{T2/5}$), 102.61 (CH, $C^{T2/5}$).
^{19}F NMR (376 MHz, $CDCl_3$): δ (ppm) –63.18 (s, CF_3).
MS (EI+): *m/z* 259.00 (M^+, 100%); calcd. for $C_{10}H_4F_3NO_2S$: 258.99.

2,3-Dichlorothieno[3',4':5,6][1,4]dioxino[2,3-b]pyridine (56Cl$_2$-PyDOT)

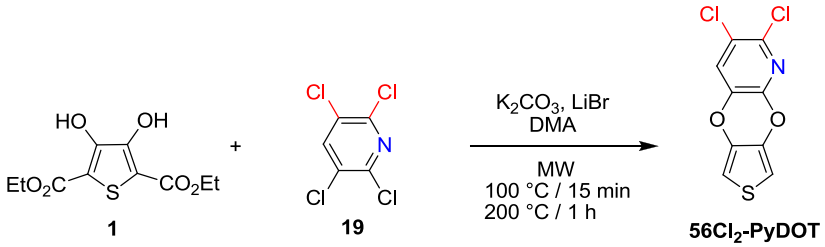

Diethyl 3,4-dihydroxy-2,5-thiophenedicarboxylate (**1**) (1.001 g, 3.85 mmol, 1.00 eq.), K_2CO_3 (0.544 g, 3.94 mmol, 1.02 eq.), 2,3,5,6-tetrachloropyridine (**19**) (0.920 g, 4.24 mmol, 1.10 eq.), LiBr (0.222 g, 2.56 mmol, 0.66 eq.) and DMA (10 mL) were placed in a 35 mL MW tube. The tube was sealed, degassed by bubbling with nitrogen (stirring) for 3 min and heated with stirring in a microwave reactor in 4 steps: 1) 50 °C / 5 min, 2) 80 °C / 15 min, 3) 100 °C / 15 min, 4) 200°C / 1 h. After cooling, the mixture was poured into water (100 mL) and stirred for 1 h. The solid was filtered off, dissolved in DCM (150 mL), dried over $MgSO_4$, filtered and the solvent was evaporated. The crude product was purified by flash chromatography on silica gel (eluent: toluene) to yield compound **56Cl$_2$-PyDOT** (166 mg, 16.6%) as light-yellow crystals. An analytically pure sample was obtained by repeated flash chromatography with PE:DCM, 2:1.
^{1}H NMR (400 MHz, $CDCl_3$): δ (ppm) 7.36 (1H, s, H^{P4}), 6.61 (1H, d, $J_{T2–T5}$ = 3.6 Hz, $H^{T2/5}$), 6.53 (1H, d, $J_{T2–T5}$ = 3.6 Hz, $H^{T2/5}$).
^{13}C NMR (100 MHz, $CDCl_3$): δ (ppm) 145.50 ($C^{P2/3/5/6}$), 139.01 ($C^{P2/3/5/6}$), 137.76 ($C^{T3/4}$), 136.85 ($C^{T3/4}$), 136.01 ($C^{P2/3/5/6}$), 127.06 (CH, C^{P4}), 124.89 ($C^{P2/3/5/6}$), 103.66 (CH, $C^{T2/5}$), 102.71 (CH, $C^{T2/5}$).
MS (EI+): *m/z* 259.00 (M^+, 100%, $^{35}Cl/^{35}Cl$), 261.00 (68%, $^{35}Cl/^{37}Cl$), 262.95 (13%, $^{37}Cl/^{37}Cl$), calcd. for $C_9H_3Cl_2NO_2S$: 258.93 (100.0%), 260.92 (68.4%), 262.92 (13.2%).

Thieno[3',4':5,6][1,4]dioxino[2,3-b]pyrazine (PzDOT)

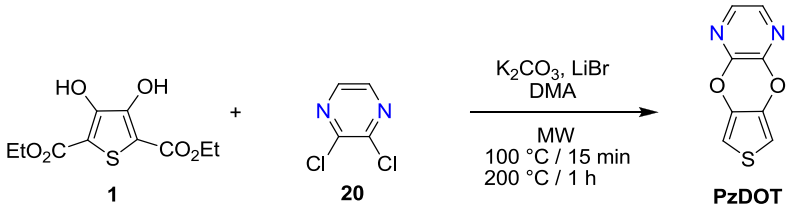

Diethyl 3,4-dihydroxy-2,5-thiophenedicarboxylate (**1**) (1.001 g, 3.85 mmol, 1.00 eq.), K_2CO_3 (0.531 g, 3.84 mmol, 1.00 eq.), 2,3-dichloropyrazine (**20**) (0.594 g, 3.99 mmol, 1.04 eq.), LiBr (0.205 g, 2.36 mmol, 0.61 eq.) and DMA (10 mL) were placed in a 35 mL MW tube. The tube was sealed, degassed by bubbling with nitrogen (stirring) for 3 min and heated with stirring in a microwave reactor in 4 steps: 1) 50 °C / 5 min, 2) 80 °C / 15 min, 3) 100 °C / 15 min, 4) 200 °C / 1 h. After cooling, the mixture was diluted with DCM (100 mL), stirred for 1 h and filtered to remove insoluble materials. The filtrate was washed with water (6 × 150 mL), dried over $MgSO_4$, filtered and the solvent was evaporated to dryness. The crude product was purified by flash chromatography on silica gel (eluent: PE:EA, 9:1) to yield compound **PzDOT** (0.283 g, 38.2%) as a white crystalline solid.

^{1}H NMR (400 MHz, $CDCl_3$, TMS): δ (ppm) 7.88 (2H, s, $H^{P5,6}$), 6.66 (2H, s, $H^{T2,5}$).

^{13}C NMR (100 MHz, $CDCl_3$): δ (ppm) 144.91 ($C^{P2,3}$), 137.51 ($C^{T3,4}$), 137.09 (CH, $C^{P5,6}$), 103.54 (CH, $C^{T2,5}$).

MS (EI+): *m/z* 192.01 (100%); calcd. for $C_8H_4N_2O_2S$: 192.00.

Thieno[3',4':5,6][1,4]dioxino[2,3-b]quinoxaline (QxDOT)

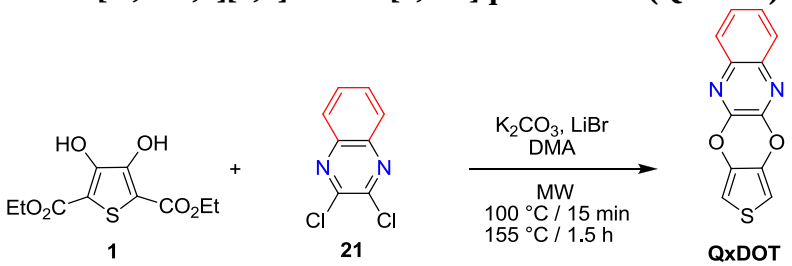

Diethyl 3,4-dihydroxy-2,5-thiophenedicarboxylate (**1**) (999 mg, 3.84 mmol, 1.00 eq.), K_2CO_3 (534 mg, 3.86 mmol, 1.01 eq.), 2,3-dichloroquinoxaline (**21**) (839 mg, 4.22 mmol, 1.10 eq.), LiBr (195 mg, 2.25 mmol, 0.6 eq.) and DMA (12 mL) were placed in a 35 mL MW tube. The tube was sealed, degassed by bubbling with nitrogen (stirring) for 3 min and heated with stirring in a microwave reactor in 4 steps: 1) 50 °C / 5 min, 2) 80 °C / 5 min, 3) 100 °C / 15 min, 4) 155 °C / 1.5 h. After cooling, the mixture was diluted with DCM (120 mL) and water (25 mL), stirred and filtered through glass wool to remove insoluble materials. The organic layer was separated, washed with water (3 × 25 mL), dried with $MgSO_4$, filtered and the solvent was evaporated. The crude product was purified by column chromatography on a silica gel (eluent: gradient from PE to DCM) to yield compound **QxDOT** (388 mg, 41.7%) as a yellowish powder.

^{1}H NMR (400 MHz, $CDCl_3$): δ (ppm) 7.85 (2H, dd, J = 6.3 Hz, 3.5 Hz, $H^{B3,6/B4,5}$), 7.62 (2H, dd, J = 6.3 Hz, 3.5 Hz, $H^{B3,6/B4,5}$), 6.75 (2H, s, $H^{T2,5}$).

^{13}C NMR (100MHz, $CDCl_3$): δ (ppm) 143.15 ($C^{P2,3}$), 138.66 ($C^{P5,6}$), 137.18 ($C^{T3,4}$), 129.09 (CH, $C^{B3,5/B4,5}$), 127.34 (CH, $C^{B3,5/B4,5}$), 103.70 (CH, $C^{T2,5}$).

MS (TOF EI+): *m/z* 242.09 (M^+, 100%); calcd for $C_{12}H_6N_2O_2S$: 242.01.

6-Bromo-5,8-difluorobenzo[b]thieno[3,4-e][1,4]dioxine (**3Br,45F$_2$-PheDOT**) and **5,8-difluorobenzo[b]thieno[3,4-e][1,4]dioxine** (**45F$_2$-PheDOT**)

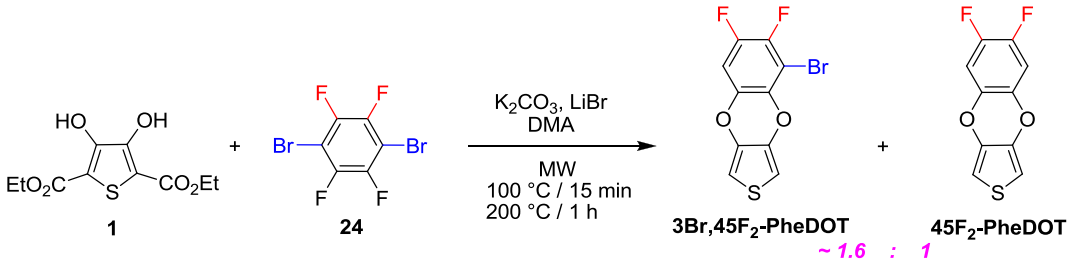

Diethyl 3,4-dihydroxy-2,5-thiophenedicarboxylate (**1**) (1.031 g, 3.96 mmol, 1.00 eq.), K_2CO_3 (0.546 g, 3.95 mmol, 1.00 eq.), 1,4-dibromo-2,3,5,6-tetrafluorobenzene (**24**) (1.216 g, 3.95 mmol, 1.00 eq.), LiBr (0.208 g, 2.40 mmol, 0.61 eq.) and DMA were placed in a 35 mL MW tube. The tube was sealed, degassed by bubbling with nitrogen (stirring) for 3 min and heated with stirring in a microwave reactor (80 W) in 4 steps: 1) 50 °C / 5 min, 2) 80 °C/ 5 min, 3) 100 °C/ 15 min, 4) 200 °C / 1 h. After cooling, the reaction mixture was transferred into water (100 mL), stirred for 1 h and the precipitate was filtered off. This solid was transferred into DCM (150 mL), stirred for 1 h for dissolution, dried over $MgSO_4$, filtered and the solvent was evaporated. The crude was purified by column chromatography on silica gel (eluent: PE) to yield a light-cream color solid (0.055 g, ~5%). The GC-MS analysis of the sample showed a mixture of two products, **3Br,45F$_2$-PheDOT** and **45F$_2$-PheDOT**, in a ratio of ca. 1.6:1. The sample showed one spot on TLC (with the same R_f as authentic **45F$_2$-PheDOT** synthesized independently in another experiment, see above) and we were unable to separate these products by flash chromatography. As the yield was low, partial debromination occurred during the reaction and the experiment did not give the expected **36Br$_2$,45F$_2$-PheDOT**, we did not make further attempts to separate the products.

3Br,45F$_2$-PheDOT:	***45F$_2$-PheDOT:***
MS (EI+): *m/z* 305.95 (M^+, 100%, ^{79}Br), 303.90 (95.5%, ^{81}Br); calcd. for $C_{10}H_3BrF_2O_2S$: 305.90 (100.0%, ^{79}Br), 303.90 (97.8%, ^{81}Br).	MS (EI+): *m/z* 226.00 (M^+, 100%); calcd. for $C_{10}H_4F_2O_2S$: 225.99.
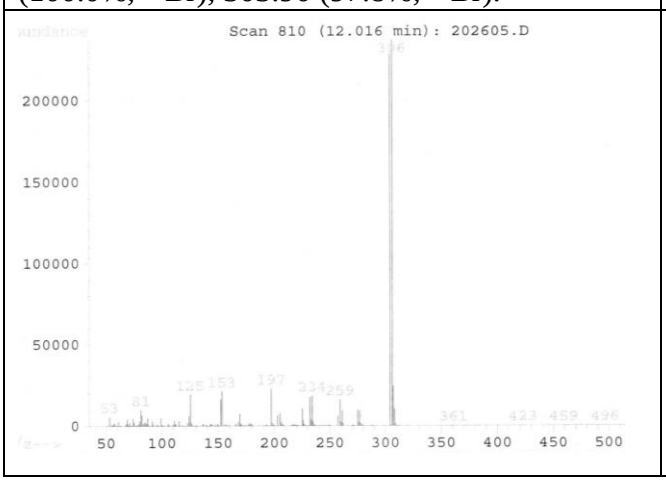	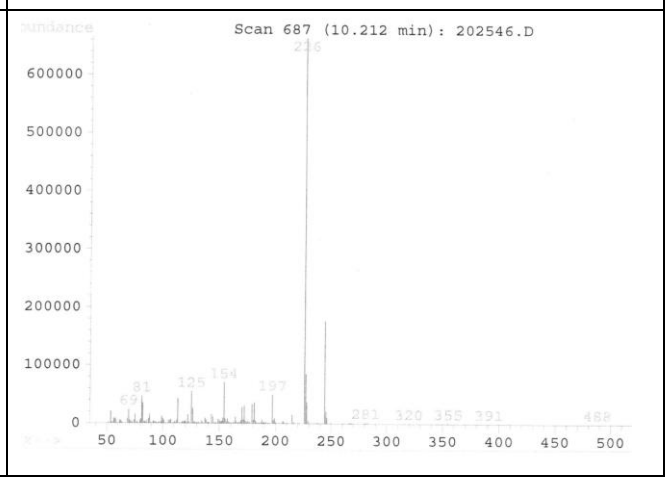

6,7-Dibromobenzo[b]thieno[3,4-e][1,4]dioxine (45Br$_2$-PheDOT), and 6-bromobenzo[b]thieno[3,4-e][1,4]dioxine (4Br-PheDOT)

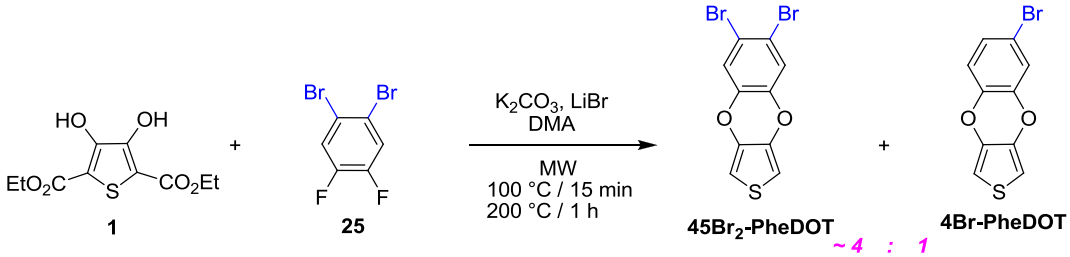

Diethyl 3,4-dihydroxy-2,5-thiophenedicarboxylate (**1**) (1.013 g, 3.89 mmol, 1.00 eq.), K_2CO_3 (0.552 g, 3.99 mmol, 1.03 eq.), 1,2-dibromo-4,5-difluorobenzene (**25**) (1.106 g, 4.07 mmol, 1.04eq.), LiBr (0.222 g, 2.56 mmol, 0.66 eq.) and DMA (10 mL) were placed in a 35 mL MW tube. The tube was sealed, degassed by bubbling with nitrogen (stirring) for 3 min and heated with stirring in a microwave reactor (80 W) in 4 steps: 1) 50 °C / 5 min, 2) 80 °C / 5 min, 3) 100 °C / 15 min, 4) 200 °C/ 1 h. Another batch of diethyl 3,4-dihydroxy-2,5-thiophenedicarboxylate (**1**) (1.012 g, 3.89 mmol, 1.00 eq.), K_2CO_3 (0.539 g, 3.90 mmol, 1.00 eq.), 1,2-dibromo-4,5-difluorobenzene (**29**) (1.137 g, 4.18 mmol, 1.08eq.), LiBr (0.209 g, 2.41 mmol, 0.62 eq.) and DMA (10 mL) was run at the same conditions. After cooling, the combined reaction mixtures were poured into water (200 mL), stirred for 1 h and the precipitate was filtered off. This solid was transferred into DCM (200 mL), stirred for 1 h, dried over $MgSO_4$, filtered and the solvent was evaporated. The crude product was purified by flash chromatography on silica gel (eluent: PE) to yield an off-white (light cream color) solid (0.258 g, ~10%). The GC-MS and ^{1}H NMR analyses of the sample showed a mixture of two products, **45Br$_2$-PheDOT** and **4Br-PheDOT**, in a ratio of ca. 4:1. The sample showed one spot on TLC and we were unable to separate these products by flash chromatography. In the ^{1}H NMR of the mixture, partly debrominated compound **4Br-PheDOT** was identified by comparison with an authentic sample prepared independently (see above) and **45Br$_2$-PheDOT** was identified by comparison with an authentic sample prepared by reaction of 4,5-dibromocatechol with 3,4-dimethoxythiophene.[13] As partial debromination occurred during the reaction and the experiment did not give the expected **45Br$_2$-PheDOT** in a pure form, we did not make further attempts to separate these products.

45Br$_2$-PheDOT: MS (EI+): *m/z* 347.95 (M$^+$, 100%, ^{79}Br/^{79}Br), 349.90 (53.3%, ^{79}Br/^{781}Br), 345.90 (50.2%, ^{81}Br/^{81}Br); calcd. for C10H4Br2O2S: 347.83 (100.0%, ^{79}Br/^{79}Br), 345.83 (50.1%, ^{79}Br/^{81}Br), 349.83 (48.4%, ^{81}Br/^{81}Br).	***4Br-PheDOT:*** MS (EI+): *m/z* 270.00 (M$^+$, 100%, ^{79}Br), 267.95 (90.0%, ^{81}Br); calcd. for $C_{10}H_5BrO_2S$: 269.92 (100.0%, ^{79}Br), 267.92 (97.8%, ^{81}Br).
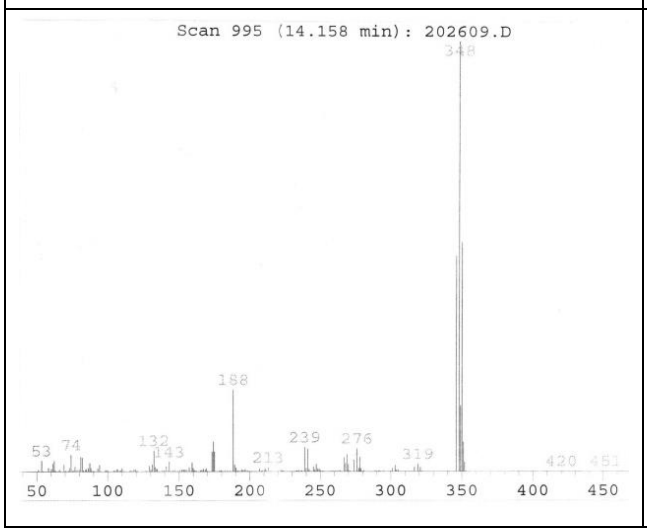	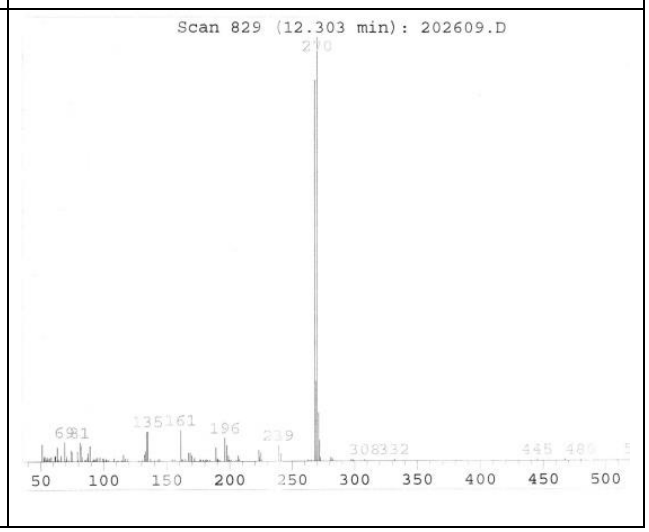

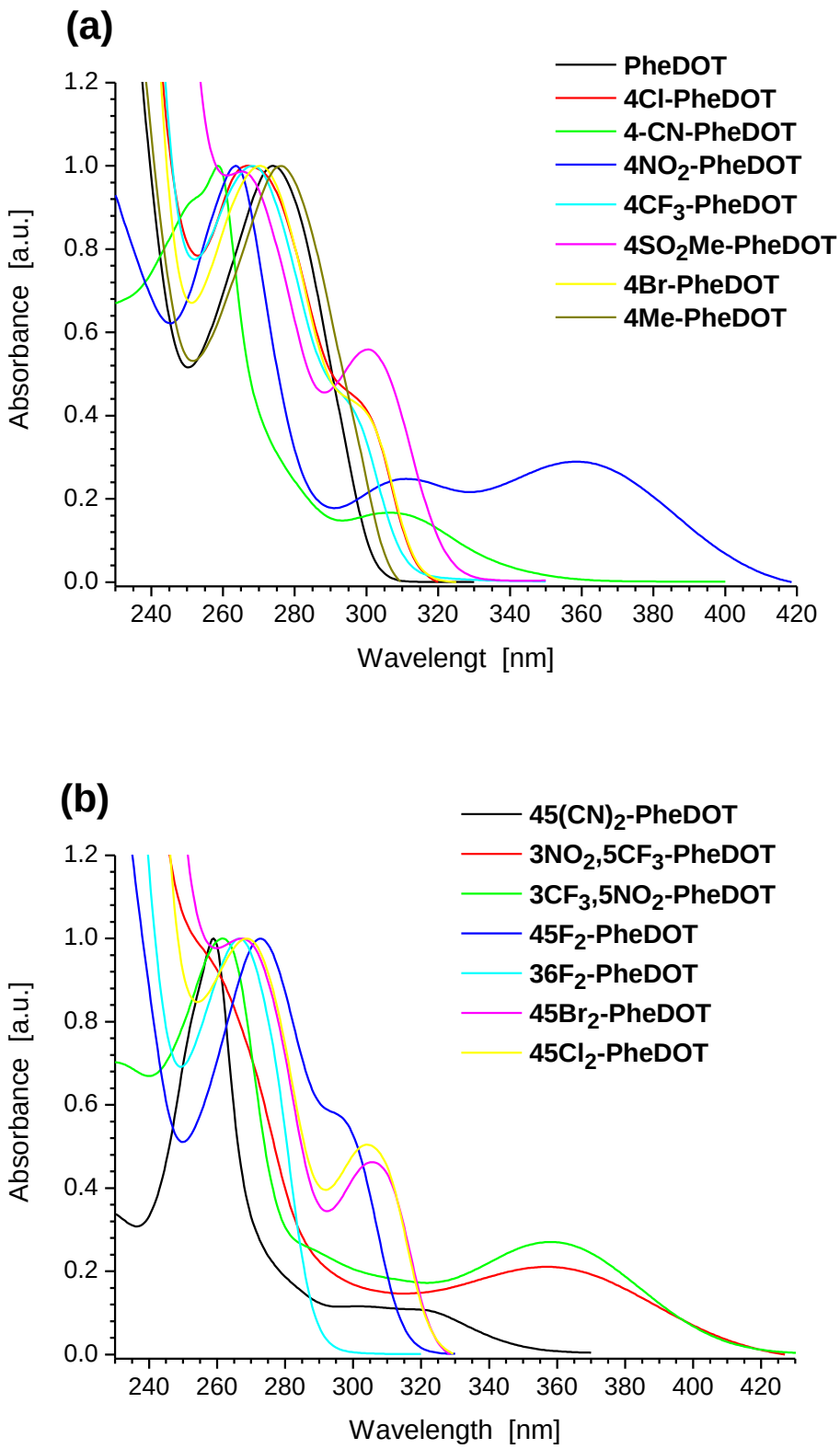

Figure S1. UV-Vis electron absorption spectra of mono- and disubstituted (at the benzene ring) **EWG-PheDOT** monomers in dichloromethane. The spectra are normalized to the maxima in the region of 260–280 nm (**45Br$_2$-PheDOT** and **45Cl$_2$-PheDOT** have been synthesized according to Ref. 13).

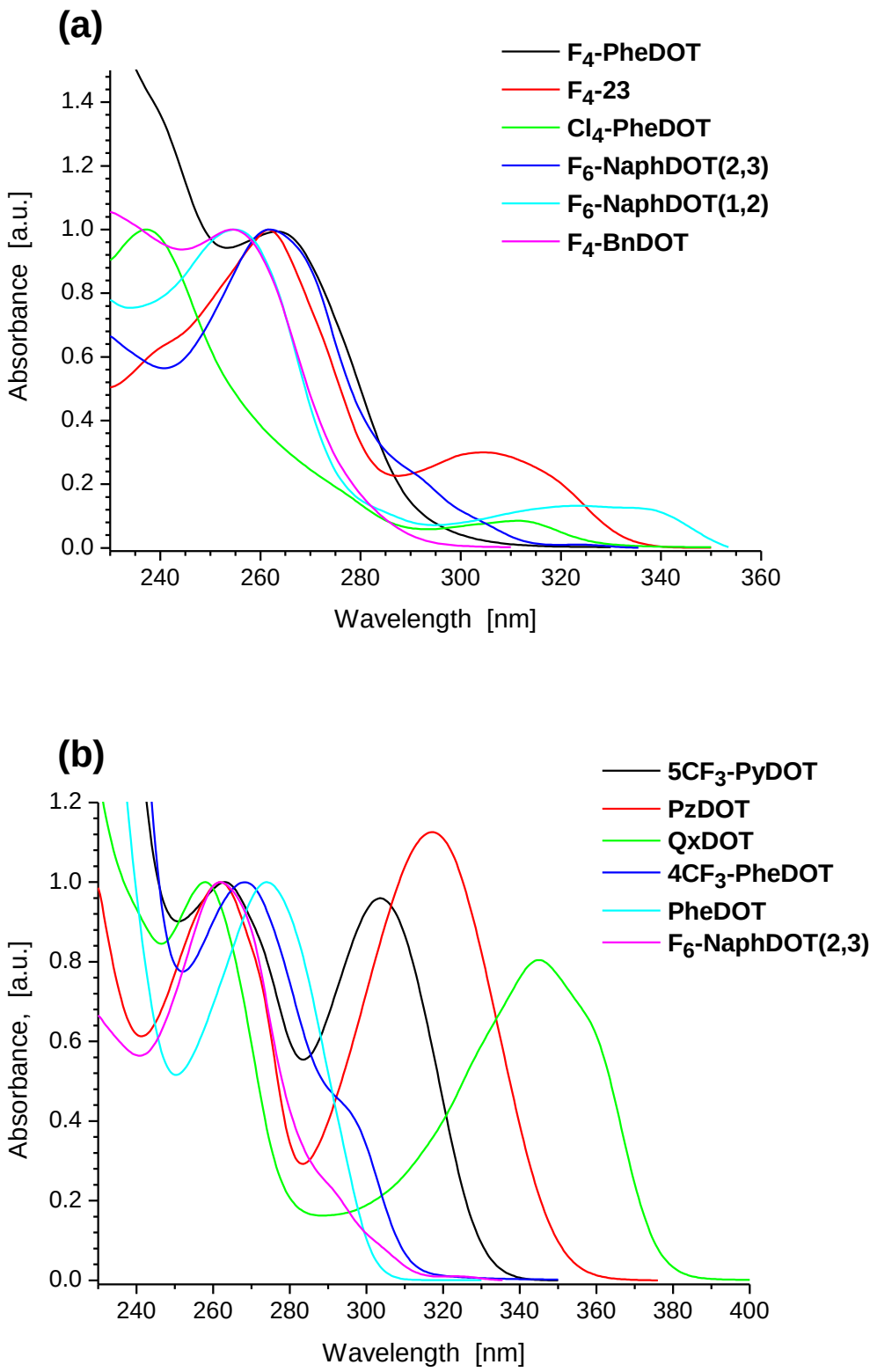

Figure S2. UV-Vis electron absorption spectra of **ArDOT** monomers in dichloromethane. The spectra are normalized to the maxima in the region of 240–280 nm.

Table S4. Crystal data and structure refinement parameters.

Compound	**F_4-23**	**36F_2-PheDOT**	**F_4-PheDOT**	**3NO_2,5CF_3-PheDOT**	**5CF_3-PyDOT**	**56Cl_2-PyDOT**	**PzDOT**	**QxDOT**
Empirical formula	$C_{13}H_6F_4O_4S$	$C_{10}H_4F_2O_2S$	$C_{10}H_2F_4O_2S$	$C_{11}H_4F_3NO_4S$	$C_{10}H_4F_3NO_2S$	$C_9H_3Cl_2NO_2S$	$C_8H_4N_2O_2S$	$C_{12}H_6N_2O_2S$
Formula weight	334.24	226.19	262.18	303.21	259.20	260.08	192.19	242.25
Temperature/K	120.0	120.0	120.0	200.0	120.0	120.0	120.0	120.0
Crystal system	orthorhombic	orthorhombic	triclinic	triclinic	monoclinic	monoclinic	monoclinic	monoclinic
Space group	$P2_12_12_1$	Pnma	P-1	P-1	$P2_1/n$	C2/c	$P2_1/c$	$P2_1/n$
a/Å	6.2517(5)	19.8371(6)	5.8022(9)	6.2118(10)	6.0124(2)	18.0302(5)	17.3384(3)	4.43002(16)
b/Å	7.3716(5)	11.5899(4)	7.6384(9)	7.0519(13)	22.0636(7)	5.89058(13)	6.74570(10)	21.1250(7)
c/Å	26.471(2)	3.70810(10)	11.243(2)	14.316(2)	7.2454(3)	18.9311(6)	14.5495(4)	10.8195(3)
α/°	90.00	90.00	108.558(15)	79.354(14)	90.00	90.00	90.00	90.00
β/°	90.00	90.00	94.513(15)	79.598(13)	97.282(3)	110.094(3)	114.8015(15)	92.714(3)
γ/°	90.00	90.00	104.161(12)	65.073(16)	90.00	90.00	90.00	90.00
Volume/$Å^3$	1219.94(16)	852.53(5)	451.33(13)	555.18(15)	953.39(6)	1888.26(9)	1544.75(6)	1011.40(6)
Z	4	4	2	2	4	8	8	4
ρ_{calc}g/cm^3	1.820	1.762	1.929	1.814	1.806	1.830	1.653	1.591
μ/mm^{-1}	0.335	0.384	0.407	0.348	0.373	0.880	0.378	0.308
F(000)	672.0	456.0	260.0	304.0	520.0	1040.0	784.0	496.0
Reflections collected	25897	15895	5934	5400	14144	14968	34104	14911
Independent reflections, R_{int}, R_σ	3576, 0.0302, 0.0175	1181, 0.0762, 0.0325	2173, 0.0568, 0.0713	2411, 0.0331, 0.0501	2527, 0.0473, 0.0353	2764, 0.0440, 0.0320	4513, 0.0729, 0.0542	2675, 0.0634, 0.0498
Data/restraints/parameters	3576/0/224	1181/0/78	2173/0/154	2411/21/192	2527/0/170	2764/0/148	4513/0/236	2675/0/178
Goodness-of-fit on F^2	1.071	1.060	1.019	1.054	1.044	1.048	1.032	1.018
R_1 indexes [I≥2σ (I)]	0.0259	0.0370	0.0581	0.0830	0.0357	0.0309	0.0433	0.0438
wR_2 indexes [all data]	0.0690	0.0910	0.1554	0.2398	0.0864	0.0743	0.0952	0.1033
Flack parameter	0.00(5)							

Figure S3 *(4 pages)*: Molecular and crystal structures of compounds **F_4-23, 36F_2-PheDOT, F_4-PheDOT, 3NO_2,4CF_3-PheDOT, 56Cl_2PyDOT, 5CF_3-PheDOT, PzDOT** and **QxDOT**.

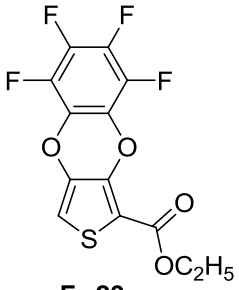

F_4-23

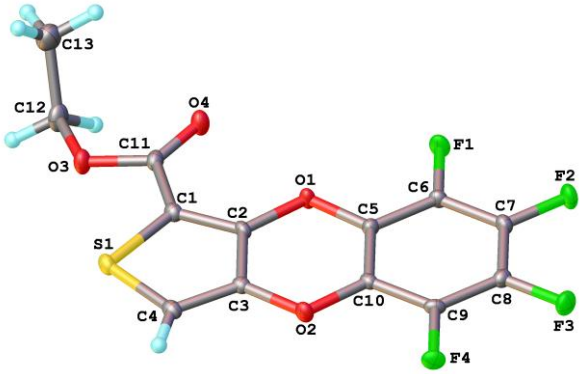

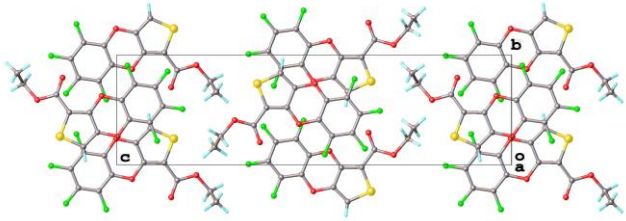

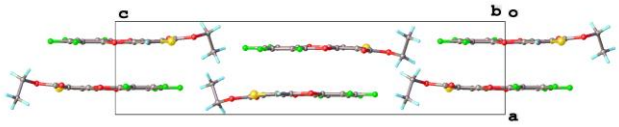

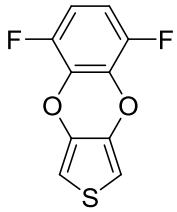

36F_2-PheDOT

(non-centrosymmetric structure; second polymorph crystal is seen)

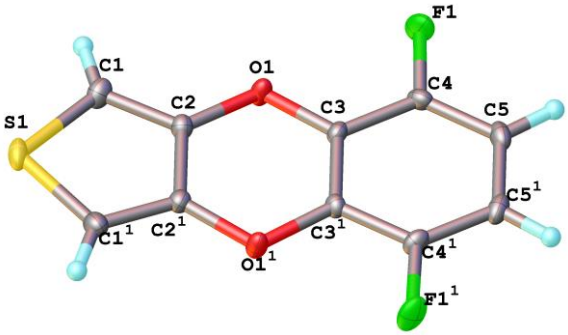

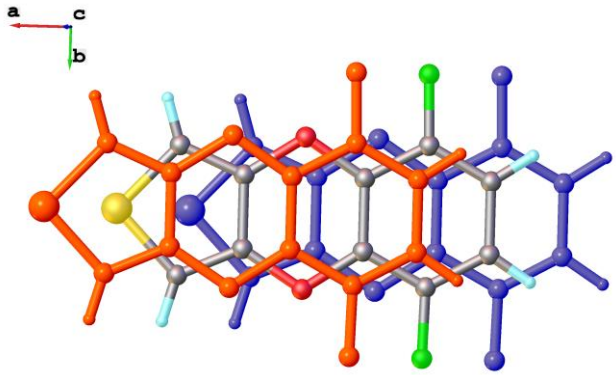

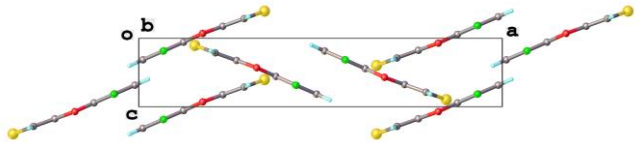

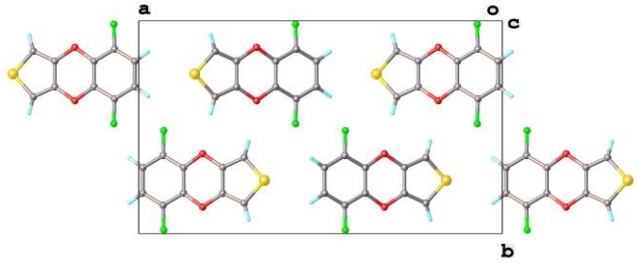

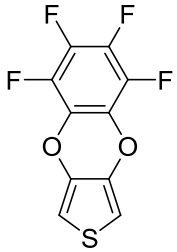

F_4-PheDOT

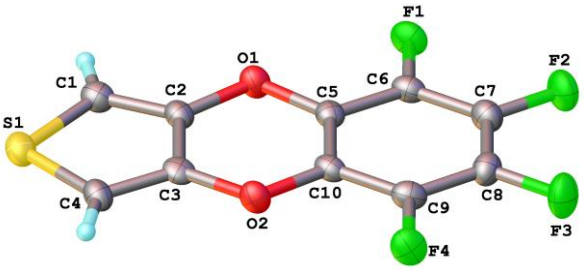

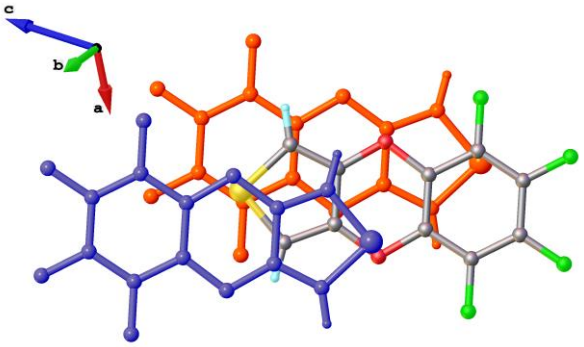

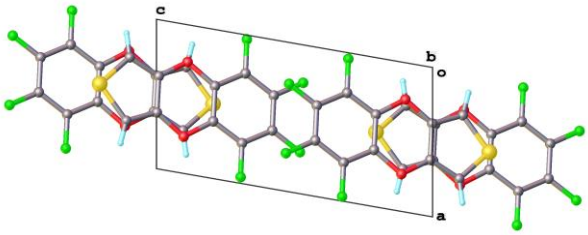

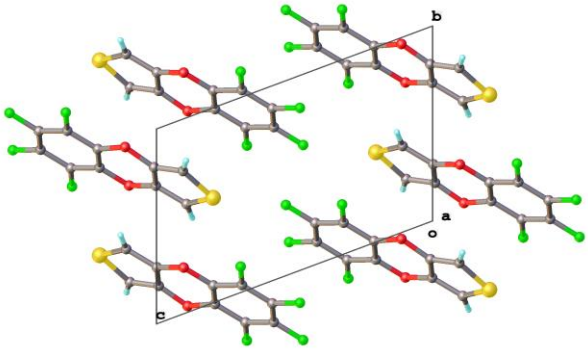

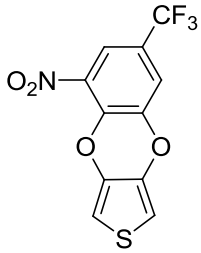

$3NO_2,4CF_3$-PheDOT

(some disorder of NO_2/CF_3 in a crystal)

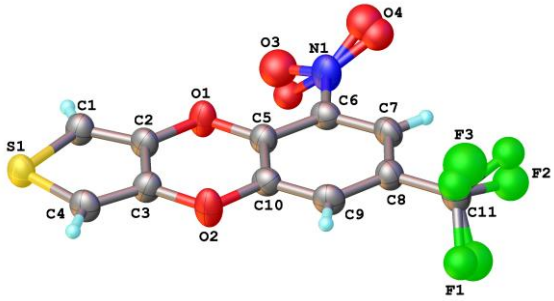

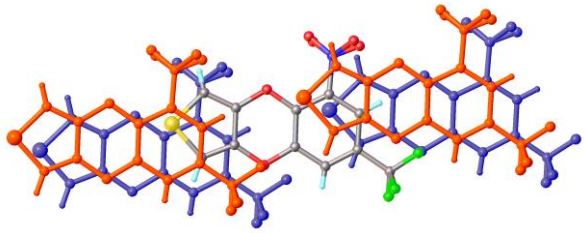

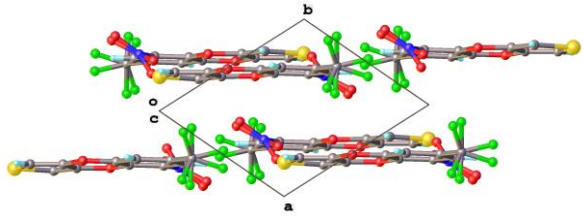

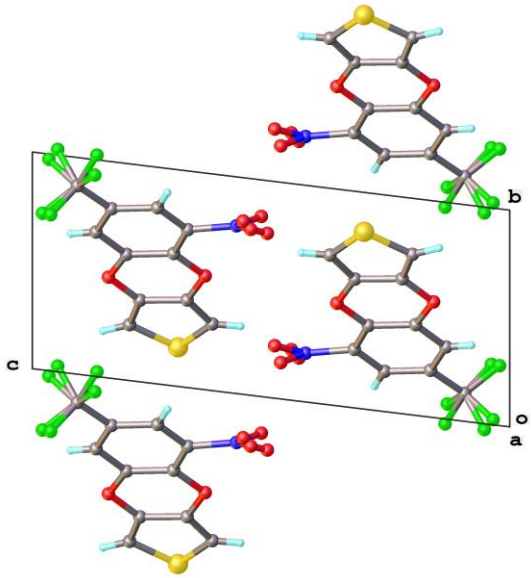

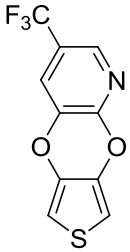

5CF$_3$-PyDOT

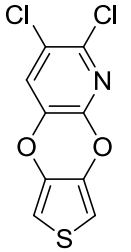

56Cl$_2$-PyDOT

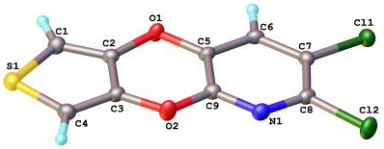

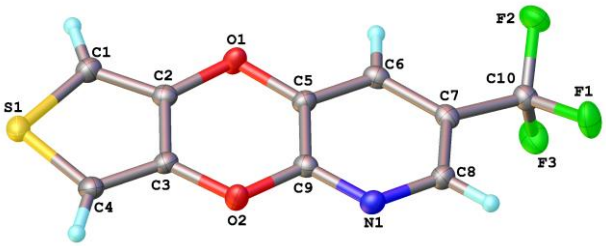

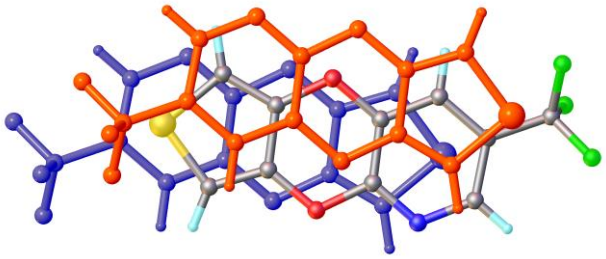

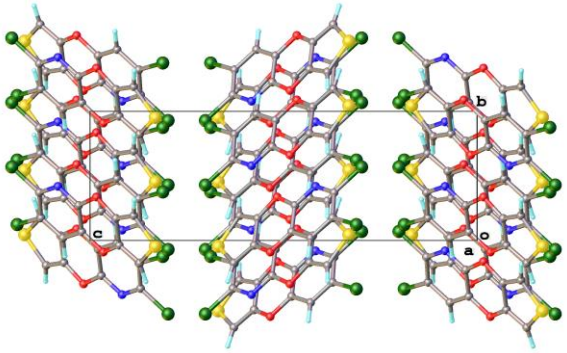

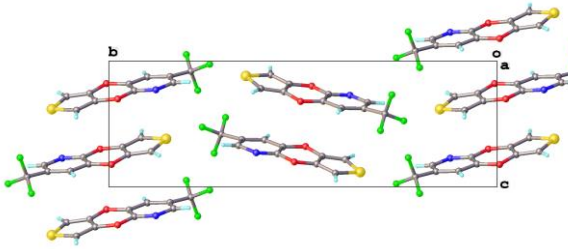

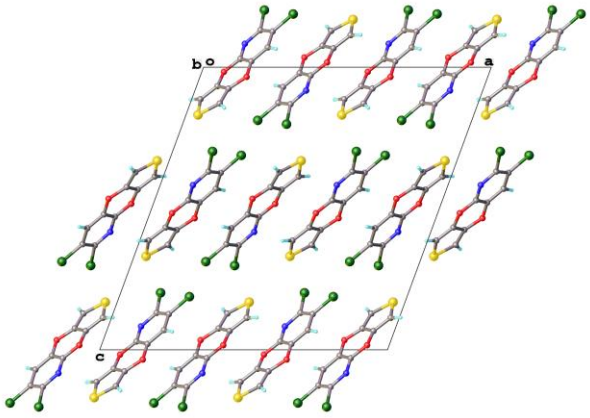

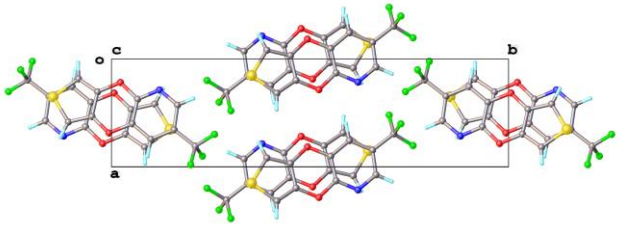

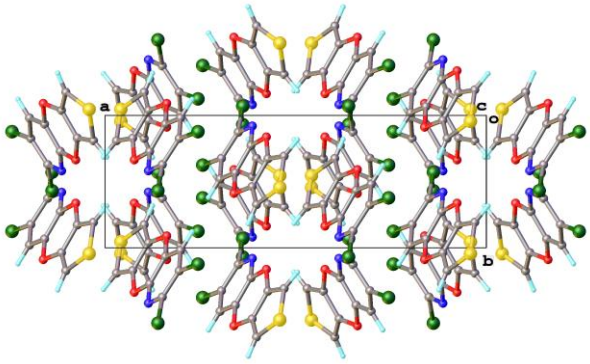

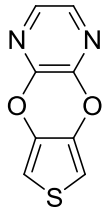

PzDOT

(twin crystals; two independent molecules in a unit cell)

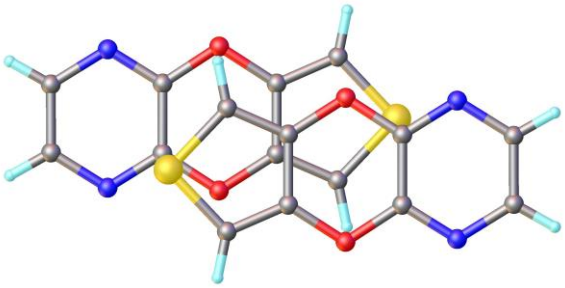

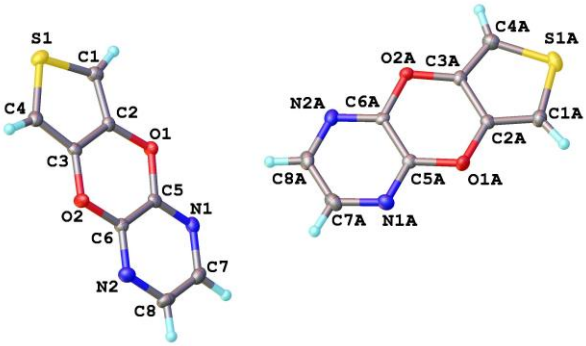

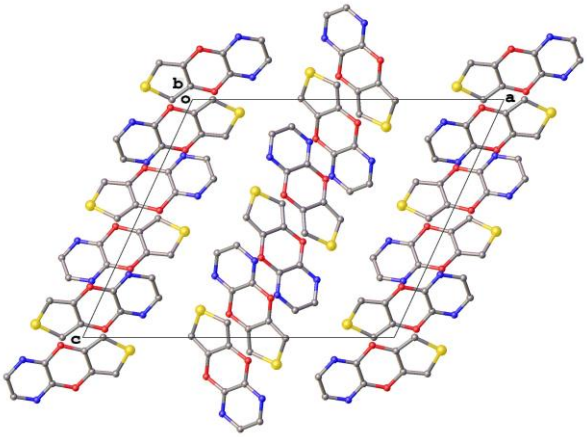

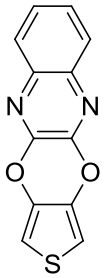

QxDOT

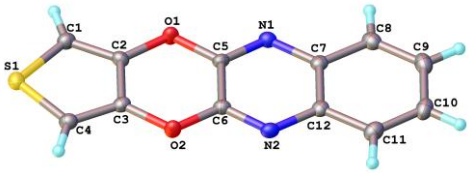

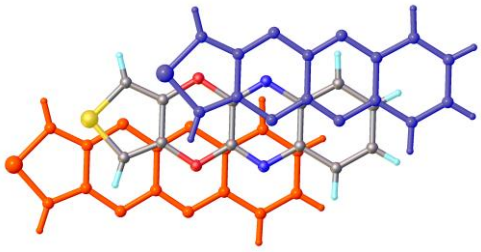

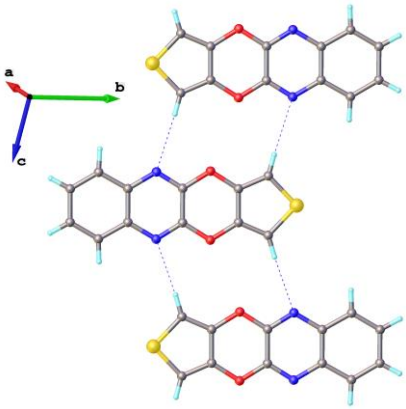

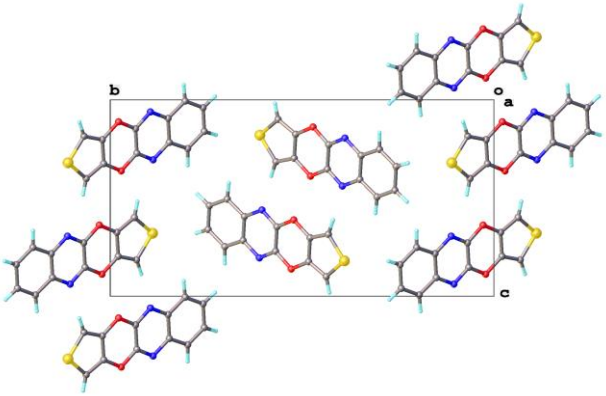

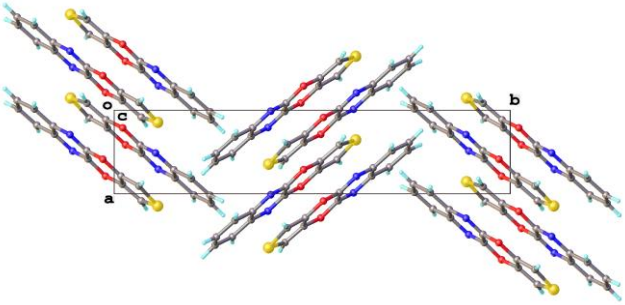

We were also able to isolate the **F4-23** intermediate from the reaction mixture in synthesis by Scheme 1 in the paper, and its structure was confirmed by a single crystal X-Ray diffraction (Figure S4). In the crystal structure of **F4-23** planar (with the exception of the terminal methyl group) molecules are arranged in layers perpendicular to the c-axis. Each layer is formed out of anti-parallel chains of molecules linked by C(thiophene)–H···O and F···O contacts. Weaker C(methylene)–H···S contacts exist between the layers. The polycyclic fragments of the molecules in adjacent parallel chains do not overlap, meaning the absence of "classical" aromatic π···π stacking in the structure. Nevertheless, the distance between molecules in parallel chains is quite short: the shortest interatomic distance is O···O 3.132(1) Å. Most probably electrostatic interactions between numerous heteroatoms are responsible for such an unusual (for planar tricyclic molecules) packing arrangement. A proper analysis of these interactions requires quantum-chemical calculations and is impossible on the basis of geometrical information obtained by X-ray method only.

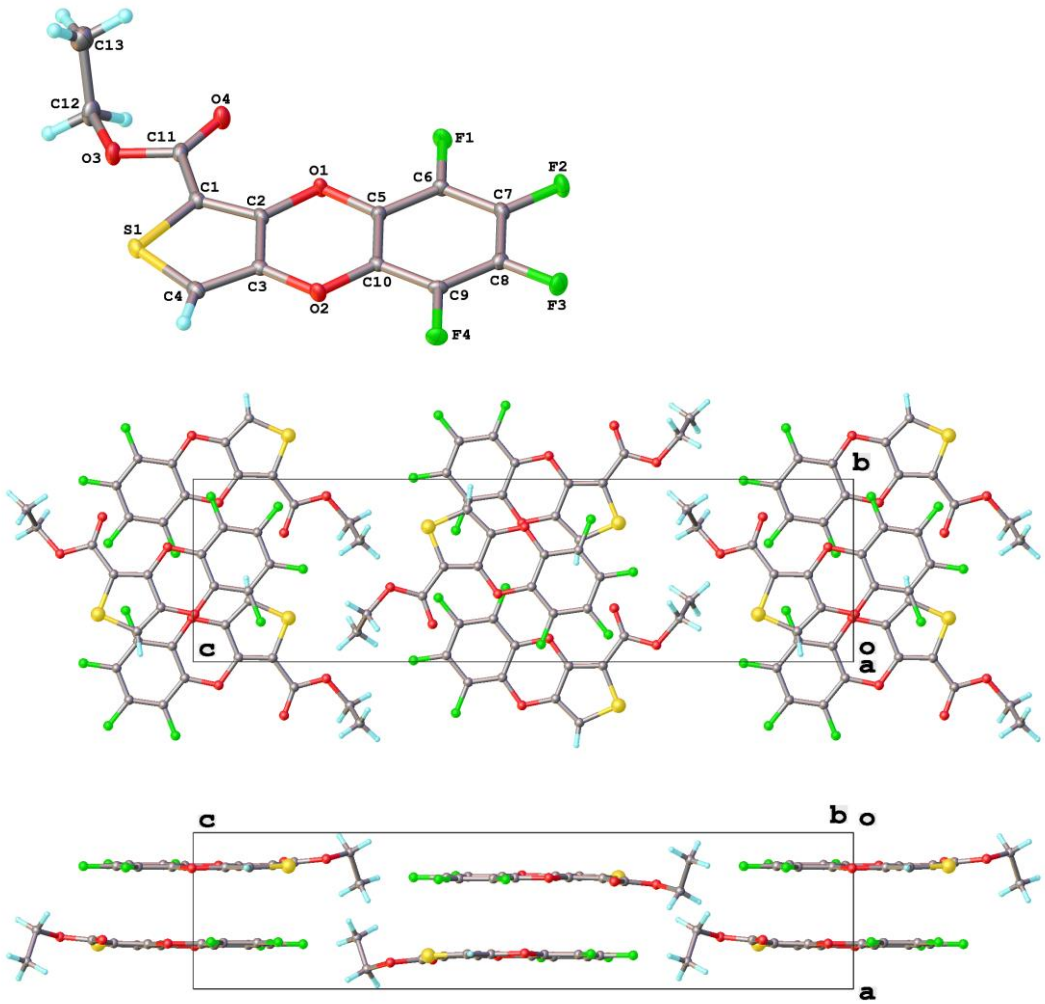

Figure S4. Molecular structure and crystal packing of compound **F4-23**.

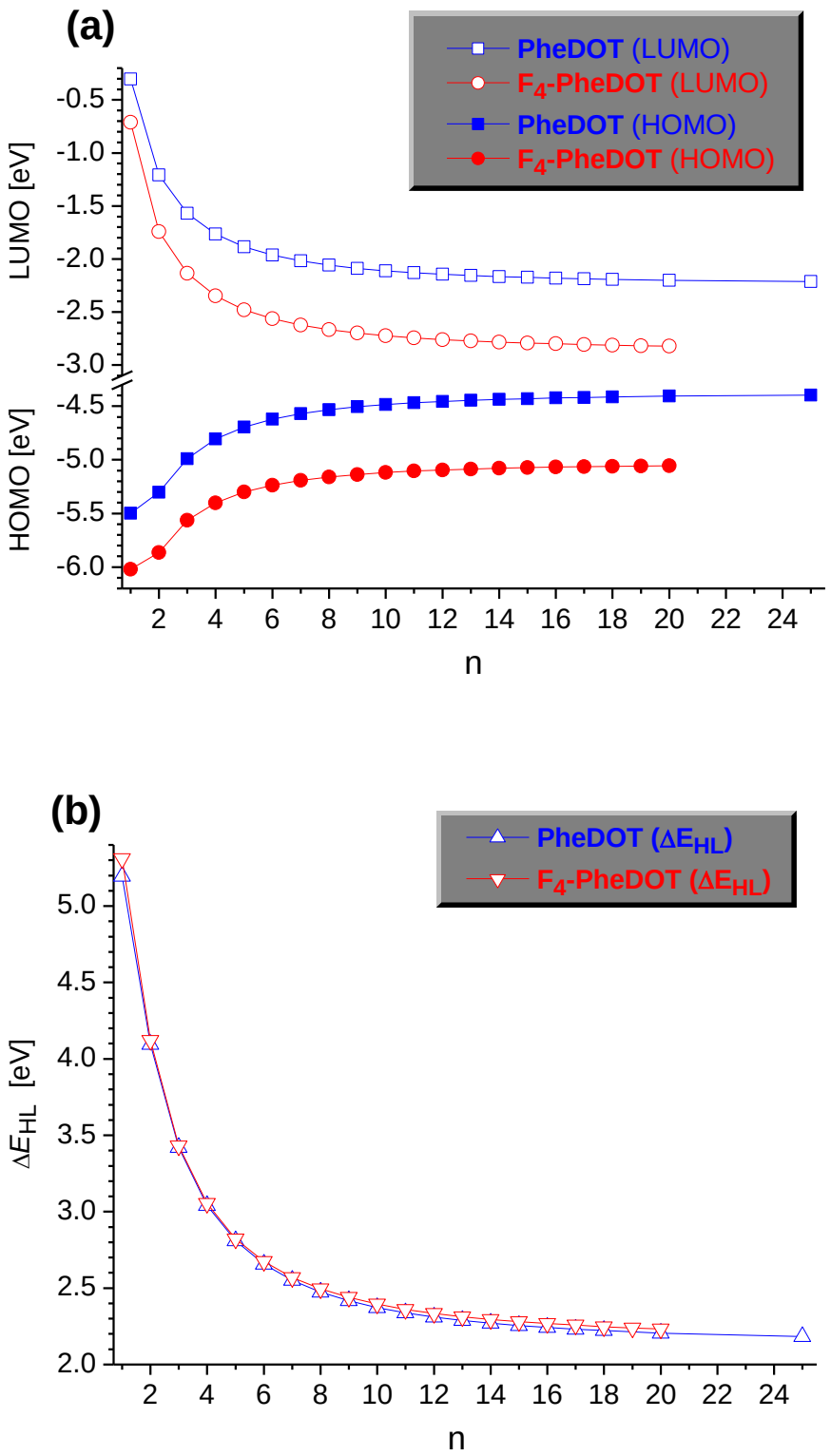

Figure S5. Chain length dependences of (a) HOMO and LUMO energies and (b) HOMO–LUMO energy gaps ΔE_{HL} for B3LYP/6-31G(d) optimized geometries (in the gas phase) of **(PheDOT)$_n$** and **(F$_4$-PheDOT)$_n$** oligomers, plotted versus a number of repeating units "n".

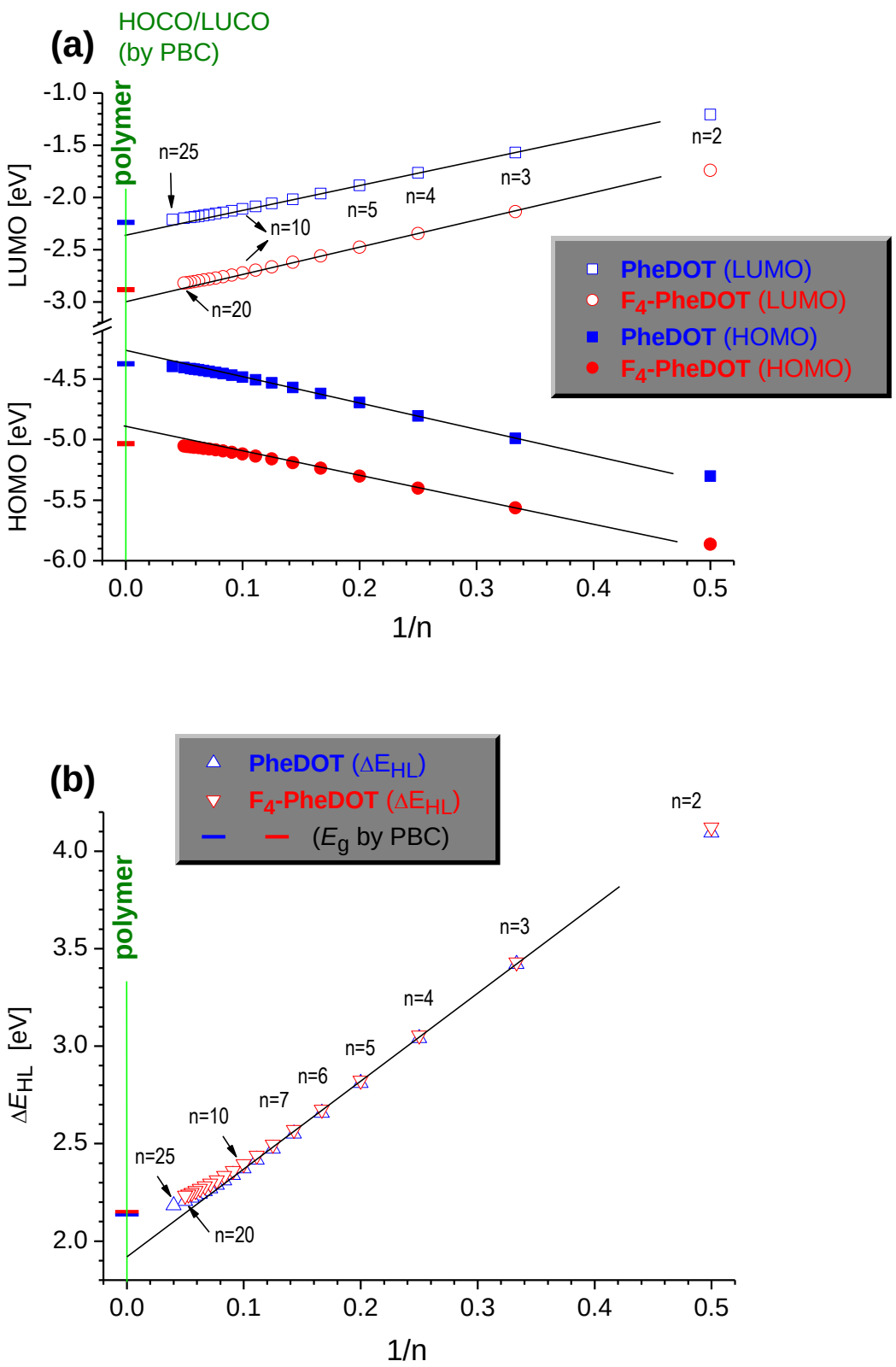

Figure S6. Chain length dependences of (a) HOMO and LUMO energies and (b) HOMO–LUMO energy gaps ΔE_{HL} for B3LYP/6-31G(d) optimized geometries (in the gas phase) of **(PheDOT)$_n$** and **(F$_4$-PheDOT)$_n$** oligomers, plotted versus a reciprocal number of repeating units, 1/n. Symbols — and — correspond to the energies (HOCO, LUCO, E_g) for polymers calculated by PBC/B3LYP/6-31G(d).

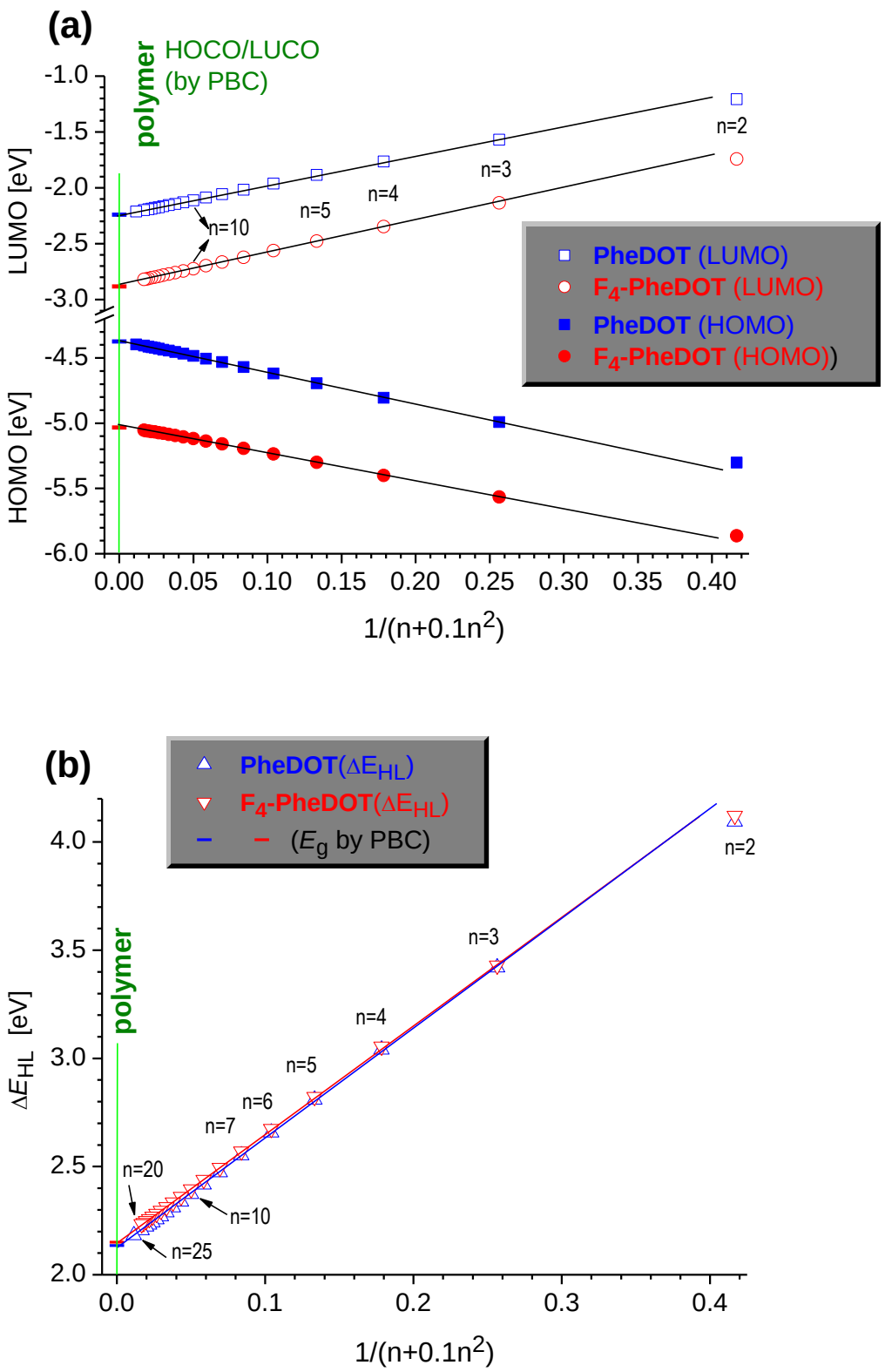

Figure S7. Chain length dependences of (a) HOMO and LUMO energies and (b) HOMO–LUMO energy gaps ΔE_{HL} for B3LYP/6-31G(d) optimized geometries (in the gas phase) of **(PheDOT)$_n$** and **(F$_4$-PheDOT)$_n$** oligomers, plotted as a function of $1/(n + 0.1n^2)$.
Symbols — and — correspond to the energies (HOCO, LUCO, E_g) for polymers calculated by PBC/B3LYP/6-31G(d).

In contrast to dependences of energies (HOMO, LUMO, ΔE_{HL}) versus 1/n, which show deviation from the linearity (saturation) with an elongation of the oligomers length, the use of the function **1/(n + 0.1n^2)** gives excellent linear dependences (see Figure S7 for magnified graphs) with correlation coefficients R ≥ 0.9998, and the extrapolated (to the infinite polymer length, n = ∞) energies excellently coincide with the energies for the polymers calculated by PBC/B3LYP/6-31G(d).

$$E_n = E_{n=\infty} + \alpha\cdot[1/(n + 0.1n^2)]$$

(PheDOT)$_n$:

LUMO [eV] = –(**2.244** ± 0.001) + (2.655 ± 0.011)·[1/(n + 0.1n^2)]
R = 0.9999, N = 18 (points n = 3...18, 20, 25)

HOMO [eV] = –(**4.364** ± 0.001) – (2.454 ± 0.008)·[1/(n + 0.1n^2)]
R = 0.9999, N = 18 (points n = 3...18, 20, 25)

ΔE_{HL} [eV] = (**2.120** ± 0.002) + (5.109 ± 0.017) ·[1/(n + 0.1n^2)]
R = 0.9999, N = 18 (points n = 3...18, 20, 25)

p[PheDOT], calculations by PBC:

LUCO = **–2.239** eV
HOCO = **–4.374** eV
E_g = **2.135**eV

(F$_4$-PheDOT)$_n$:

LUMO [eV] = –(**2.868** ± 0.002) + (2.889 ± 0.012)·[1/(n + 0.1n^2)]
R = 0.9999, N = 18 (points n = 3...20)

HOMO [eV] = –(**5.015** ± 0.001) – (2.143 ± 0.010)·[1/(n + 0.1n^2)]
R = 0.9998, N = 18 (points n = 3...20)

ΔE_{HL} [eV] = (**2.147** ± 0.001) + (5.032 ± 0.015) ·[1/(n + 0.1n^2)]
R =0.9999 , N = 18 (points n = 3...20)

p[F$_4$-PheDOT], calculations by PBC:

LUCO = **–2.882** eV
HOCO = **–5.033** eV
E_g = **2.151**eV

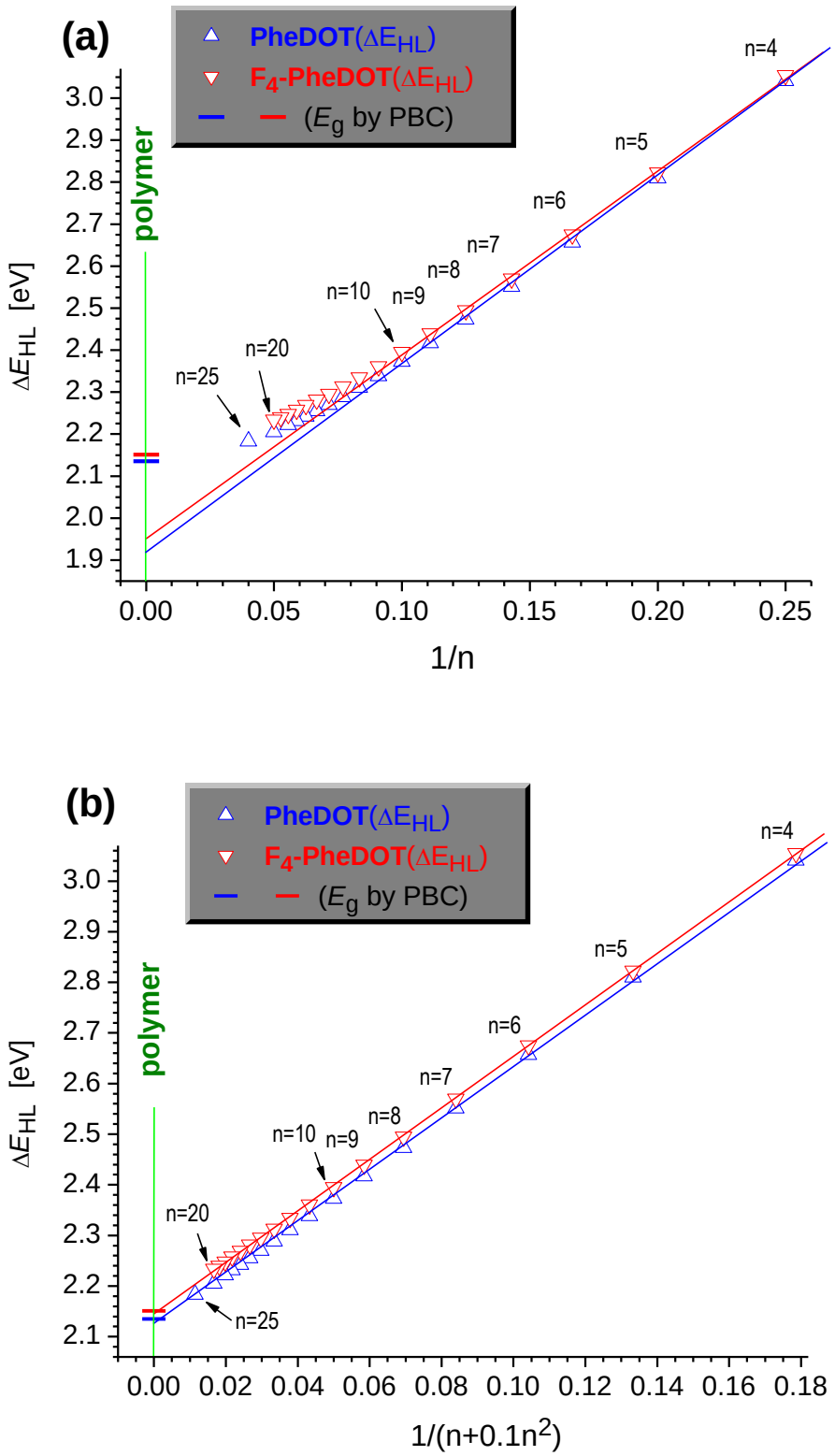

Figure S8. Magnified graphs (for n = 4 – 25, from Figures S4 and S5) of B3LYP/6-31G(d) calculated energy gaps ΔE_{HL} for **(PheDOT)$_n$** and **(F$_4$-PheDOT)$_n$**: comparison of correlations versus (a) 1/n and (b) $1/(n + 0.1n^2)$.

Table S5. Total energies, HOMO/LUMO energy levels and the HOMO–LUMO gaps for **(PheDOT)$_n$** and **(F$_4$-PheDOT)$_n$** oligomers by B3LYP/6-31G(d) calculations in the gas phase.

(PheDOT)$_n$

n	1/n	1/(n+0.1n^2)	Total energy, hartree	HOMO, eV	LUMO, eV	ΔE_{HL}, eV
1	1	0.9091	–933.27336120	–5.499	–0.304	5.196
2	0.5000	0.4167	–1865.3590544	–5.303	–1.208	4.095
3	0.3333	0.2564	–2797.4456125	–4.991	–1.571	3.420
4	0.2500	0.1786	–3729.5318205	–4.806	–1.764	3.041
5	0.2000	0.1333	–4661.6187163	–4.695	–1.885	2.810
6	0.1667	0.1042	–5593.7044558	–4.620	–1.963	2.657
7	0.1429	0.0840	–6525.7918588	–4.570	–2.018	2.551
8	0.1250	0.0694	–7457.8778554	–4.532	–2.058	2.473
9	0.1111	0.0585	–8389.9650029	–4.506	–2.088	2.417
10	0.1000	0.0500	–9322.0512785	–4.484	–2.111	2.373
11	0.0909	0.0433	–10254.1381466	–4.468	–2.123	2.339
12	0.0833	0.0379	–11186.2245524	–4.455	–2.144	2.311
13	0.0769	0.0334	–12118.3112902	–4.445	–2.156	2.289
14	0.0714	0.0298	–13050.3978619	–4.437	–2.166	2.271
15	0.0667	0.0267	–13982.4844337	–4.429	–2.174	2.256
16	0.0625	0.0240	–14914.5709395	–4.423	–2.181	2.242
17	0.0588	0.0218	–15846.6575770	–4.418	–2.187	2.232
18	0.0556	0.0198	–16778.7441030	–4.414	–2.192	2.222
25	0.0400	0.0114	–23303.3501514	–4.396	–2.213	2.183

(F$_4$-PheDOT)$_n$

n	1/n	1/(n+0.1n^2)	Total energy, hartree	HOMO, eV	LUMO, eV	ΔE_{HL}, eV
1	1	0.9091	–1330.1652878	–6.022	–0.710	5.311
2	0.5000	0.4167	–2659.1424162	–5.864	–1.741	4.122
3	0.3333	0.2564	–3988.1206097	–5.565	–2.136	3.429
4	0.2500	0.1786	–5317.0989362	–5.401	–2.347	3.054
5	0.2000	0.1333	–6646.0773958	–5.301	–2.478	2.823
6	0.1667	0.1042	–7975.0556120	–5.236	–2.562	2.675
7	0.1429	0.0840	–9304.0341761	–5.192	–2.622	2.570
8	0.1250	0.0694	–10633.0124079	–5.150	–2.665	2.494
9	0.1111	0.0585	–11961.9910497	–5.137	–2.698	2.439
10	0.1000	0.0500	–13290.9693471	–5.119	–2.724	2.395
11	0.0909	0.0433	–14619.9478397	–5.105	–2.745	2.361
12	0.0833	0.0379	–15948.9261401	–5.094	–2.760	2.334
13	0.0769	0.0334	–17277.9045610	–5.086	–2.773	2.313
14	0.0714	0.0298	–18606.8829648	–5.078	–2.783	2.295
15	0.0667	0.0267	–19935.8614073	–5.073	–2.791	2.281
16	0.0625	0.0240	–21264.8398646	–5.068	–2.799	2.269
17	0.0588	0.0218	–22593.8182640	–5.064	–2.806	2.258
18	0.05556	0.01984	–23922.7954363	–5.060	–2.812	2.248
19	0.05263	0.01815	–25251.7721790	–5.058	–2.818	2.240
20	0.0500	0.0167	–26580.7515697	–5.055	–2.821	2.234

Table S6. HOMO, LUMO energy levels and the HOMO–LUMO energy gaps (ΔE_{HL}) of dimers **(ArDOT)$_2$** by B3LYP/6-31G(d) calculations in the gas phase.

	Dimers **(ArDOT)$_2$**	Total energy, hartree	HOMO, eV	LUMO, eV	ΔE_{HL},[a] eV
1	**[(4MeO)$_2$-PheDOT]$_2$**	–2323.4326423	–4.895	–1.040	3.855
2	**(4MeO-PheDOT)$_2$**	–2094.4015000	-5.142	-1.134	4.008
3	**(4Me-PheDOT)$_2$**	–1943.9948689	–5.225	–1.148	4.077
4	**(PheDOT)$_2$**	–1865.3590543	–5.303	–1.208	4.095
5	**(36F$_2$-PheDOT)$_2$**	–2262.2632089	–5.577	–1.465	4.111
6	**(4F-PheDOT)$_2$**	–2063.8215136	–5.464	–1.368	4.096
7	**(4Br-PheDOT)$_2$**	–7007.5652927	–5.563	–1.463	4.100
8	**(4Cl-PheDOT)$_2$**	–2784.5474279	–5.572	–1.468	4.104
9	**(45F$_2$-PheDOT)$_2$**	–2262.2698477	–5.612	–1.512	4.100
10	**(4CF$_3$-PheDOT)$_2$**	–2539.4325592	–5.701	–1.582	4.119
11	**(4MeSO$_2$-PheDOT)$_2$**	–3041.1303425	–5.843	–1.729	4.114
12	**(F4-PheDOT)$_2$**	–2659.1424161	–5.864	–1.742	4.122
13	**(45Cl$_2$-PheDOT)$_2$**	–3703.7258360	–5.766	–1.658	4.108
14	**(Cl$_4$-PheDOT)$_2$**	–5542.0642800	–5.990	–1.869	4.120
15	**(3NO$_2$,5CF$_3$-PheDOT)$_2$**	–2948.4047350	–6.148	–2.842	3.306
16	**(4CN-PheDOT)$_2$**	–2049.8433341	–5.917	–1.845	4.073
17	**(4NO$_2$-PheDOT)$_2$**	–2274.3601970	–6.003	–2.587	3.416
18	**(3CF$_3$,5NO$_2$-PheDOT)$_2$**	–2352.9989481	–5.947	–2.513	3.434
19	**(45(CN)$_2$-PheDOT)$_2$**	–2234.3133927	–6.415	–2.582	3.833
20	**(NaphDOT(2,3))$_2$**	–2172.6473759	–5.260	–1.313	3.947
21	**[F$_6$-NaphDOT(2,3)]$_2$**	–3363.3433721	–5.773	–1.874	3.899
22	**[F$_6$-NaphDOT(1,2)]$_2$**	–3363.3378313	–5.798	–1.918	3.881
23	**(PyDOT)$_2$**	–1897.4408713	–5.509	–1.365	4.145
24	**(5CF$_3$-PyDOT)$_2$**	–2571.5109075	–5.899	–1.754	4.145
25	**(56Cl$_2$-PyDOT)$_2$**	–3735.8092468	–5.966	–1.825	4.141
26	**(PzDOT)$_2$**	–1929.5159146	–5.764	–1.641	4.124
27	**(QxDOT)$_2$**	–2236.8167607	–5.701	–1.968	3.734
28	**(F$_4$-BnDOT)$_2$** cisoid[b]	–2737.7710399	–5.437	–1.340	4.097
29	**(F$_4$-BnDOT)$_2$** transoid[b]	–2737.7710008	–5.439	–1.343	4.096

[a] ΔE_{HL} = LUMO – HOMO.
[b] "Cisoid" and "transoid" belongs to the relative orientation of non-planar seven-member rings in the dimers.

Table S7. HOCO, LUCO energy levels and the band gaps (E_g,) of **p[ArDOT]** polymers by PBC/B3LYP/6-31G(d) calculations in the gas phase

p[ArDOT]	Total energy,[a] hartree	HOCO, eV	LUCO, eV	E_g,[b] eV	ΔHOCO,[c] eV	ΔE_g,[d] meV
p[4MeO-PheDOT]	–2093.2153646	–4.329	–2.204	2.126	0.040	–10
p[4Me-PheDOT]	–1942.8090085	–4.270	–2.147	2.123	0.104	–13
p[PheDOT]	–1864.1731432	–4.374	–2.239	2.135	**0**	**0**
p[36F$_2$-PheDOT]	–2261.0764465	–4.552	–2.390	2.162	–0.178	26
p[4F-PheDOT]	–2062.6355280	–4.644	–2.511	2.133	-0.27	–2
p[4Br-PheDOT]	–7006.3793017	–4.770	–2.631	2.139	–0.396	4
p[4Cl-PheDOT]	–2783.3613276	–4.790	–2.650	2.140	–0.416	5
p[45F$_2$-PheDOT]	–2261.0829434	–4.893	–2.755	2.138	–0.519	2
p[4CF$_3$-PheDOT]	–2538.2463064	–4.953	–2.809	2.144	–0.579	9
p[4MeSO$_2$-PheDOT]	–3039.9466487	–4.980	–2.831	2.149	–0.606	14
p[F$_4$-PheDOT]	–2657.9557189	–5.033	–2.882	2.151	–0.659	16
p[45Cl$_2$-PheDOT]	–3702.5384442	–5.059	–2.919	2.140	–0.685	5
p[4CN-PheDOT]	–2947.2281140	–5.324	–3.173	2.152	–0.950	16
p[4NO$_2$-PheDOT]	–2048.6563942	–5.370	–3.230	2.140	–0.996	5
p[45(CN)2-PheDOT]	–2273.1744023	–6.017	–3.847	2.170	–1.643	35
p[NaphDOT(2,3)]	–2351.8121007	–4.393	–2.364	2.029	–0.019	–106
p[F$_6$-NaphDOT(2,3)]	–2233.1177820	–4.950	–2.913	2.037	–0.576	–98
p[PyDOT]	–2171.4611856	–4.471	–2.315	2.156	–0.097	21
p[5CF$_3$-PyDOT]	–3362.1576614	–5.055	–2.887	2.169	–0.681	33
p[56Cl$_2$-PyDOT]	–3362.1542424	–5.157	–2.988	2.169	–0.783	34
p[PzDOT]	–1896.2573156	–4.684	–2.507	2.177	–0.310	41
p[QxDOT]	–2570.3264606	–4.639	–2.583	2.056	–0.265	–79

[a] Absolute energies per unit cell.
[b] E_g = LUCO – HOCO.
[c] ΔHOCO = HOCO(**p[ArDOT]**) – HOCO(**p[PheDOT]**)
[d] ΔE_g = E_g(**p[ArDOT]**) – E_g(**p[PheDOT]**)

Table S8. Short S⋯O contacts and selected bond distances in **p[ArDOTs]** for optimized polymer structures by PBC/B3LYP/6-31G(d).

p[ArDOT]	S⋯O	(Ph)C1–O (Ph)C2–O	O–C3(Th) O–C4(Th)	(Th–Th) C2–C5'	Thiophene C2–C3	Thiophene C3–C4
p[4MeO-PheDOT]	2.944 2.949	1.385	1.372	1.437	1.378	1.413
p[4Me-PheDOT]	2.947	1.384	1.372	1.437	1.379	1.413
p[PheDOT]	2.947	1.384	1.372	1.437	1.379	1.413
p[36F$_2$-PheDOT]	2.951	1.377	1.374	1.442	1.378	1.413
p[4F-PheDOT]	2.947	1.383	1.373	1.437	1.378	1.412
p[4Br-PheDOT]	2.943 2.952	1.382	1.373	1.436	1.378	1.412
p[4Cl-PheDOT]	2.944 2.951	1.382	1.373	1.437	1.378	1.412
p[45F$_2$-PheDOT]	2.947	1.382	1.373	1.437	1.378	1.412
p[4CF$_3$-PheDOT]	2.943 2.954	1.381	1.373	1.437	1.378	1.412
p[4MeSO$_2$-PheDOT]	2.894 2.996	1.380	1.375	1.435	1.378	1.411
p[F$_4$-PheDOT]	2.951	1.376	1.375	1.441	1.378	1.413
p[45Cl$_2$-PheDOT]	2.948	1.380	1.373	1.437	1.378	1.412
p[4CN-PheDOT]	2.934 2.965	1.380	1.373	1.437	1.378	1.411
p[4NO$_2$-PheDOT]	2.916 2.980	1.379	1.373	1.436	1.378	1.411
p[45(CN)2-PheDOT]	2.955	1.376	1.374	1.438	1.378	1.411
p[NaphDOT(2,3)]	2.950	1.382	1.371	1.436	1.379	1.411
p[F$_6$-NaphDOT(2,3)]	2.951	1.374	1.373	1.438	1.379	1.410
p[PyDOT]	2.948 2.932	1.380	1.374	1.435	1.378	1.411
p[5CF$_3$-PyDOT]	2.944 2.938	1.376	1.375	1.435	1.378	1.410
p[56Cl$_2$-PyDOT]	2.935 2.946	1.375	1.375	1.436	1.378	1.411
p[PzDOT]	2.942	1.374	1.376	1.438	1.378	1.411
p[QxDOT]	2.945	1.373	1.374	1.437	1.379	1.409
RANGE (lowest-highest)	*2.894–2.996*	*1.373–1.385*	*1.371–1.376*	*1.435–1.442*	*1.378–1.379*	*1.409–1.413*

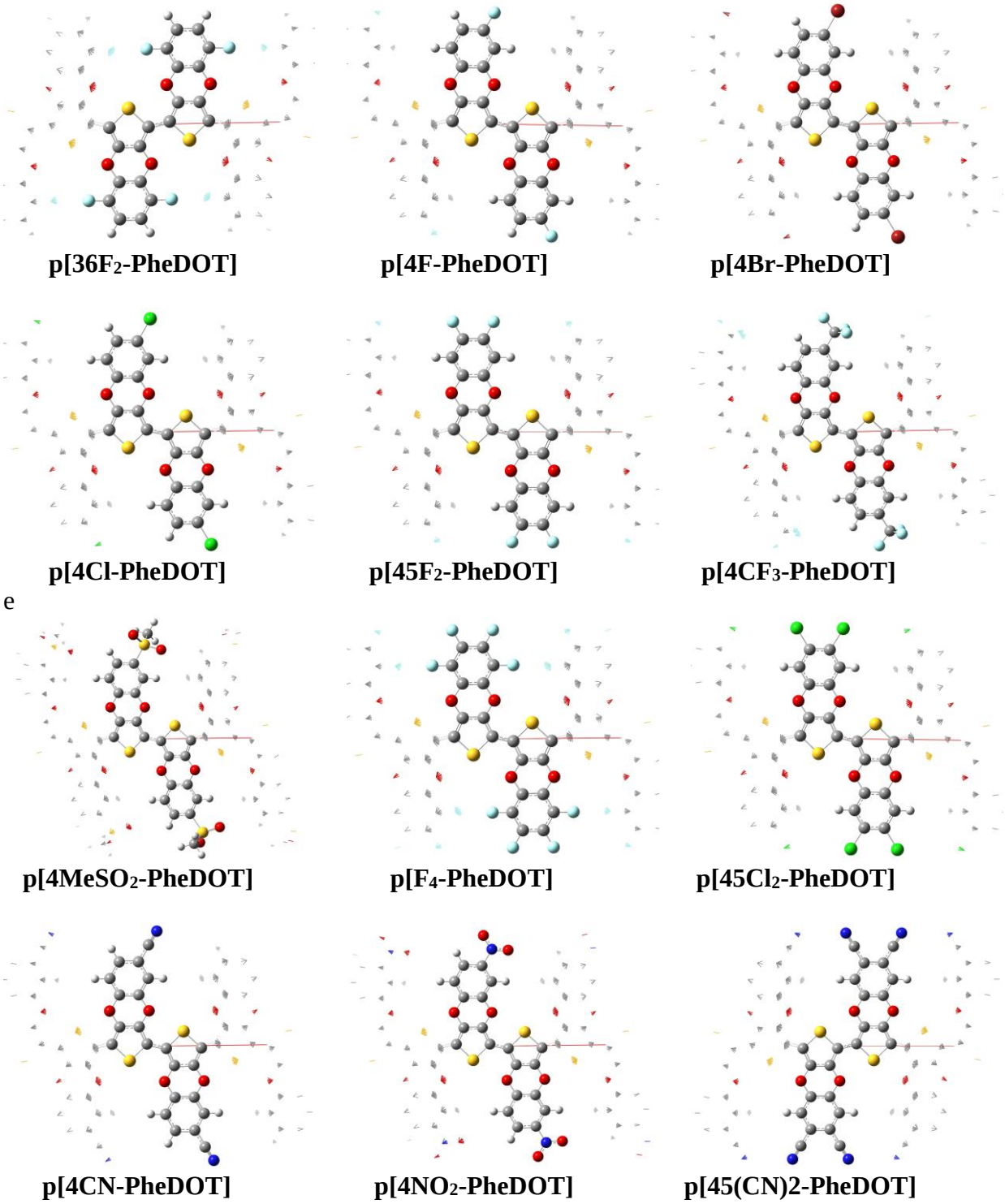

Figure S9. Unit cells for the optimized structures of **p[EWG-PheDOT]** polymers calculated at PBC/B3LYP/6-31G(d). Replication of the unit cells is shown as shadow atoms/bonds. Absolute energies (per unit cell), HOCO and LUCO energies and the band gaps E_g are given in the Table S7.

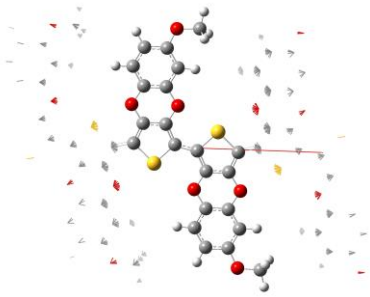

p[4MeO-PheDOT]

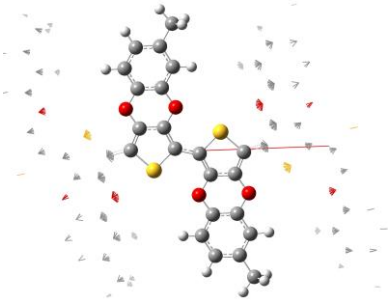

p[4Me-PheDOT]

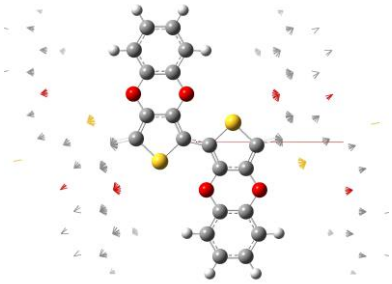

p[PheDOT]

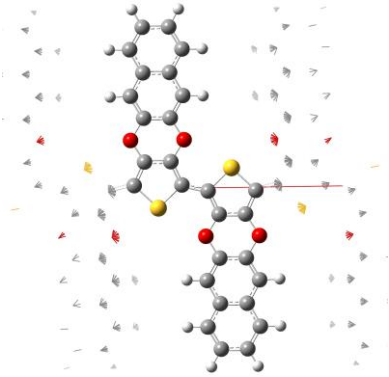

p[NaphDOT(2,3)]

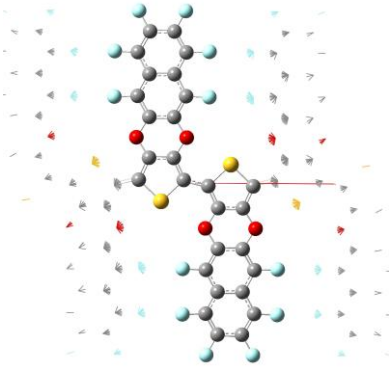

p[F_6-NaphDOT(2,3)]

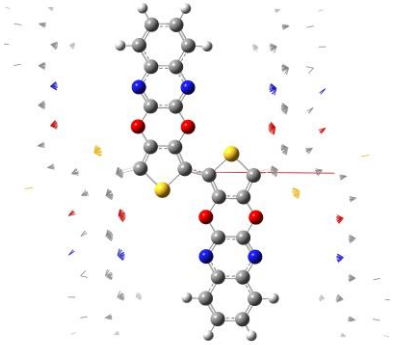

p[QxDOT]

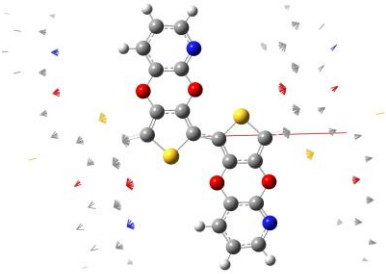

p[PyDOT]

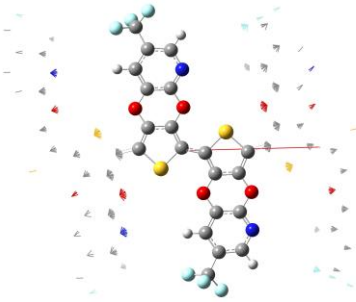

p[5CF_3-PyDOT]

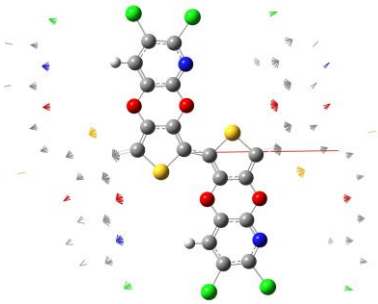

p[56Cl_2-PyDOT]

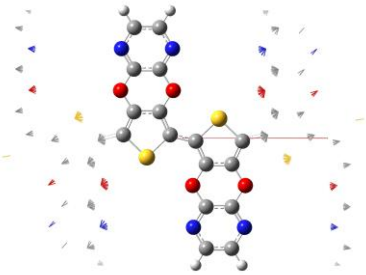

p[PzDOT]

Figure S10. Unit cells for the optimized structures of other **p[Ar-DOT]** polymers calculated at PBC/B3LYP/6-31G(d). Replication of the unit cells is shown as shadow atoms/bonds. Absolute energies (per unit cell), HOCO and LUCO energies and the band gaps E_g are given in the Table S7.

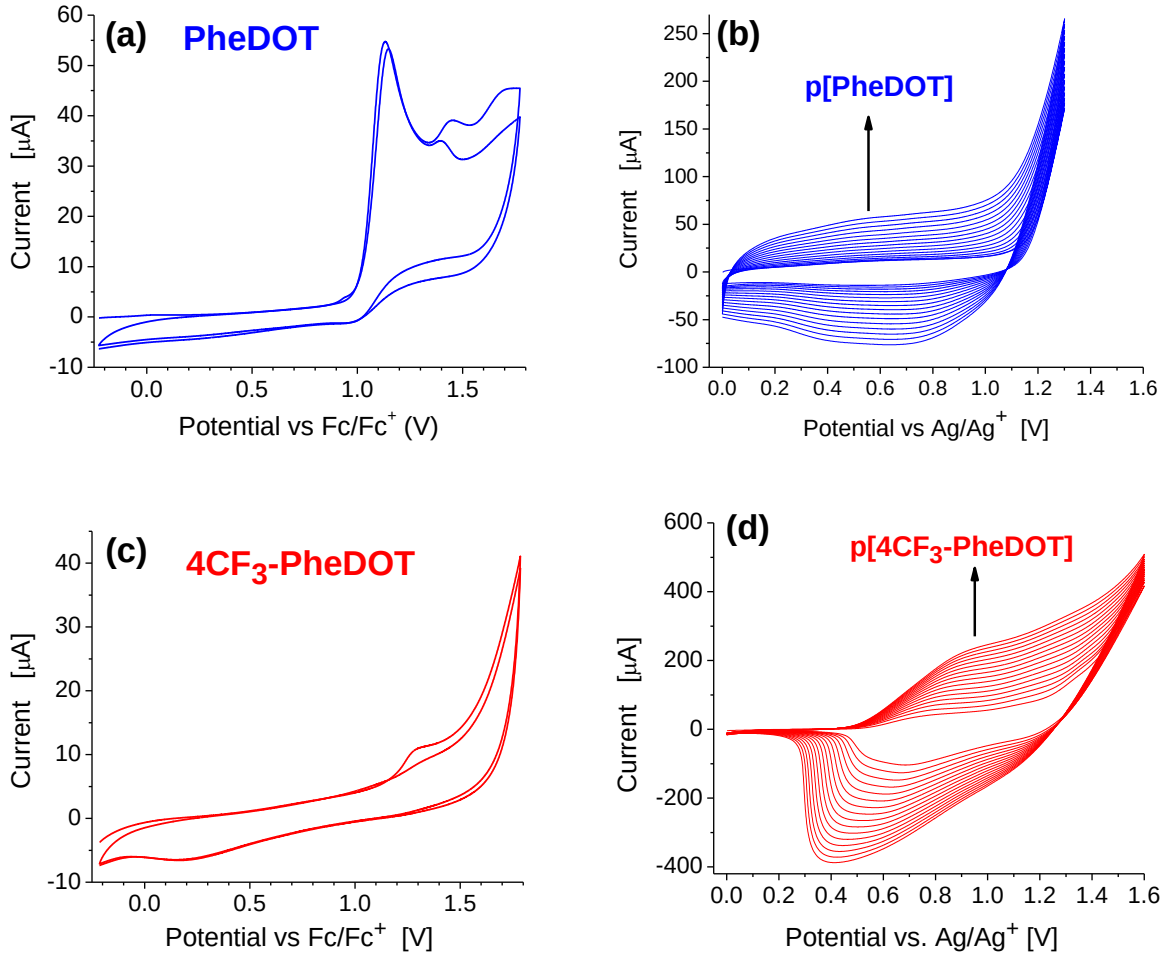

Figure S11. (a,c) Cyclic voltammograms of **PheDOT** and **4CF$_3$-PheDOT** (~1 mM) in dichloromethane, 0.2 M Bu_4NPF_6, scan rate 100 mV/s. (b,d) Potentiodynamic electropolymerization of **PheDOT** and **4CF$_3$-PheDOT** (~100 mM) in dichloromethane, 0.2 M Bu_4NPF_6, scan rate 100 mV/s.

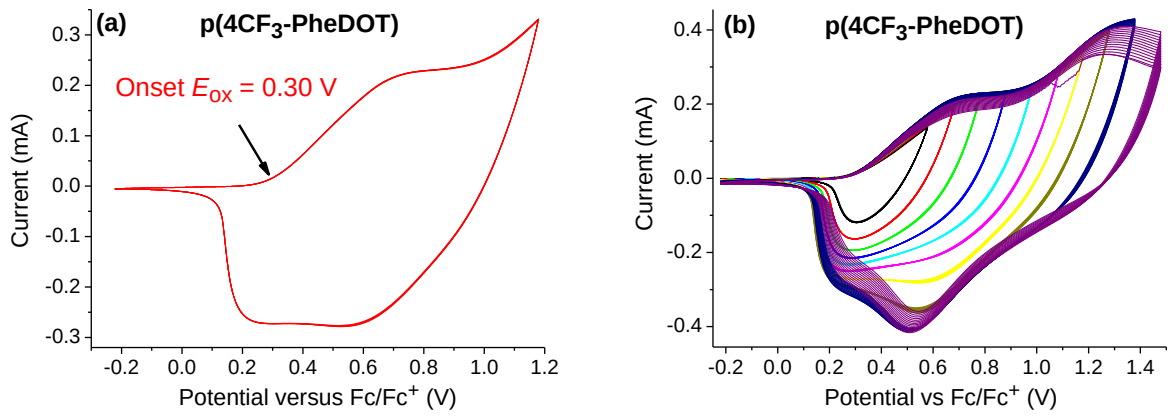

Figure S12. Cyclic voltammograms of **p[4CF$_3$-PheDOT]** films in DCM solution, 0.1 M Bu_4NPF_6, scan rate 100 mV/s. (a) Six consecutive scand on p-doping / dedoping. (b) Recurrent p-doping / dedoping of **p[4CF$_3$-PheDOT]** to different maximal p-doping potentials: the polymer shows good reversibility and stability on cycling up to potentials of ~1.2–1.3 V. Overdoping the films by applying the potentials of >1.4 V leads to some degradation of the polymer films.

References

1 O. Hinsberg, *Berichte*, 1910, **43**, 901.

2 (a) E. W. Fager, *J. Am. Chem. Soc.*, 1945, **67**, 2217–2218. (b) C. G. Overberger and J. Lakl**,** *J. Am. Chem. Soc.*, 1951, **73**, 2956–2957. (c) V. N. Gogte, L. G. Shah, B. D. Tilak, K. N. Gadekar and M. B. Sahasrabudhe, *Tetrahedron*, 1967, **23**, 2437–2441. (d) T. Soganci, G. Kurtay, M. Ak and M. Güllü, *RSC Adv.*, 2015, **5**, 2630–2639. (e) N. Agarwal, C.-H. Hung and M. Ravikanth, *Tetrahedron*, 2004, **60**, 10671–10680.

3 Gaussian 09, Revision A02, M. J. Frisch, G. W. Trucks, H. B. Schlegel, G. E. Scuseria, M. A. Robb, J. R. Cheeseman, G. Scalmani, V. Barone, B. Mennucci, G. A. Petersson, H. Nakatsuji, M. Caricato, X. Li, H. P. Hratchian, A. F. Izmaylov, J. Bloino, G. Zheng, J. L. Sonnenberg, M. Hada, M. Ehara, K. Toyota, R. Fukuda, J. Hasegawa, M. Ishida, T. Nakajima, Y. Honda, O. Kitao, H. Nakai, T. Vreven, J. A. Montgomery Jr., J. E. Peralta, F. Ogliaro, M. J. Bearpark, J. Heyd, E. N. Brothers, K. N. Kudin, V. N. Staroverov, R. Kobayashi, J. Normand, K. Raghavachari, A. P. Rendell, J. C. Burant, S. S. Iyengar, J. Tomasi, M. Cossi, N. Rega, N. J. Millam, M. Klene, J. E. Knox, J. B. Cross, V. Bakken, C. Adamo, J. Jaramillo, R. Gomperts, R. E. Stratmann, O. Yazyev, A. J. Austin, R. Cammi, C. Pomelli, J. W. Ochterski, R. L. Martin, K. Morokuma, V. G. Zakrzewski, G. A. Voth, P. Salvador, J. J. Dannenberg, S. Dapprich, A. D. Daniels, Ö. Farkas, J. B. Foresman, J. V. Ortiz, J. Cioslowski and D. J. Fox, Gaussian, Inc., Wallingford CT, 2009.

4 (a) A. D. Becke, *Phys. Rev. A*, 1988, **38**, 3098–3100. (b) A. D. Becke, *J. Chem. Phys.*, 1993, **98**, 5648–5652.

5 C. Lee, W. Yang and R. G. Parr, *Phys. Rev. B*, 1988, **37**, 785–789.

6 (a) E. Poverenov, Y. Sheynin, N. Zamoshchik, A. Patra, G. Leitus, I. F. Perepichka and M. Bendikov, *J. Mater. Chem.*, 2012, **22**, 14645–14655. (b) S. S. Zade, N. Zamoshchik and M. Bendikov, *Acc. Chem. Res.*, 2011, **44**, 14–24. (c) S. S. Zade and M. Bendikov, *Org. Lett.*, 2006, **8**, 5243–5246. (d) S. Shao, J. Shi, I. Murtaza, P. Xu, Y. He, S. Ghosh, X. Zhu, I. F. Perepichka and H. Meng, *Polym. Chem.*, 2017, **8**, 769–784.

7 O. V. Dolomanov, L. J. Bourhis, R. J. Gildea, J. A. K. Howard and H. Puschmann, *J. Appl. Cryst.*, 2009, **42**, 339–341.

8 G. M. Sheldrick, *Acta Cryst.*, 2008, **A64**, 112–122.

9 S. Roquet, P. Leriche, I. Perepichka, B. Jousselme, E. Levillain, P. Frère, J. Roncali, *J. Mater. Chem.*, 2004, **14**, 1396–1400.

10 I. F. Perepichka, S. Roquet, P. Leriche, J.-M. Raimundo, P. Frère and J. Roncali, *Chem. Eur. J.*, 2006, **12**, 2960–2966.

11 We have isolated an intermediate **F_4-23** when the reaction was performed at higher temperature of 140–160 ºC (see below).

12 Easier decarboxyethylation of the first CO_2Et group in the intermediate **22** (without EWG) was observed before [Ref. 9 above]: in conventional heating reaction of thiophene **1** with o-chloronitrobenzene (**2**) at 100 ºC, a mixture of mono- and disubstituted thiophenes (**22** and **23**) were formed. An absence of such products in the reaction with hexafluorobenzene (**15**) (Table S2, entries 1, 2) is indicative of its substantially lower reactivity in S_NAr reaction.

13 **45Br_2-PheDOT** and **45Cl_2-PheDOT** were synthesized by reflux of 4,5-dibromocatechol or 4,5-dibromocatechol with 3,4-dimethoxythiophene in benzene or toluene in the presence of *p*-toluenesulfonic acid, similarly to unsubstituted **PheDOT** (Ref. 6a, 9) and isolated with low yields of 1.3 and 5%, respectively (M. P. Krompiec, S. N. Baxter and I. F. Perepichka, unpublished results).

6-Chlorobenzo[b]thieno[3,4-e][1,4]dioxine (**4Cl-PheDOT**)

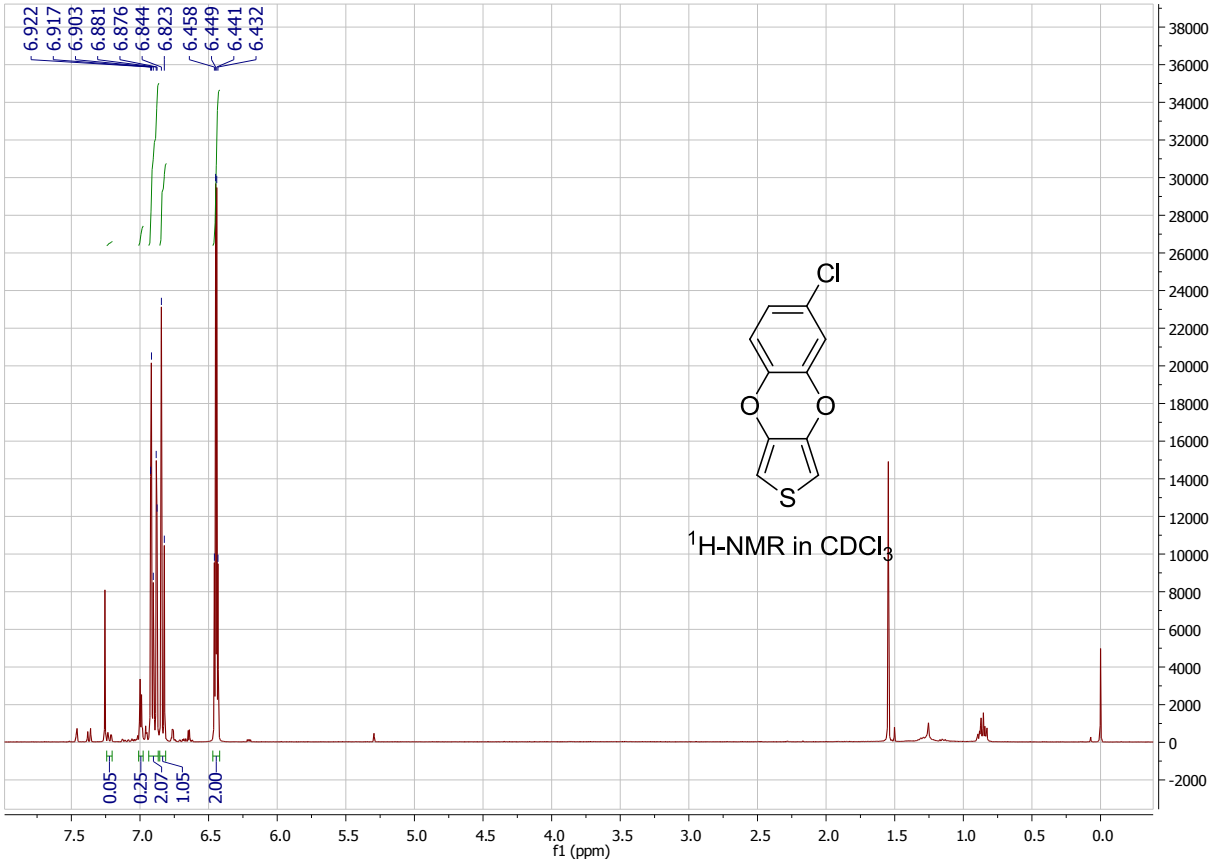

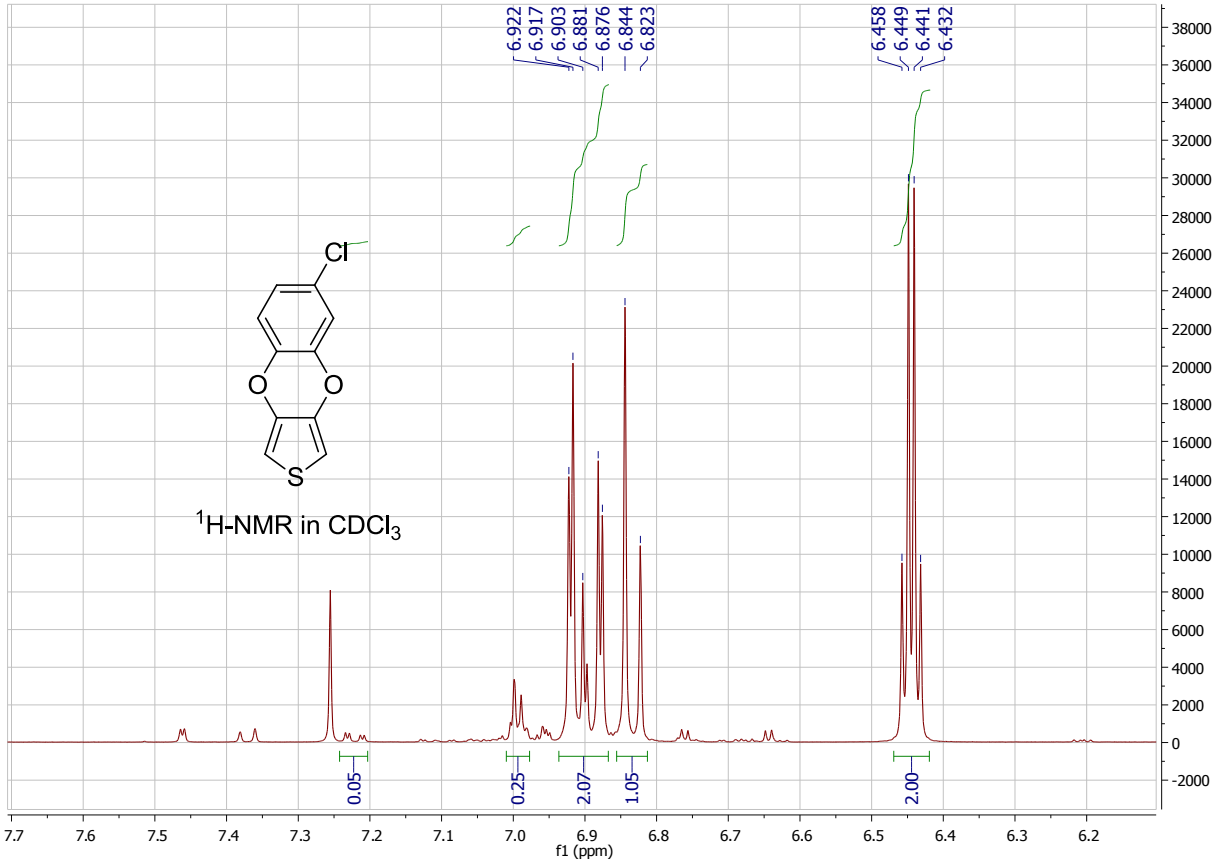

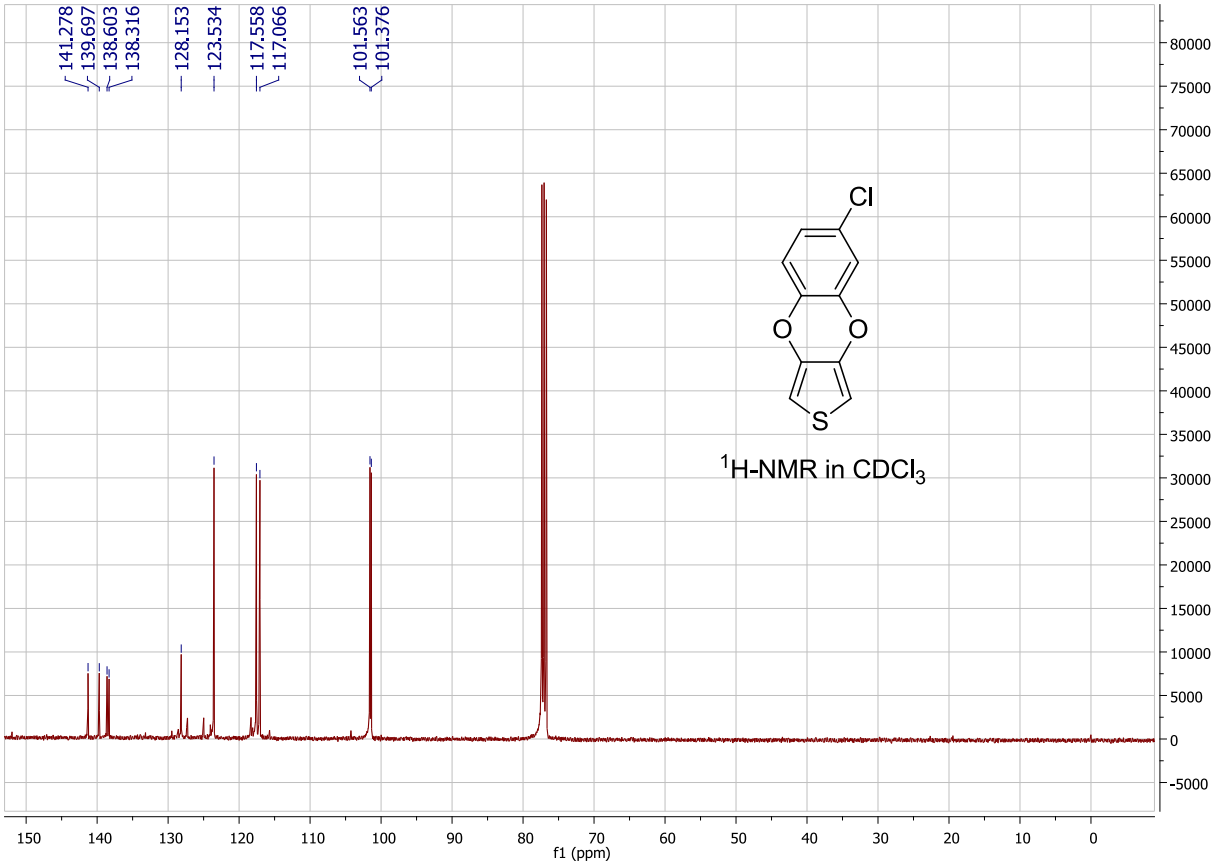
141.278
139.697
138.603
138.316
128.153
123.534
117.558
117.066
101.563
101.376
Cl
O
O
S
^{1}H-NMR in $CDCl_3$
f1 (ppm)

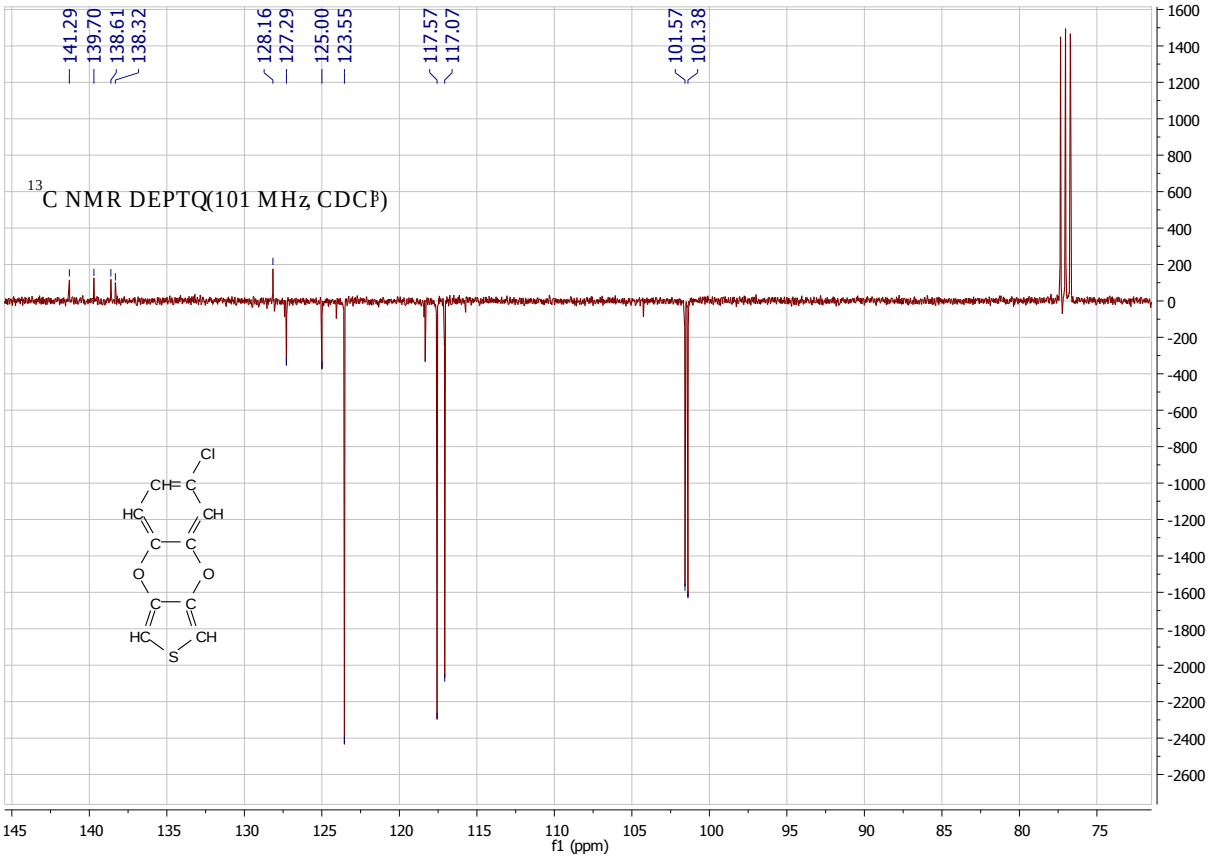
141.29
139.70
138.61
138.32
128.16
127.29
125.00
123.55
117.57
117.07
101.57
101.38
^{13}C NMR DEPTQ(101 MHz, $CDCl_3$)
Cl
CH
C
HC
CH
C
C
O
O
C
C
HC
CH
S
f1 (ppm)

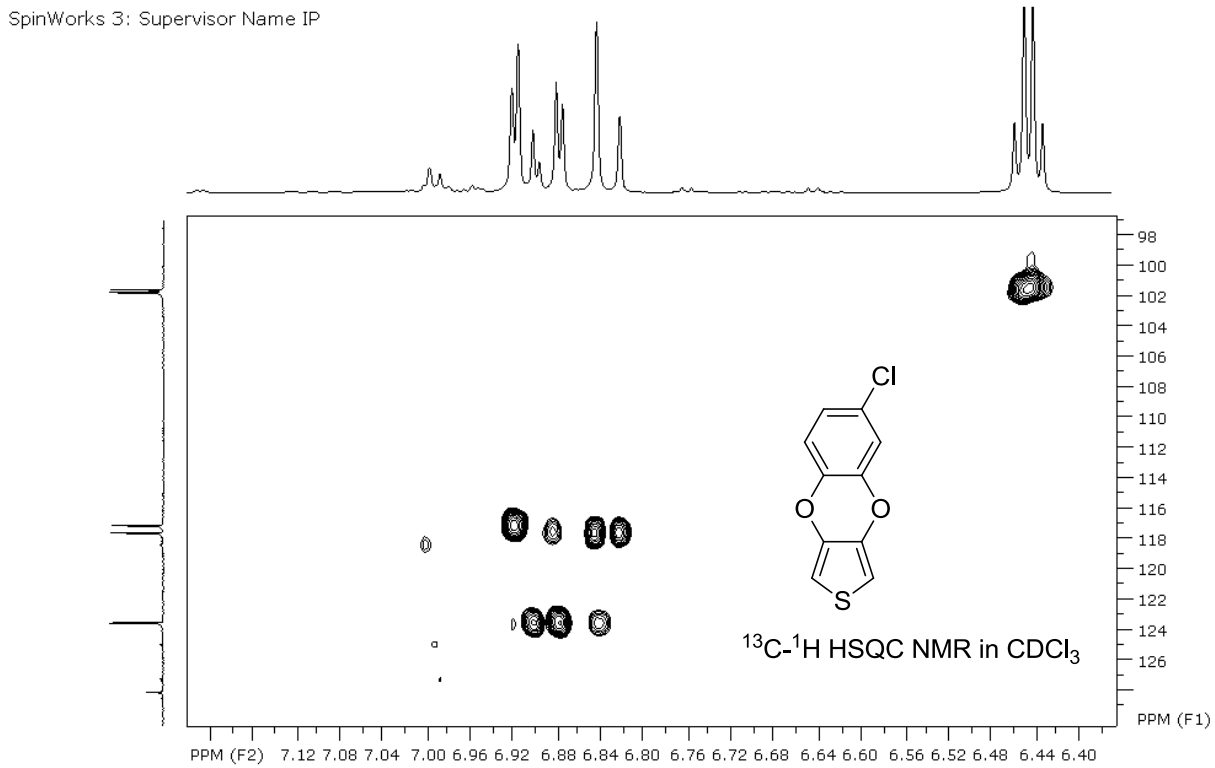

file: ...71-79\mpk-72b\31-MPK72B-HSQC.b\ser
expt: <hsqcedetgpsisp2.3>
transmitter freq: 400.131668 MHz
time domain size: 2048 by 256 points
width (F2): 3030.30 Hz = 7.5733 ppm = 1.4796 Hz/pt
number of scans: 2

F2: freq. of 0 ppm: 400.1300109 MHz
processed size: 1024 complex points
window function: Sine Squared
shift: 90.0 degrees
Hz/cm: 17.115 ppm/cm: 0.04277

F1: freq. of 0 ppm: 100.6127690 MHz
processed size: 1024 complex points
window function: Sine Squared
shift: 90.0 degrees
Hz/cm: 307.587 ppm/cm: 3.05692

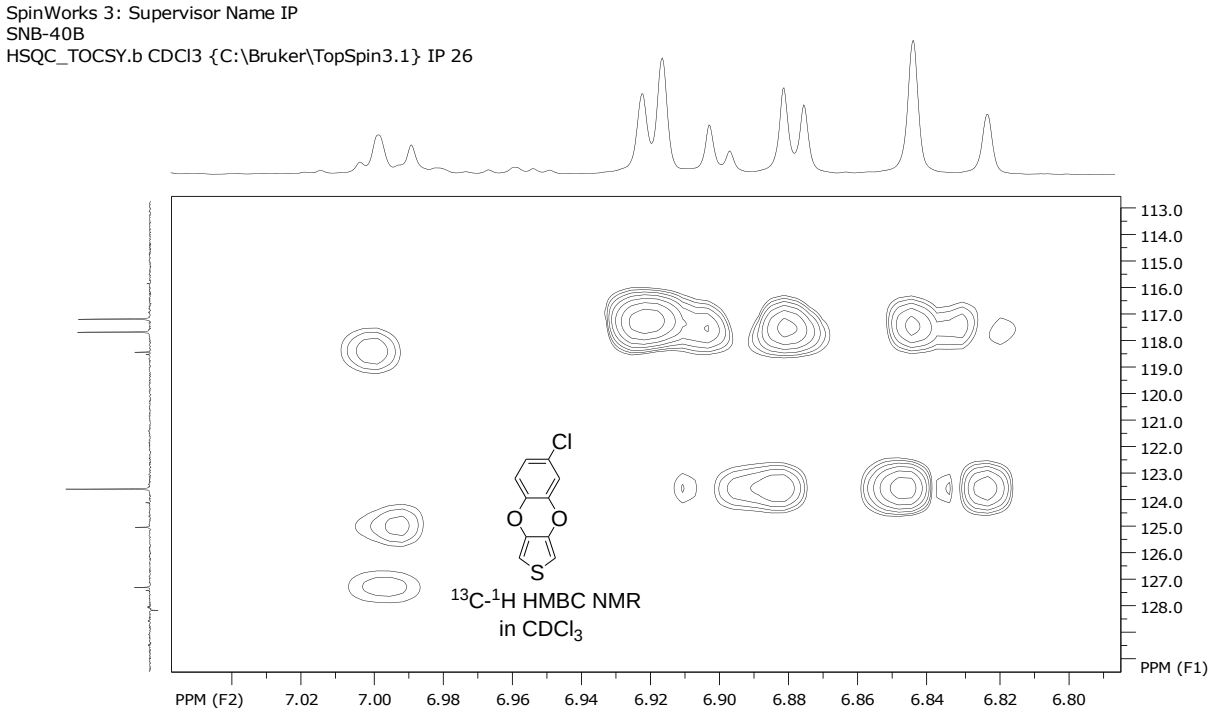

file: ...ata\SNB-40B\July 25\HSQC_TOCSY\ser
expt: <hsqcdietgpsisp.2>
transmitter freq: 400.131670 MHz
time domain size: 2048 by 256 points
width (F2): 3012.05 Hz = 7.5276 ppm = 1.4707 Hz/pt
number of scans: 8

F2: freq. of 0 ppm: 400.1300112 MHz
processed size: 1024 complex points
window function: Sine Squared
shift: 90.0 degrees
Hz/cm: 4.967 ppm/cm: 0.01241

F1: freq. of 0 ppm: 100.6127690 MHz
processed size: 1024 complex points
window function: Sine Squared
shift: 90.0 degrees
Hz/cm: 164.077 ppm/cm: 1.63066

6-Bromobenzo[b]thieno[3,4-e][1,4]dioxine (**4Br-PheDOT**)

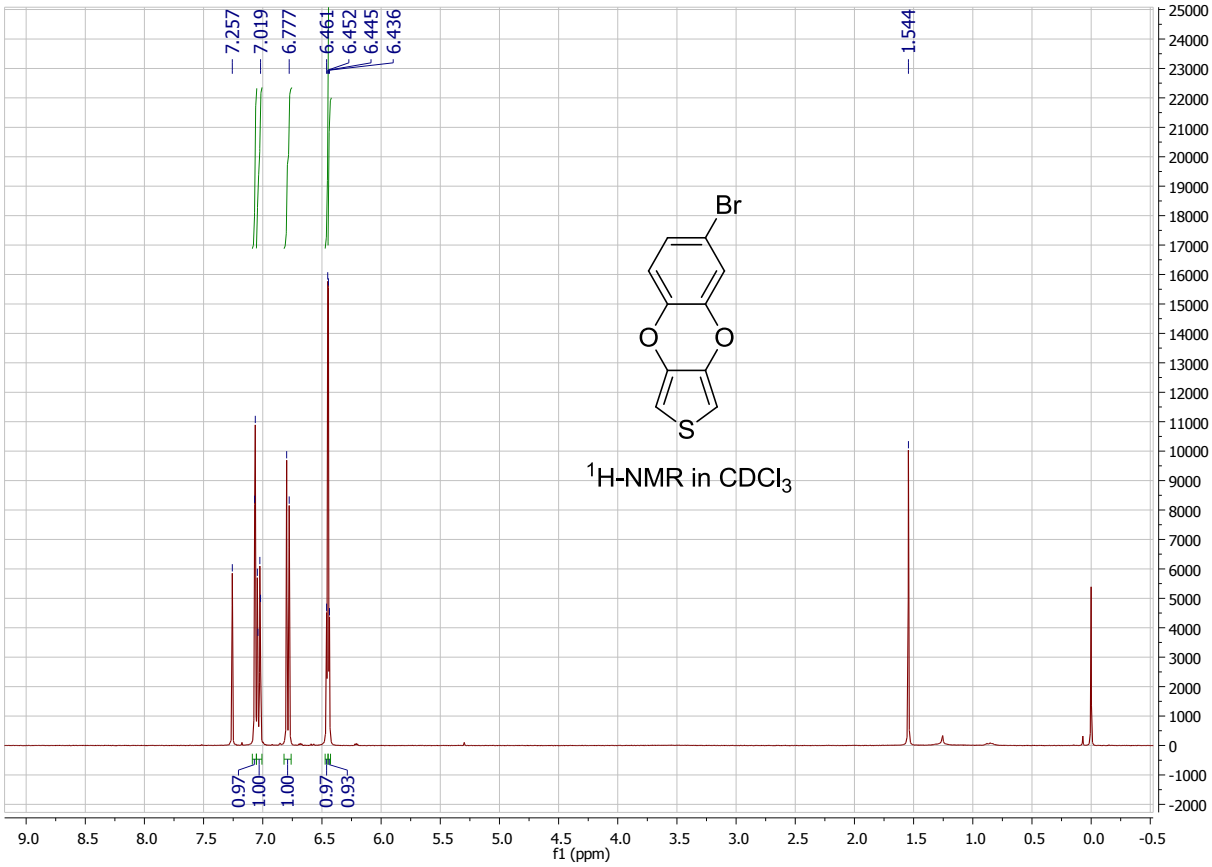

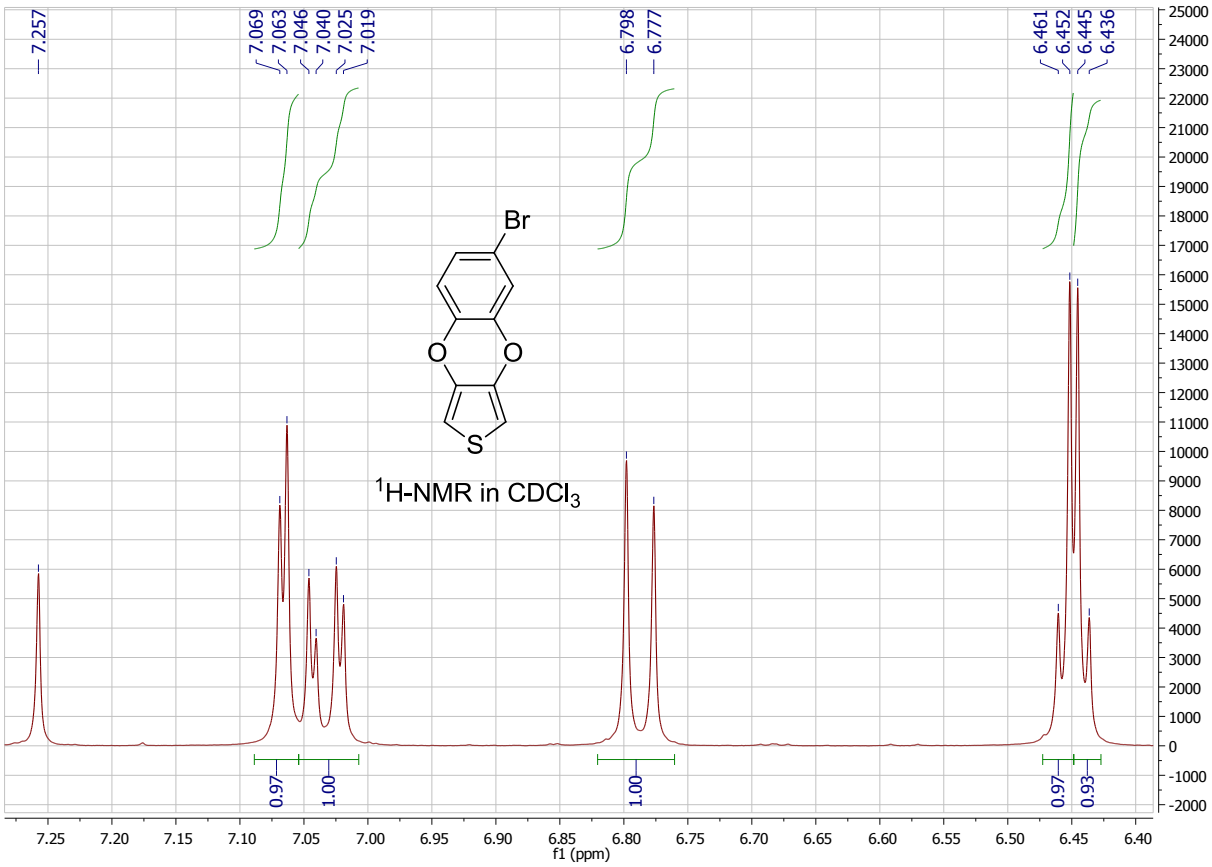

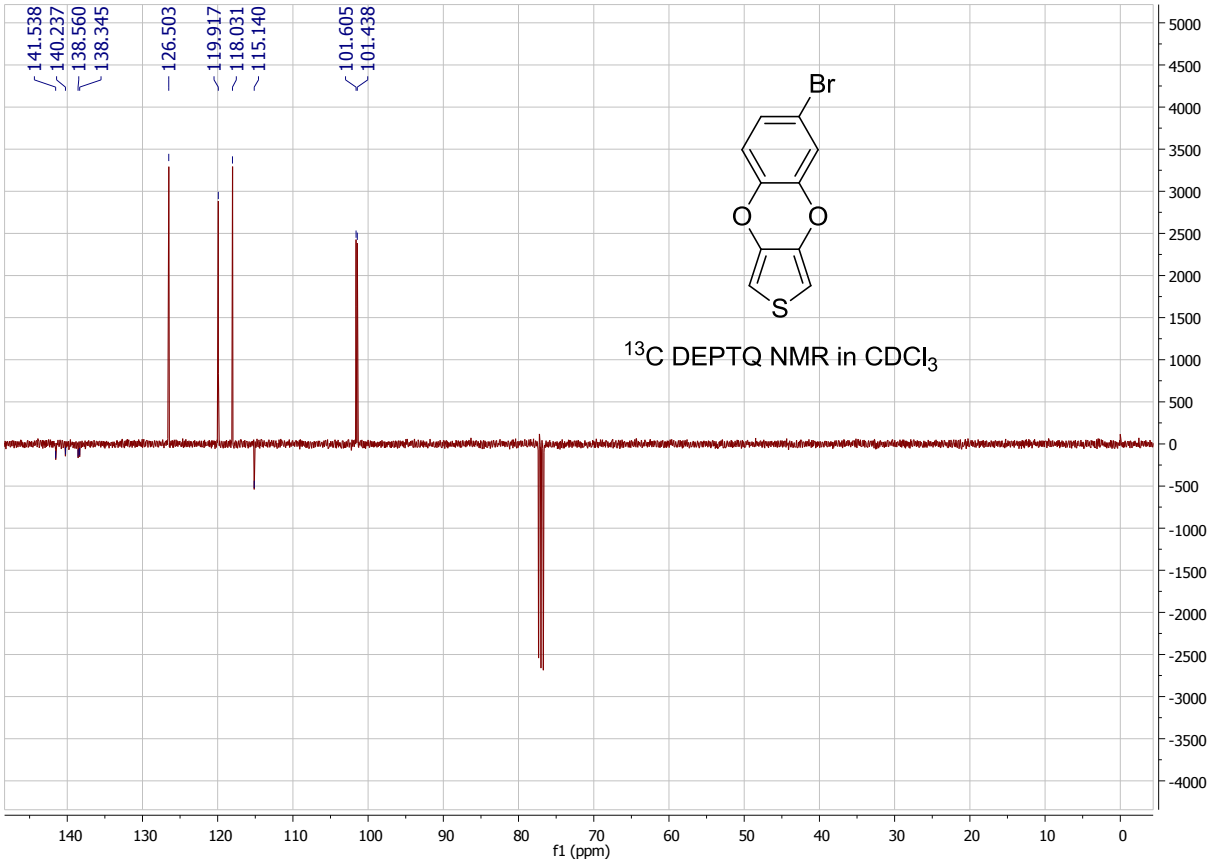
141.538
140.237
138.560
138.345
126.503
119.917
118.031
115.140
101.605
101.438
Br
O
O
S
13C DEPTQ NMR in CDCl3
f1 (ppm)

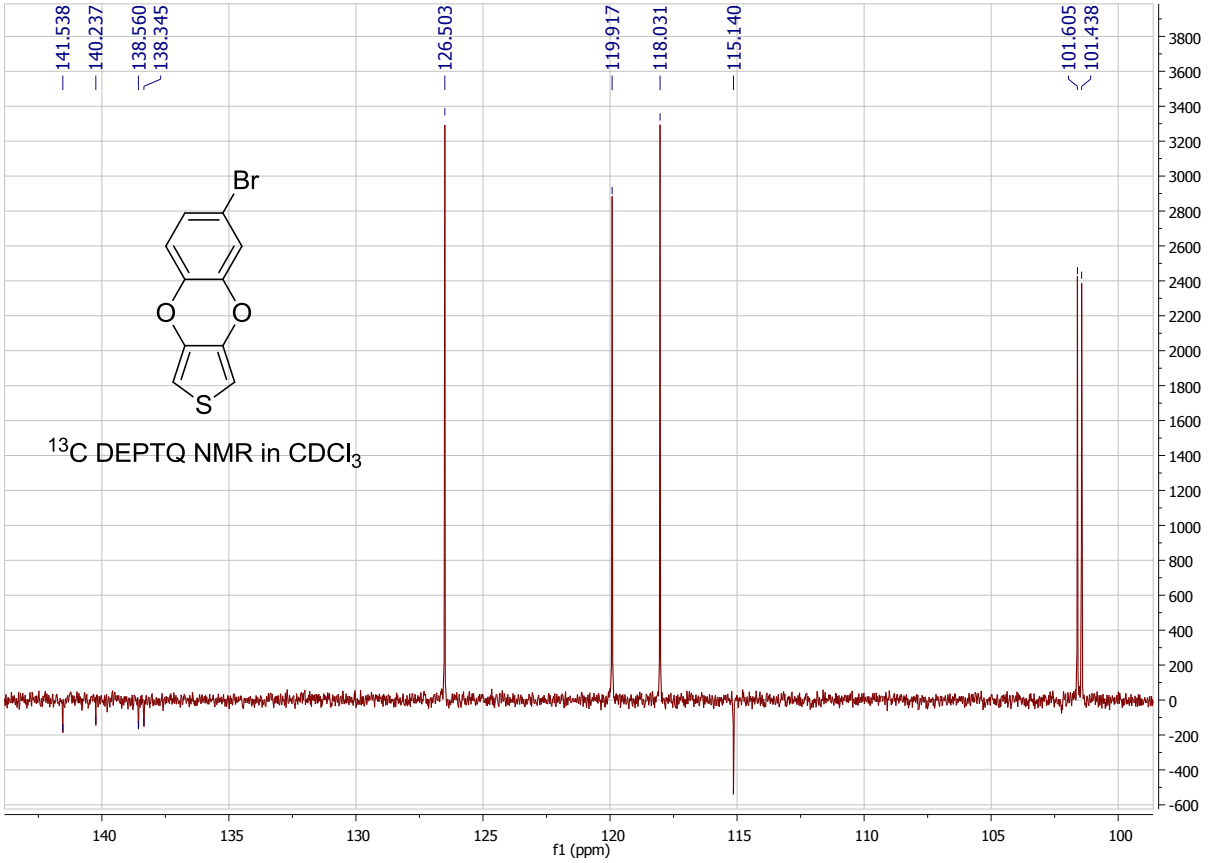
141.538
140.237
138.560
138.345
126.503
119.917
118.031
115.140
101.605
101.438
Br
O
O
S
13C DEPTQ NMR in CDCl3
f1 (ppm)

SpinWorks 3: Supervisor Name IP

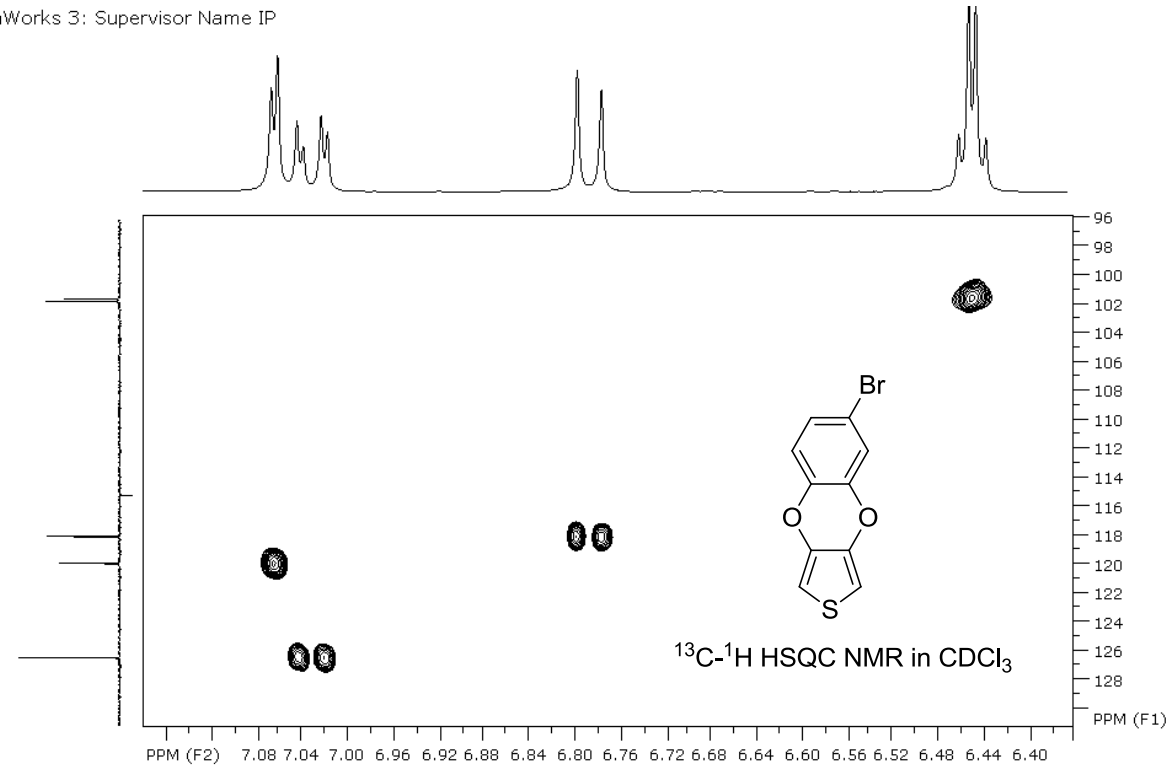

file: ...4Br-PheDOT\51-MPK-71A11-HSQC.b\ser
expt: <hsqcedetgpsisp2.3>
transmitter freq: 400.131582 MHz
time domain size: 2048 by 256 points
width (F2): 2808.99 Hz = 7.0202 ppm = 1.3716 Hz/pt
number of scans: 2

F2: freq. of 0 ppm: 400.1300106 MHz
processed size: 1024 complex points
window function: Sine Squared
shift: 90.0 degrees
Hz/cm: 16.379 ppm/cm: 0.04093

F1: freq. of 0 ppm: 100.6127690 MHz
processed size: 1024 complex points
window function: Sine Squared
shift: 90.0 degrees
Hz/cm: 323.480 ppm/cm: 3.21488

SpinWorks 3: Supervisor Name IP
MPK-71A11
HMBC.b CDCl3 {C:\Bruker\TopSpin3.2} sam 12

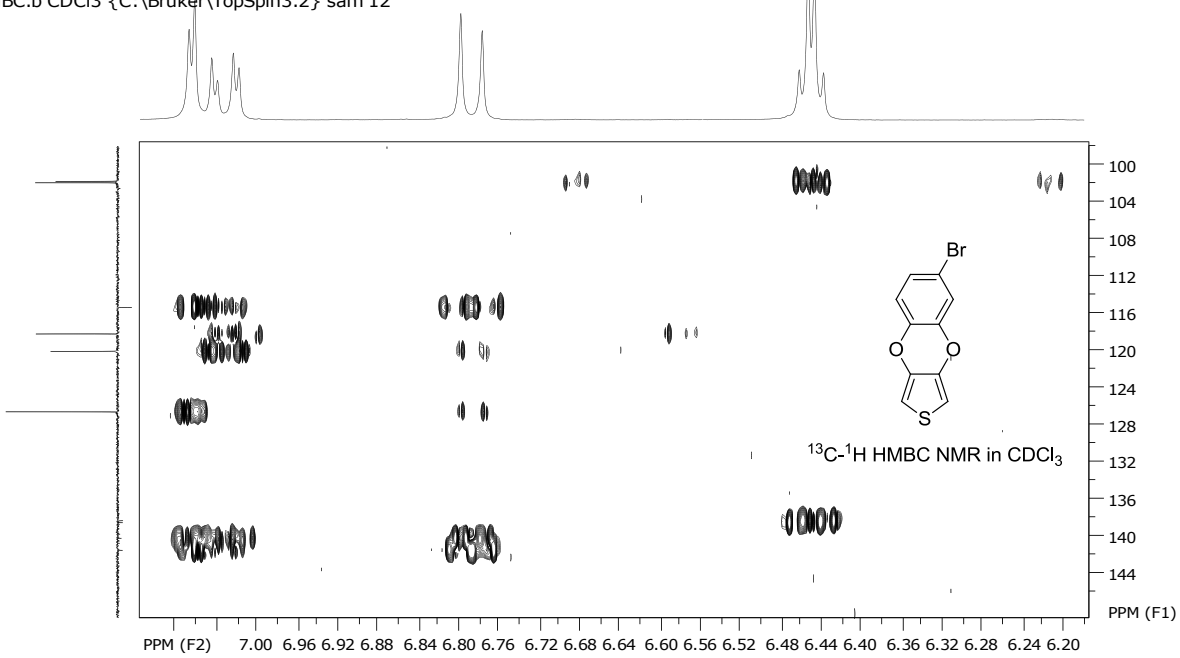

file: ...4Br-PheDOT\52-MPK-71A11-HMBC.b\ser
expt: <hmbcetgpl3nd>
transmitter freq: 400.131582 MHz
time domain size: 4096 by 256 points
width (F2): 2808.99 Hz = 7.0202 ppm = 0.6858 Hz/pt
number of scans: 4

F2: freq. of 0 ppm: 400.1300106 MHz
processed size: 2048 complex points
window function: Sine
shift: 45.0 degrees
Hz/cm: 17.138 ppm/cm: 0.04283

F1: freq. of 0 ppm: 100.6127690 MHz
processed size: 1024 complex points
window function: Sine Squared
shift: 90.0 degrees
Hz/cm: 468.870 ppm/cm: 4.65968

Benzo[b]thieno[3,4-e][1,4]dioxine-6-carbonitrile (**4CN-PheDOT**)

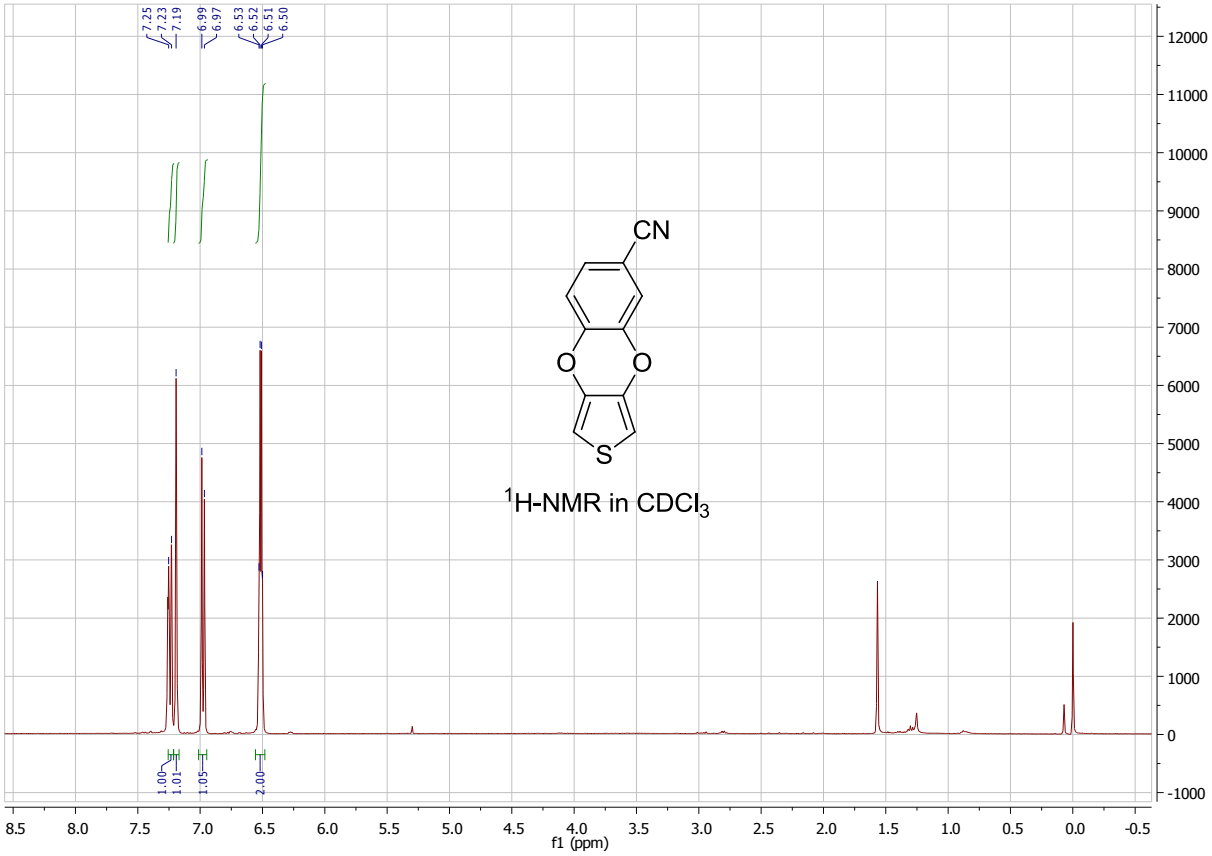

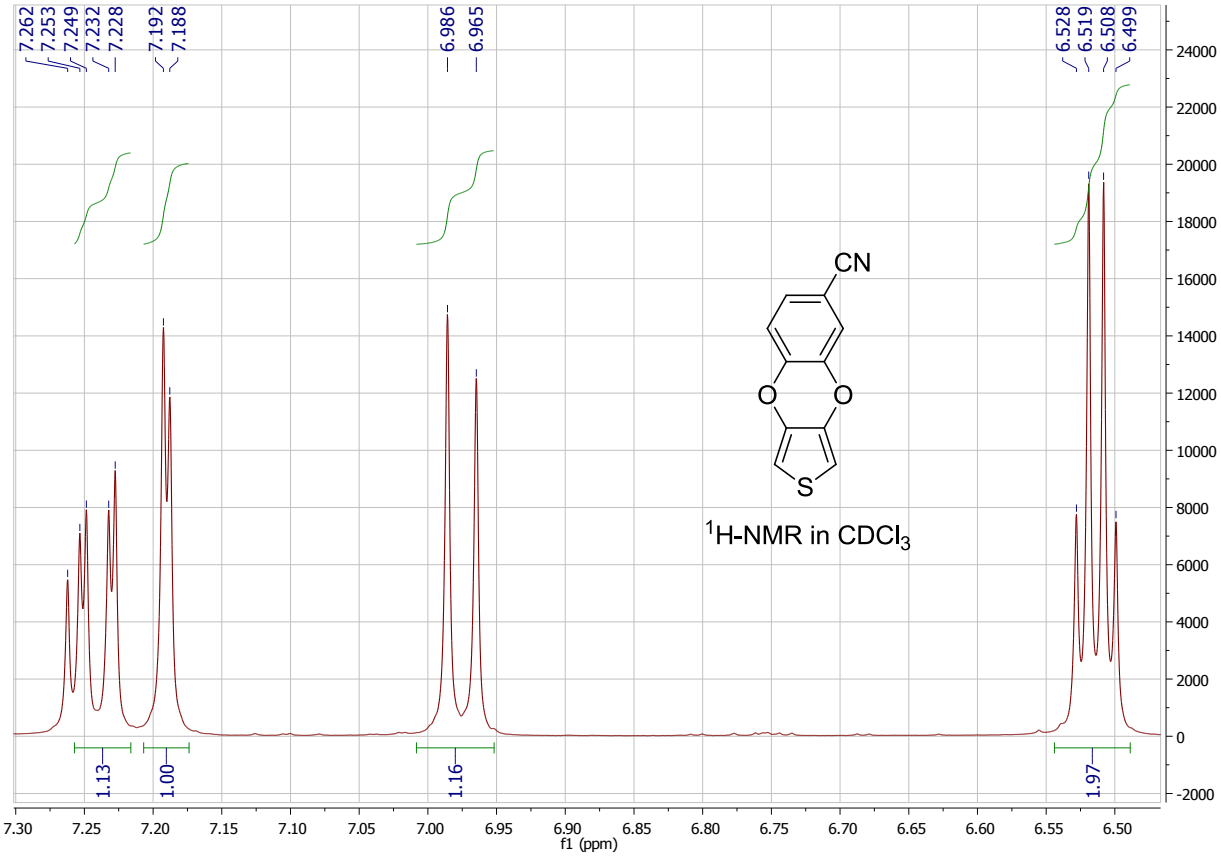

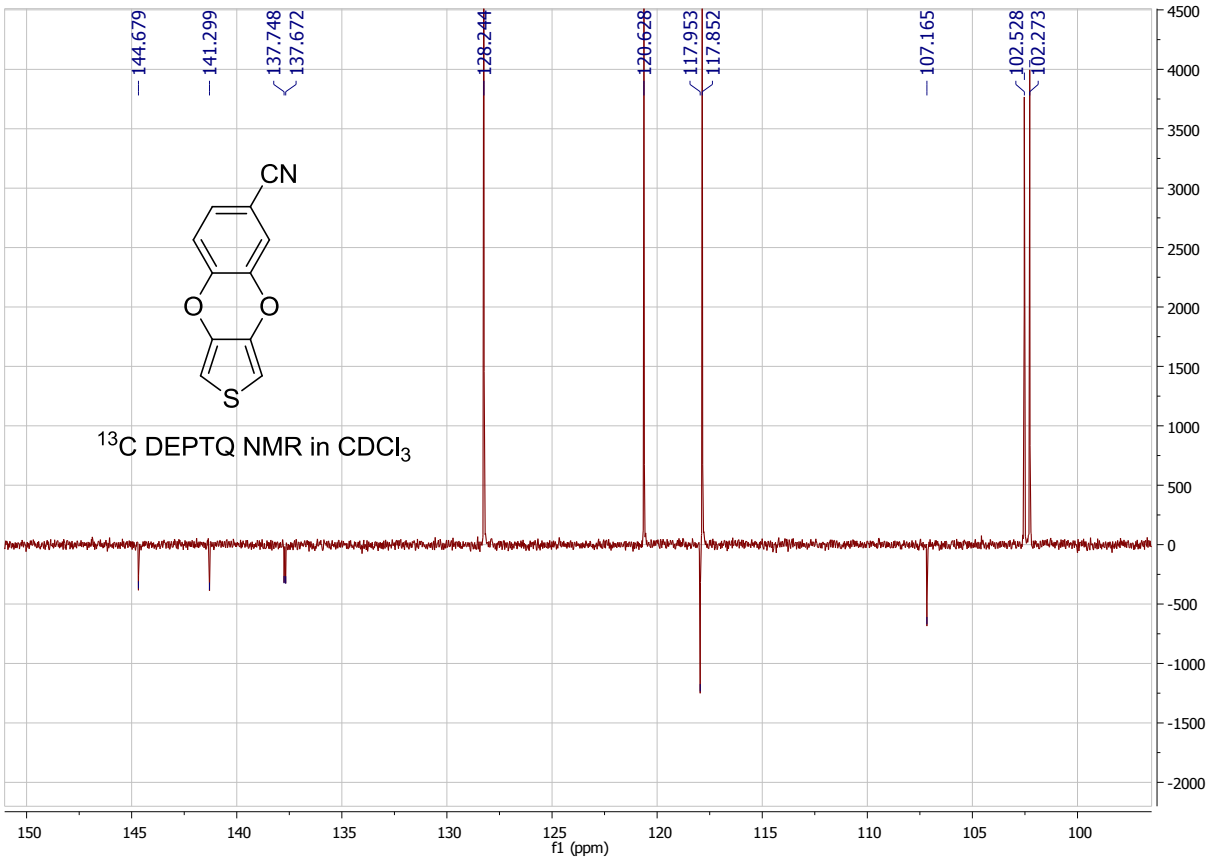
144.679
141.299
137.748
137.672
128.244
120.628
117.953
117.852
107.165
102.528
102.273
CN
O
O
S
13C DEPTQ NMR in CDCl3
f1 (ppm)

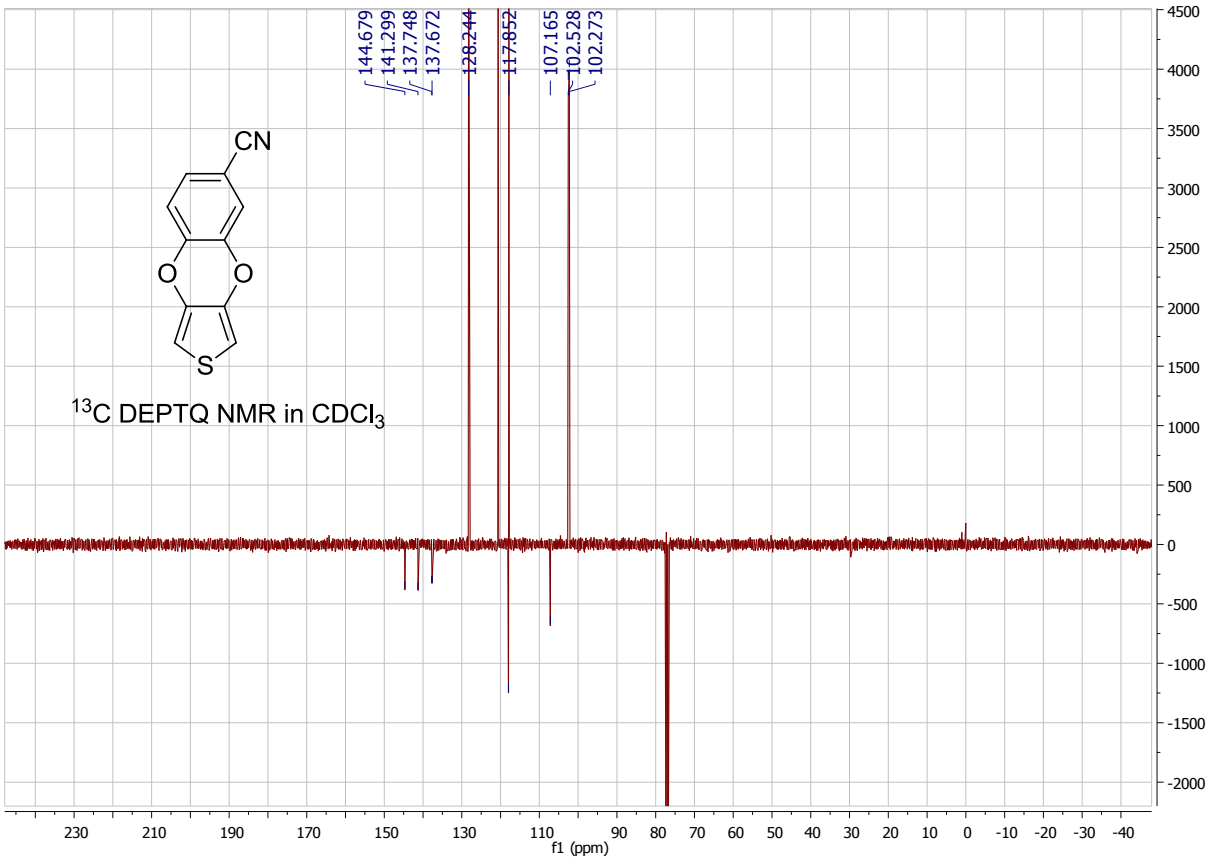
144.679
141.299
137.748
137.672
128.244
117.852
107.165
102.528
102.273
CN
O
O
S
13C DEPTQ NMR in CDCl3
f1 (ppm)

SpinWorks 3: Supervisor Name IP
SNB-34C
HSQC.b CDCl3 {C:\Bruker\TopSpin3.1} IP 7

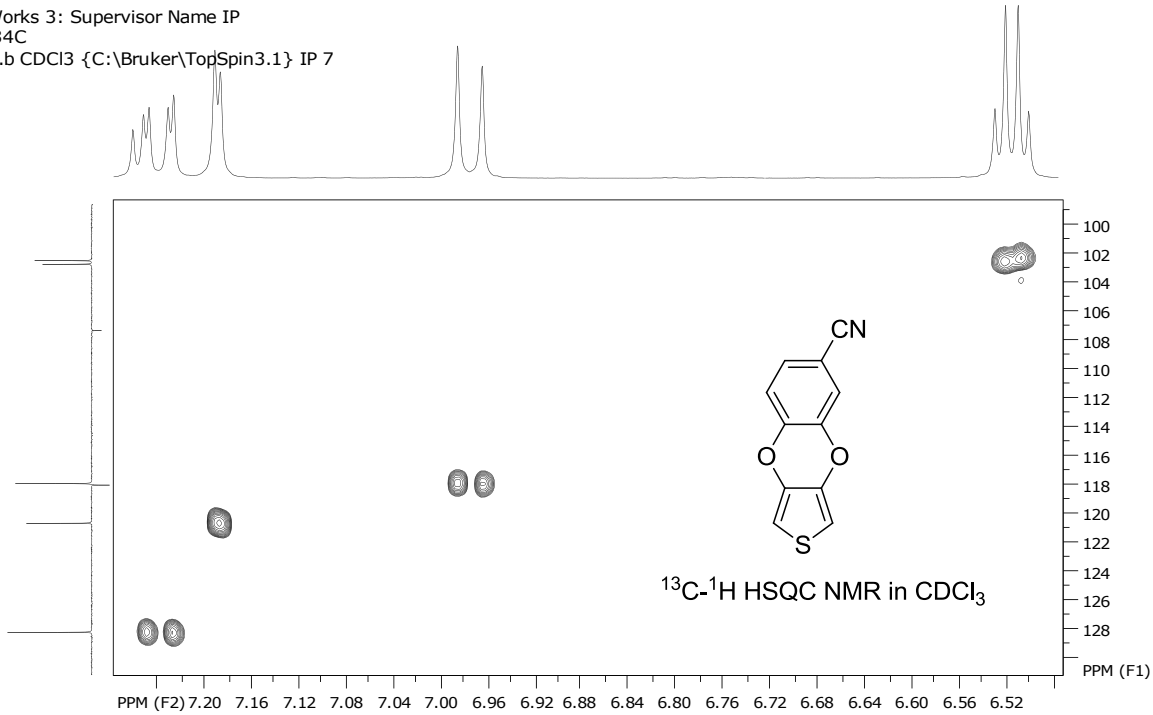

file: ...ated\SNB-34C\53-SNB-34C-HSQC.b\ser
expt: <hsqcedetgpsisp2.3>
transmitter freq: 400.131656 MHz
time domain size: 2048 by 256 points
width (F2): 2994.01 Hz = 7.4826 ppm = 1.4619 Hz/pt
number of scans: 2

F2: freq. of 0 ppm: 400.1300088 MHz
processed size: 1024 complex points
window function: Sine Squared
shift: 90.0 degrees
Hz/cm: 14.649 ppm/cm: 0.03661

F1: freq. of 0 ppm: 100.6127690 MHz
processed size: 1024 complex points
window function: Sine Squared
shift: 90.0 degrees
Hz/cm: 301.160 ppm/cm: 2.99305

6-Nitrobenzo[b]thieno[3,4-e][1,4]dioxine (**4NO$_2$-PheDOT**)

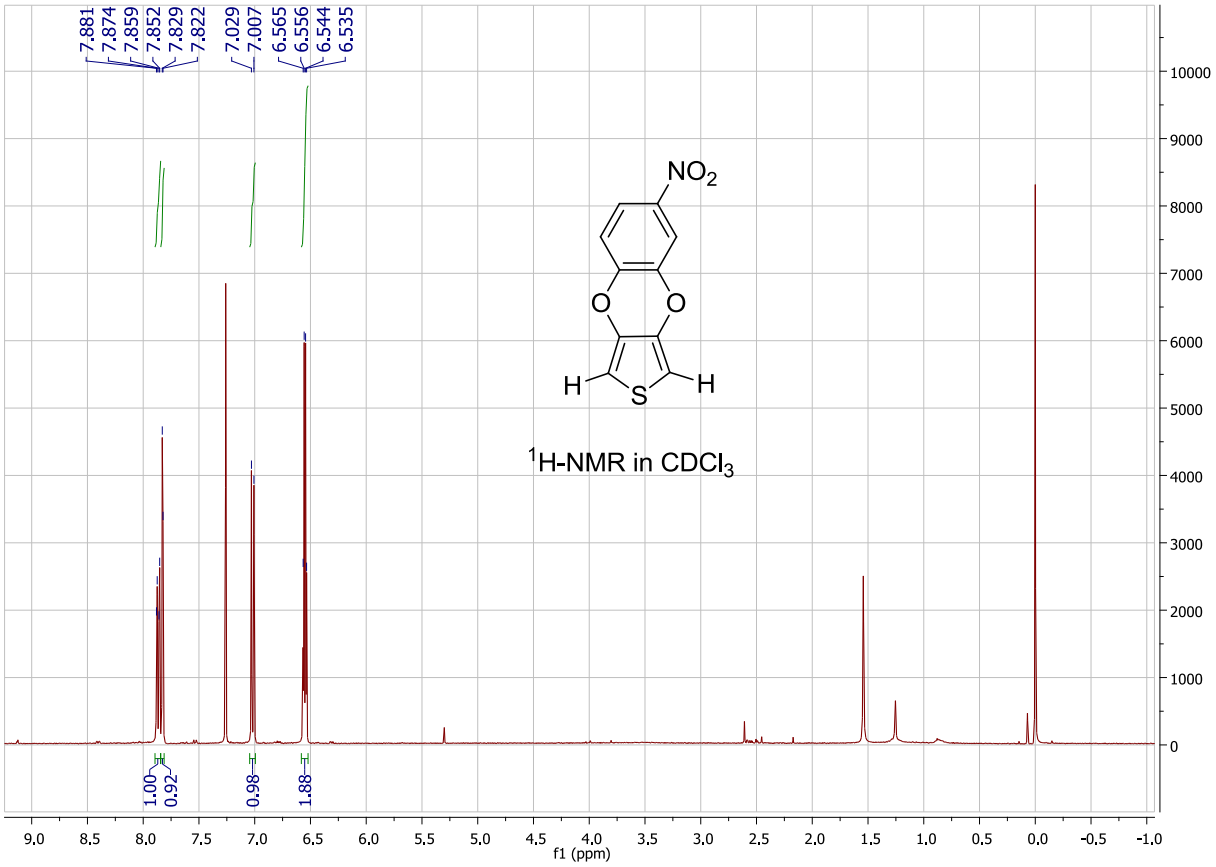

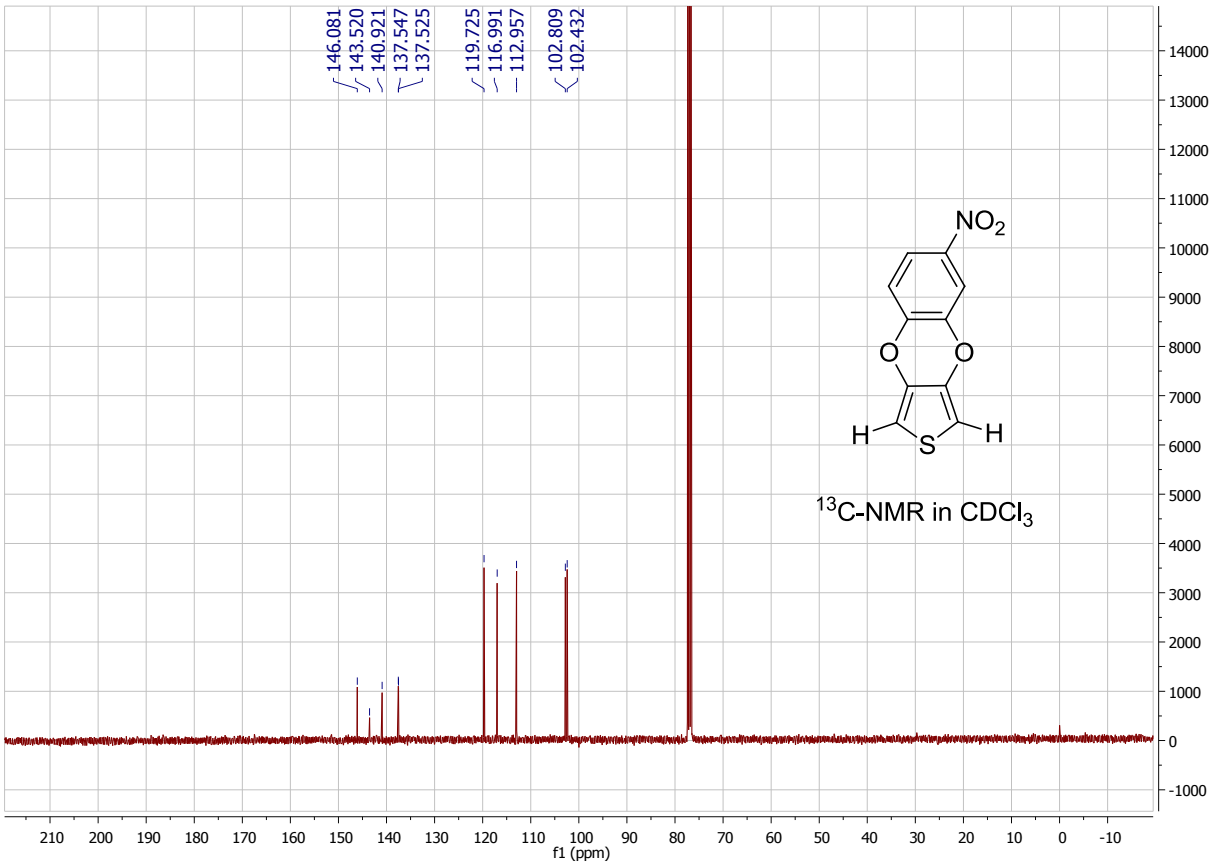

6-(Trifluoromethyl)benzo[b]thieno[3,4-e][1,4]dioxine (**4CF$_3$-PheDOT**)

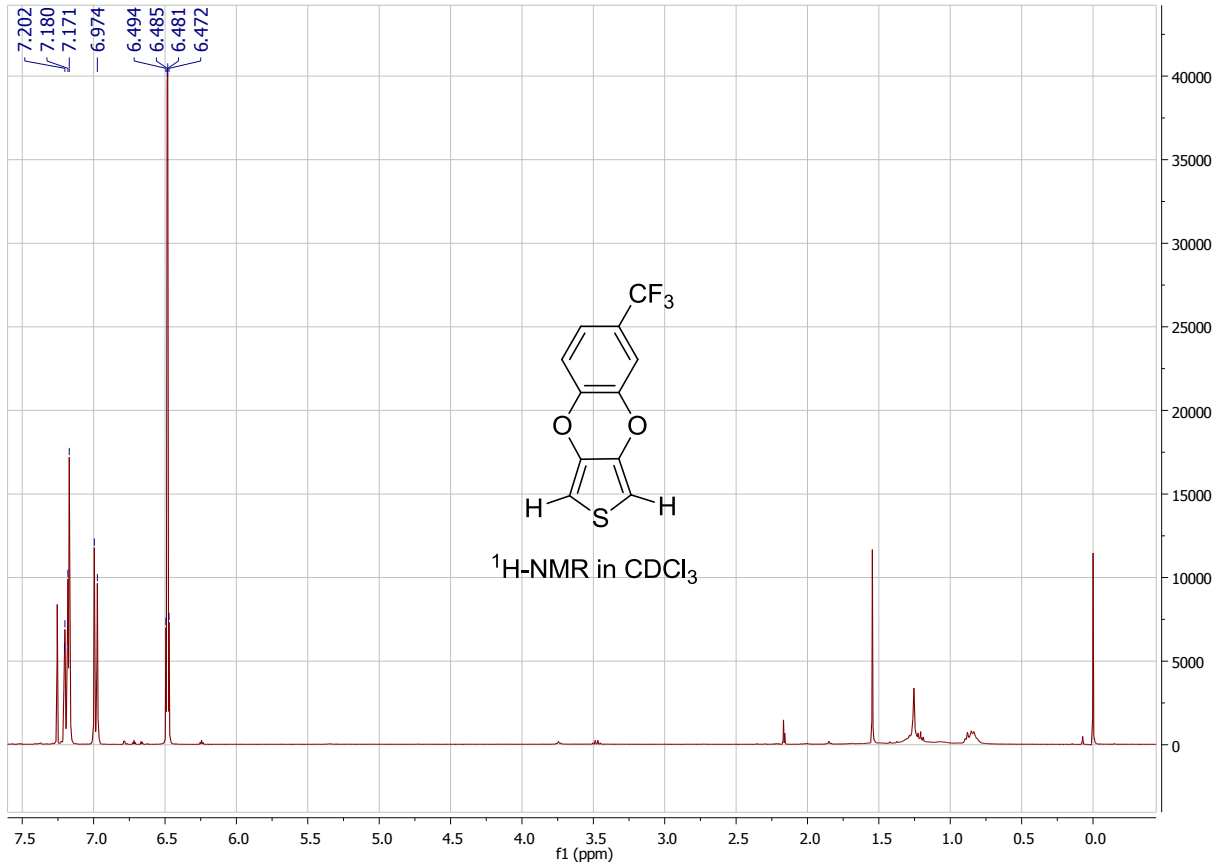

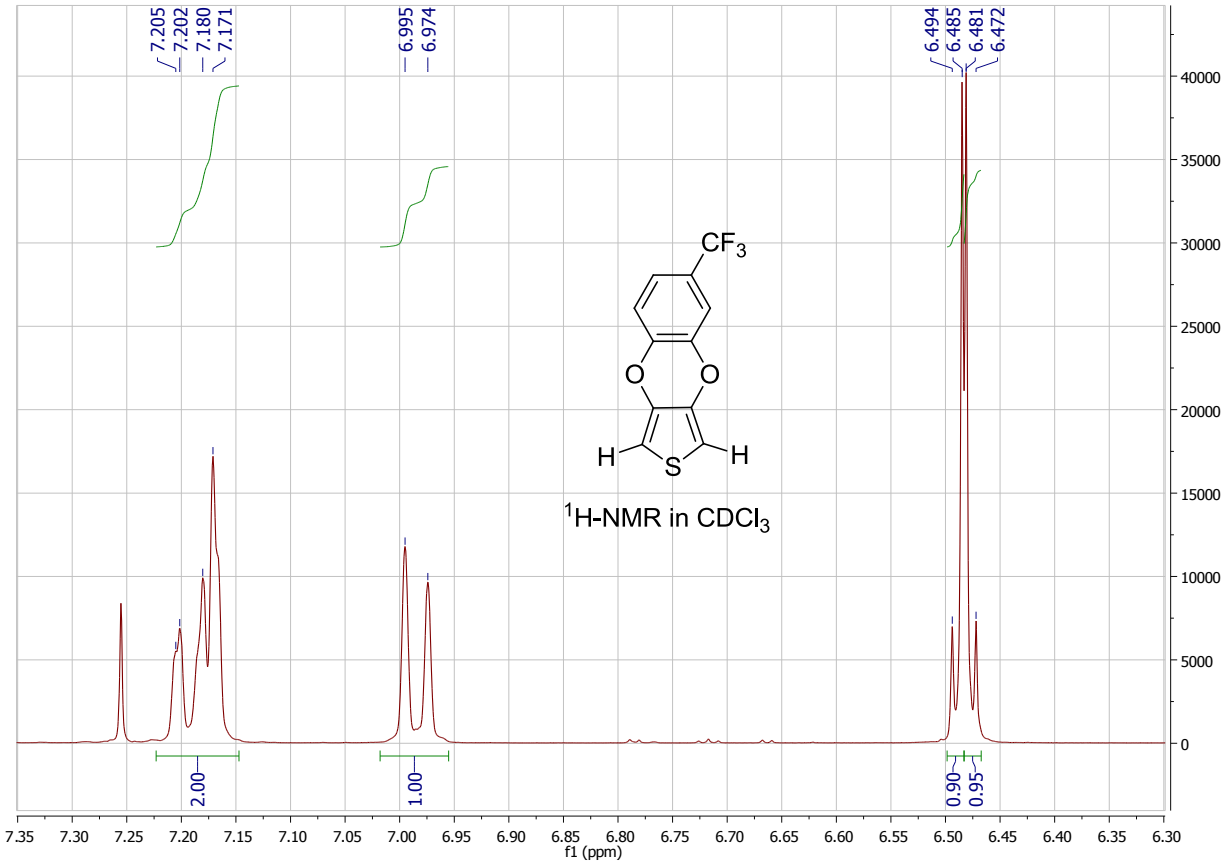

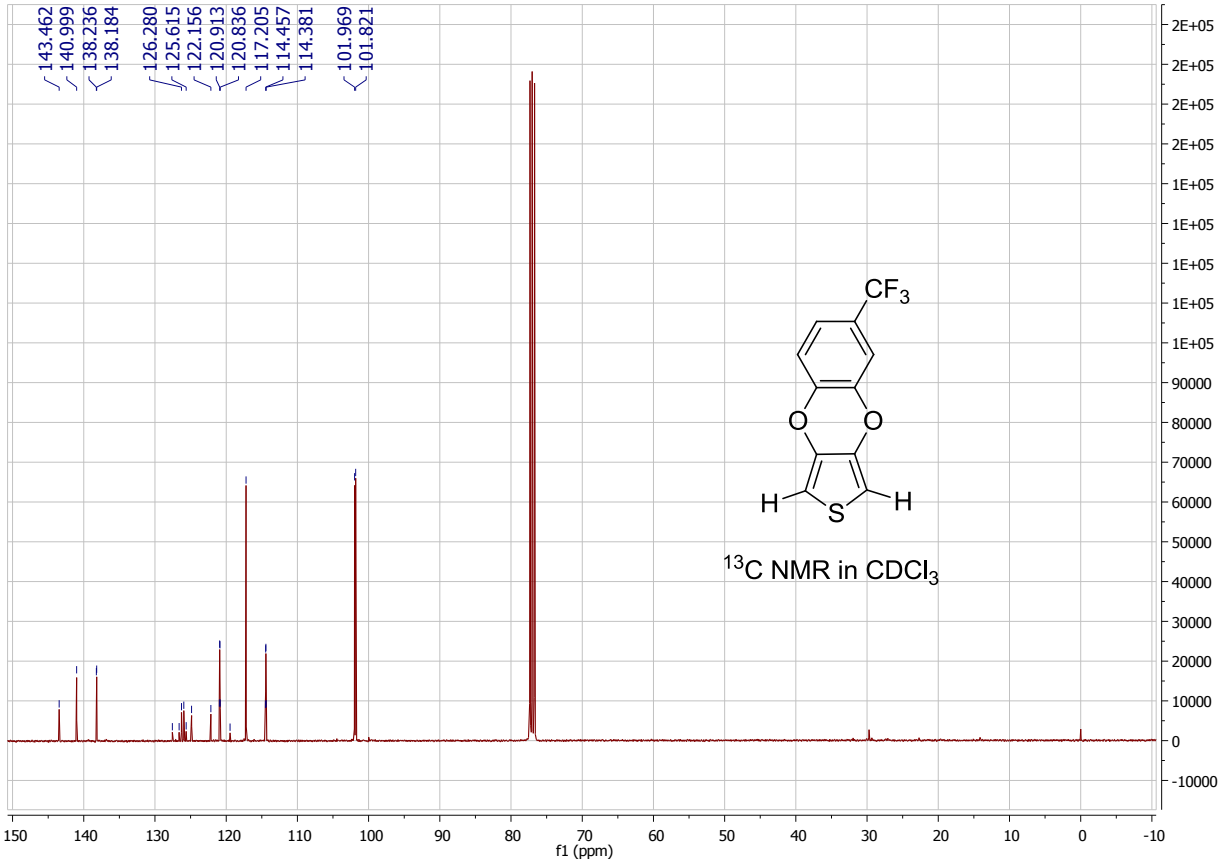
143.462
140.999
138.236
138.184
126.280
125.615
122.156
120.913
120.836
117.205
114.457
114.381
101.969
101.821
CF3
O
O
H
S
H
13C NMR in CDCl3
f1 (ppm)

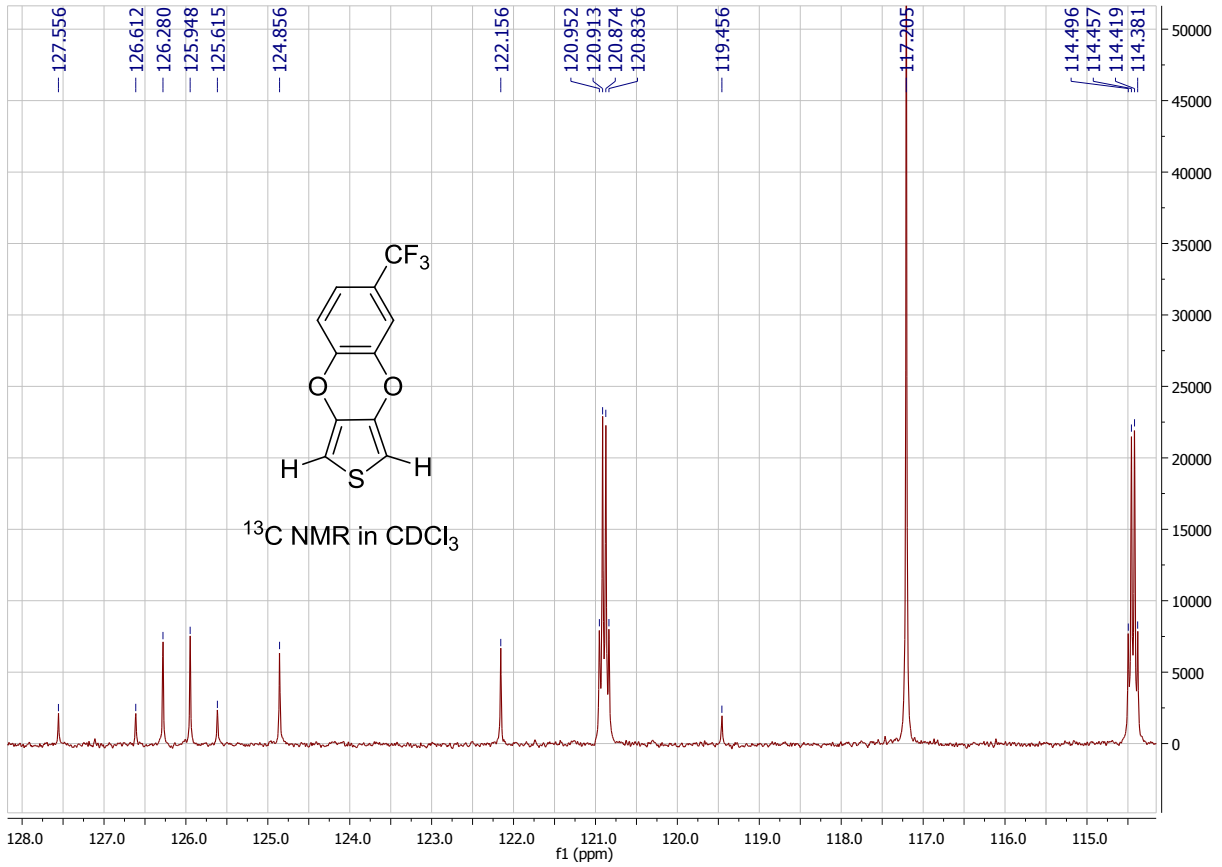
127.556
126.612
126.280
125.948
125.615
124.856
122.156
120.952
120.913
120.874
120.836
119.456
117.205
114.496
114.457
114.419
114.381
CF3
O
O
H
S
H
13C NMR in CDCl3
f1 (ppm)

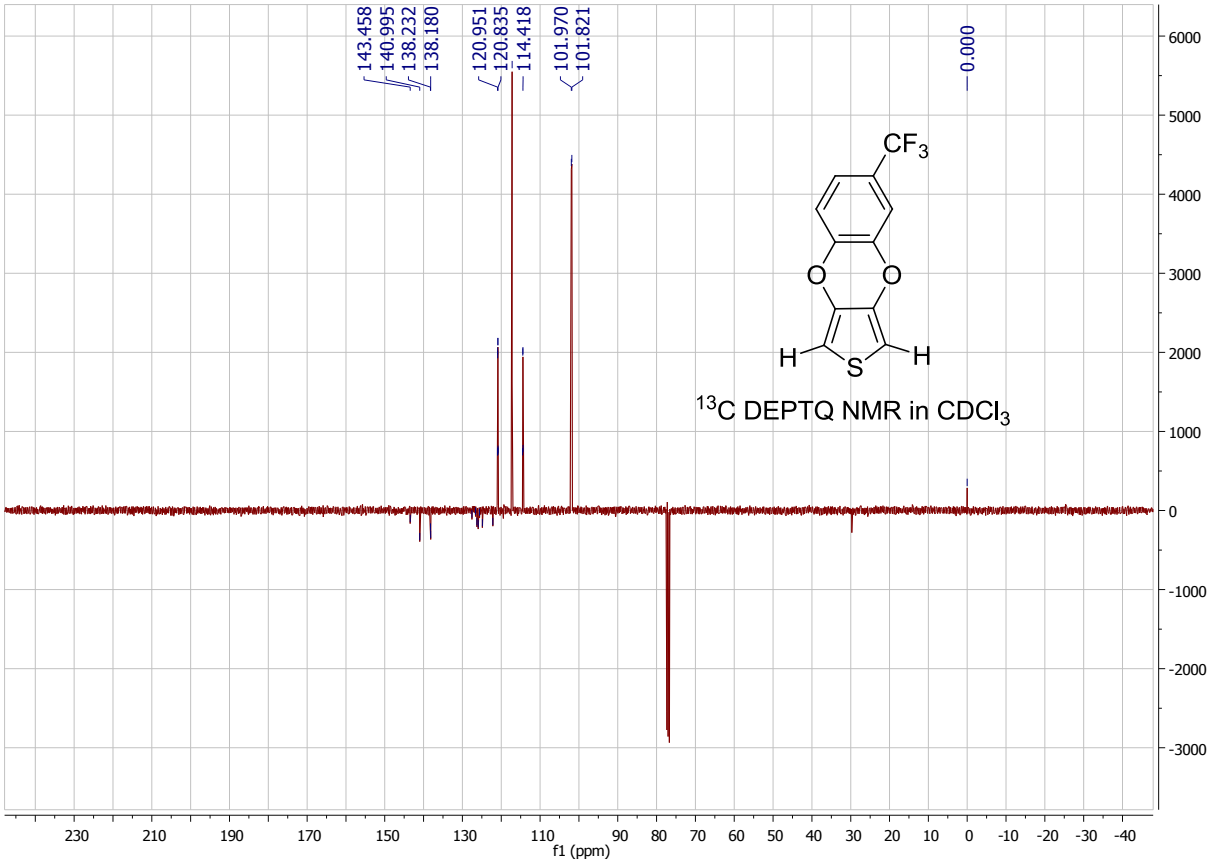
143.458
140.995
138.232
138.180
120.951
120.835
114.418
101.970
101.821
0.000
CF3
O
O
H
S
H
13C DEPTQ NMR in CDCl3
f1 (ppm)

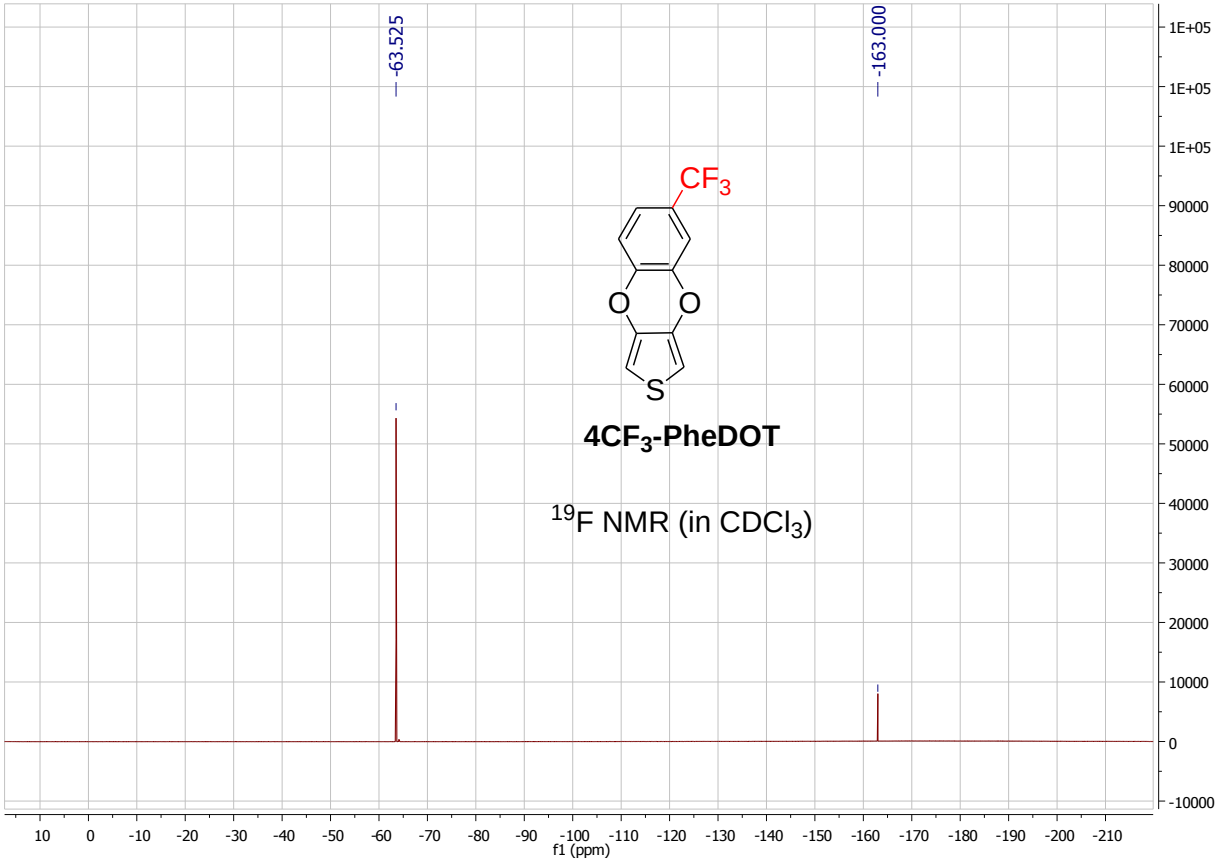
-63.525
-163.000
CF3
O
O
S
4CF3-PheDOT
19F NMR (in CDCl3)
f1 (ppm)

SpinWorks 3: Supervisor Name IP

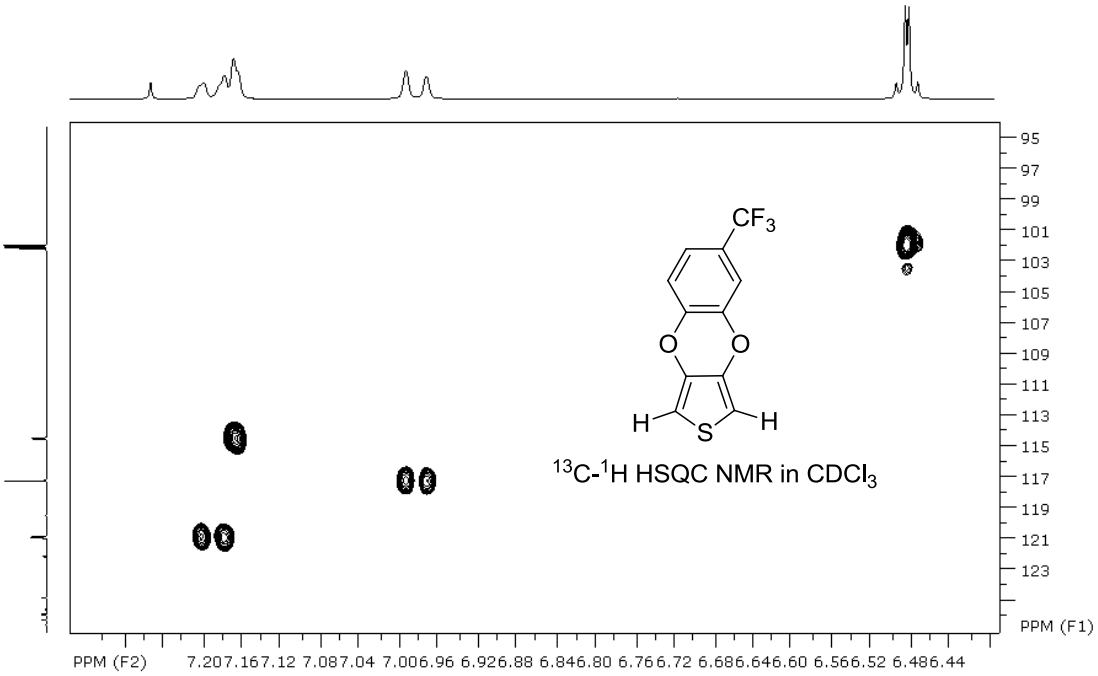

file: ...eated\snb38B\11-SNB-38B-HSQC.b\ser
expt: <hsqcedetgpsisp2.3>
transmitter freq: 400.131644 MHz
time domain size: 2048 by 256 points
width (F2): 3012.05 Hz = 7.5276 ppm = 1.4707 Hz/pt
number of scans: 2

F2: freq. of 0 ppm: 400.1300117 MHz
processed size: 1024 complex points
window function: Sine Squared
shift: 90.0 degrees
Hz/cm: 18.913 ppm/cm: 0.04727

F1: freq. of 0 ppm: 100.6127690 MHz
processed size: 1024 complex points
window function: Sine Squared
shift: 90.0 degrees
Hz/cm: 303.030 ppm/cm: 3.01164

SpinWorks 3: Supervisor Name IP

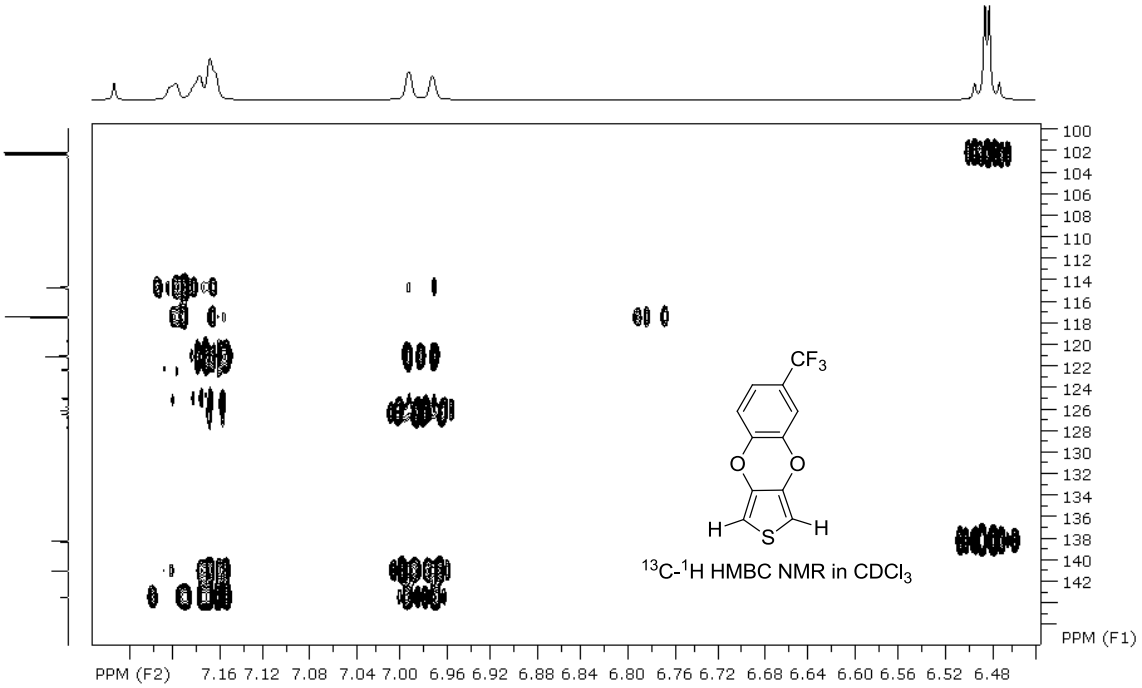

file: ...eated\snb38B\12-SNB-38B-HMBC.b\ser
expt: <hmbcetgpl3nd>
transmitter freq: 400.131644 MHz
time domain size: 4096 by 256 points
width (F2): 3012.05 Hz = 7.5276 ppm = 0.7354 Hz/pt
number of scans: 4

F2: freq. of 0 ppm: 400.1300117 MHz
processed size: 2048 complex points
window function: Sine
shift: 45.0 degrees
Hz/cm: 16.726 ppm/cm: 0.04180

F1: freq. of 0 ppm: 100.6127690 MHz
processed size: 1024 complex points
window function: Sine Squared
shift: 90.0 degrees
Hz/cm: 442.769 ppm/cm: 4.40029

6-(Methylsulfonyl)benzo[b]thieno[3,4-e][1,4]dioxine **(4MeSO$_2$-PheDOT)**

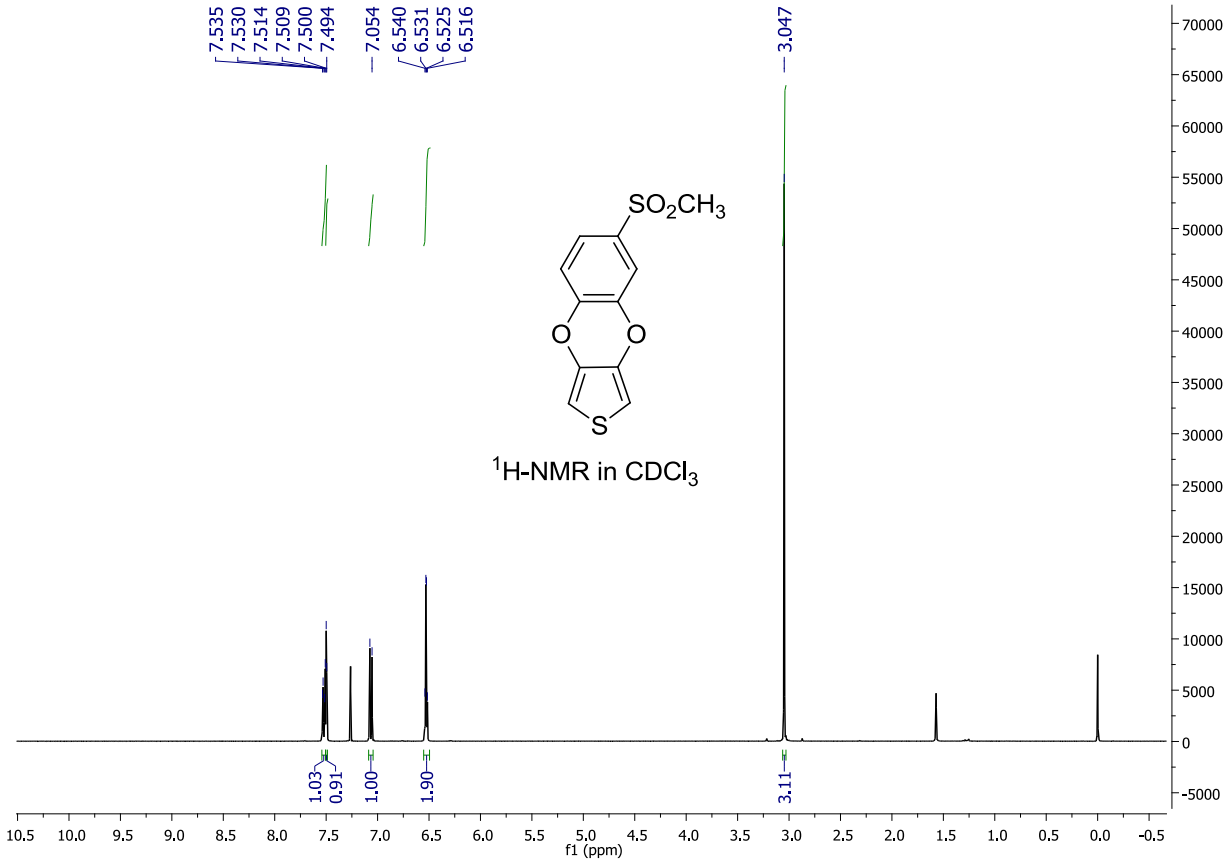

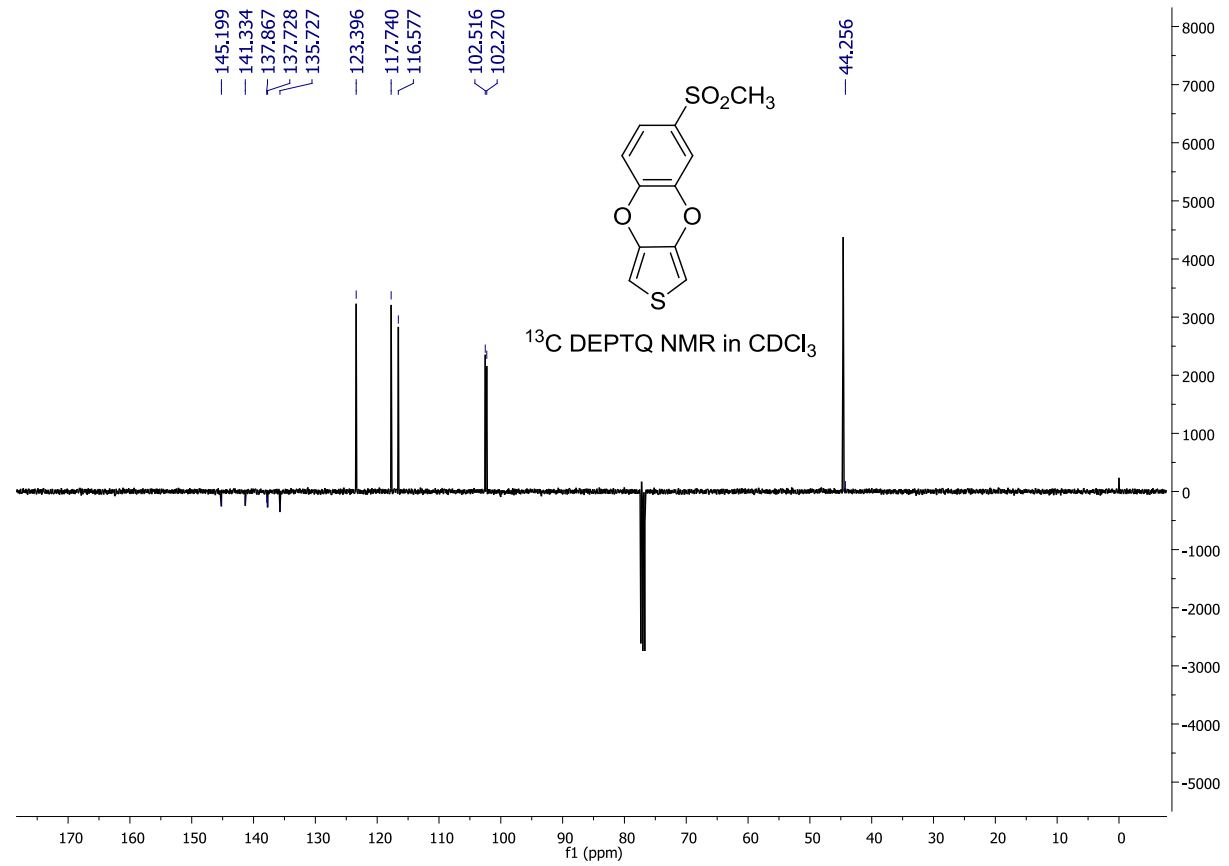

5-Nitro-7-(trifluoromethyl)benzo[b]thieno[3,4-e][1,4]dioxine (**3NO$_2$,5CF$_3$-PheDOT**)

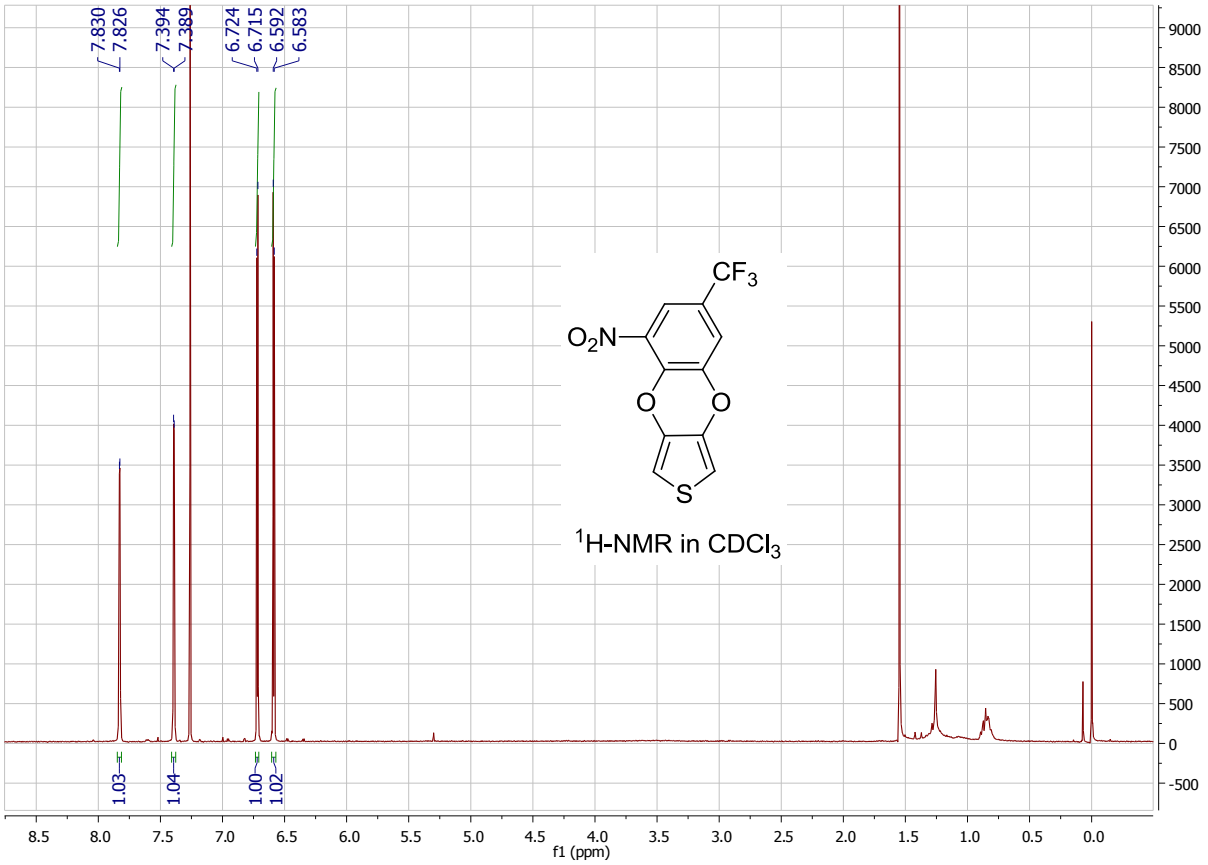

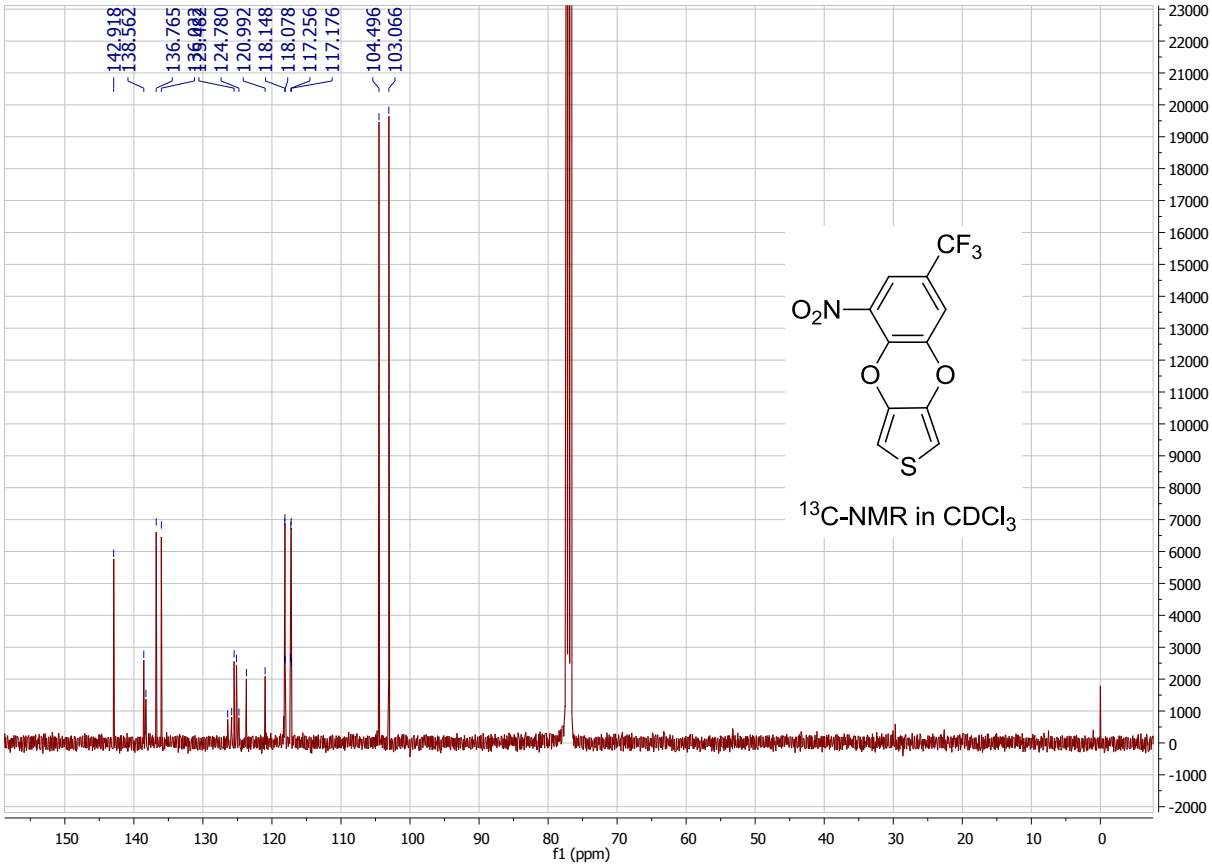

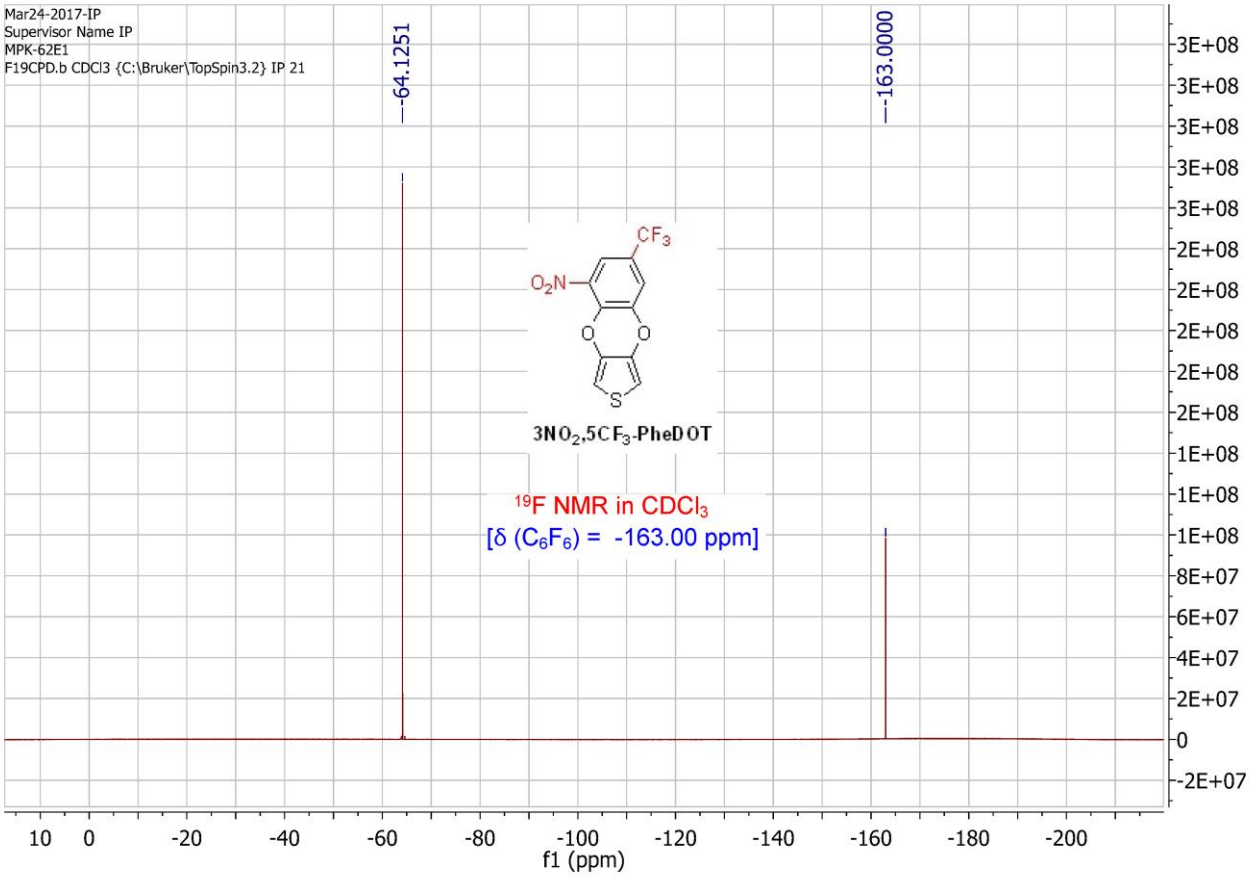
Mar24-2017-IP
Supervisor Name IP
MPK-62E1
F19CPD.b CDCl3 {C:\Bruker\TopSpin3.2} IP 21
-64.1251
-163.0000
CF3
O2N
O
O
S
3NO2,5CF3-PheDOT
19F NMR in CDCl3
[δ (C6F6) = -163.00 ppm]
3E+08
2E+08
1E+08
8E+07
6E+07
4E+07
2E+07
0
-2E+07
10
0
-20
-40
-60
-80
-100
-120
-140
-160
-180
-200
f1 (ppm)

7-Nitro-5-(trifluoromethyl)benzo[b]thieno[3,4-e][1,4]dioxine (**3CF$_3$,5NO$_2$-PheDOT**)

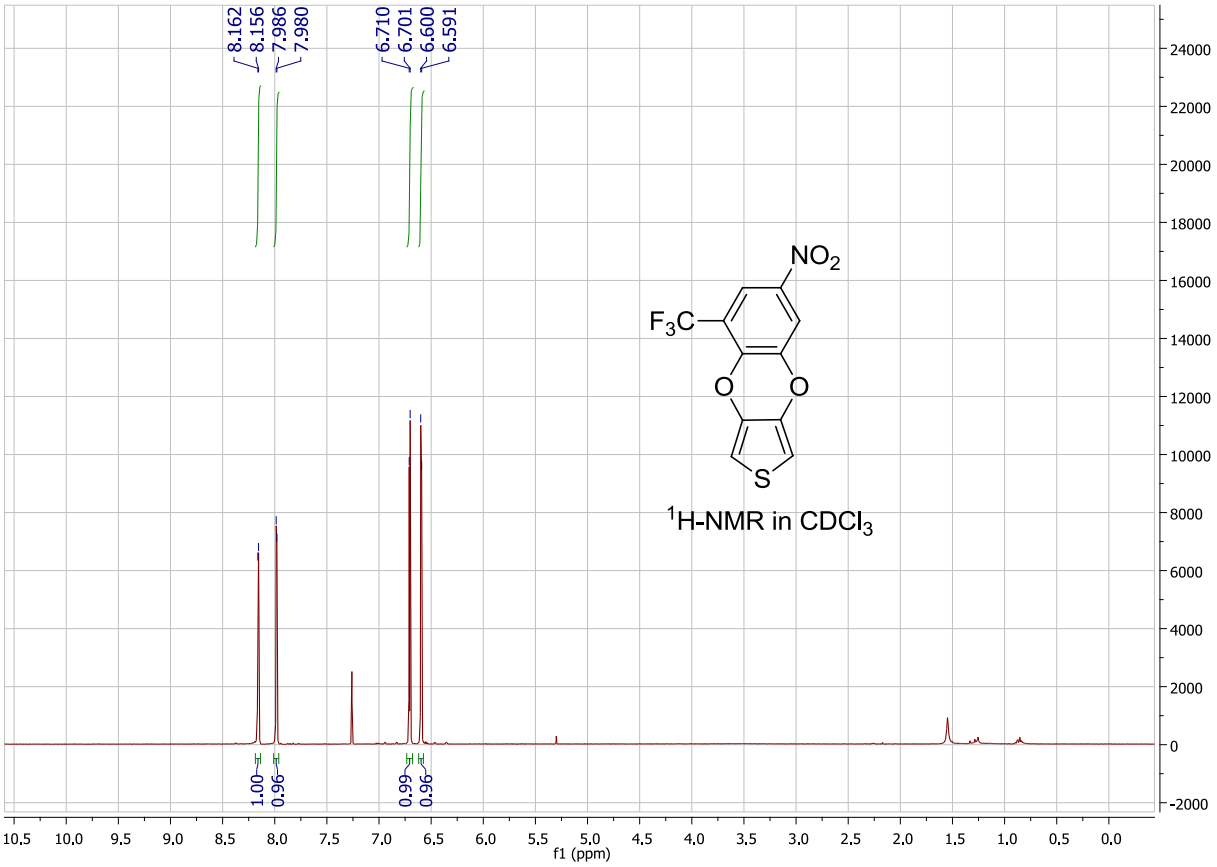

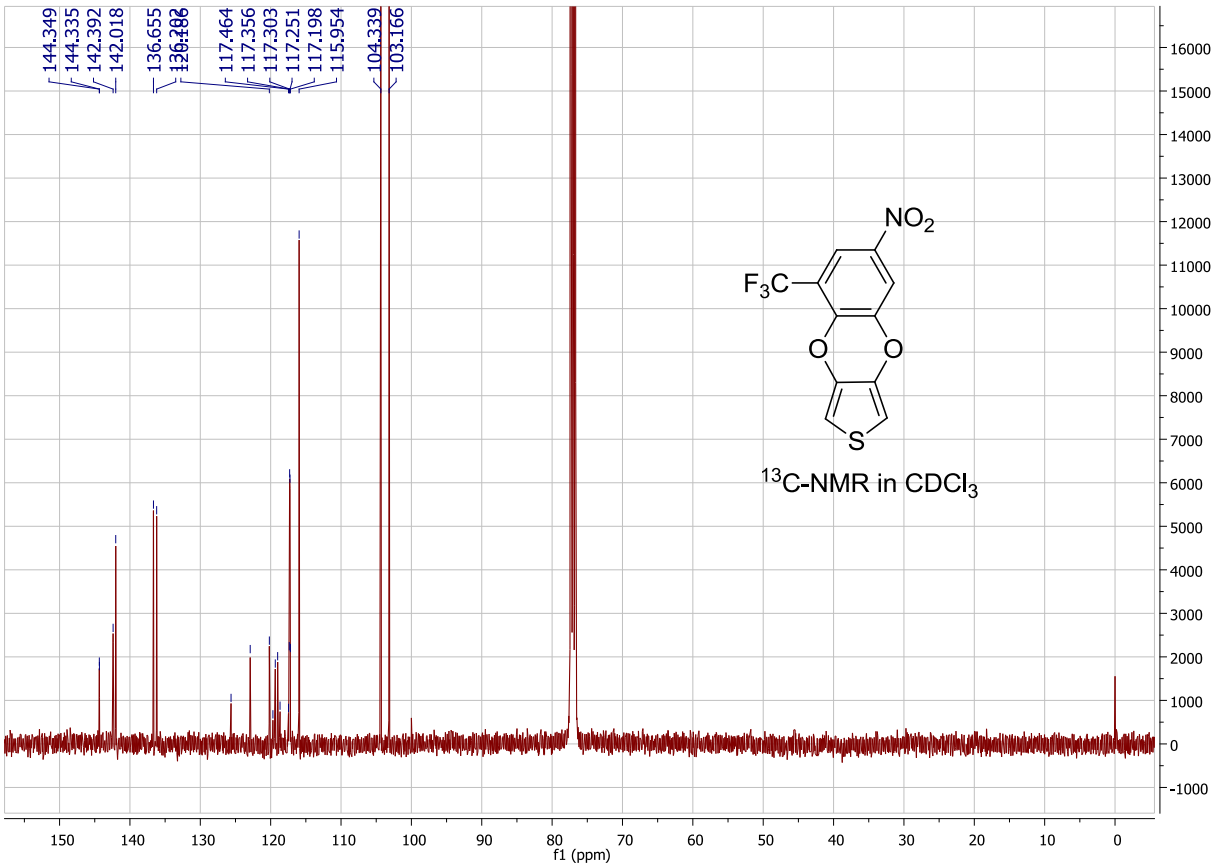

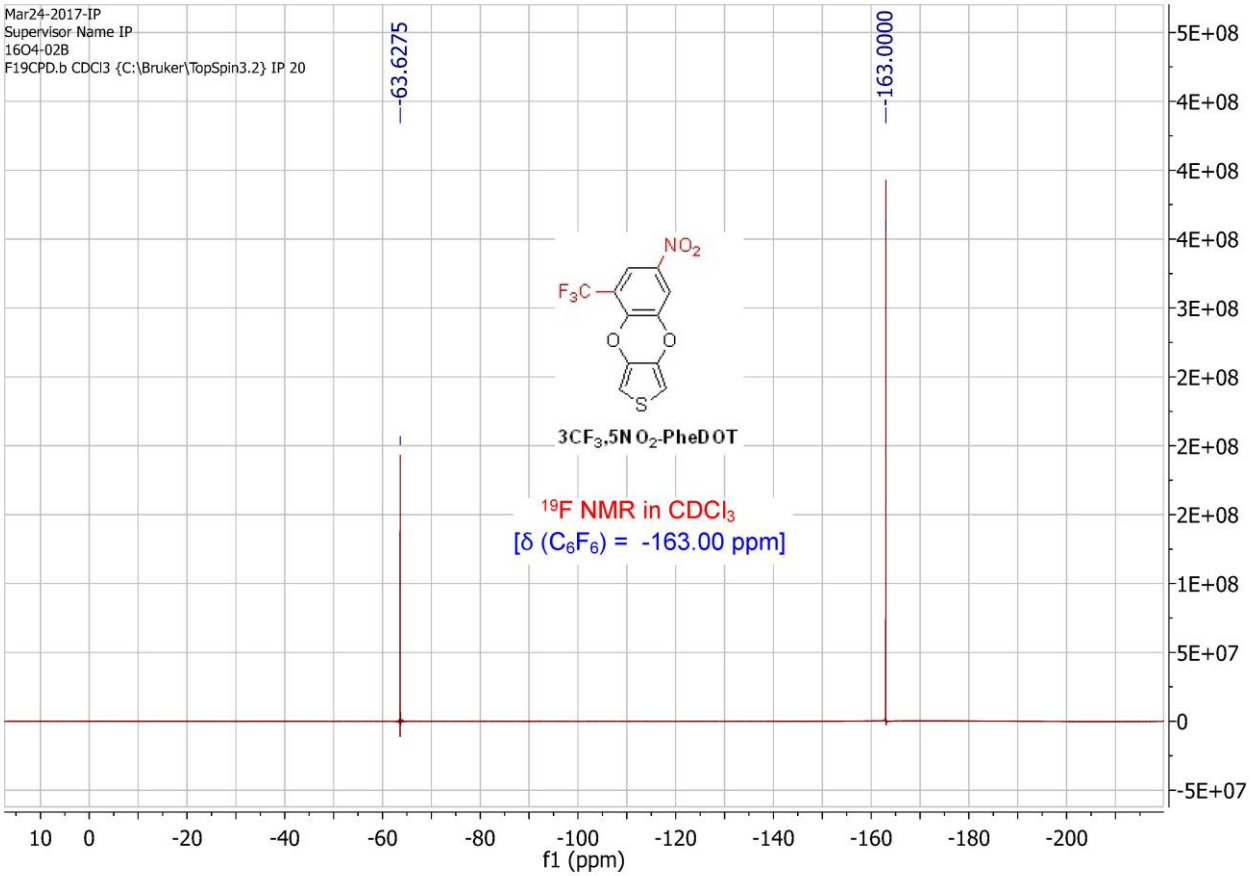
Mar24-2017-IP
Supervisor Name IP
16O4-02B
F19CPD.b CDCl3 {C:\Bruker\TopSpin3.2} IP 20
-63.6275
-163.0000
NO2
F3C
O
O
S
3CF3,5NO2-PheDOT
19F NMR in CDCl3
[δ (C6F6) = -163.00 ppm]
5E+08
4E+08
4E+08
4E+08
3E+08
2E+08
2E+08
2E+08
1E+08
5E+07
0
-5E+07
10
0
-20
-40
-60
-80
-100
-120
-140
-160
-180
-200
f1 (ppm)

5,6,7,8-Tetrachlorobenzo[b]thieno[3,4-e][1,4]dioxine **(Cl_4-PheDOT)**

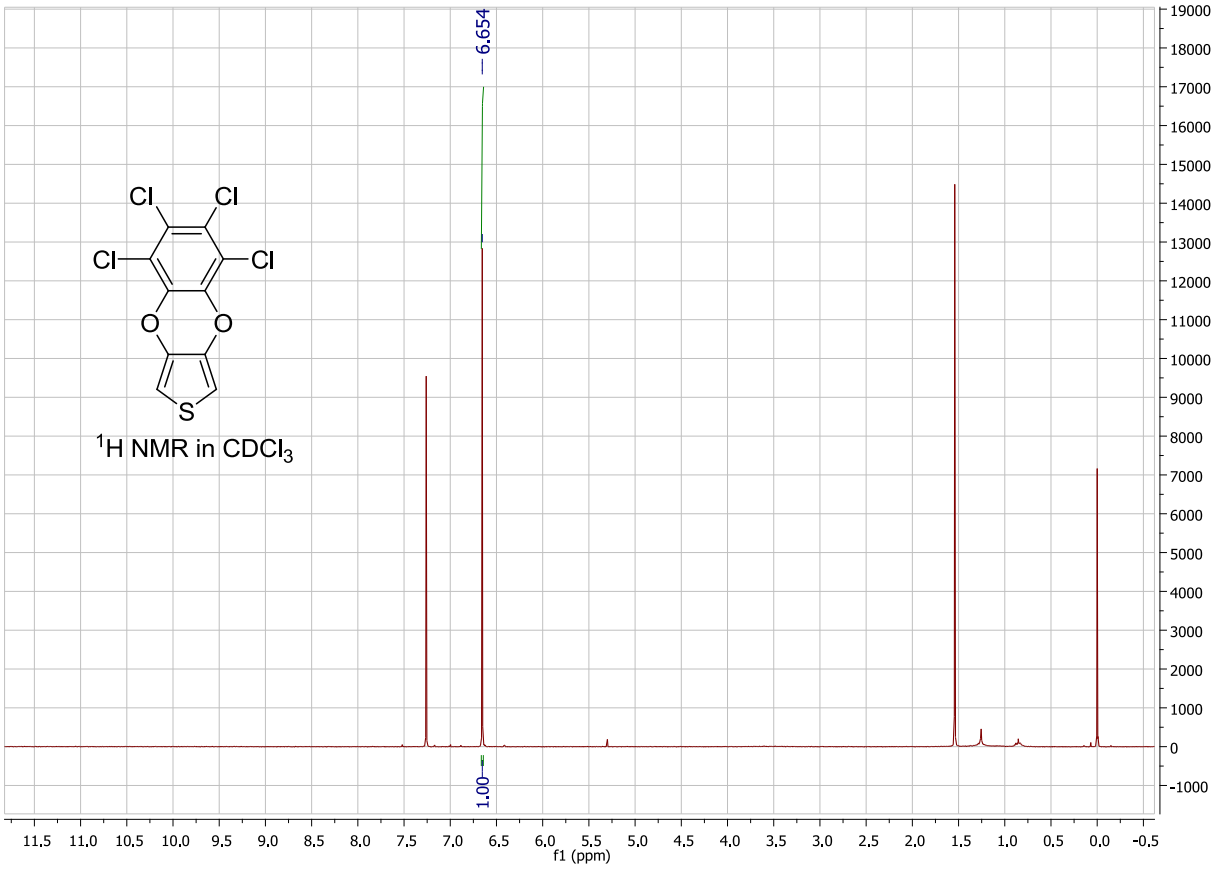

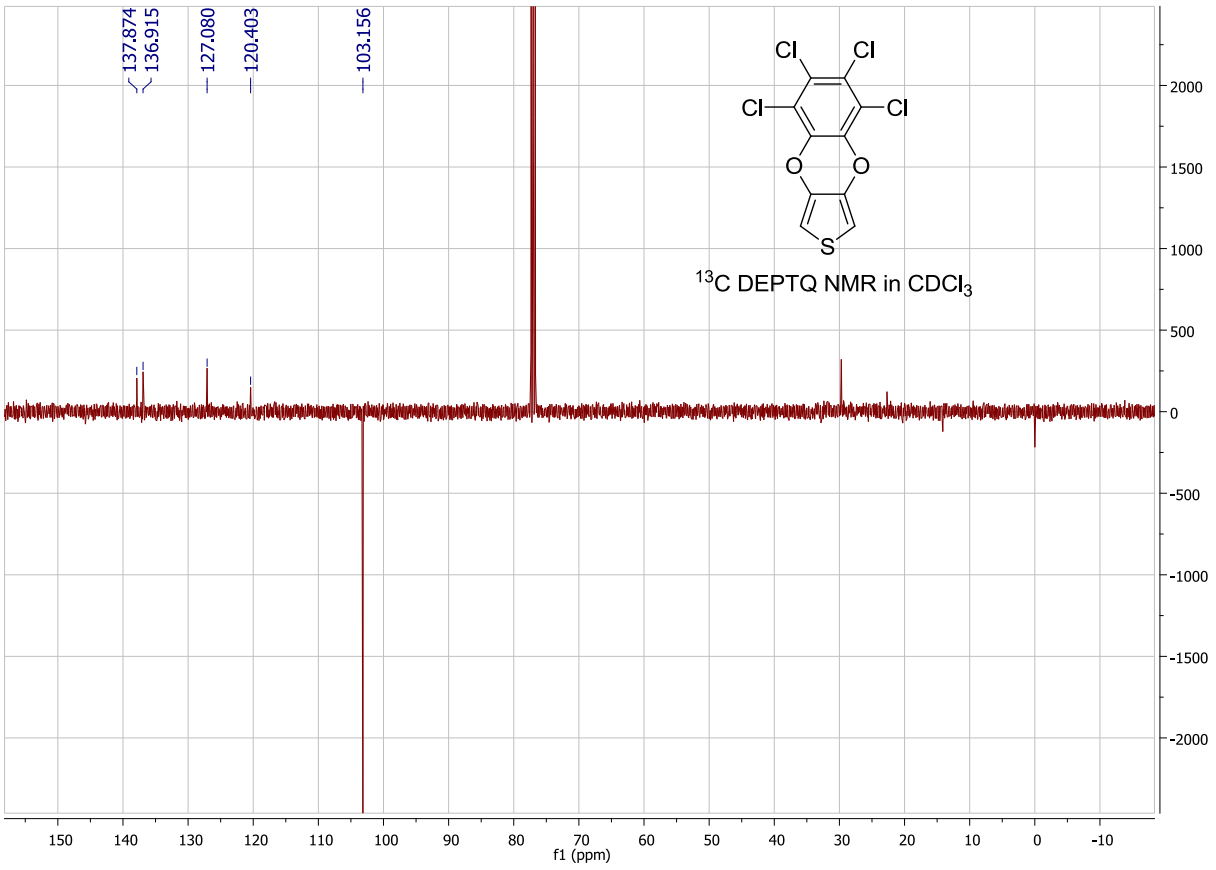

Benzo[b]thieno[3,4-e][1,4]dioxine-6,7-dicarbonitrile **(45(CN)$_2$-PheDOT)**

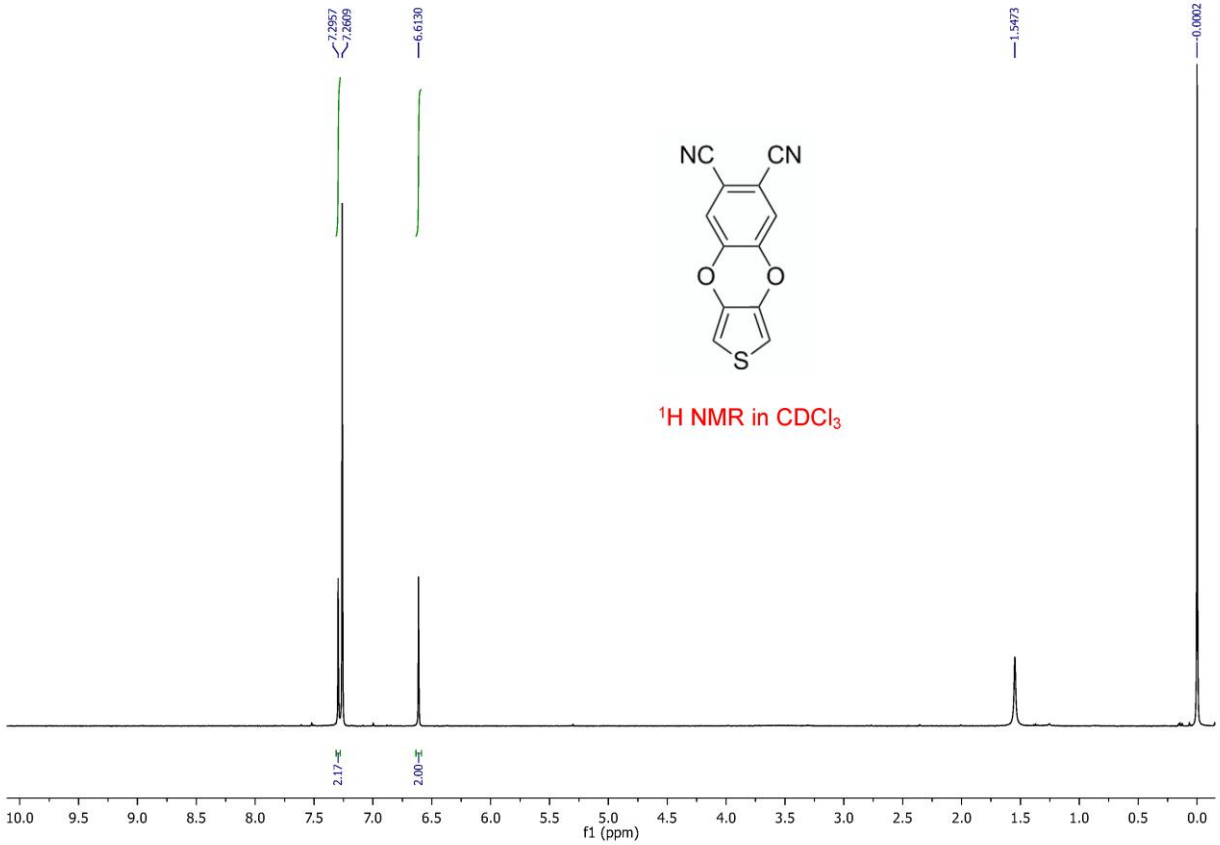

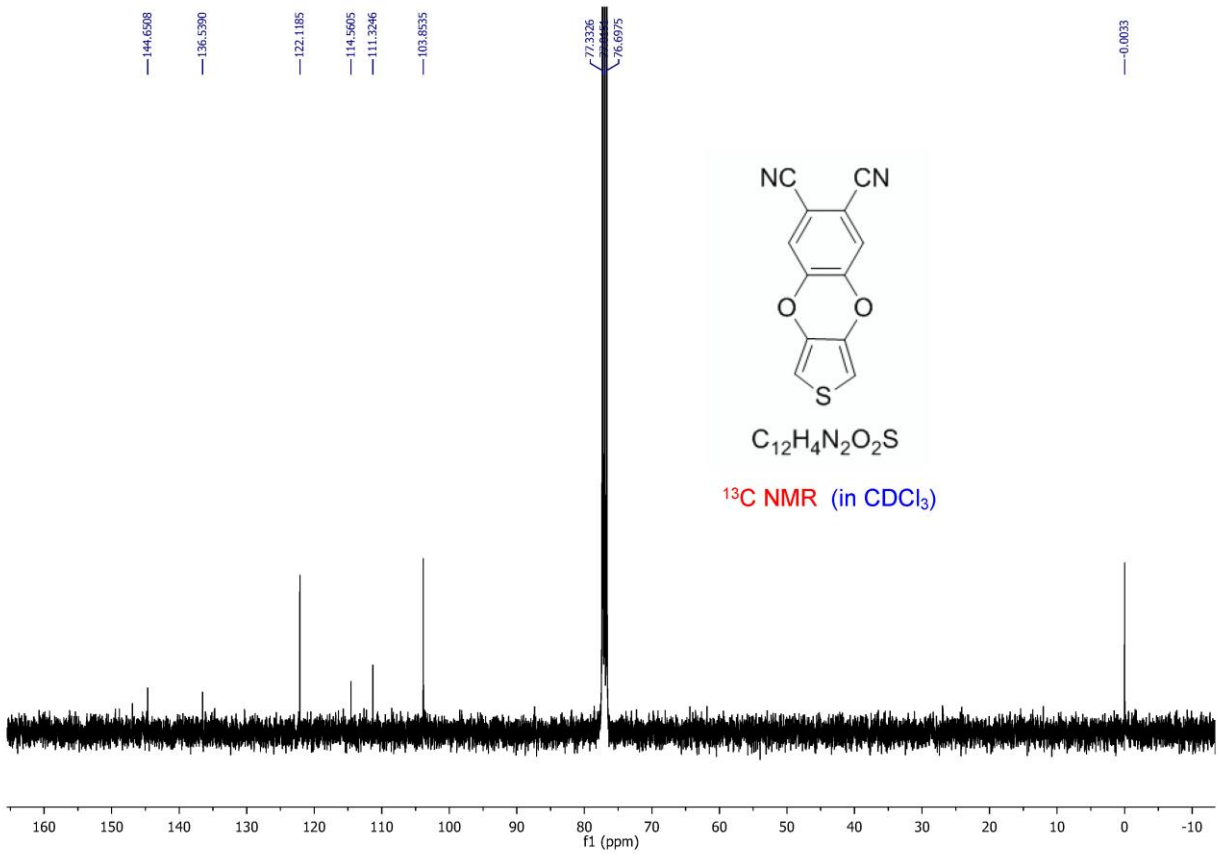

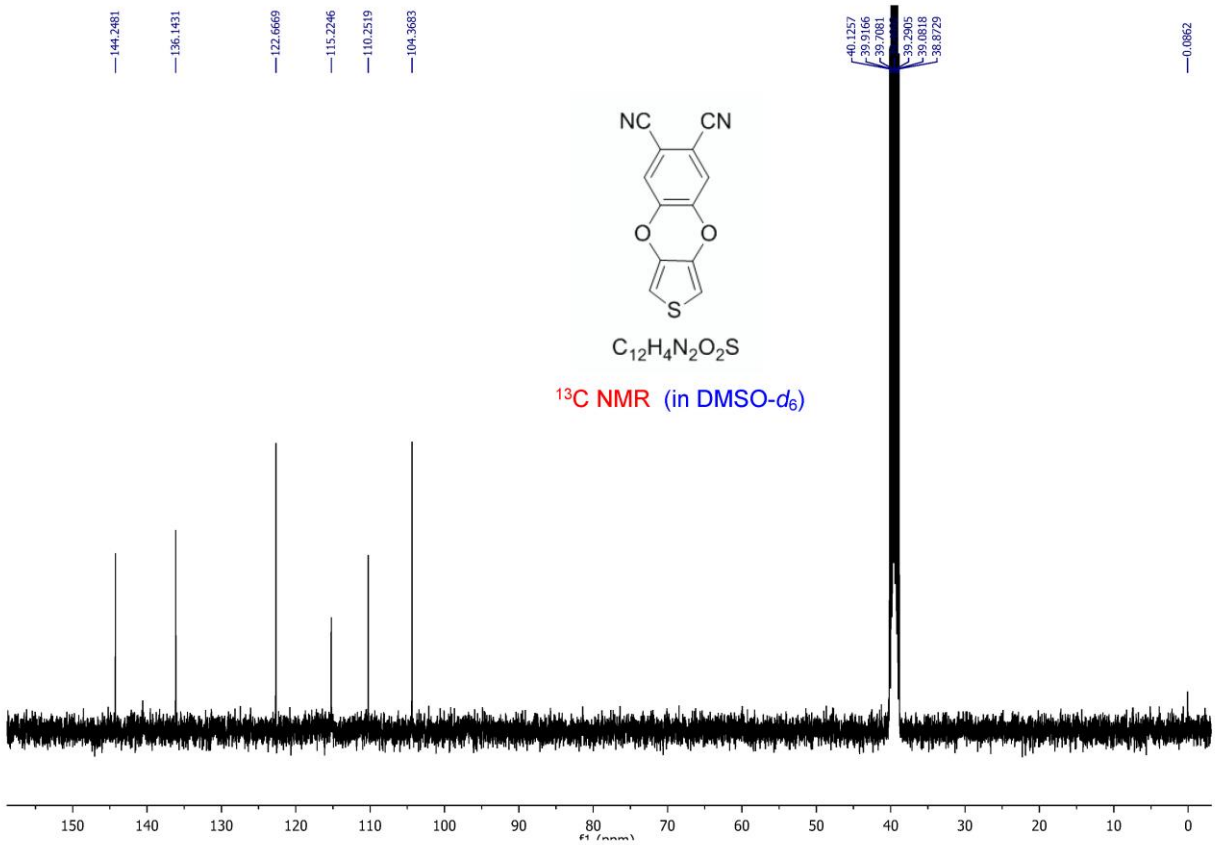
144.2481
136.1431
122.6669
115.2246
110.2519
104.3683
40.1257
39.9166
39.7081
39.2905
39.0818
38.8729
0.0862
NC
CN
O
O
S
$C_{12}H_4N_2O_2S$
^{13}C NMR (in DMSO-d_6)
150
140
130
120
110
100
90
80
70
60
50
40
30
20
10
0

6,7-Difluorobenzo[b]thieno[3,4-e][1,4]dioxine (**45F$_2$-PheDOT**)

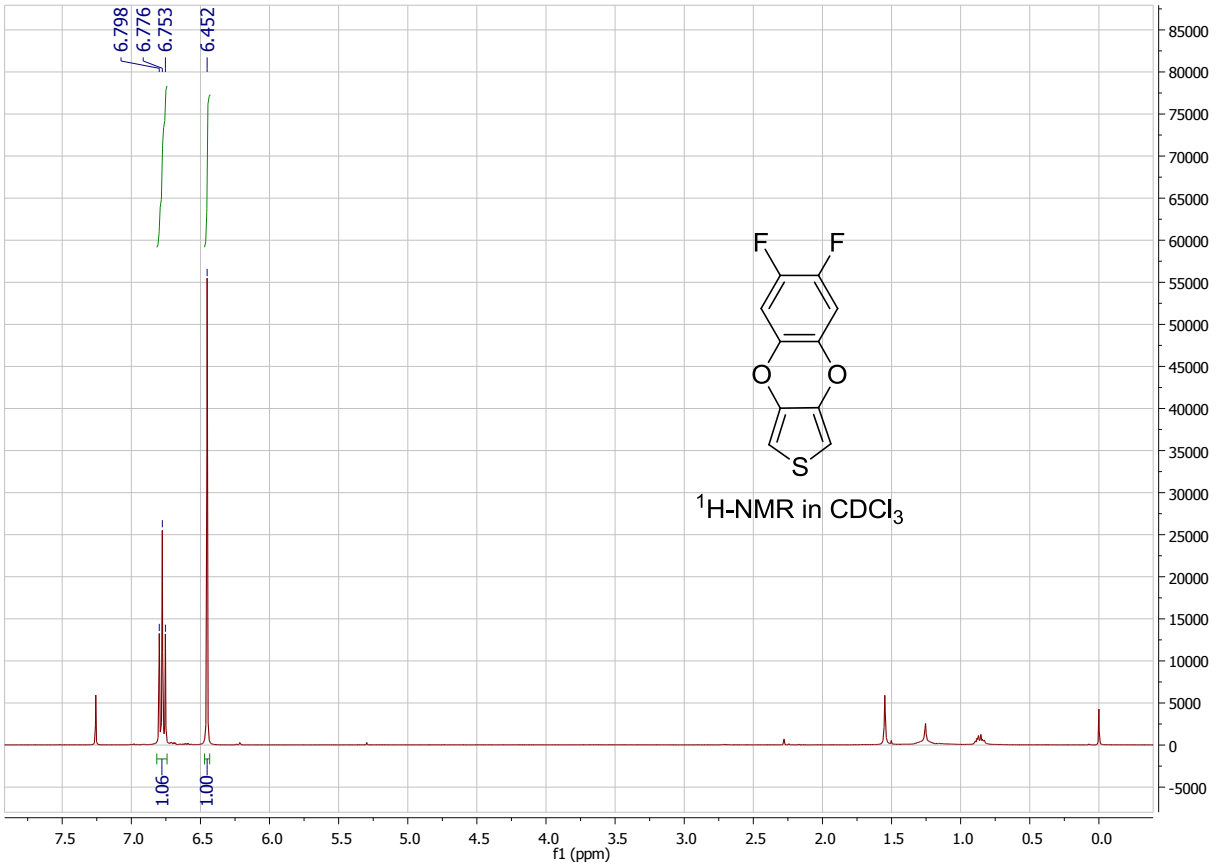

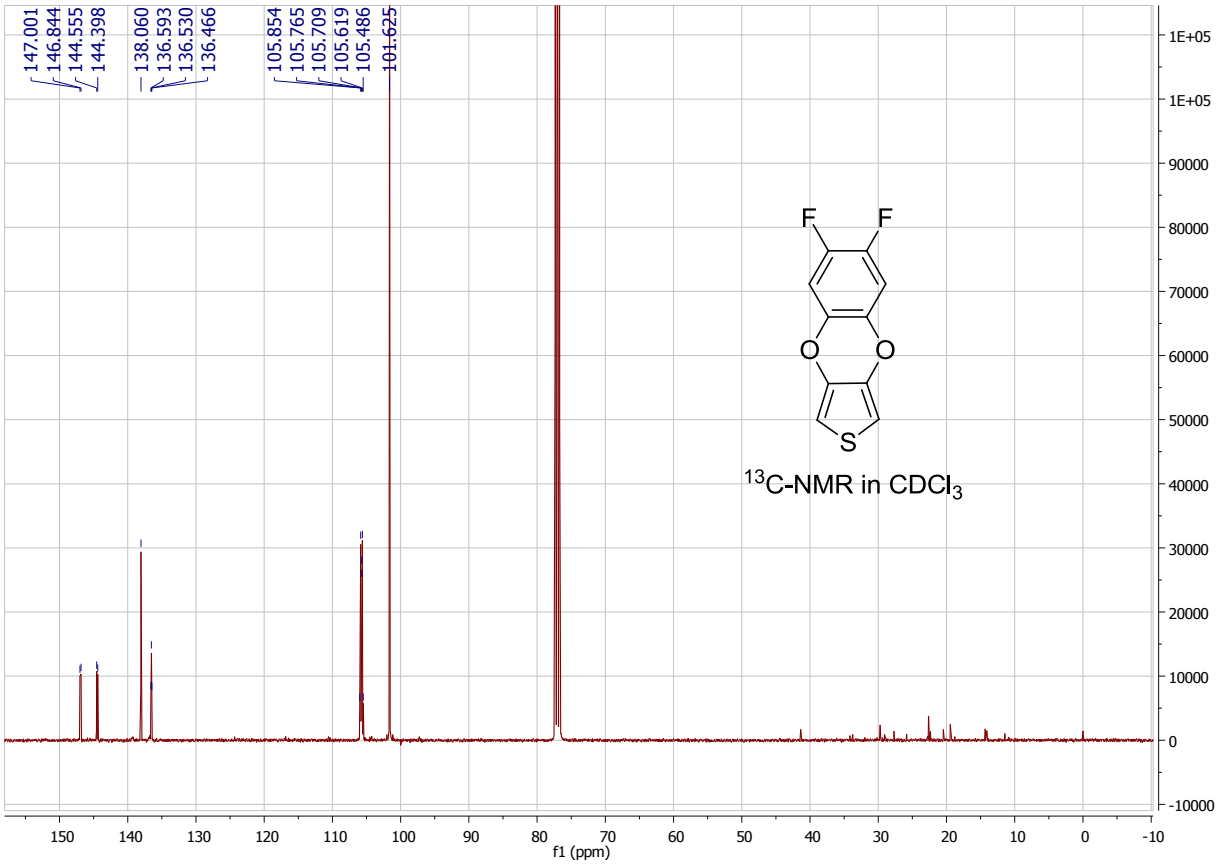

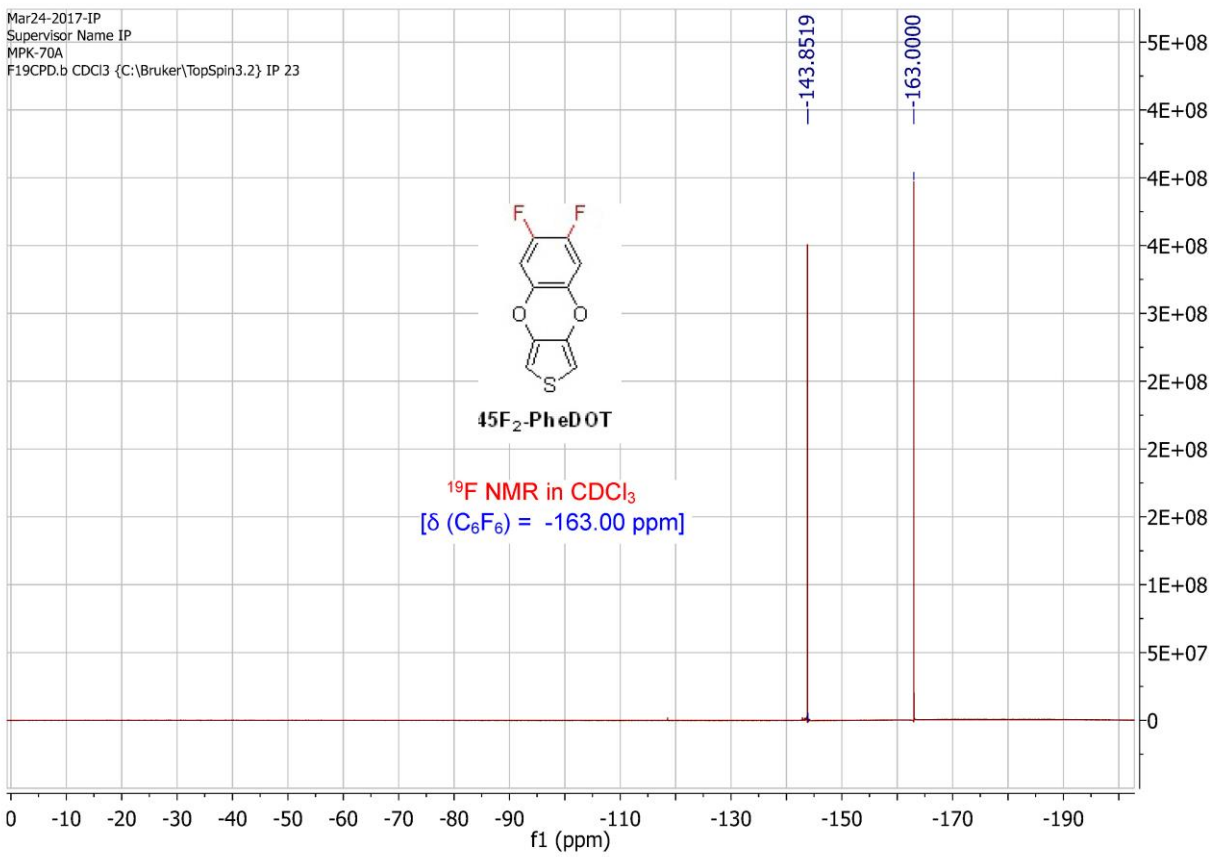
Mar24-2017-IP
Supervisor Name IP
MPK-70A
F19CPD.b CDCl3 {C:\Bruker\TopSpin3.2} IP 23
-143.8519
-163.0000
F
F
O
O
S
45F2-PheDOT
19F NMR in CDCl3
[δ (C6F6) = -163.00 ppm]
5E+08
4E+08
4E+08
4E+08
3E+08
2E+08
2E+08
2E+08
1E+08
5E+07
0
0 -10 -20 -30 -40 -50 -60 -70 -80 -90 -110 -130 -150 -170 -190
f1 (ppm)

5,8-Difluorobenzo[b]thieno[3,4-e][1,4]dioxine **(36F$_2$-PheDOT)**

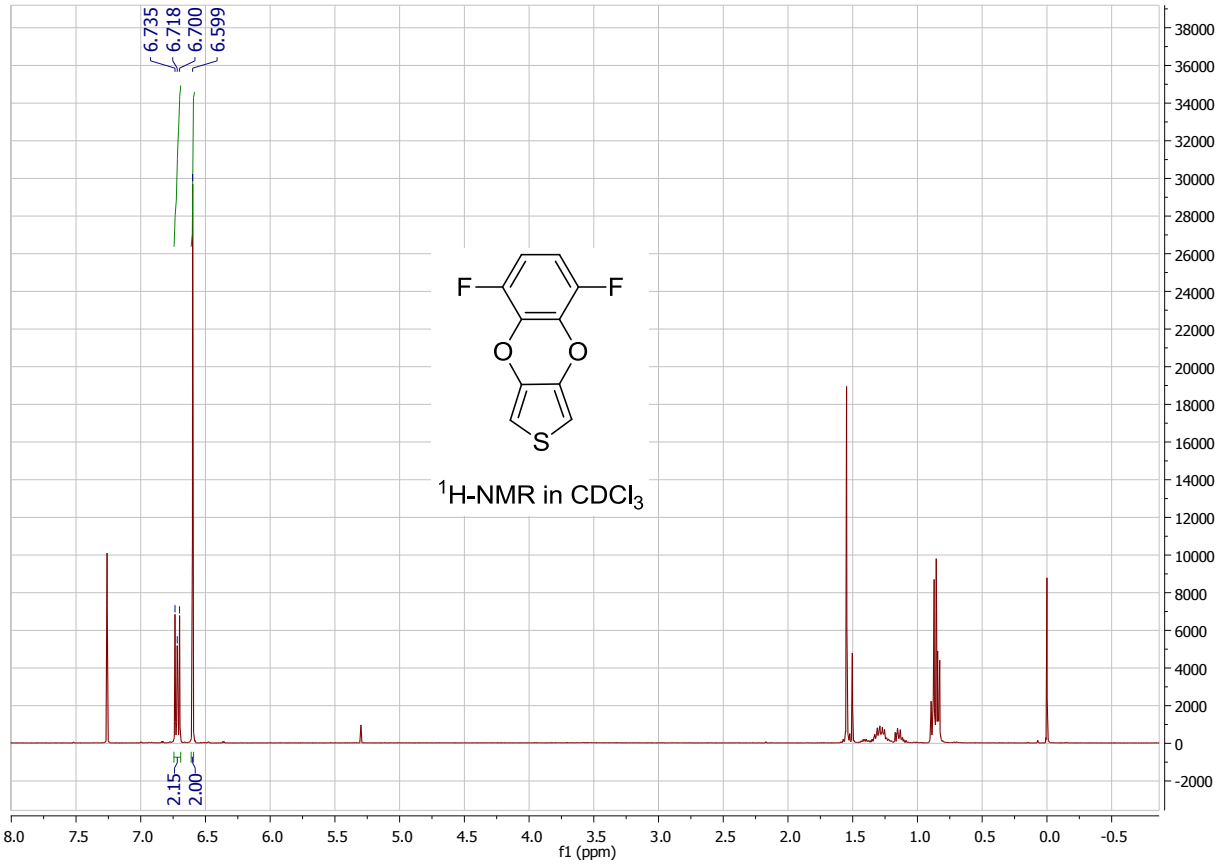

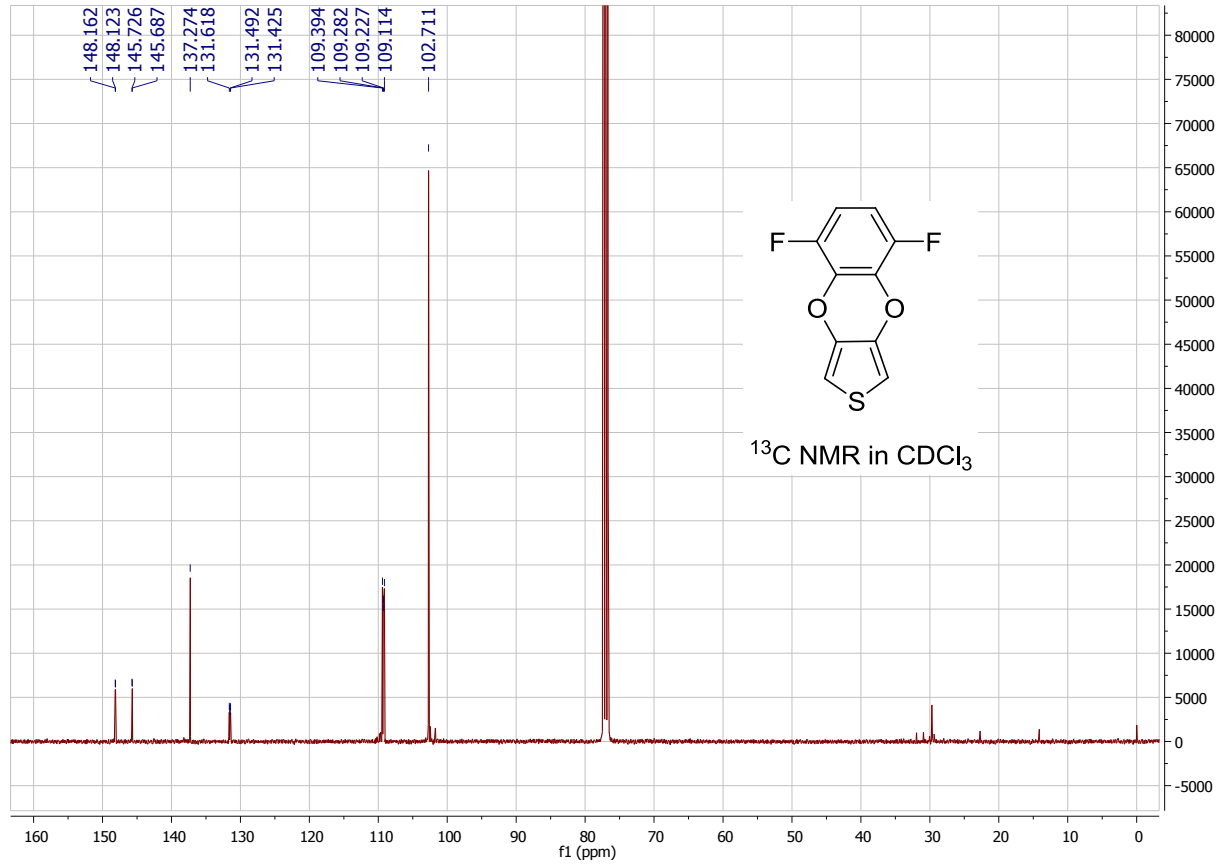

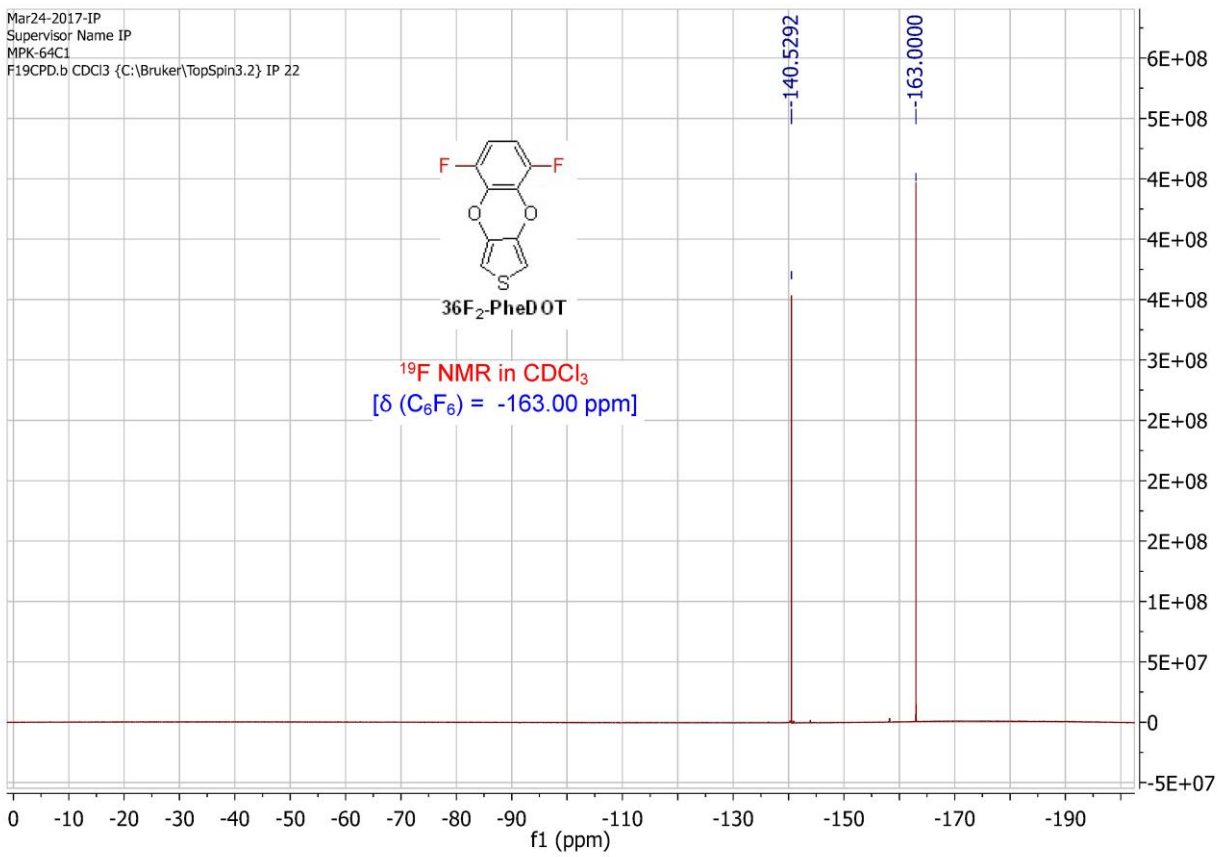
Mar24-2017-IP
Supervisor Name IP
MPK-64C1
F19CPD.b CDCl3 {C:\Bruker\TopSpin3.2} IP 22
-140.5292
-163.0000
F
F
O
O
S
36F2-PheDOT
19F NMR in CDCl3
[δ (C6F6) = -163.00 ppm]
6E+08
5E+08
4E+08
4E+08
4E+08
3E+08
2E+08
2E+08
2E+08
1E+08
5E+07
0
-5E+07
0 -10 -20 -30 -40 -50 -60 -70 -80 -90 -110 -130 -150 -170 -190
f1 (ppm)

5,6,7,8-Tetrafluorobenzo[b]thieno[3,4-e][1,4]dioxine (**F_4-PheDOT**)

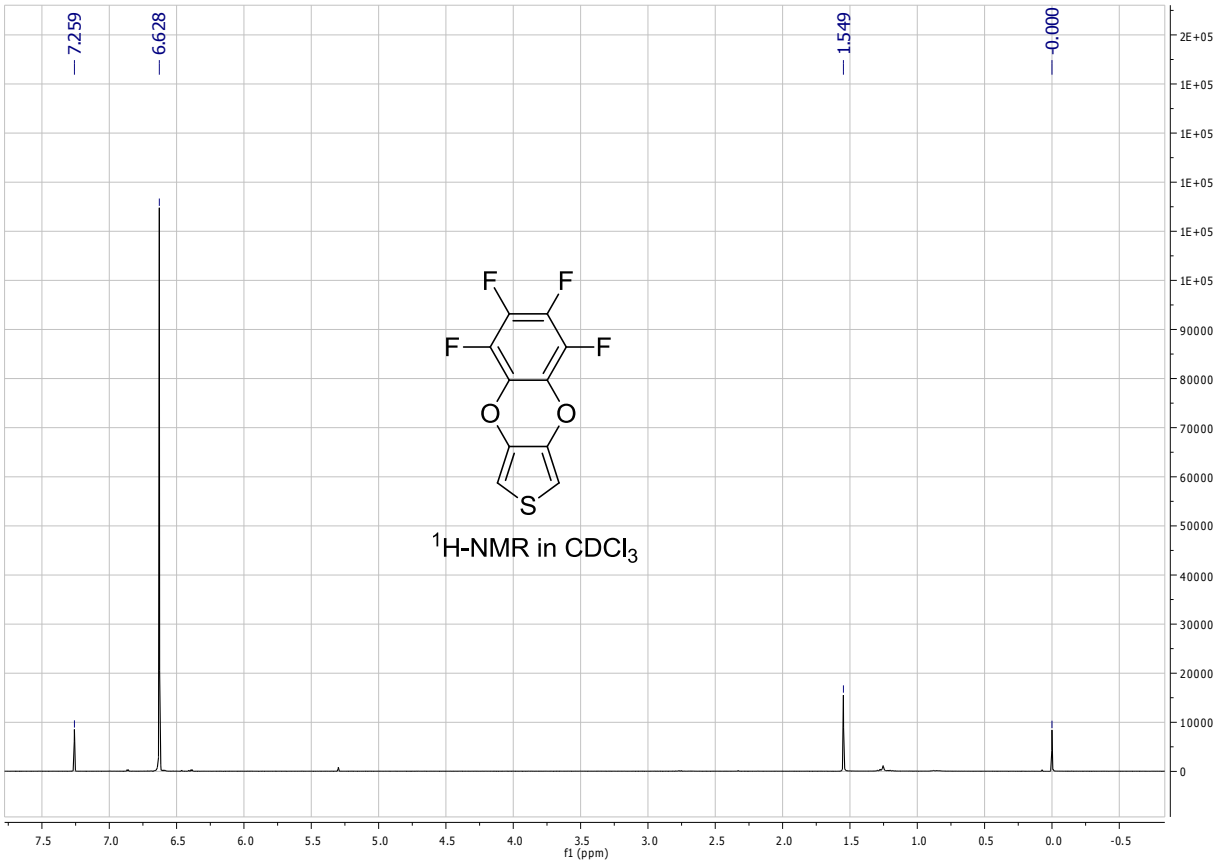

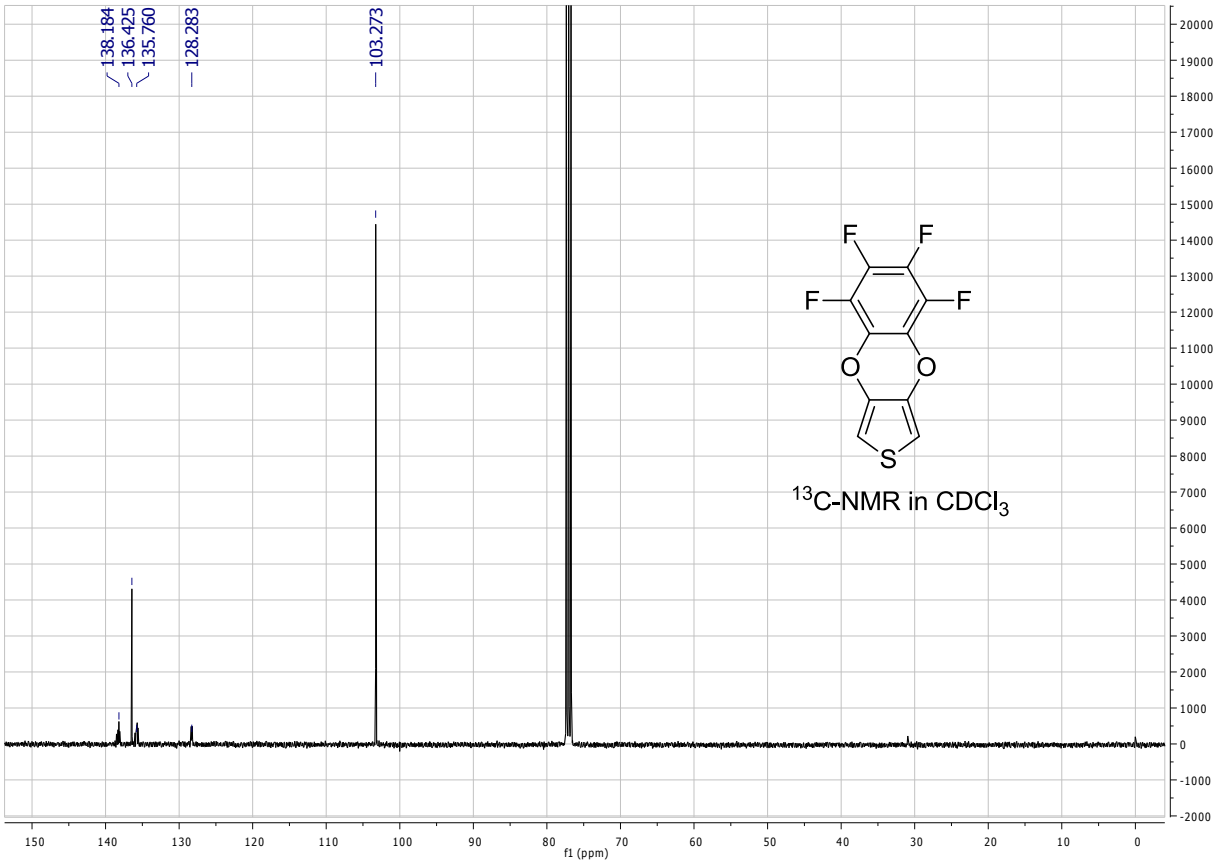

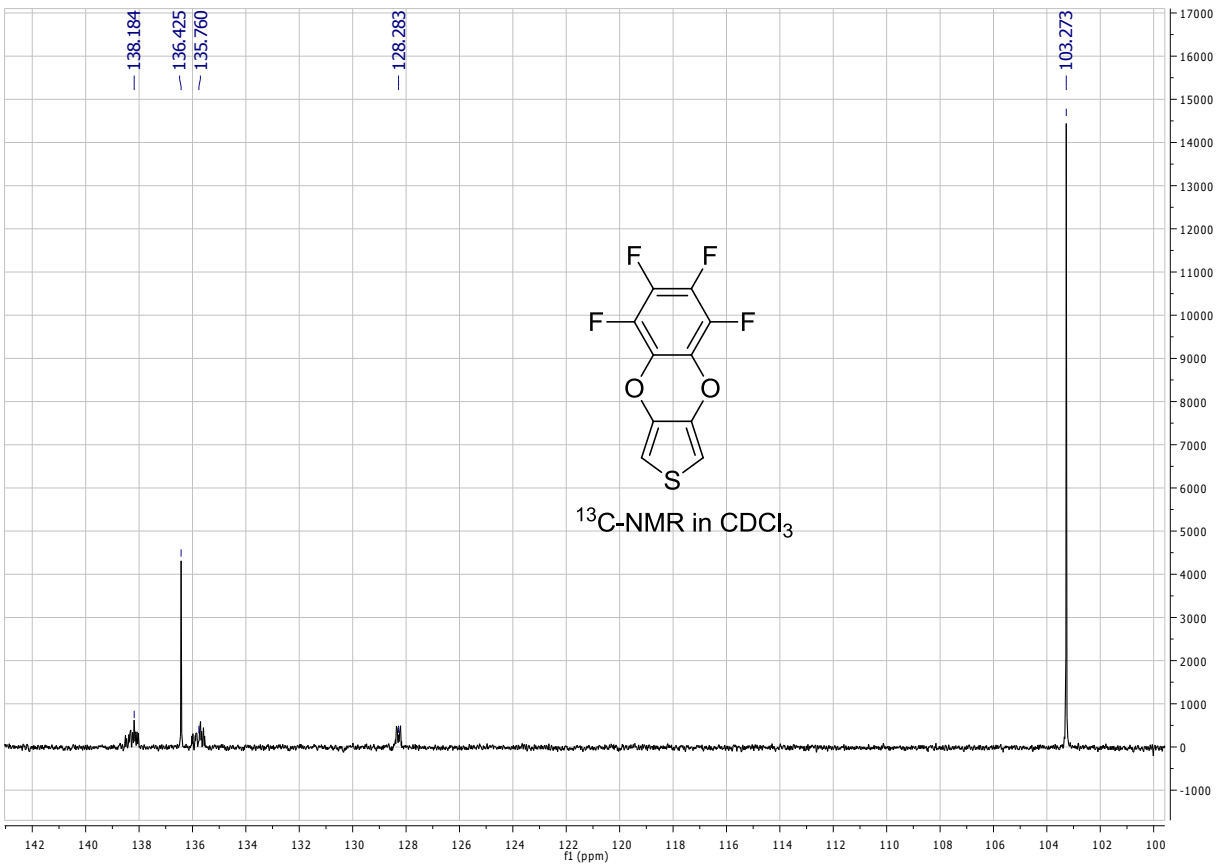
138.184
136.425
135.760
128.283
103.273
F
F
F
F
O
O
S
^{13}C-NMR in $CDCl_3$
f1 (ppm)

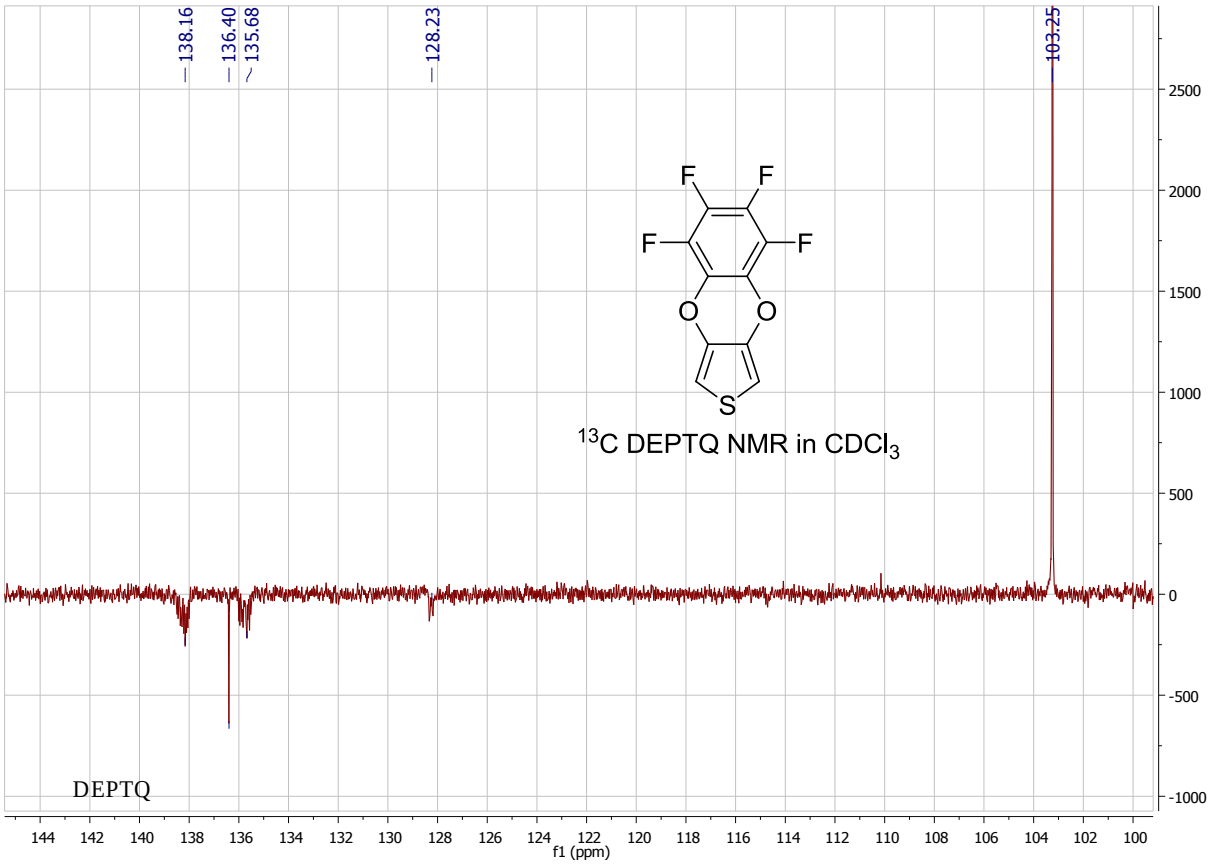
138.16
136.40
135.68
128.23
103.25
F
F
F
F
O
O
S
^{13}C DEPTQ NMR in $CDCl_3$
DEPTQ
f1 (ppm)

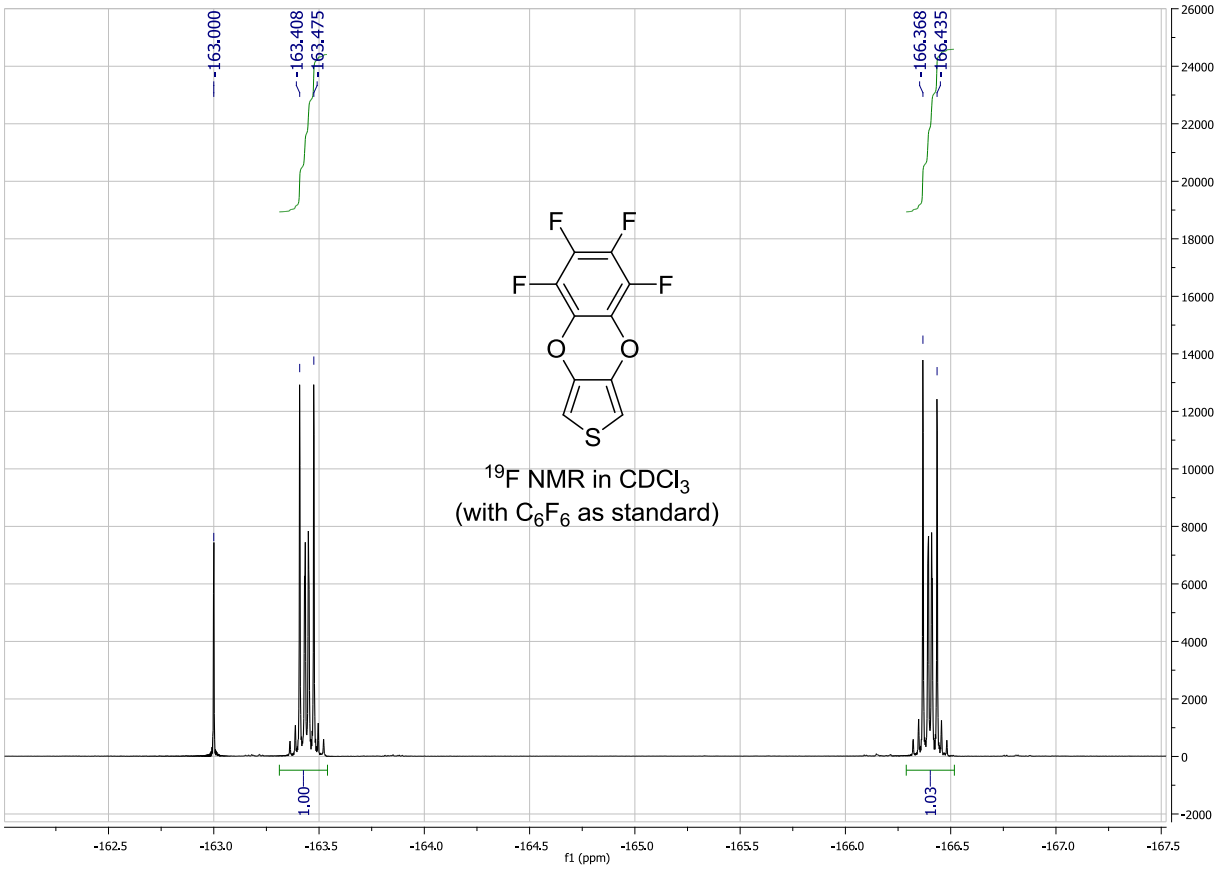

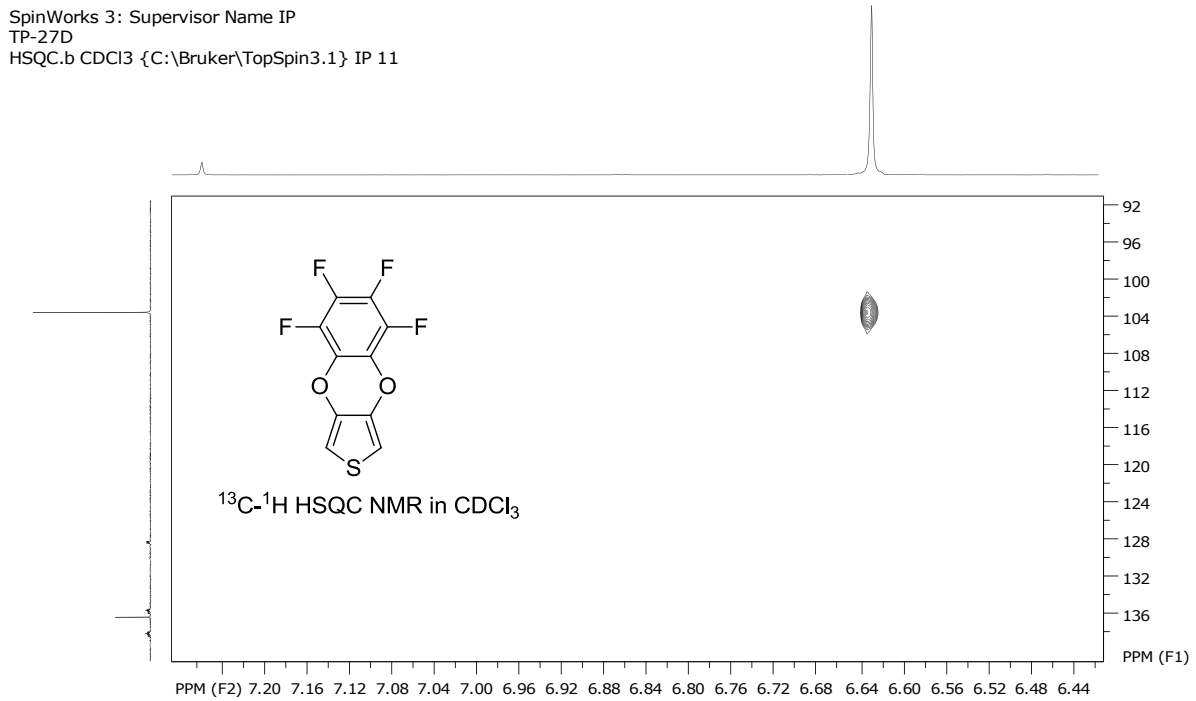

file: ...PheDOT_tp_27d\36-TP-27D-HSQC.b\ser
expt: <hsqcedetgpsisp2.3>
transmitter freq: 400.131549 MHz
time domain size: 2048 by 256 points
width (F2): 2762.43 Hz = 6.9038 ppm = 1.3488 Hz/pt
number of scans: 2

F2: freq. of 0 ppm: 400.1300094 MHz
processed size: 1024 complex points
window function: Sine Squared
shift: 90.0 degrees
Hz/cm: 15.901 ppm/cm: 0.03974

F1: freq. of 0 ppm: 100.6127690 MHz
processed size: 1024 complex points
window function: Sine Squared
shift: 90.0 degrees
Hz/cm: 459.036 ppm/cm: 4.56208

Ethyl 5,6,7,8-tetrafluorobenzo[b]thieno[3,4-e][1,4]dioxine-1-carboxylate (**F_4-23**)

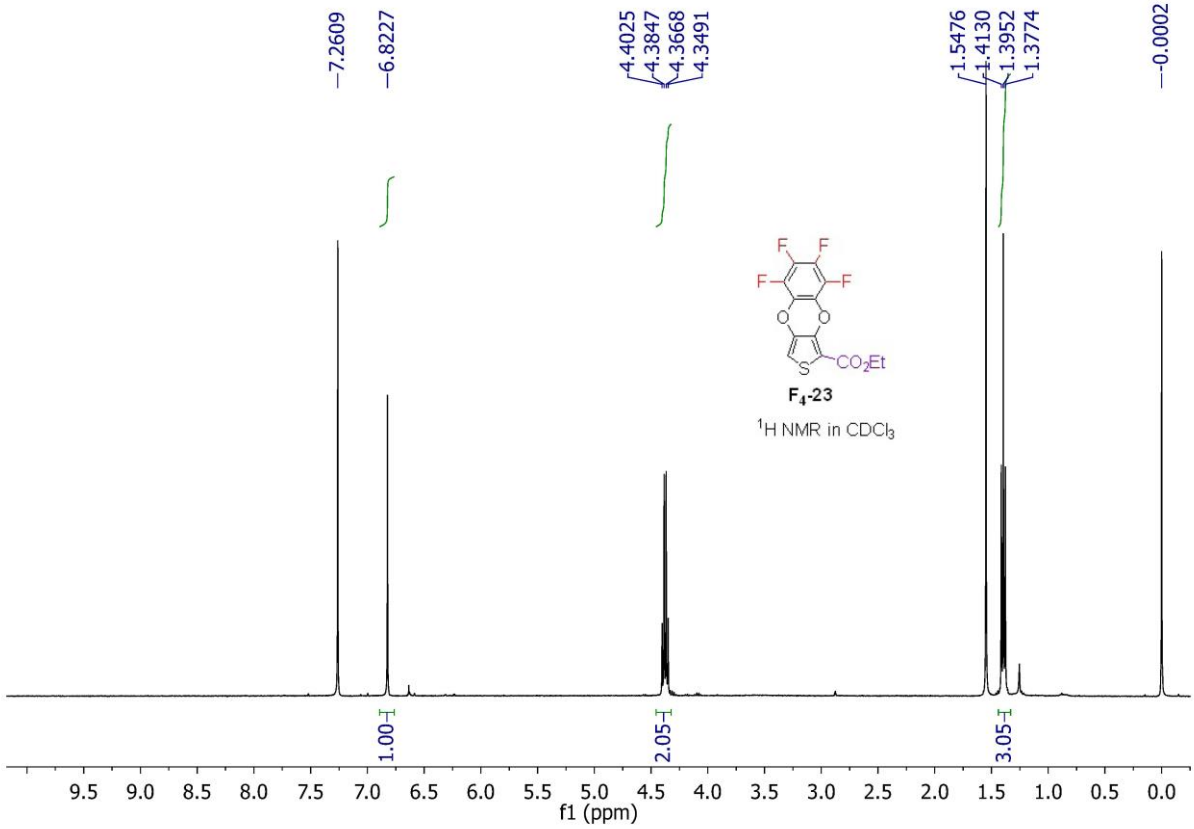

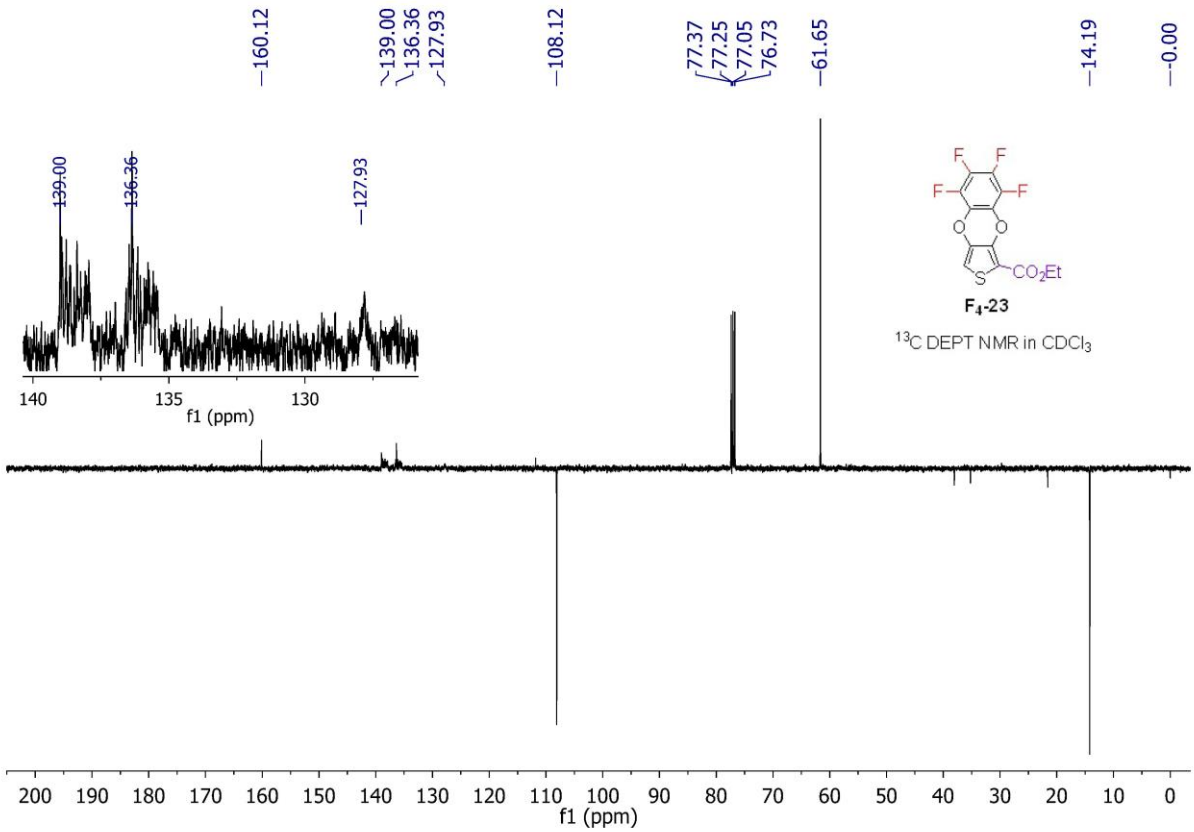

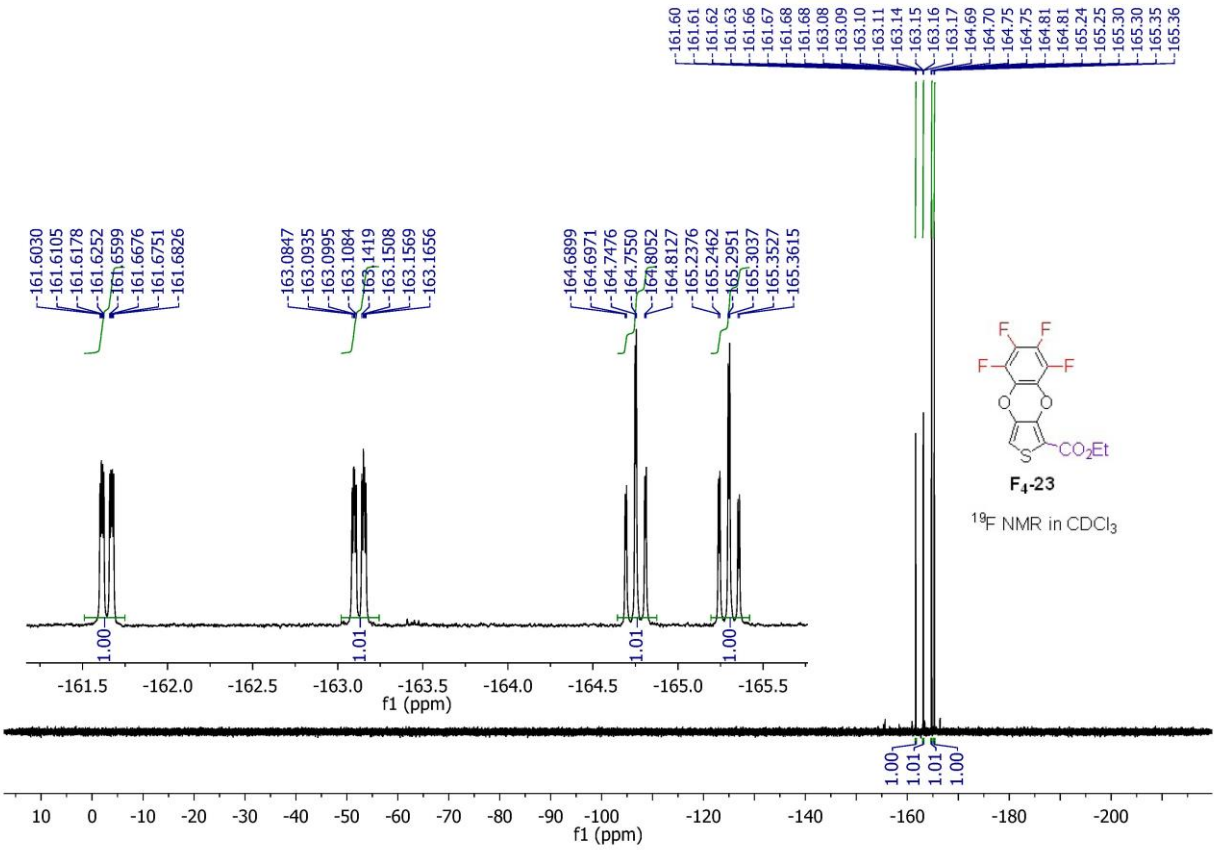
F4-23
19F NMR in CDCl3
f1 (ppm)

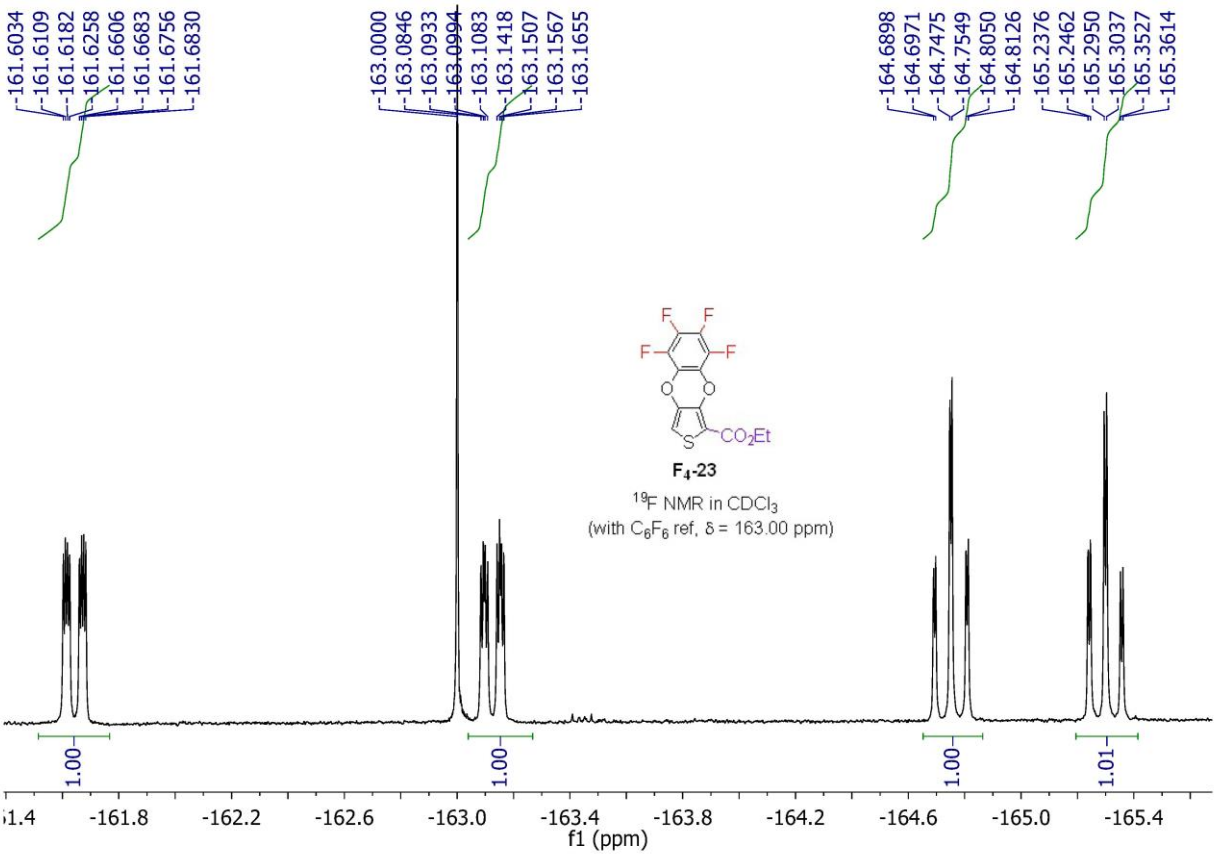
F4-23
19F NMR in CDCl3
(with C6F6 ref, δ = 163.00 ppm)
f1 (ppm)

1,2,3,4,5,6-Hexafluoronaphtho[1,2-b]thieno[3,4-e][1,4]dioxine **{F_6-NaphDOT(1,2)}**

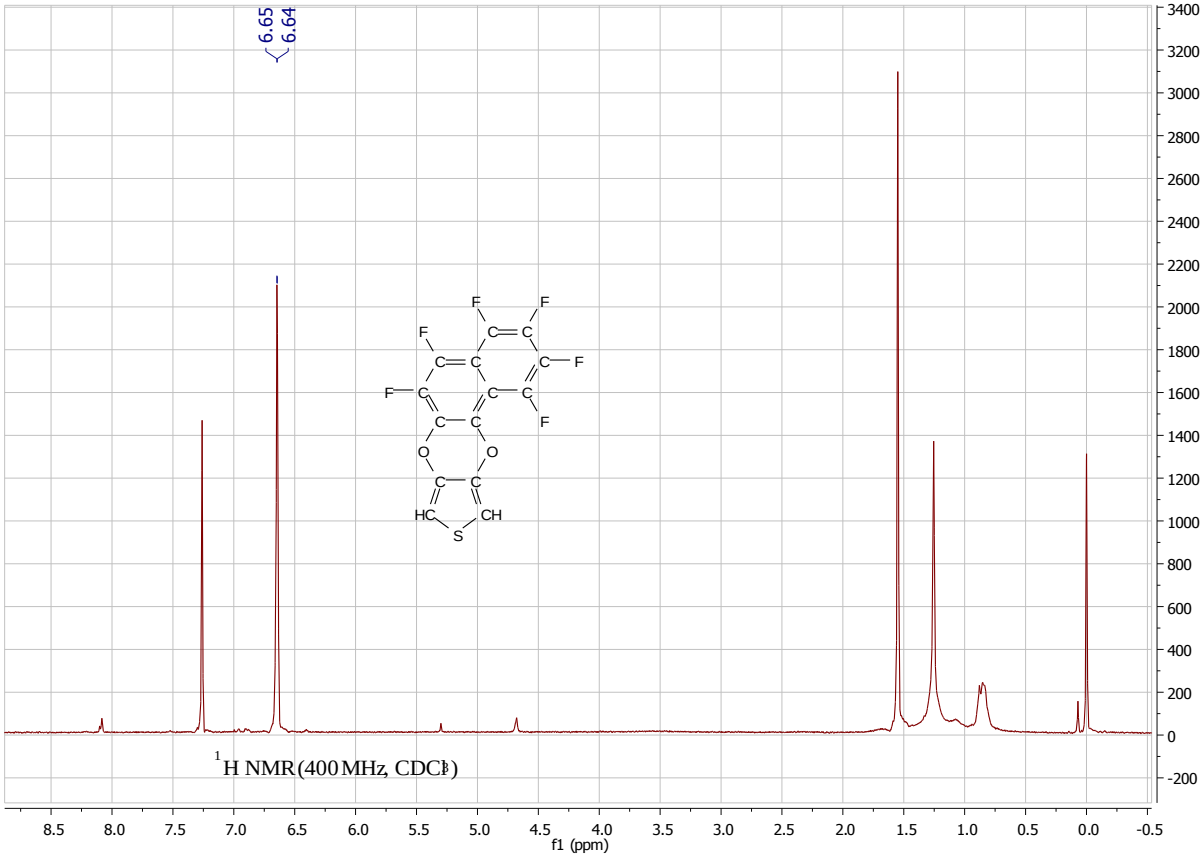

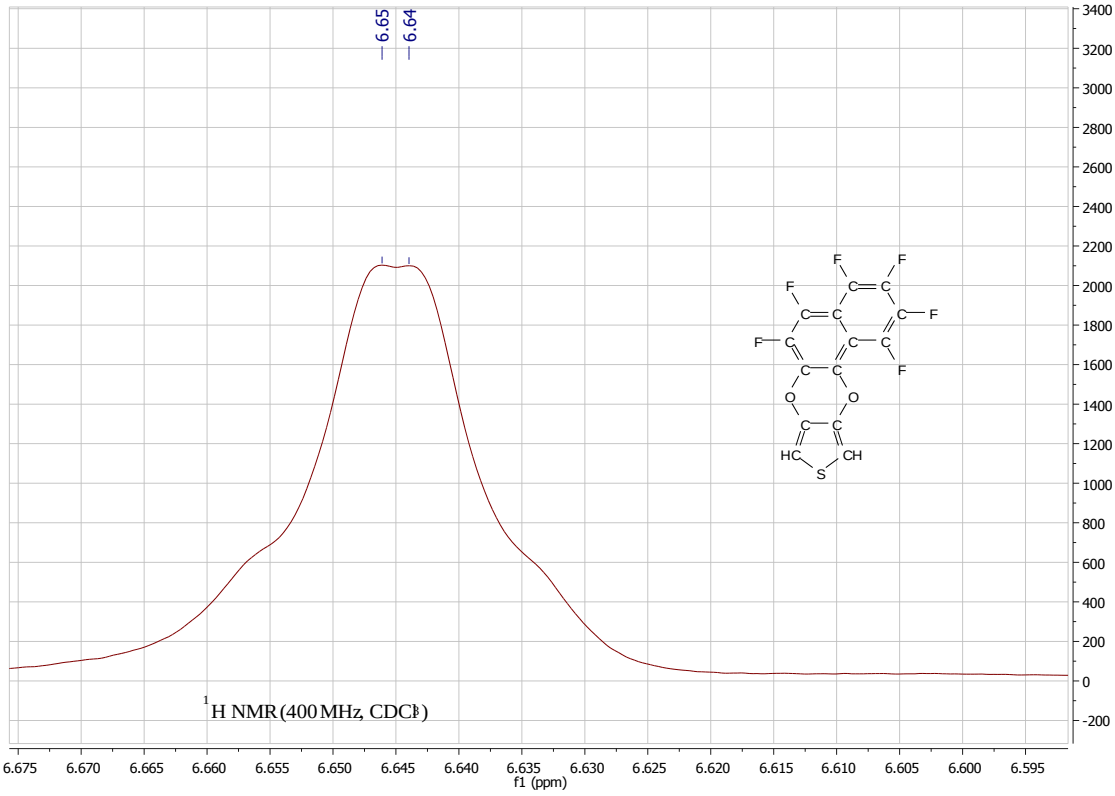

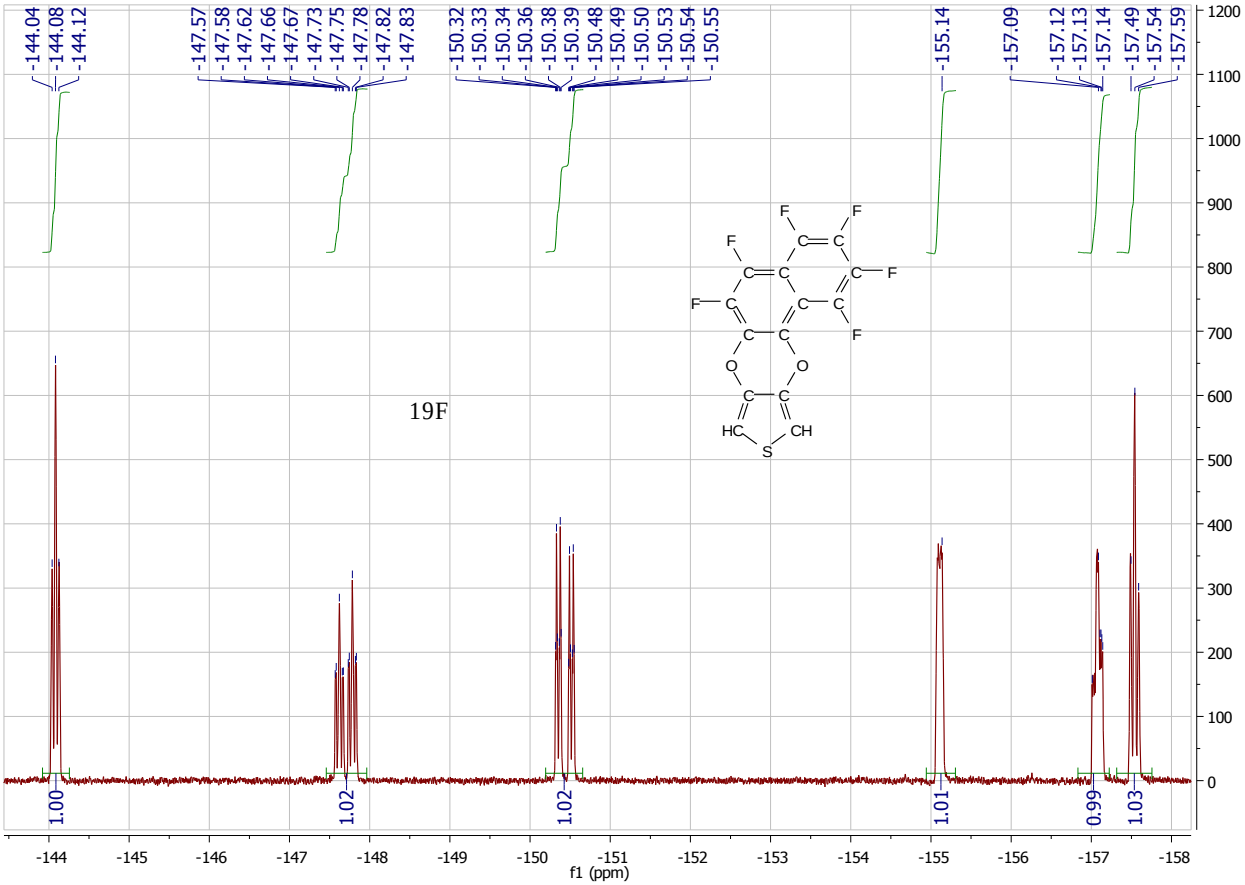
-144.04
-144.08
-144.12
-147.57
-147.58
-147.62
-147.66
-147.67
-147.73
-147.75
-147.78
-147.82
-147.83
-150.32
-150.33
-150.34
-150.36
-150.38
-150.39
-150.48
-150.49
-150.50
-150.53
-150.54
-150.55
-155.14
-157.09
-157.12
-157.13
-157.14
-157.49
-157.54
-157.59
19F
1.00
1.02
1.02
1.01
0.99
1.03
f1 (ppm)

5,6,7,8,9,10-Hexafluoronaphtho[2,3-b]thieno[3,4-e][1,4]dioxine **{F6-NaphDOT(2,3)}**

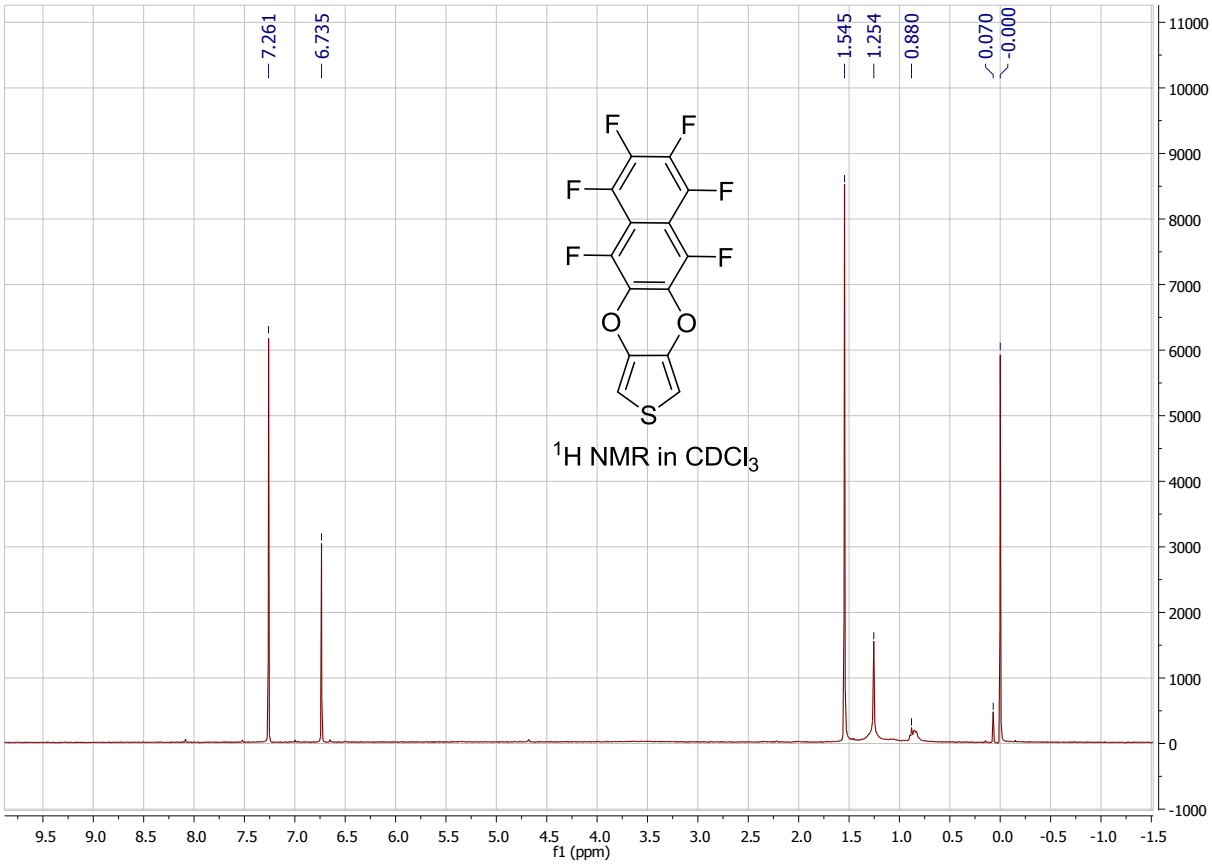

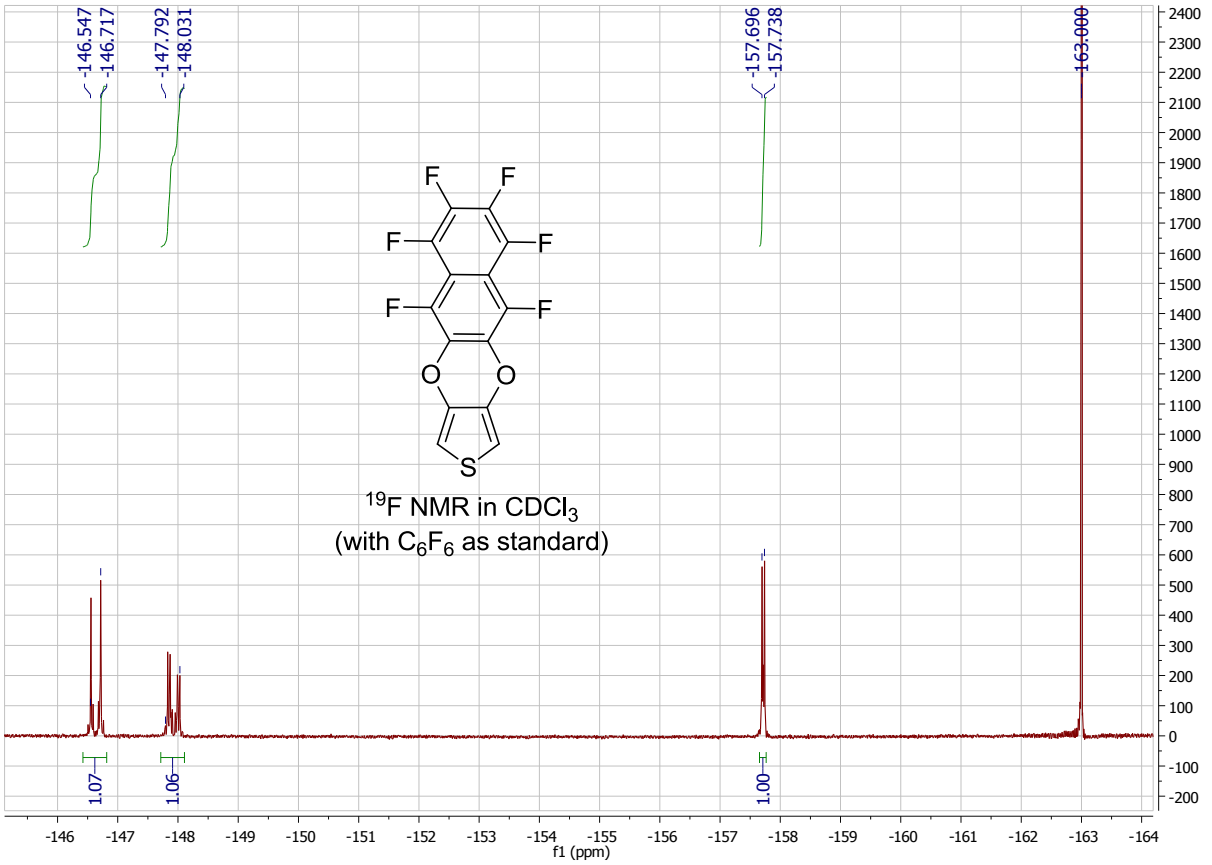

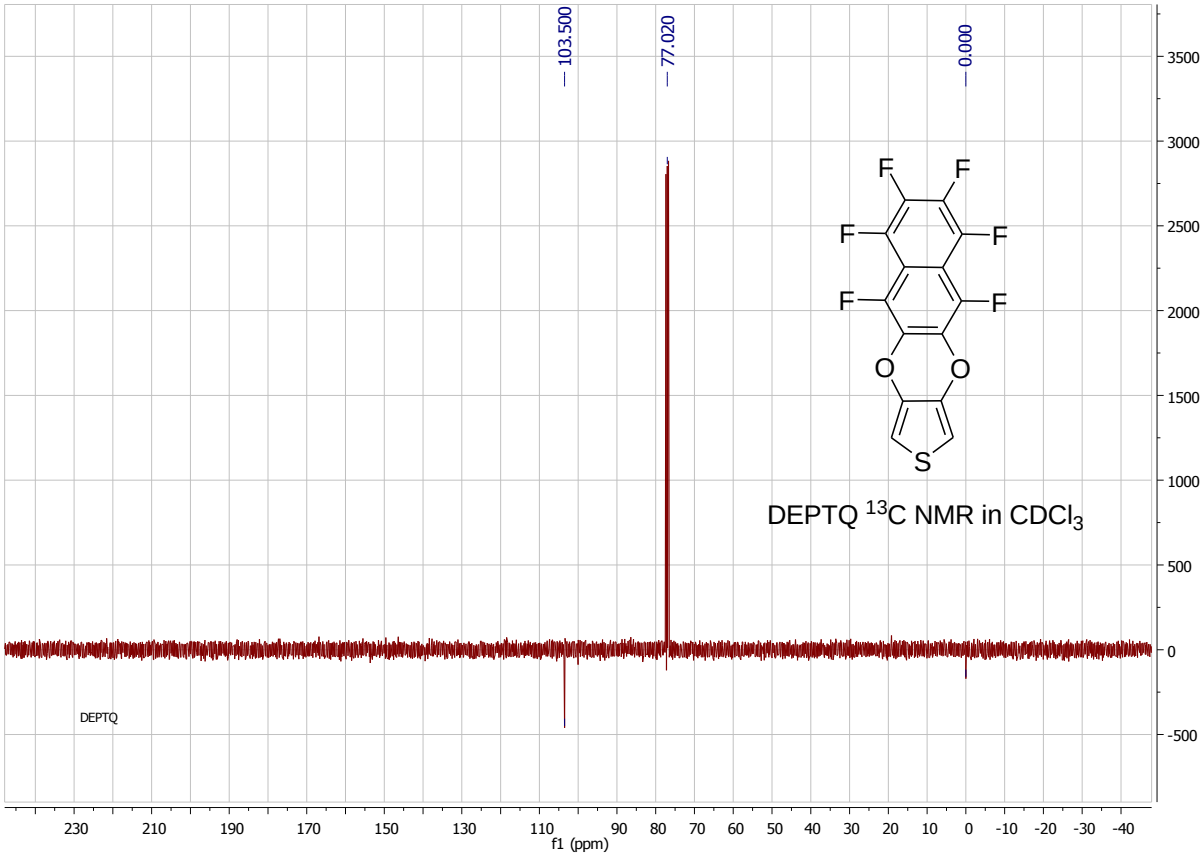
103.500
77.020
0.000
F
F
F
F
F
F
O
O
S
DEPTQ ^{13}C NMR in $CDCl_3$
DEPTQ
3500
3000
2500
2000
1500
1000
500
0
-500
230
210
190
170
150
130
110
90
80
70
60
50
40
30
20
10
0
-10
-20
-30
-40
f1 (ppm)

5,6,7,8-Tetrafluoro-9H-benzo[e]thieno[3,4-b][1,4]dioxepine (**F4-BnDOT**)

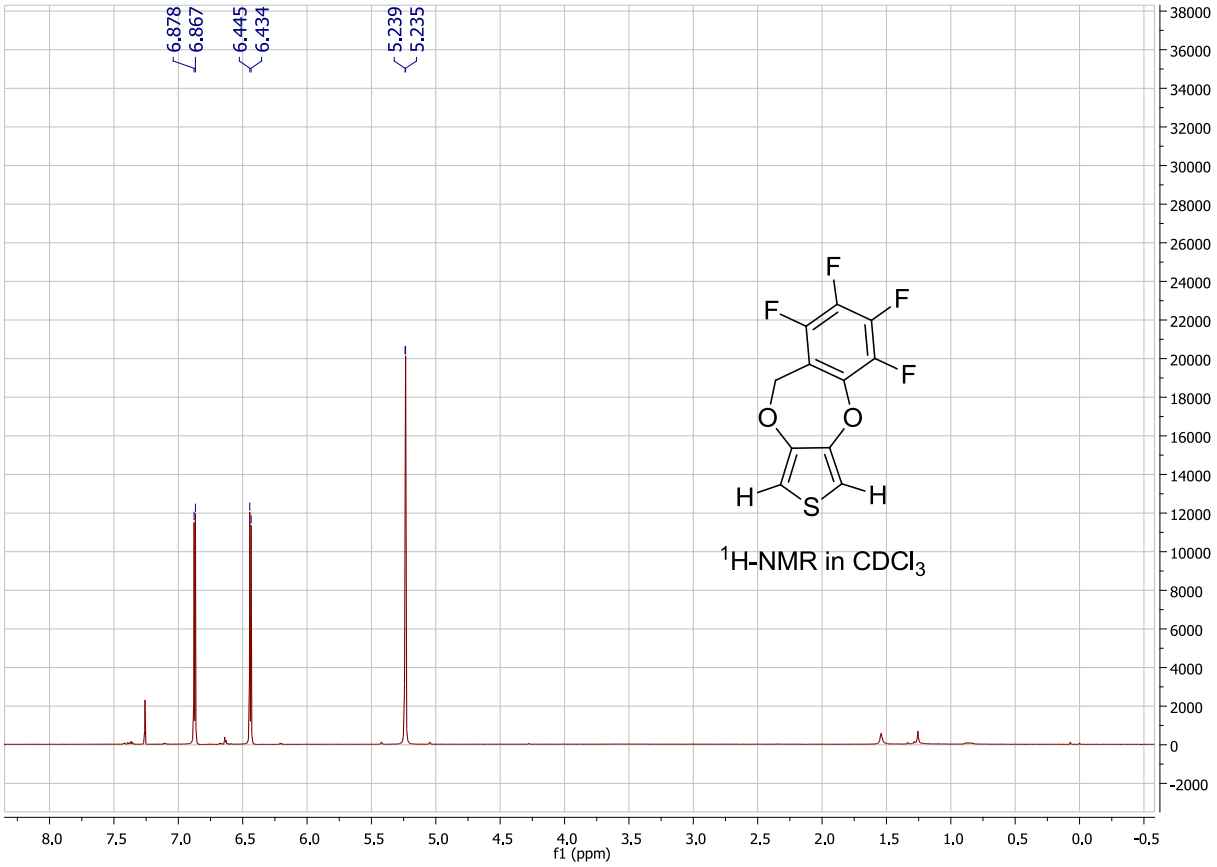

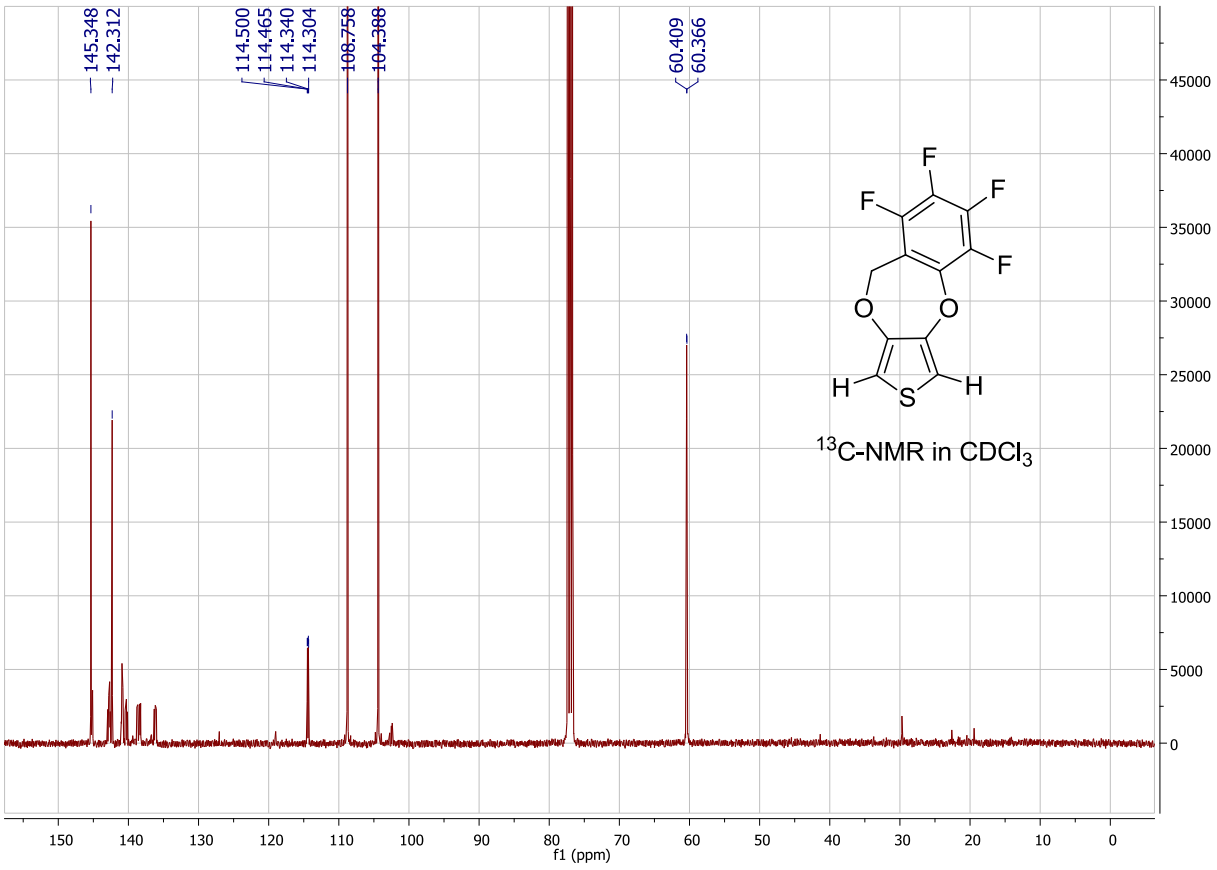

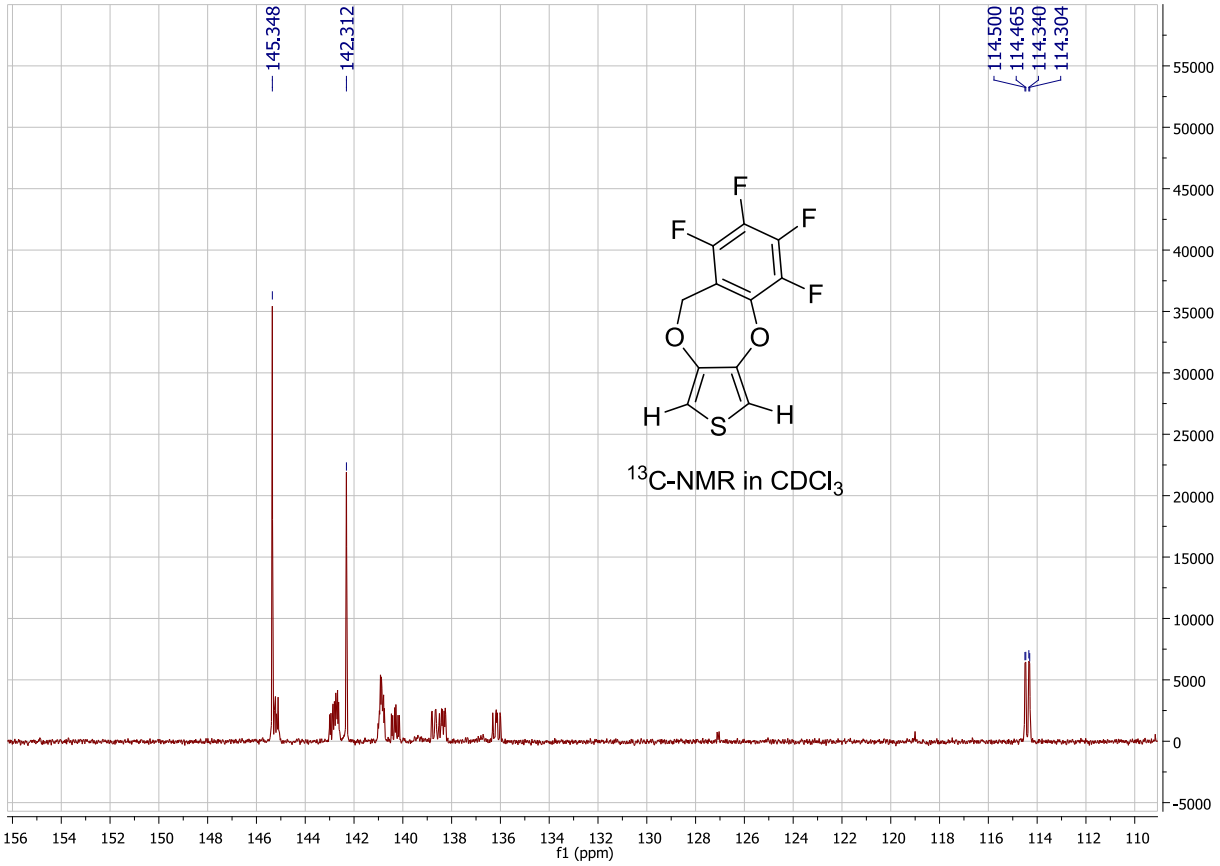
145.348
142.312
114.500
114.465
114.340
114.304
F
F
F
F
O
O
H
S
H
^{13}C-NMR in $CDCl_3$
f1 (ppm)

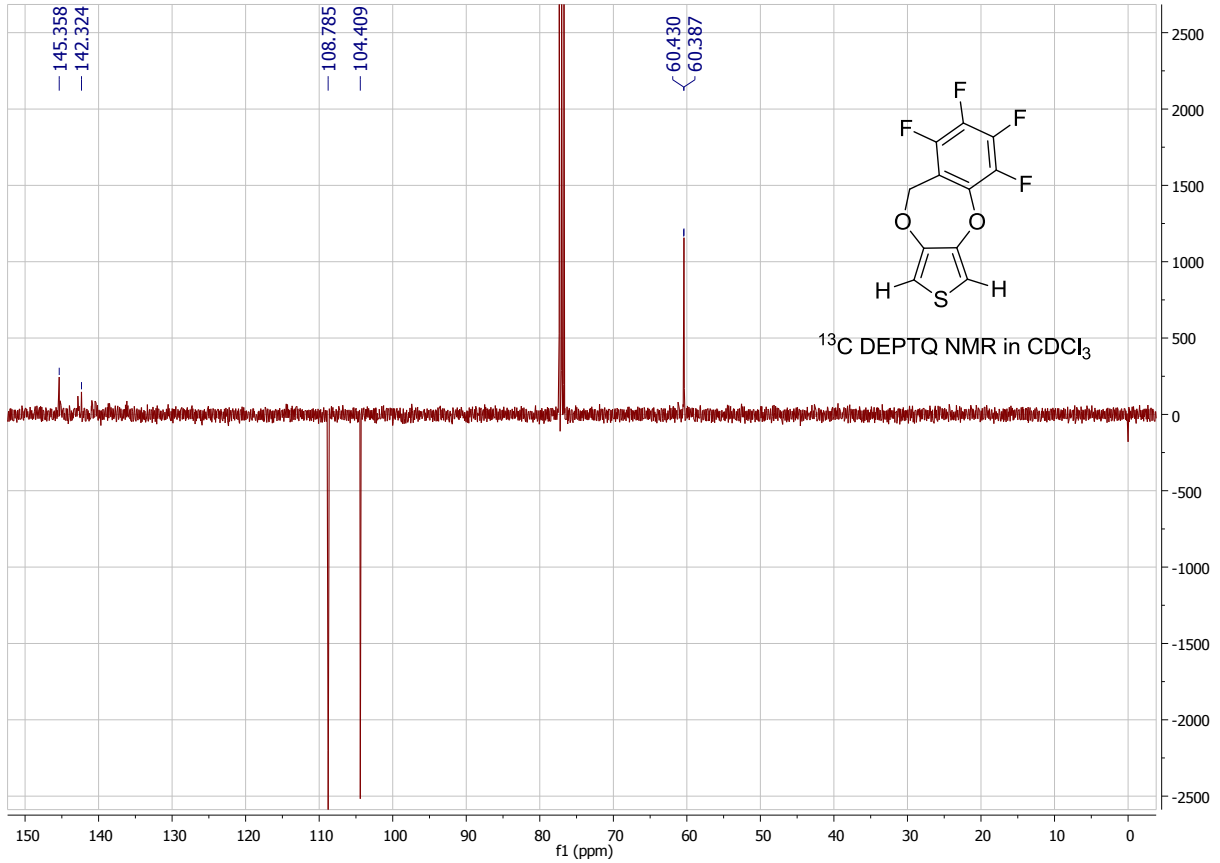
145.358
142.324
108.785
104.409
60.430
60.387
F
F
F
F
O
O
H
S
H
^{13}C DEPTQ NMR in $CDCl_3$
f1 (ppm)

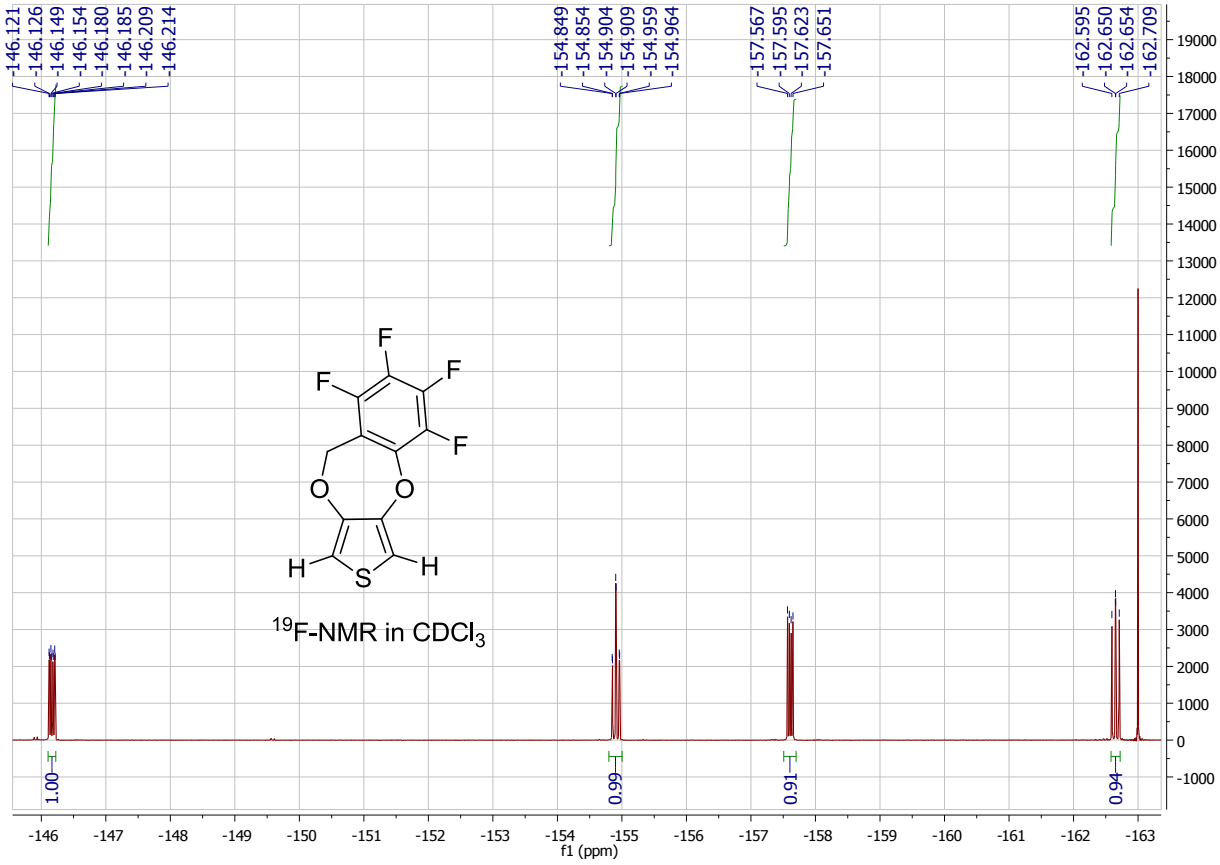

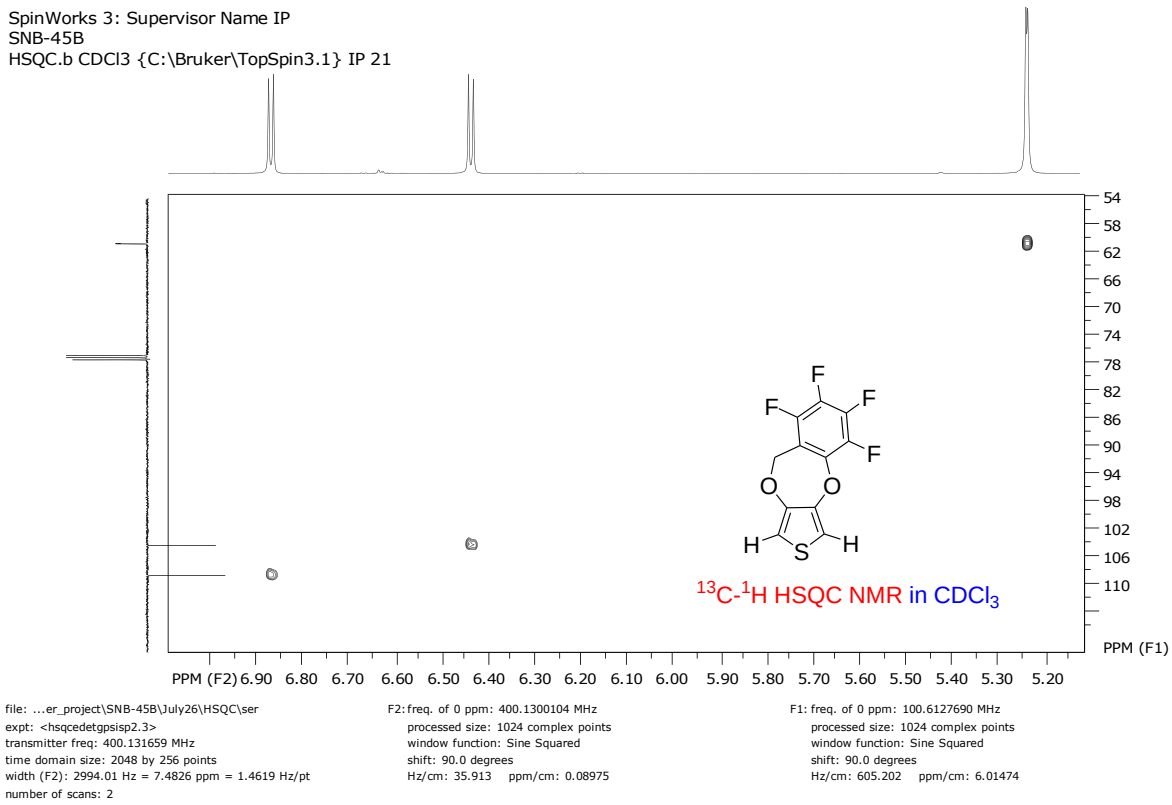

file: ...er_project\SNB-45B\July26\HSQC\ser
expt: <hsqcedetgpsisp2.3>
transmitter freq: 400.131659 MHz
time domain size: 2048 by 256 points
width (F2): 2994.01 Hz = 7.4826 ppm = 1.4619 Hz/pt
number of scans: 2

F2: freq. of 0 ppm: 400.1300104 MHz
processed size: 1024 complex points
window function: Sine Squared
shift: 90.0 degrees
Hz/cm: 35.913 ppm/cm: 0.08975

F1: freq. of 0 ppm: 100.6127690 MHz
processed size: 1024 complex points
window function: Sine Squared
shift: 90.0 degrees
Hz/cm: 605.202 ppm/cm: 6.01474

3-Trifluoromethylthieno[3',4':5,6][1,4]dioxino[2,3-b]pyridine (**5CF₃-PyDOT**)

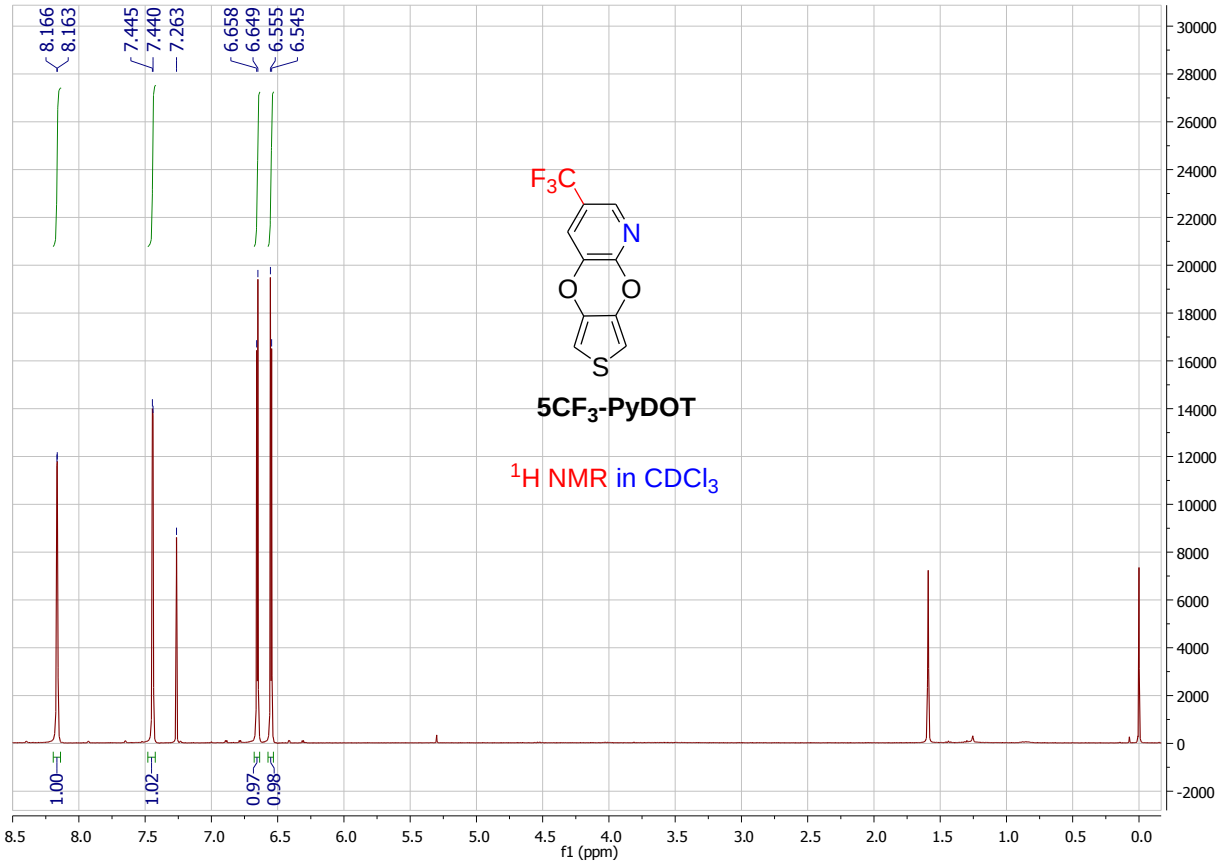

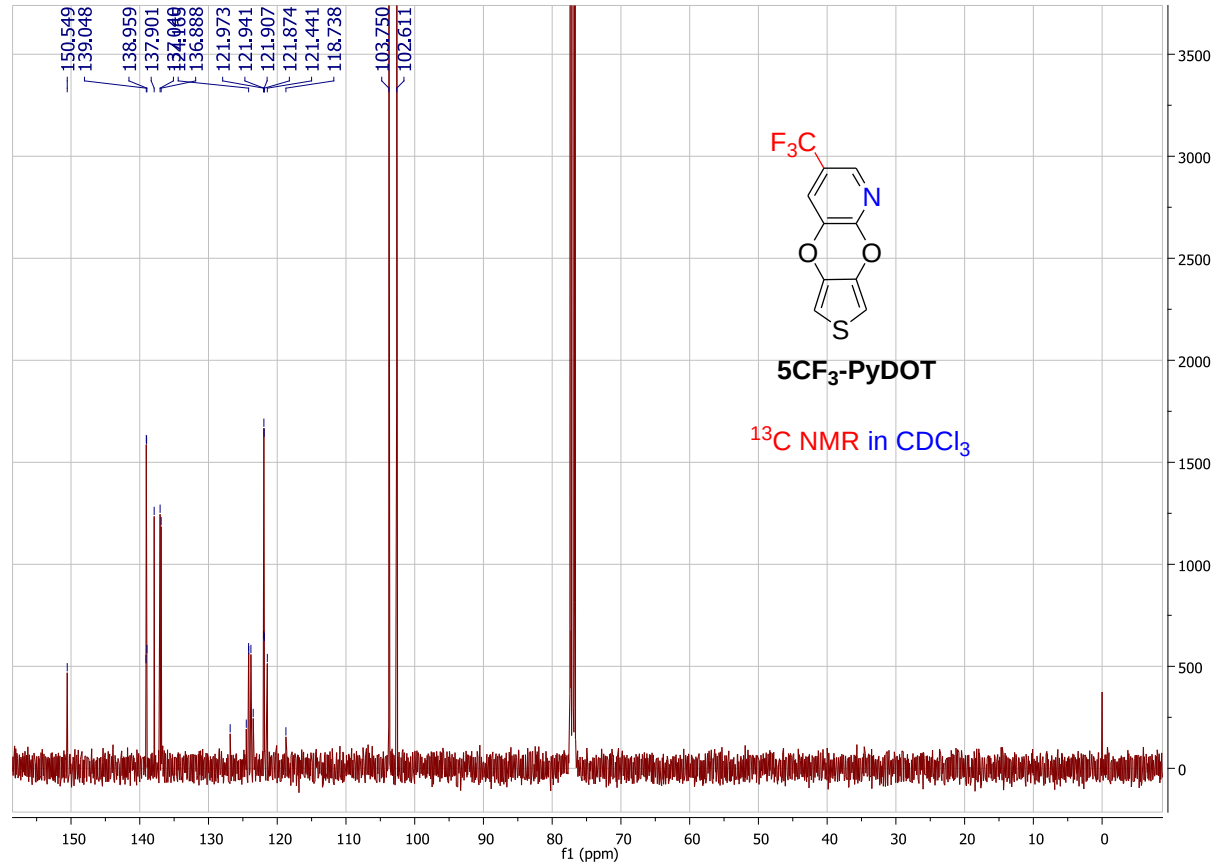

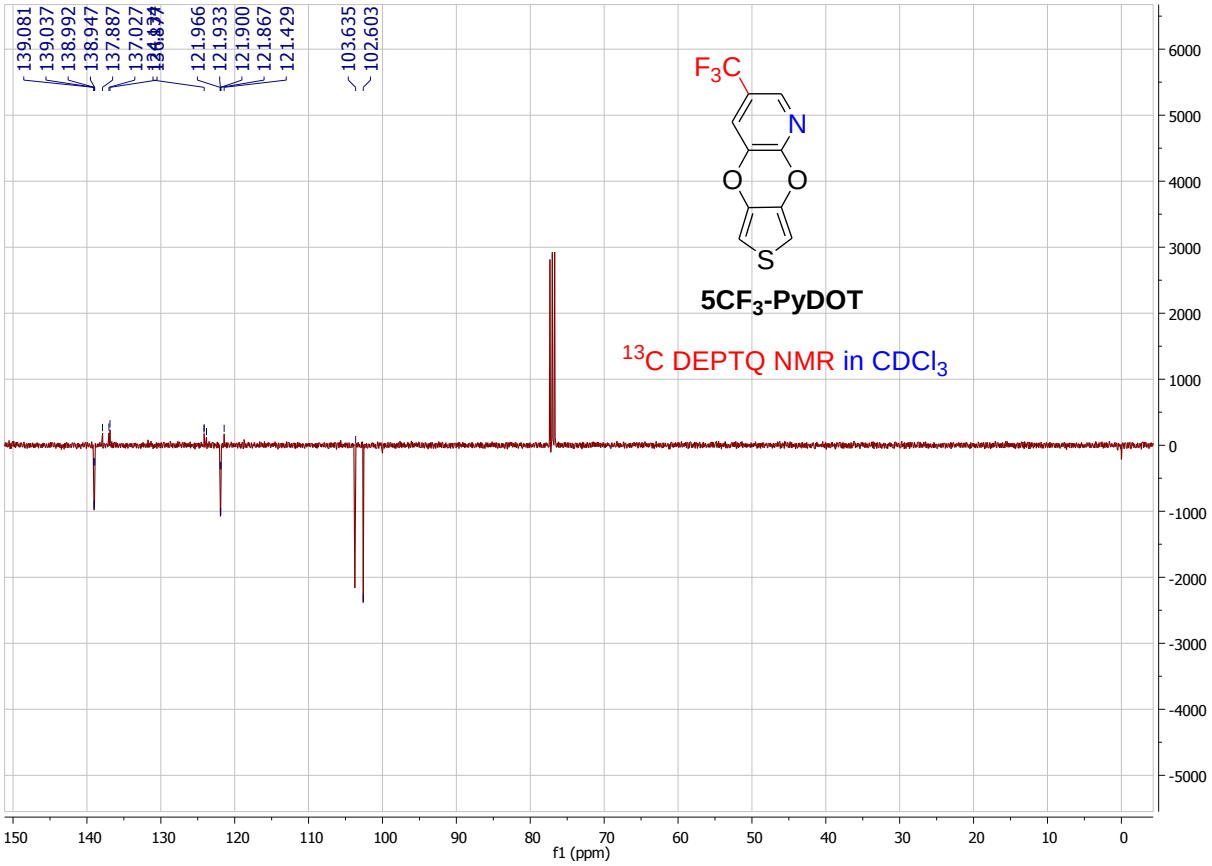
139.081
139.037
138.992
138.947
137.887
137.027
121.966
121.933
121.900
121.867
121.429
103.635
102.603
F3C
N
O
O
S
5CF3-PyDOT
13C DEPTQ NMR in CDCl3
f1 (ppm)

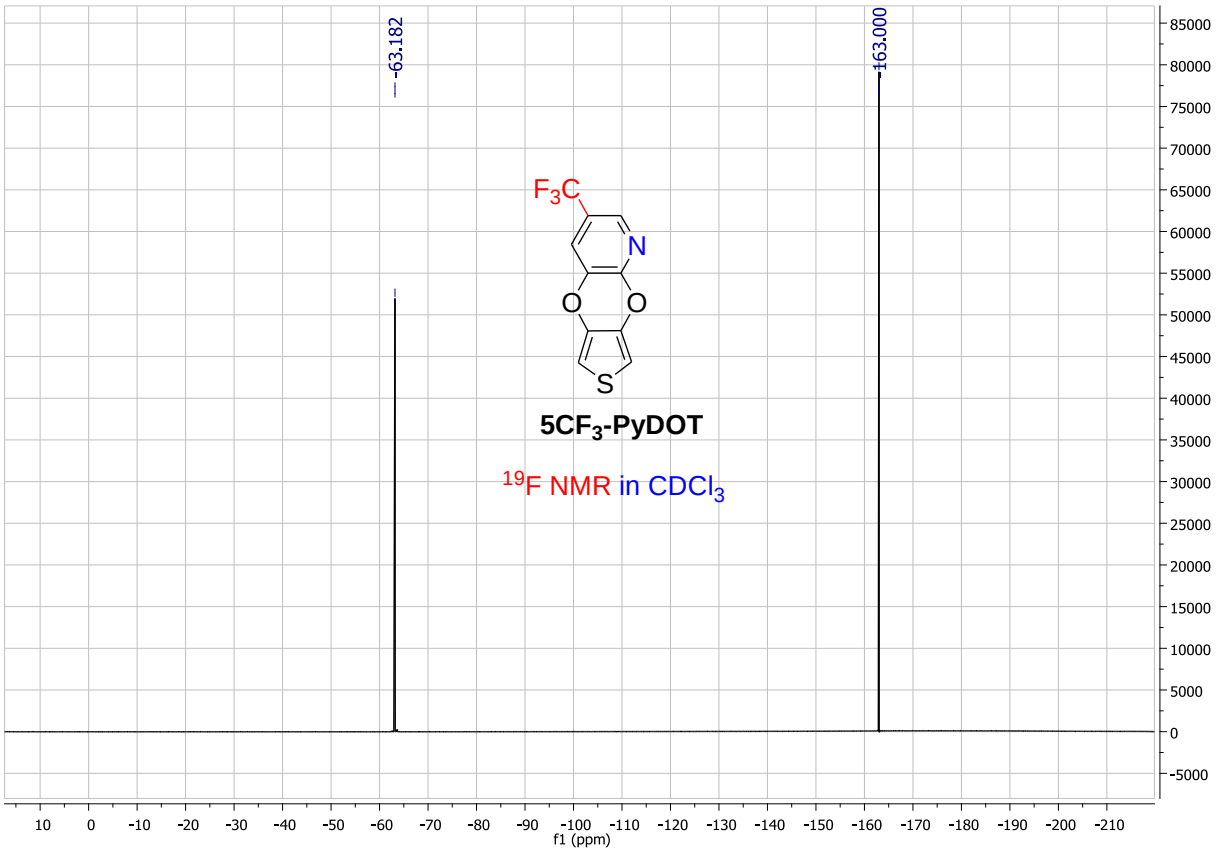
-63.182
-163.000
F3C
N
O
O
S
5CF3-PyDOT
19F NMR in CDCl3
f1 (ppm)

2,3-Dichlorothieno[3',4':5,6][1,4]dioxino[2,3-b]pyridine (**56Cl$_2$-PyDOT**)

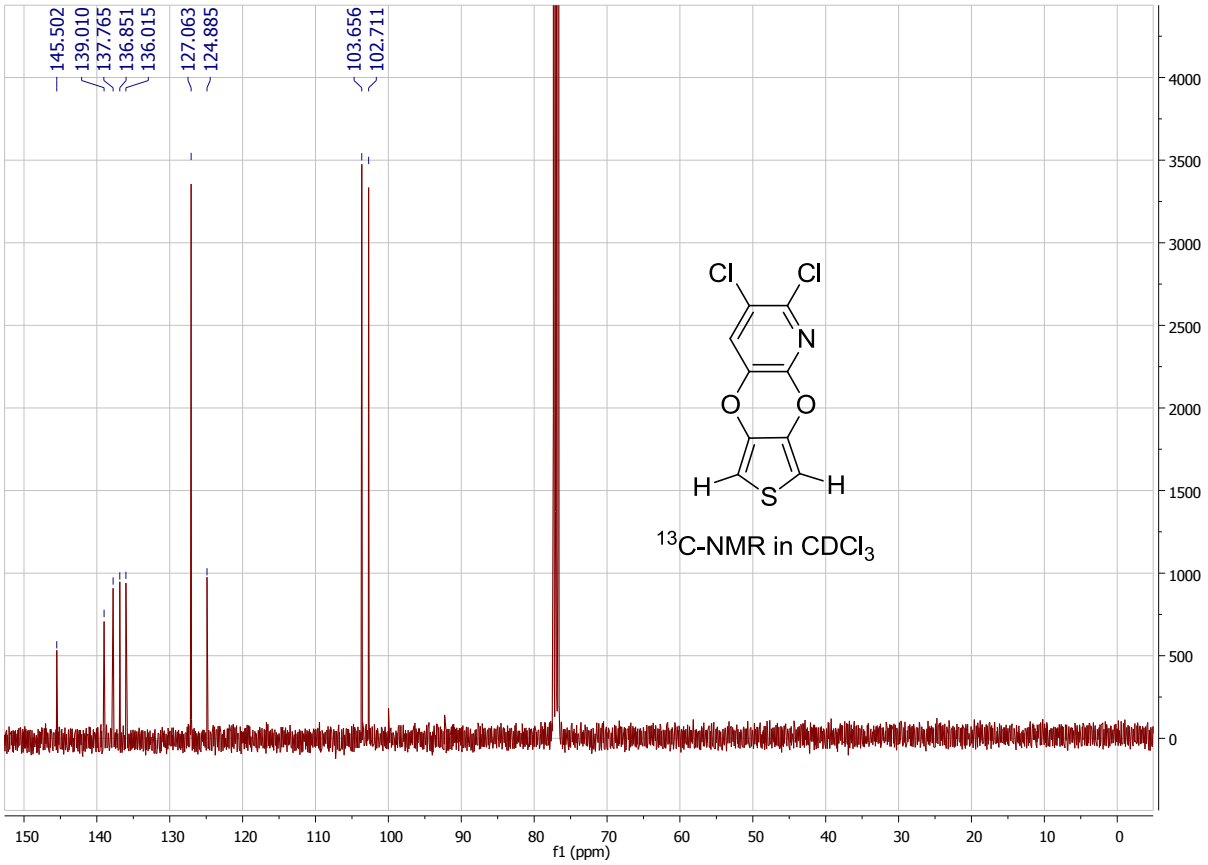

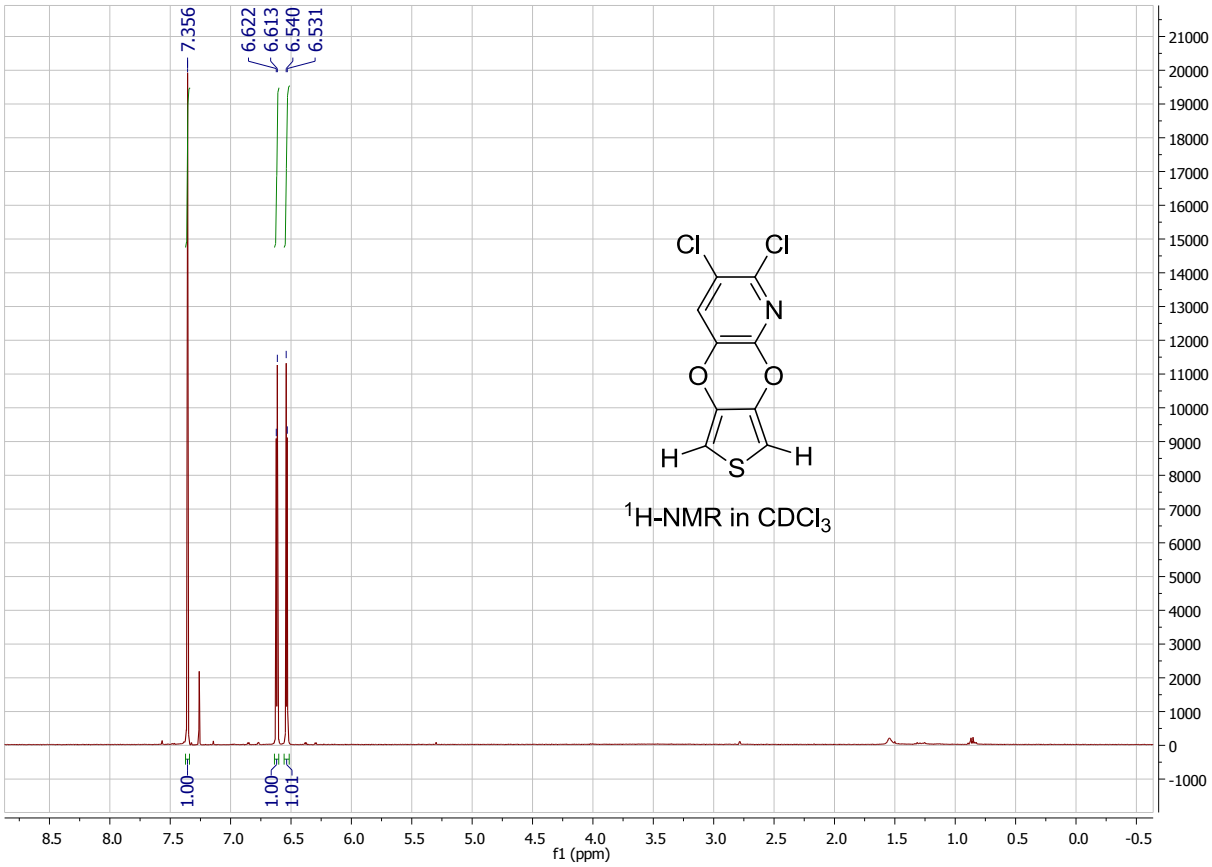

SpinWorks 3: Supervisor Name IP
SNB-47BP
HSQC.b CDCl3 {C:\Bruker\TopSpin3.2} sam 10

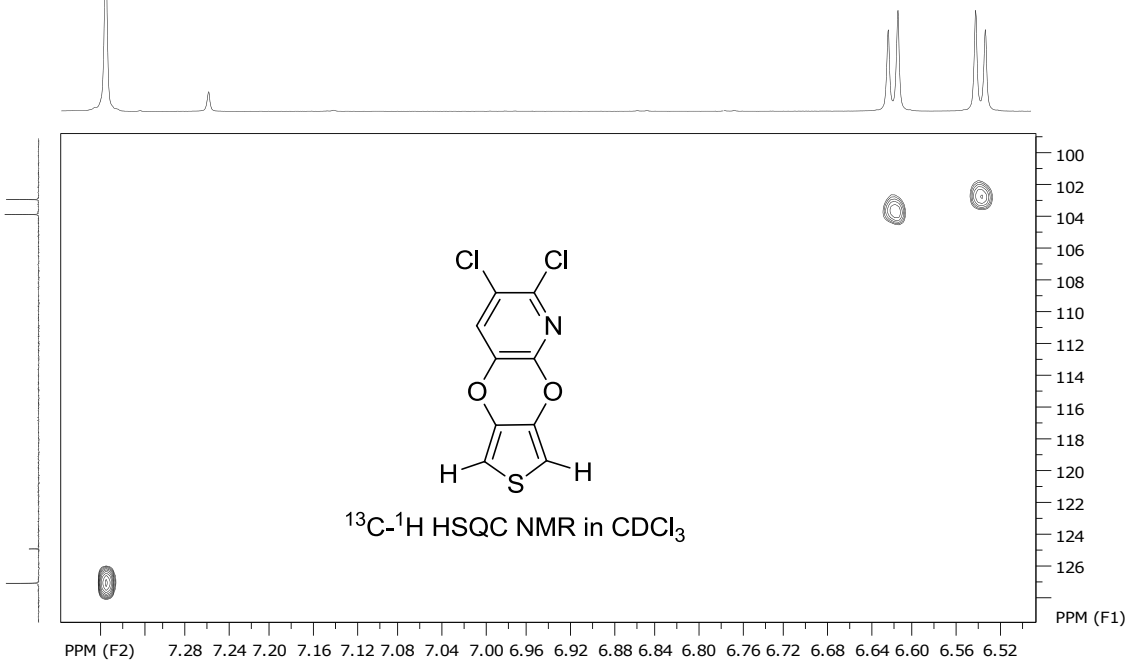

file: ...d\snb_47bp\101-SNB-47BP-HSQC.b\ser
expt: <hsqcedetgpsisp2.3>
transmitter freq: 400.131694 MHz
time domain size: 2048 by 256 points
width (F2): 3048.78 Hz = 7.6194 ppm = 1.4887 Hz/pt
number of scans: 2

F2: freq. of 0 ppm: 400.1300097 MHz
processed size: 1024 complex points
window function: Sine Squared
shift: 90.0 degrees
Hz/cm: 16.571 ppm/cm: 0.04141

F1: freq. of 0 ppm: 100.6127684 MHz
processed size: 1024 complex points
window function: Sine Squared
shift: 90.0 degrees
Hz/cm: 281.170 ppm/cm: 2.79438

SpinWorks 3: Supervisor Name IP
SNB-47BP
HMBC.b CDCl3 {C:\Bruker\TopSpin3.2} sam 10

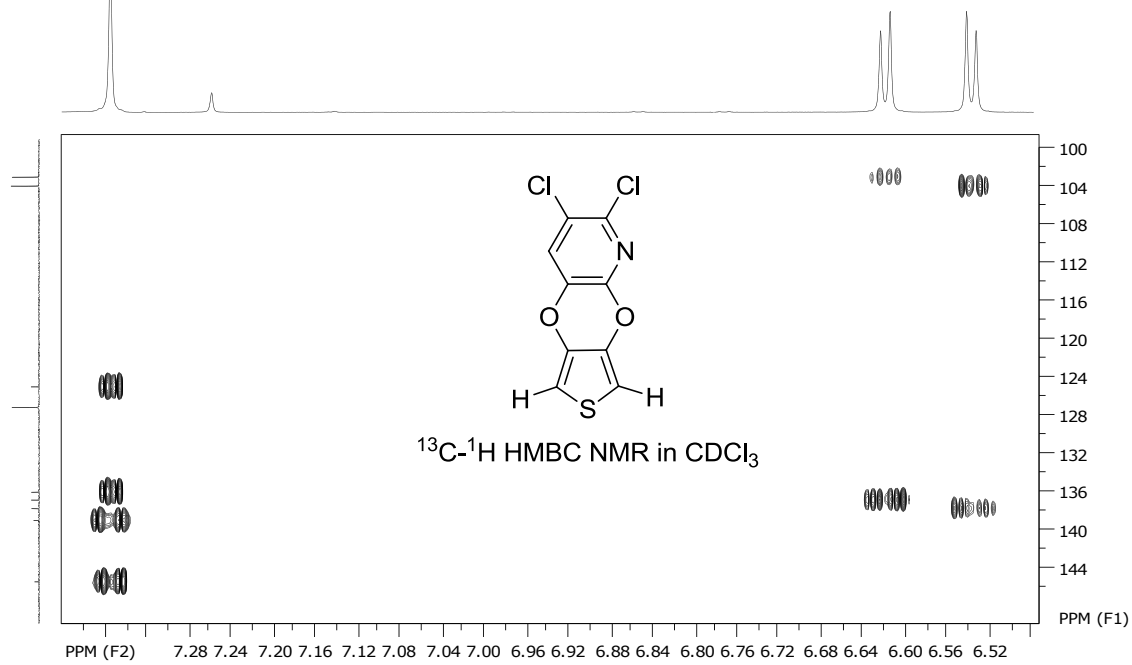

file: ...d\snb_47bp\102-SNB-47BP-HMBC.b\ser
expt: <hmbcetgpl3nd>
transmitter freq: 400.131694 MHz
time domain size: 4096 by 256 points
width (F2): 3048.78 Hz = 7.6194 ppm = 0.7443 Hz/pt
number of scans: 4

F2: freq. of 0 ppm: 400.1300098 MHz
processed size: 2048 complex points
window function: Sine
shift: 45.0 degrees
Hz/cm: 16.881 ppm/cm: 0.04219

F1: freq. of 0 ppm: 100.6127679 MHz
processed size: 1024 complex points
window function: Sine Squared
shift: 90.0 degrees
Hz/cm: 468.609 ppm/cm: 4.65708

Thieno[3',4':5,6][1,4]dioxino[2,3-b]pyrazine **(PzDOT)**

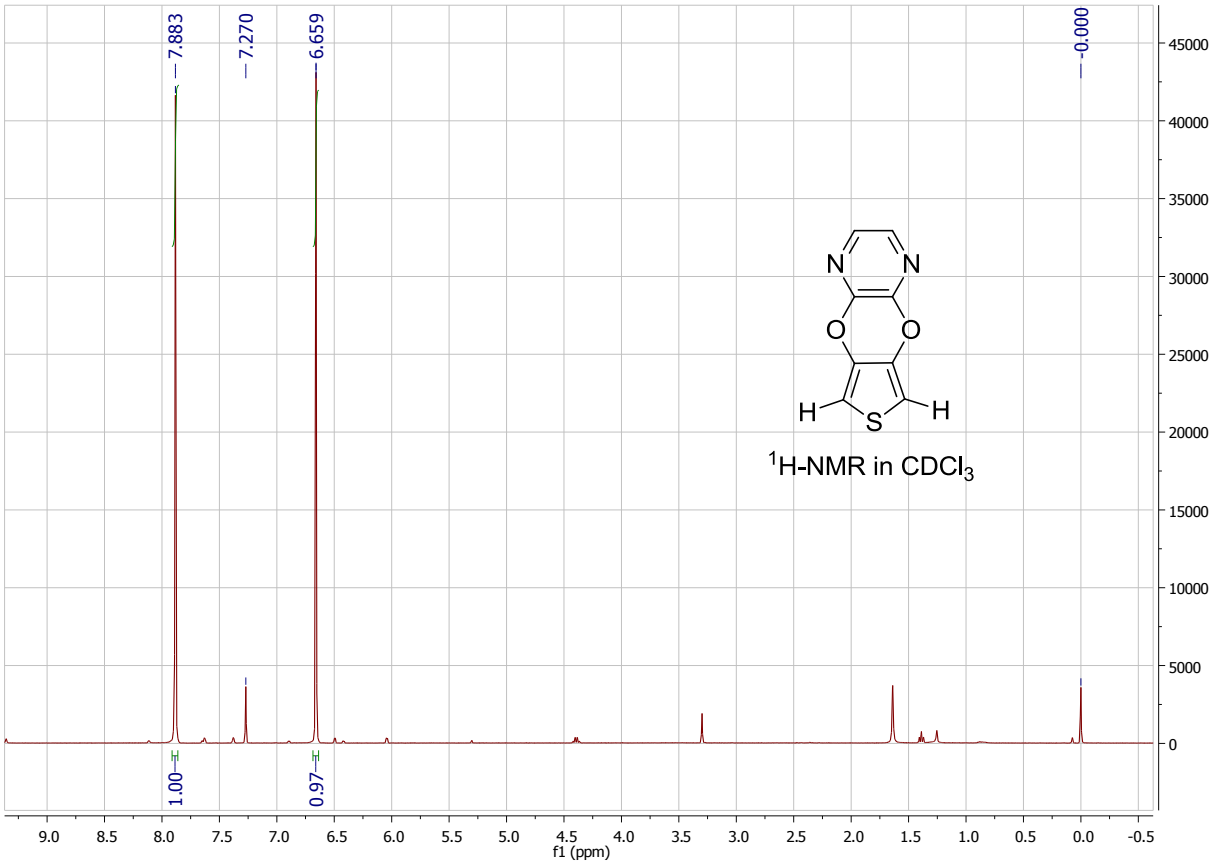

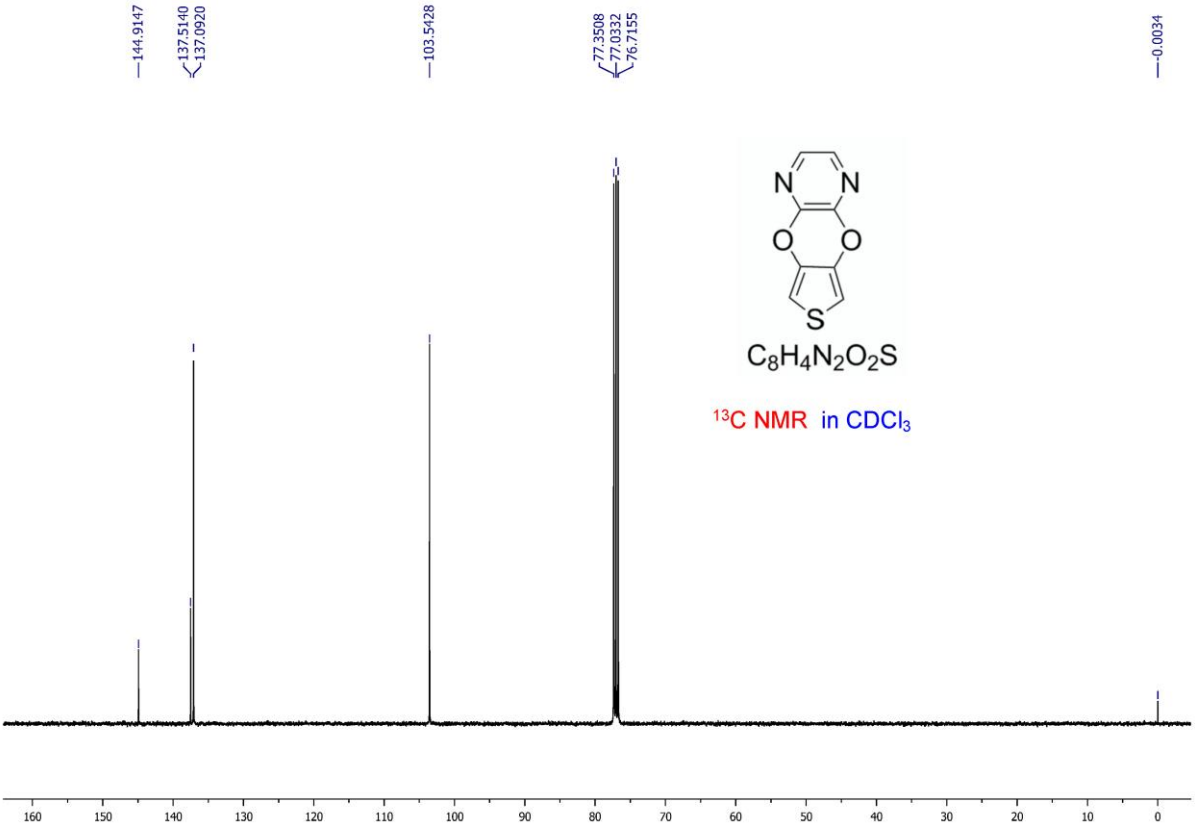

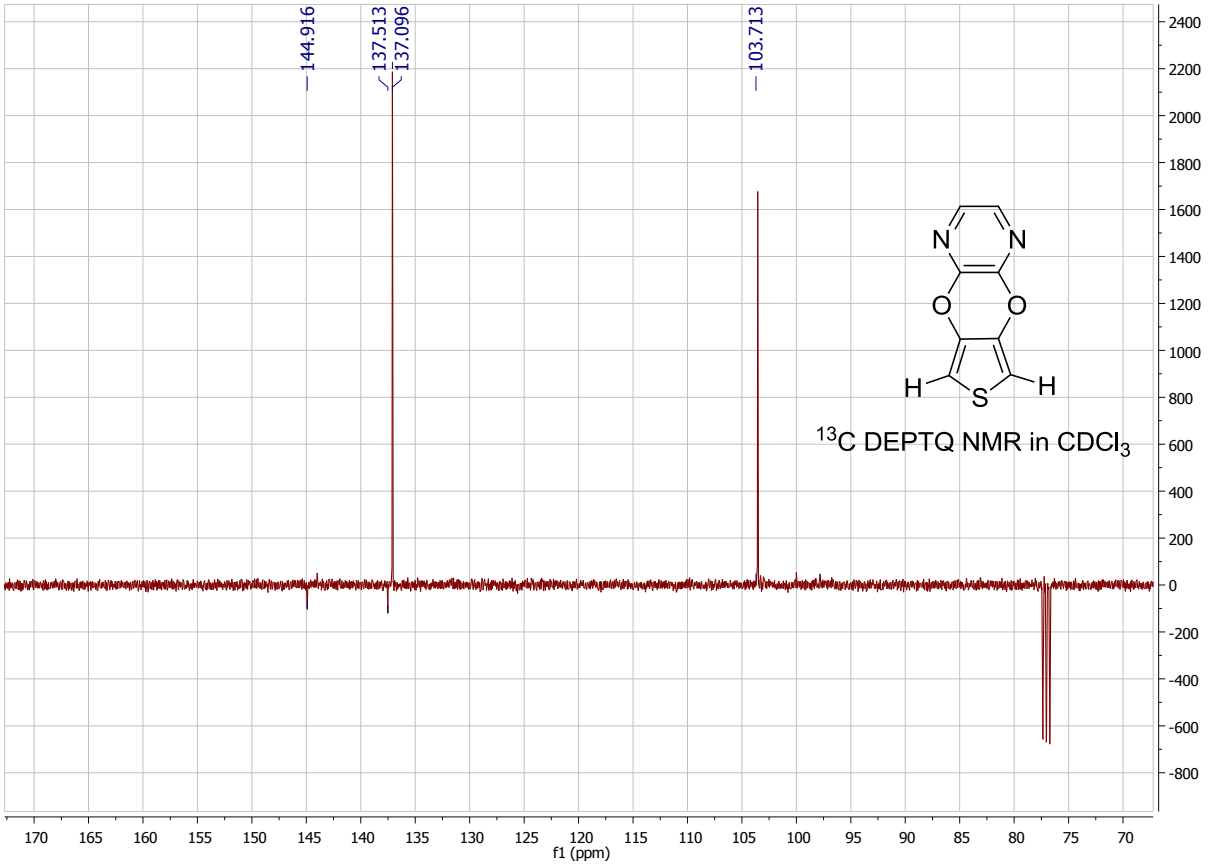
144.916
137.513
137.096
103.713
N
N
O
O
H
S
H
13C DEPTQ NMR in CDCl3
f1 (ppm)

SpinWorks 3: Supervisor Name IP

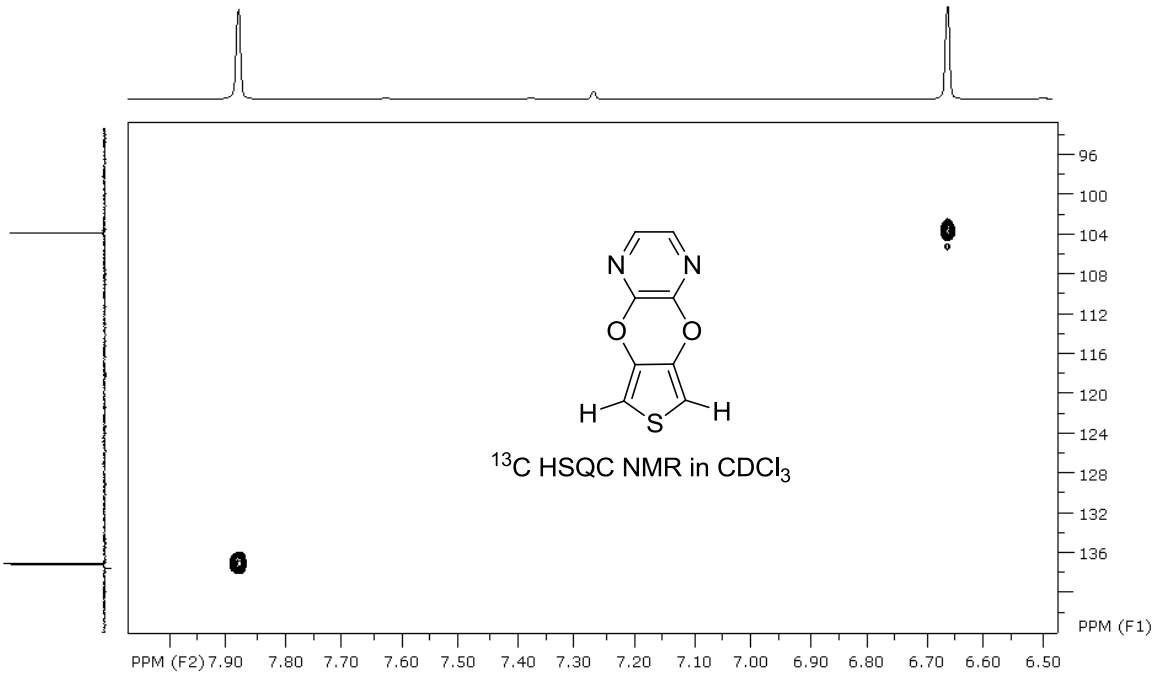

file: ...r_project\SNB-39B\July 19\HSQC\ser
expt: <hsqcedetgpsisp2.3>
transmitter freq: 400.132054 MHz
time domain size: 2048 by 256 points
width (F2): 3846.15 Hz = 9.6122 ppm = 1.8780 Hz/pt
number of scans: 2

F2: freq. of 0 ppm: 400.1300057 MHz
processed size: 1024 complex points
window function: Sine Squared
shift: 90.0 degrees
Hz/cm: 31.945 ppm/cm: 0.07984

F1: freq. of 0 ppm: 100.6127690 MHz
processed size: 1024 complex points
window function: Sine Squared
shift: 90.0 degrees
Hz/cm: 469.355 ppm/cm: 4.66464

SpinWorks 3: HMBC spectrum of SNB-39B

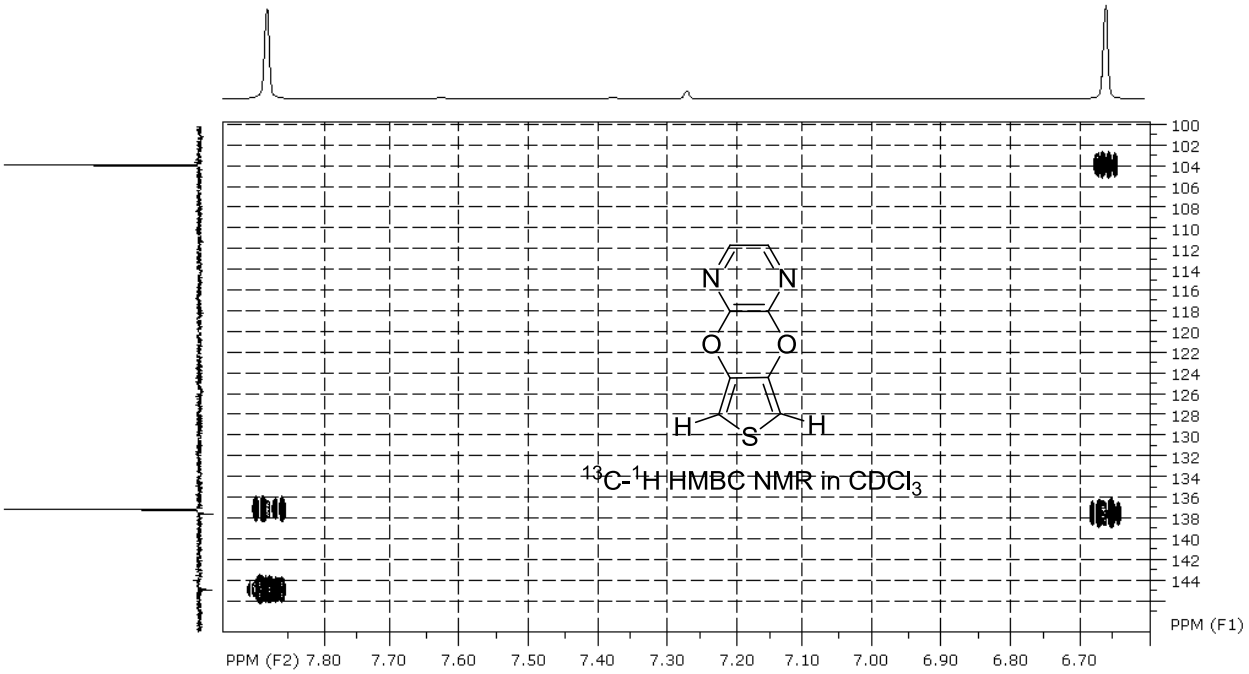

file: ...r_project\SNB-39B\July 19\HMBC\ser
expt: <hmbcetgpl3nd>
transmitter freq: 400.132054 MHz
time domain size: 4096 by 256 points
width (F2): 3846.15 Hz = 9.6122 ppm = 0.9390 Hz/pt
number of scans: 4

F2: freq. of 0 ppm: 400.1300057 MHz
processed size: 2048 complex points
window function: Sine
shift: 45.0 degrees
Hz/cm: 26.938 ppm/cm: 0.06732

F1: freq. of 0 ppm: 100.6127690 MHz
processed size: 1024 complex points
window function: Sine Squared
shift: 90.0 degrees
Hz/cm: 450.079 ppm/cm: 4.47293

Thieno[3',4':5,6][1,4]dioxino[2,3-b]quinoxaline **(QxDOT)**

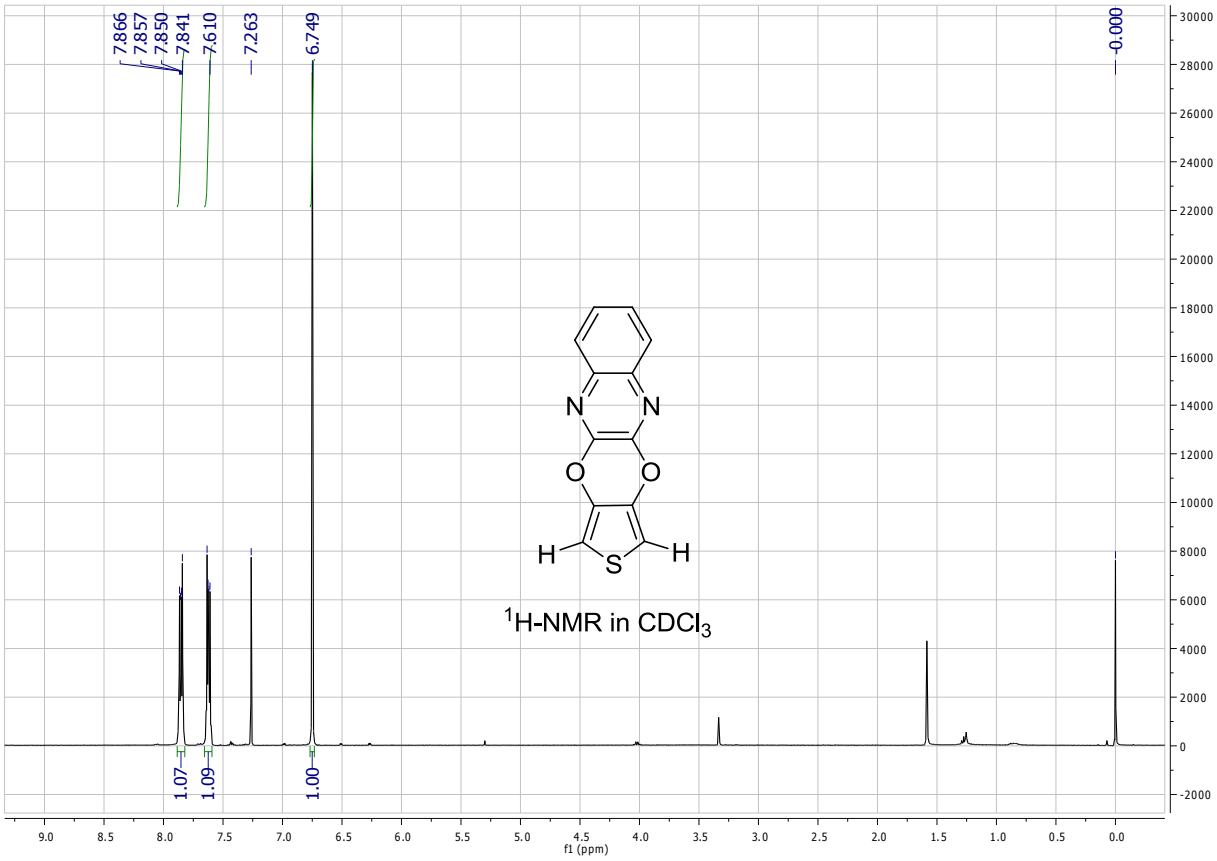

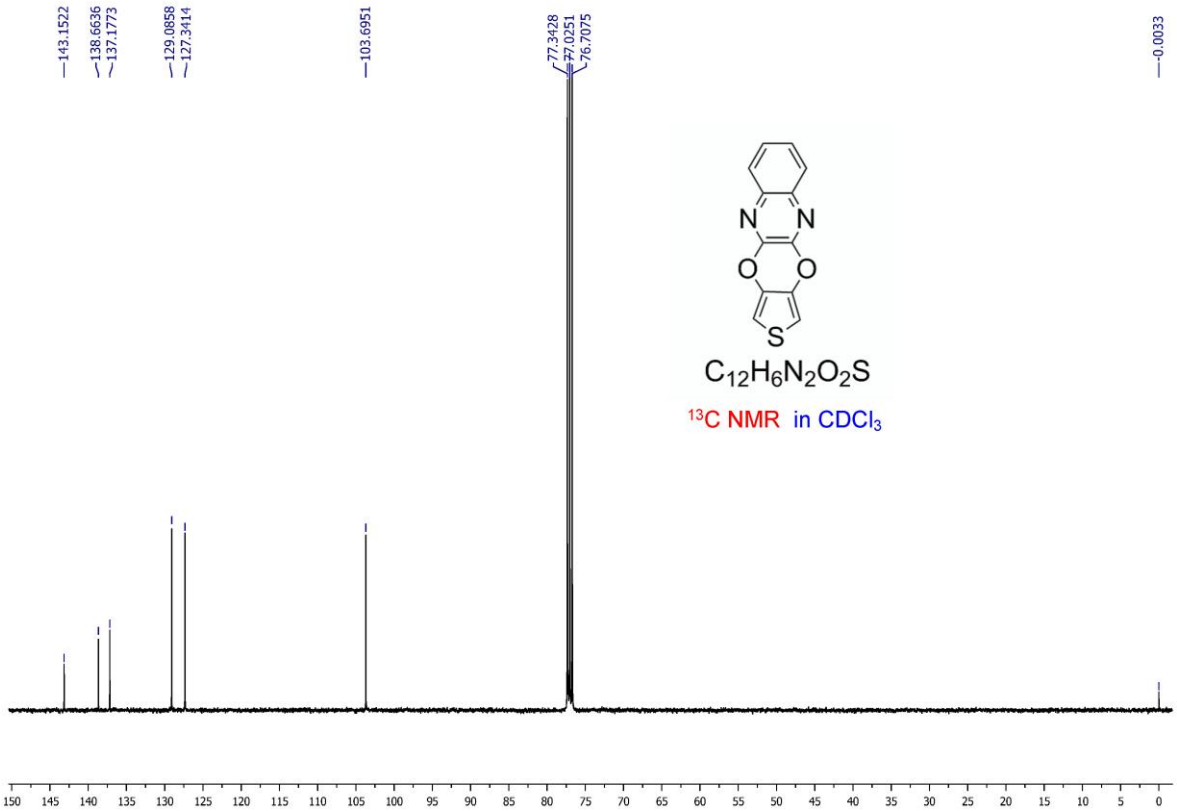

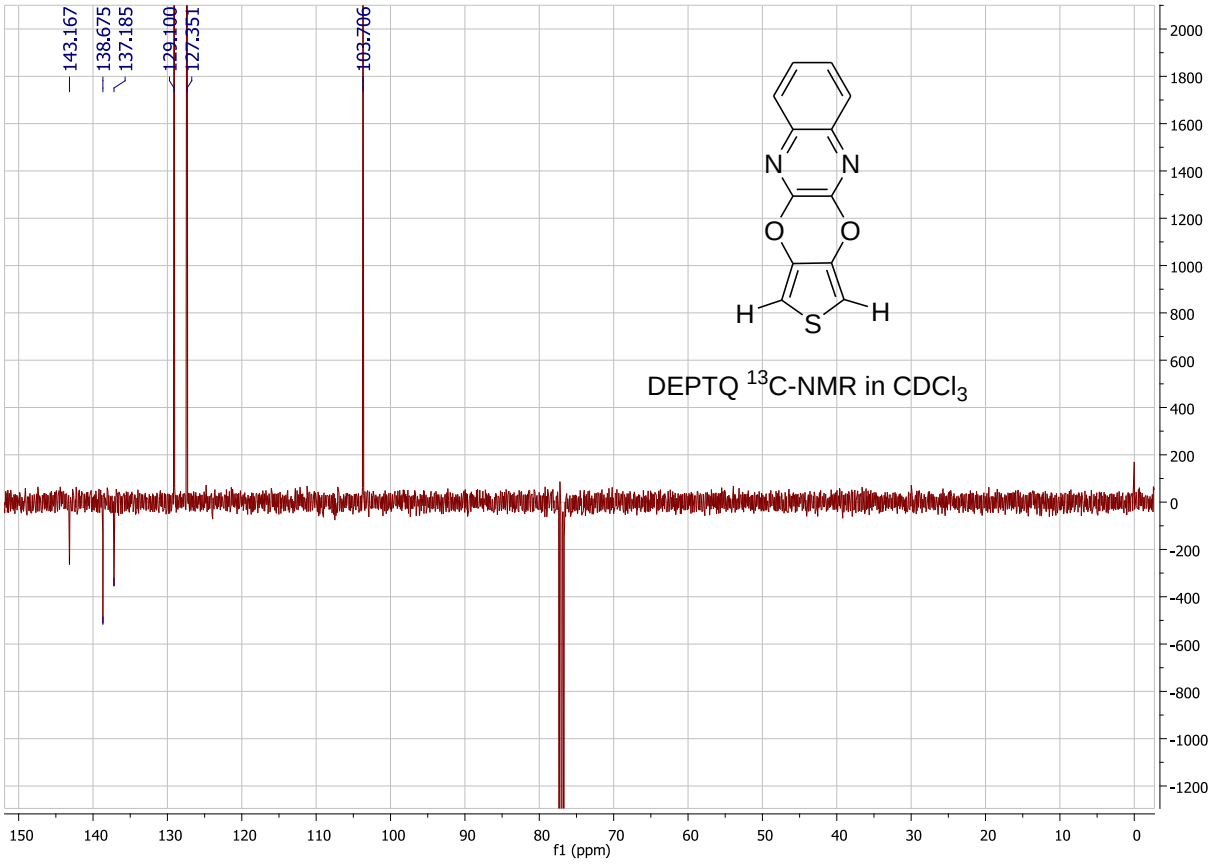
143.167
138.675
137.185
129.100
127.351
103.706
N
N
O
O
H
S
H
DEPTQ 13C-NMR in CDCl3
f1 (ppm)

SpinWorks 3: Supervisor Name IP
MPK-57B4
HSQC.b CDCl3 {C:\Bruker\TopSpin3.1} IP 34

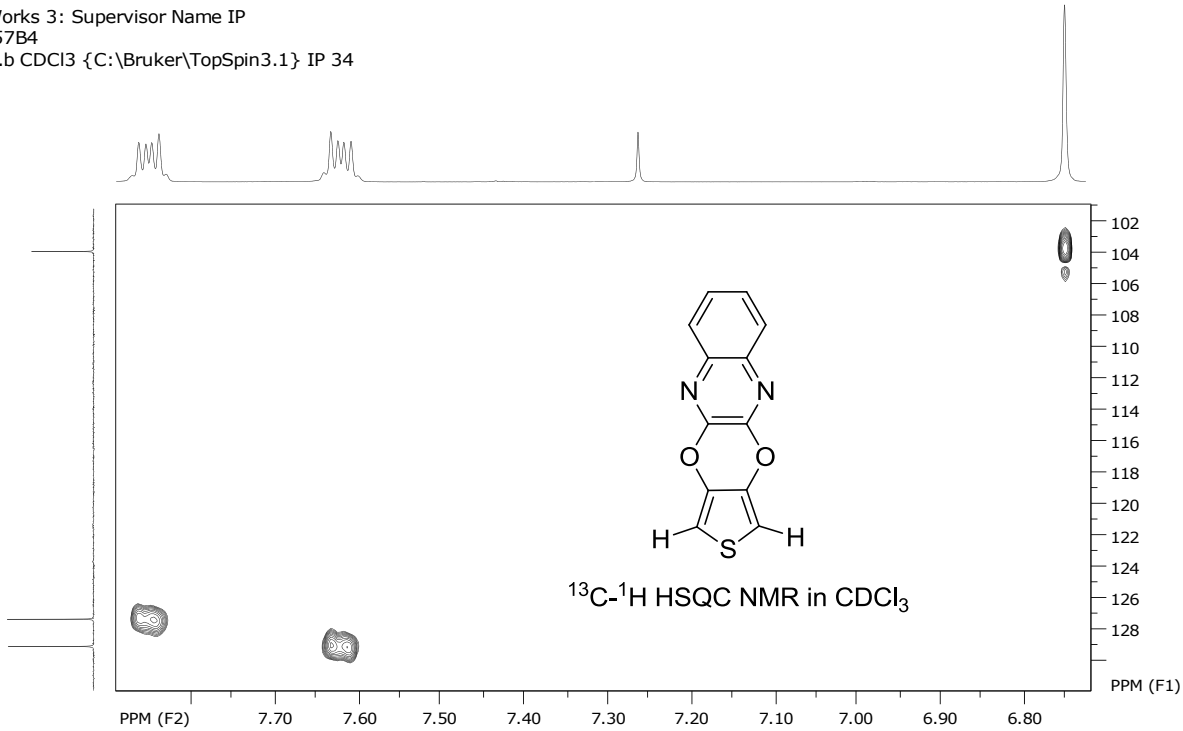

file: ...0-60\mpk_57\53-MPK-57B4-HSQC.b\ser
expt: <hsqcedetgpsisp2.3>
transmitter freq: 400.131763 MHz
time domain size: 2048 by 256 points
width (F2): 3184.71 Hz = 7.9592 ppm = 1.5550 Hz/pt
number of scans: 2

F2: freq. of 0 ppm: 400.1300084 MHz
processed size: 1024 complex points
window function: Sine Squared
shift: 90.0 degrees
Hz/cm: 21.302 ppm/cm: 0.05324

F1: freq. of 0 ppm: 100.6127690 MHz
processed size: 1024 complex points
window function: Sine Squared
shift: 90.0 degrees
Hz/cm: 283.687 ppm/cm: 2.81940

SpinWorks 3: Supervisor Name IP
MPK-57B4
HMBC.b CDCl3 {C:\Bruker\TopSpin3.1} IP 34

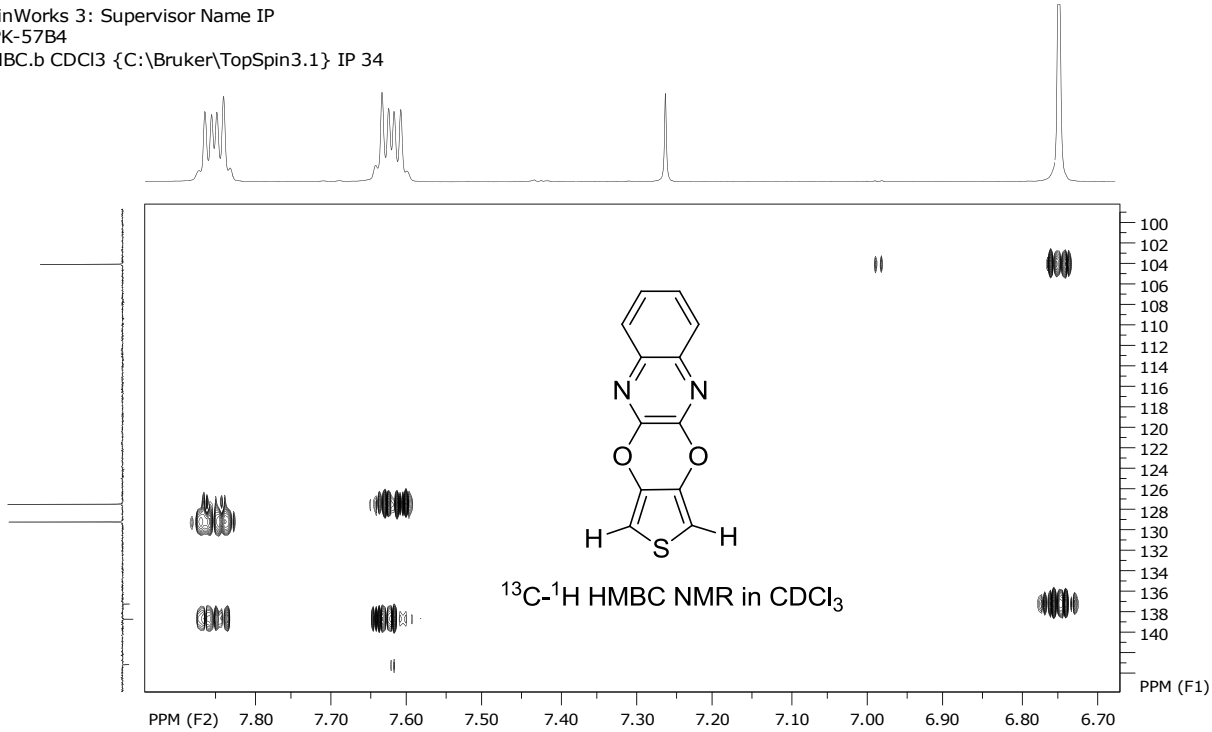

file: ...0-60\mpk_57\54-MPK-57B4-HMBC.b\ser
expt: <hmbcetgpl3nd>
transmitter freq: 400.131763 MHz
time domain size: 4096 by 256 points
width (F2): 3184.71 Hz = 7.9592 ppm = 0.7775 Hz/pt
number of scans: 4

F2: freq. of 0 ppm: 400.1300084 MHz
processed size: 2048 complex points
window function: Sine
shift: 45.0 degrees
Hz/cm: 23.096 ppm/cm: 0.05772

F1: freq. of 0 ppm: 100.6127690 MHz
processed size: 1024 complex points
window function: Sine Squared
shift: 90.0 degrees
Hz/cm: 435.681 ppm/cm: 4.32984